



Kent Academic Repository

Addison, Anthony William (1970) *Rhodium Chemistry, a Synthetical and Spectroscopic Study*. Doctor of Philosophy (PhD) thesis, University of Kent.

Downloaded from

<https://kar.kent.ac.uk/79264/> The University of Kent's Academic Repository KAR

The version of record is available from

<https://doi.org/10.22024/UniKent/01.02.79264>

This document version

UNSPECIFIED

DOI for this version

Licence for this version

CC BY-NC-ND (Attribution-NonCommercial-NoDerivatives)

Additional information

Versions of research works

Versions of Record

If this version is the version of record, it is the same as the published version available on the publisher's web site. Cite as the published version.

Author Accepted Manuscripts

If this document is identified as the Author Accepted Manuscript it is the version after peer review but before type setting, copy editing or publisher branding. Cite as Surname, Initial. (Year) 'Title of article'. To be published in *Title of Journal*, Volume and issue numbers [peer-reviewed accepted version]. Available at: DOI or URL (Accessed: date).

Enquiries

If you have questions about this document contact ResearchSupport@kent.ac.uk. Please include the URL of the record in KAR. If you believe that your, or a third party's rights have been compromised through this document please see our [Take Down policy](https://www.kent.ac.uk/guides/kar-the-kent-academic-repository#policies) (available from <https://www.kent.ac.uk/guides/kar-the-kent-academic-repository#policies>).

RHODIUM CHEMISTRY,
A SYNTHETICAL AND SPECTROSCOPIC STUDY.

A Thesis
submitted for the Degree of

Doctor of Philosophy

of the

UNIVERSITY OF KENT AT CANTERBURY

by

Anthony William Addison

B.Sc.(N.S. Wales)

September, 1970.

Acknowledgements.

I should like to thank my supervisor , Dr. Bob Gillard, to whom I am indebted for his enthusiastic guidance and encouragement over the past three years.

I am indebted to him and to Drs. Brian Heaton and Huw Vaughan for their cooperation and patient instruction in the Chemical Art.

I wish to thank Dr. J. A. Creighton & Mr. K. M. Thomas for their comments regarding the spectroscopic aspects of this work; also Miss J. Roye for transducing my manuscript into type , Miss L. Hurst for diagrams, and Miss L. Stevenson and Mrs. J. Teverson for all their help.

I thank Drs. G. Luckhurst & J. Wright for ESR spectra and X-ray powder photographs respectively, and Mrs. M. J. Clark for all those C, H, N-analyses !

Finally , let me express my gratitude to my friends and colleagues for making my stay at U.K.C. an enjoyable and memorable one.

I acknowledge the financial support provided by the Medical Research Council through the Biological Inorganic Chemistry Research Fund.

Abstract

The reductant-catalysed synthesis of complexes of the type trans[RhL₄X₂]X.nH₂O has been used to prepare compounds with L=pyridine and substituted pyridines; X = Cl, Br, I and extended to include L = isoquinoline, pyrimidine, pyrazole and thiazole, as well as the bis-chelates with 1:10-phenanthroline and 2,2'-bipyridyl and a polymeric triamine complex with L = pyrazine. The exchange of chloride for bromide in the monoheterocyclic amine complexes is catalysed by ethanol; a five-hundred-fold rate increase is observed for the halide exchange when the L = thiazole complex is ethanol catalysed. The inhibiting effect of oxygen on the substitution reactions is related to the eventual formation of binuclear cationic complexes of the type [Rh₂L₈X₂O₂]Y_n.mH₂O which have been isolated and characterised for L = pyridine, 4-methylpyridine, X = Cl, Y = ClO₄⁻, BF₄⁻ n = 3. They contain a bridging superoxide ligand whose relationship to the colours and magnetic properties of these and other complexes is discussed. The complexes with X = H₂O are weak acids and deprotonate to X = OH⁻. The μ-superoxodirrhodium(III) complexes are strong one-electron oxidants in aqueous solution (E^{0'} ~ +0.95 v.) and are converted to the corresponding μ-peroxodirrhodium(III) complexes (n = 2) by

base. These latter may be reoxidised quantitatively in acid solution, in which medium, however, they also disproportionate and hydrolyse slowly.

The reactions of the trans[RhL₄X₂]X. salts (L = pyridine, X = Cl⁻, Br⁻) with other ligands, Y, with and without added catalyst are studied. The species RhL₃XY₂ (X = Cl, Y = NO₂; X = Cl, Br, Y = NCO); [RhL₄Y₂]⁺ (Y = N₃, I); RhL₃Y₃ (Y = NO₂, N₃, I); [RhL₂Y₄]⁻ (Y = N₃) are prepared thus and characterised by analytical and spectroscopic methods.

Hydrolysis of the trans[RhL₄X₂]⁺ ions is effected by fluoride, acetate and hydroxyl ions, and salts of the species trans[RhL₄XY]ⁿ⁺ have been obtained (L = pyridine, X = Cl, Br ≠ Y = OH, OH₂, Cl); the aquo-complexes are weak acids whose pK_a values have been determined. The compounds synthesised are surveyed polarographically, and comment made on the relationships between half-wave potentials, spectroscopic properties and (auto)catalytic behaviour.

From the oxalato-complexes, RhL₃XOx, (L = pyridine, substituted pyridine; X = Cl, Br) the compounds RhL₃X₂Y (X = Cl, Br, Y = Cl, Br) are synthesised and characterised. Their electronic spectra and those of the other compounds are rationalised empirically. The low-frequency Raman and infrared spectra in the metal-ligand stretching region of these and several trans[ML₄X₂]ⁿ⁺ species (M = Co, Rh, Pt,

L = monoheterocyclic amine, X = Cl, Br) have been obtained and are discussed in terms of two simple valence force field models and rationalised on the basis of simplistic application of group theory.

Aspects of the interaction of molecular oxygen with transition metal centres are presented in terms of a donor-acceptor interaction with oxygen acting as a Lewis acid.

Solvates and adducts of both complex salts and uncharged complexes are prepared and examined with respect to their properties of stabilisation of unusual species and the probability of hydrogen bond formation with halo-carbons.

Symbols and Abbreviations

δ	(in vibrational tables) a bending mode
ϵ	molar absorbance ($l \cdot \text{mol}^{-1} \text{cm}^{-1}$)
λ	wavelength, in
nm.	nanometre
()	in spectroscopic tables, denotes a shoulder
ν	a frequency, or the mode associated with it thus ν_a , ν_s are antisymmetric and symmetric ν
Λ	molar conductivity ($\text{cm}^2 \text{ohm}^{-1} \text{mol}^{-1}$)
kK	kiloKayser ($1 \text{ kK} = 1000 \text{ cm}^{-1}$)
c-	<u>cis</u>
t-	<u>trans</u>
<u>fac</u>	the facial (1,2,3-) isomer
<u>mer</u>	the meridional (1,2,6-) isomer
UV	ultraviolet
i.r.	infrared
SCE	saturated calomel electrode
A	NH_3 (in a complex)
D	deuterium (deuteriochloroform of solvation in 4.3)
S	chloroform of solvation
py	pyridine (Dpy = pentadeuteriopyridine)
pic	\uparrow -picoline
n-Zpy	pyridine with the Z-substituent in the n-position
lut	lutidine (3,5-dimethylpyridine)
en	ethylenediamine
pn	propylenediamine
Ox	oxalate dianion
prm	pyrimidine
pzl	pyrazole
pzn	pyrazine
thz	thiazole
iquin	<u>isoquinoline</u>
bipy	2,2'-bipyridyl

phen	1:10-phenanthroline
cyclam	1,4,8,11-tetra-azacyclotetradecane
trien	triethylenetetramine
salen	N,N'-ethylenebis(salicyladehydimate) dianion
acacen	N,N'-ethylenebis(acetylacetonimate) dianion
DMSO	dimethyl sulphoxide
DMF	dimethyl formamide
Me	methyl
Et	ethyl
Pr	propyl

Table of Contents.

<u>Chapter 1</u>	<u>Pyridine base Complexes of Rhodium(III)</u>	
1.1	Introduction.	1
1.2	Preparation of trans-dihalotetramine salts.	5
1.3	Structure and stability.	6
1.4	Trans-[Rh py ₄ I ₂] ⁺ .	10
1.5	Other heterocyclic ligands.	12
1.6	Electronic spectra.	17
1.7	Trans[Rh(thiazole) ₄ Cl ₂] ⁺ and bromide.	19
1.8	Solvates and adducts.	24
1.9	Vibrational studies.	
	(i) The co-ordinated ligand.	27
	(ii) Metal-ligand vibrations.	30
<u>Chapter 2</u>	<u>Superoxide complexes of rhodium.</u>	
2.1	Initial observations.	43
2.2	Preparation of complexes.	44
2.3	Characterisation.	45
2.4	Magnetic properties.	47
2.5	Redox properties.	50
2.6(i)	Spectroscopy and reactivity	57
	(ii) Spectroscopy and structure.	58
2.7	Rationalisation of the preparation.	70
<u>Chapter 3</u>	<u>Reactions of trans[Rh py₄X₂]⁺.</u>	
3.1	Catalysis and inhibition.	77
3.2	Substitution reactions.	
	(i) Iodide.	80
	(ii) Azide.	80
	(iv) Cyanate.	87
	(v) Nitrite.	89
	(vi) Ethylenediamine.	91
	(vii) 1,3-Dicarbonyls.	93
	(viii) Phenanthroline and bipyridyl.	93

Cont.

Contents (cont.)

<u>Ch.</u>	<u>3.3</u>	The hydrolysis of $\text{trans}[\text{Rh py}_4\text{X}_2]^+$	
	(i)	Experimental observations.	98
	(ii)	Spectroscopic characterisation and pK_a	101
	<u>3.4</u>	Polarographic studies.	106
<u>Chapter 4</u>		<u>Tripyridinerhodium(III) compounds.</u>	
	<u>4.1</u>	Halo-oxalatotripyridinerhodium(III)	115
	<u>4.2(i)</u>	Reaction with hydrohalogenic acids.	119
	(ii)	Electronic spectra.	122
	(iii)	Empirical rules for Rh(III) spectra.	128
	(iv)	Vibrational modes of Rhpy_3X_2 .	132
	<u>4.3</u>	Halocarbon solvates.	
	(i)	Formation and composition.	142
	(ii)	Vibrational spectra and structure.	149
<u>Chapter 5</u>			
	<u>5.1</u>	Aspects of autoxidation.	155
	<u>5.2</u>	Conclusion.	164
<u>Chapter 6</u>		<u>Experimental.</u>	
	A	Instrumentation.	172
	B	Analyses.	176
	C	Reagents.	176
	D	Preparations of compounds.	177
	E	Redox equivalent weights.	198
		<u>Appendices (i)-(iv).</u>	

I Declare that I have not submitted any part of this work for any qualification in any other institution.

A. W. Addison

Canterbury, 1970.

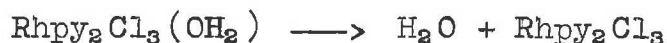
Chapter 1

Pyridine Base Complexes of Rhodium(III)

1.1 Introduction

The ability of nitrogenous bases to combine with metal ions is a familiar aspect of inorganic chemistry which has been known for over a century. The use of heterocyclic nitrogen bases such as pyridine to fulfil this role has also been well documented over many years. Jørgensen's⁽¹⁾ synthesis of transdichlorotetrapyridinerhodium(III)chloride was one of the first pyridine complexes, and preceded the preparation of complexes of rhodium with other heterocyclic bases by more than fifty years⁽²⁾, but his characterisation was of the anhydrous salt, which is not readily prepared from the hydrated golden yellow laths. It is noteworthy that in the same publication Jørgensen discusses the evidence at hand at that time for the accepted atomic weight of rhodium. Jørgensen then turned to the further investigation of the ammine⁽³⁾ complexes of rhodium(III) which were to take part in the later controversial theories of Werner⁽⁴⁾ regarding the structure of coordination compounds, now a classic thesis in the development of modern chemistry.

Little of significance in the chemistry of the rhodium-pyridine system was then published until the nineteen twenties, when Delépine⁽⁵⁾ synthesised several complexes under milder conditions than those used by Jørgensen. In conjunction with studies on similar iridium(III) complexes, he synthesised several rhodium complexes and characterised them as Rhpy_3Cl_3 (one isomer), $\text{Rhpy}_4\text{Cl}_3 \cdot 6\text{H}_2\text{O}$, salts of cis- and trans- $[\text{Rhpy}_2\text{Cl}_4]^-$ as orange and red materials respectively, the cis-isomer being hydrolysable to $[\text{Rhpy}_2(\text{OH}_2)\text{Cl}_3] \cdot \text{H}_2\text{O}$, which he showed to be acidic by preparation of the salt $\text{Ag}[\text{Rhpy}_2(\text{OH})\text{Cl}_3] \cdot 2\text{H}_2\text{O}$. Similarly, the transtetrachlorodipyridinerhodium(III) anion was hydrolysed to give an aquo-complex, which could be dehydrated by heating;



The pink compound formed has since been shown⁽⁶⁾ to be polymeric $[\text{Rhpy}_2\text{Cl}_3]_n$, and quarter of a century after his first publication on the subject, Delépine⁽⁷⁾ described the action of sunlight on Rhpy_3Cl_3 in solution to give the pink compound, as well as the photosensitised conversion of Rhpy_3Cl_3 to the chloro-aquo compound and his previously described complex salts $[\text{Rhpy}_4\text{Cl}_2][\text{Rhpy}_2\text{Cl}_4]$. The original work⁽⁵⁾ includes salts of the anion $[\text{Rhpy}_2\text{Cl}_3(\text{OH})]^-$, while

in concluding Delépine commented "On n'a pas pu préparer $\text{Rh}^{\text{IV}}(\text{C}^5\text{H}^5\text{N})_2\text{Cl}_4$ ". His work was followed a few years later⁽⁸⁾ by a lengthy publication describing the examination of analogous bromorhodium complexes by Poulenc, working in the same laboratory, as the extension of an investigation of bromorhodate(III) anions. Poulenc added the $[\text{Rhpy}_5\text{Br}_5]^-$ species to the types known, and showed that only one isomer of Rhpy_3Br_3 was preparable, and it was much later that Holtzclaw and Collman⁽⁹⁾ separated fac and mer- Rhpy_3Cl_3 . Poulenc also demonstrated the photosensitivity of the bromo-complexes by preparing Rhpy_3Br_3 from Rhpy_4Br_3 photochemically. C.K. Jørgensen⁽¹⁰⁾ has examined Delepine's compounds by electronic spectroscopy and concluded that the previous cis and trans formulations were correct.

Dwyer and Nyholm⁽¹¹⁾ examined the effect of hypophosphorous acid on rhodium(III) pyridine complexes, expecting the formation of "rhodous" complexes through reduction of the rhodium(III) species. Unfortunately, their lack of facilities for C, H and N analyses or i.r. spectroscopy led them to misformulate many of their compounds, so that their $[\text{Rhpy}_6]^{3+}$ species were later found⁽¹²⁾ merely to be the hydrated salts $[\text{Rhpy}_4\text{X}_2]\text{X} \cdot 5\text{H}_2\text{O}$, for example. In the same studies, a compound claimed to contain the $[\text{Rhpy}_5\text{H}]^{2+}$ ion was isolated as the iodide

salt; it had an i.r. band attributable to $\sim(\text{Rh-H})$. Since then, the action of borohydride on ethylenediamine and pyridine complexes has been evidenced to yield hydrido-rhodium species^(13,14), and the position of H^- in the spectrochemical series toward rhodium(III) has been discussed⁽¹⁵⁾.

In effect, Dwyer and Nyholm⁽¹¹⁾ discovered the catalytic influence of reducing agents on the overall reaction



and similarly for the bromide. However it was not until ten years later that Delépine⁽¹⁶⁾ realised that the influence of simple alcohols, glycols and sugars on the reaction of aqueous pyridine with chlororhodium(III) species was of just this type, and later his study was extended by a coworker⁽¹⁷⁾ and became a convenient synthetic route, These catalytic effects are reconsidered later in this work.

Recently, interest in pyridine complexes has been aroused in a different quarter, since the discovery⁽¹⁸⁾ of their antibacterial action, and their ability to induce anomalous morphology in the gram-negative bacteria Escherichia coli at sub-lethal levels.

1.2 Preparation of trans Dihalotetraminerhodium(III)

Salts

Compounds of the type $\text{trans}[\text{RhL}_4\text{X}_2]\text{Y}\cdot n\text{H}_2\text{O}$ were prepared by the catalytic procedure, using aqueous ethanol as the reaction medium. The general method used to to quickly add a warm solution of excess heterocyclic base ligand in ethanol to a warm solution of the rhodium halide in aqueous ethanol, the ligand:metal ratio being ca. 6:1.

Pyridine readily forms thus the complexes trans $[\text{Rhp}_4\text{Cl}_2]\text{Cl}\cdot 5\text{H}_2\text{O}$ and $[\text{Rhp}_4\text{Br}_2]\text{Br}\cdot 5\text{H}_2\text{O}$. One notes that both carry water of crystallisation, and the formulation has led to discrepancies in the past. Pentahydration is favoured by the C, H analyses (Table 1.1) and by an experiment in which quantitative precipitation of the anhydrous perchlorate salt of $\text{Rhp}_4\text{Cl}_2^+$ gave a value of 4.6 for n in $\text{Rhp}_4\text{Cl}_3\cdot n\text{H}_2\text{O}$. Salts of the RhL_4X_2^+ species are readily formed in aqueous solution merely by the addition of the sodium salt or acid of the appropriate anion, and this simple metathesis is used throughout to precipitate ClO_4^- , BF_4^- or PF_6^- . The 4-methylpyridine complex, $\text{Rhpic}_4\text{Cl}_3$ crystallises from solution as large golden yellow plates which may be dried carefully to yield an 8-9 hydrate, the crystals of which crumble if

warmed, efflorescing to the trihydrate. The 3- and 4-alkylpyridines readily yield $RhL_4Cl_2^+$ complexes by the catalytic preparation, the solubility in organic solvents increasing as the degree of alkylation increases, and the solubility in water decreasing. The acetylpyridine complex is too soluble in water or alcohols to be crystallised as the chloride, so was prepared as the perchlorate salt.

The preparative procedure was extended to encompass other substituted pyridines, as well as various different nitrogen heterocycle archetypes, of which pyridine itself is an example.

1.3 The Interdependence of Structure and Stability

The synthesis of the $RhL_4X_2^+$ species was not always successful. However, the failures are usually readily explained. Thus in the case of pentafluoropyridine, quinoline, and 2-methylpyridine, there was little evidence of reaction. Furthermore, the addition of 10 M HCl to the reaction mixture, followed by warming, generated the cherry-pink colour of the penta- and hexa-chlororhodate anions, while the $RhL_4X_2^+$ species which have been prepared, are quite stable toward hot HCl.

Table 1.1a

Analytical Properties of Rhodium Heterocyclic Base Complexes $[\text{RhL}_2\text{X}_2]\text{Y}_n\text{nH}_2\text{O}$

L	X	Y	n ^a	f. %C		f. %H		f. %N		Other%	
				f.	c.	f.	c.	f.	c.	f.	c.
Pyridine	Cl	Cl	5	39.2	39.0	5.2	4.9	9.0	9.1	H ₂ O	13.9 14.6
"	Cl	ClO ₄	0	40.8	40.8	3.4	3.4	9.4	9.5		
"	Cl	BF ₄	0	41.9	41.7	3.3	3.5	9.9	9.7		
"	Cl	PF ₆	0	38.0	37.8	3.4	3.2	8.7	8.8		
"	Br	Br	5	32.1	31.7	3.6	3.8	7.8	7.7		
"	Br	ClO ₄	0	35.4	35.4	3.0	3.0	8.4	8.3		
"	I	I	3	27.9	28.0	2.1	3.1	7.4	6.5		
"	I	ClO ₄	0	32.2	31.1	3.2	2.6	8.0	7.2	Cl	3.9 4.7
										I	30.0 32.9
4-methylpyridine	Cl	Cl	3	45.5	45.3	4.5	5.3	8.7	8.8		
"	Cl	ClO ₄	0	44.5	44.6	4.3	4.4	8.7	8.7		
"	Cl	BF ₄	0	45.4	45.5	4.6	4.5	9.1	8.9		
4-ethylpyridine	Cl	ClO ₄	0	47.9	47.9	5.0	5.2	8.0	8.0		
3,5-dimethylpyridine	Cl	Cl	1	50.9	51.4	6.1	5.8	8.5	8.6		
3-chloropyridine	Cl	Cl	5	32.1	31.9	3.4	3.5	7.3	7.4	Cl	32.9 32.9
3-acetylpyridine	Cl	ClO ₄	0 ^b	43.8	44.4	3.7	3.7	7.2	7.4		
isoquinoline	Cl	Cl	3	55.1	55.4	3.8	4.4	7.3	7.2		
thiazole	Cl	Cl	5	22.5	22.5	3.6	3.5	9.0	8.8		
"	Br	Br	2	20.2	20.0	3.0	2.2	7.9	7.8		
pyrazole	Cl	Cl	5	25.2	25.2	4.6	4.6	19.6	19.6		
pyrimidine	Cl	ClO ₄	0	32.4	32.4	2.7	2.7	18.9	18.9		

a: evidenced by $\nu(\text{O-H})$ in i.r. spectrumb: $\nu(\text{C=O})$, 1700 cm^{-1} (v.s.) in i.r.

c: calculated

f: found

Table 1.1(b)

Analytical Properties of Rhodium Heterocyclic Base Compounds

Compound	%C		%H		%N		%Other	
	f.	c.	f.	c.	f.	c.	f.	c.
[Rh bi py ₂ Cl ₂]Cl.2H ₂ O	43.3	43.0	3.6	3.6	10.3	10.0		
[Rh phen ₂ Cl ₂]Cl.3H ₂ O	46.2	46.2	3.5	3.6	9.2	9.0		
[Rh phen ₂ I ₂]I.2H ₂ O	32.6	32.8	2.3	2.3	6.4	6.4	I,	41.6 43.2
Rh z n ₃ Cl ₃	31.6	32.1	2.2	2.7	18.6	18.7		
Rh(C lpy) ₃ Cl ₃	32.5	32.8	2.1	2.2	7.4	7.6		
[Rh py ₄ ClBr]ClO ₄ ^a	38.0	37.9	3.2	3.2	8.8	8.8		

a: prepared as in Chapter 4.

The structure of the $\text{Rhpy}_4\text{Cl}_2^+$ ion has been determined⁽¹⁹⁾ by an X-ray diffraction study and it has the trans-configuration, with Rh-Cl distances of 2.34\AA , and Rh-N bond lengths of 2.09\AA . The noteworthy feature of the ion is that the four per se planar pyridine ligands are neither horizontal nor vertical to the ClRhCl axis, but inclined at an angle ($40^\circ - 50^\circ$) to it. The ion has the appearance of a propeller for this reason, and as this configuration is associated with helicity, the ion is, theoretically, resolvable into R and S forms. Indeed, the instantaneous configuration must be one of these enantiomers, as molecular models suggest strongly that the pyridine rings can rotate only in phase with each other to invert the configuration. However, the rate of inversion is unknown, and vice versa, no trans Mpy_4X_2^+ species has yet been resolved. The necessity for concerted rotation of the ligands about the Rh-N axes is reminiscent of the so-called "cogwheel effect" proposed⁽²⁰⁾ as existing between the methyl substituents in the dimesityl carbonium ion, in which the aryl rings rotate relatively freely, even at -60°C , but which apparently must involve concerted "meshing" of the methyl groups as they move past one another. Unfortunately, the vibrational spectra of $\text{Rhpy}_4\text{X}_2^+$ species appear not to contain any transition which may be associated with changes

in the rotational states of the rings, unless it occurs below ca. 200 cm^{-1} in which case the rate of inversion, and hence of racemisation will be high enough at room temperature to prevent resolution, since $kT = 208.5 \text{ cm}^{-1}$ at 300°K . In addition, the ^1H n.m.r. spectra⁽²¹⁾ of various of the tetrakis (alkylpyridine) complexes do not offer any evidence for restricted rotation (33°C) but nor do they disprove its existence.

Both the crystal structure and the molecular models imply that the axial (halide) ligands may interact with the α -protons on the pyridine ring (Figure 1.1) in the same way as they cause interaction between rings.

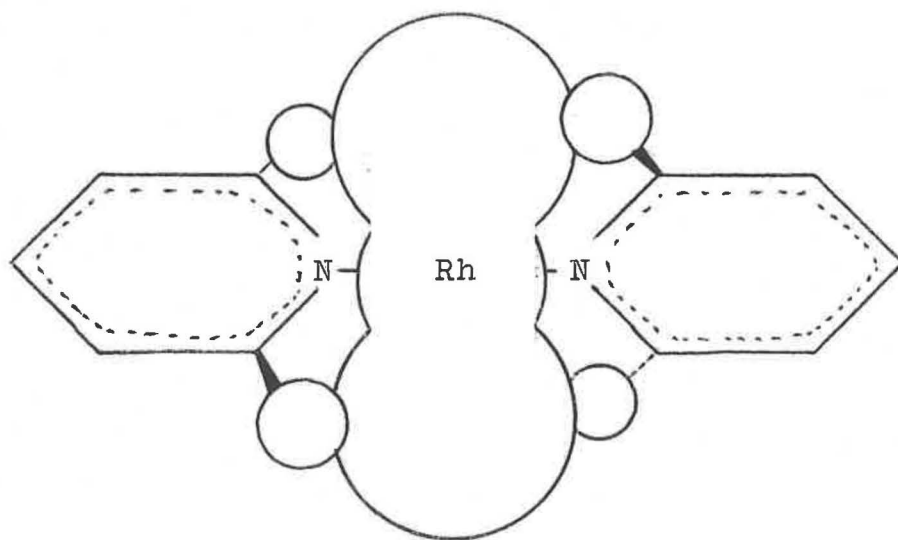
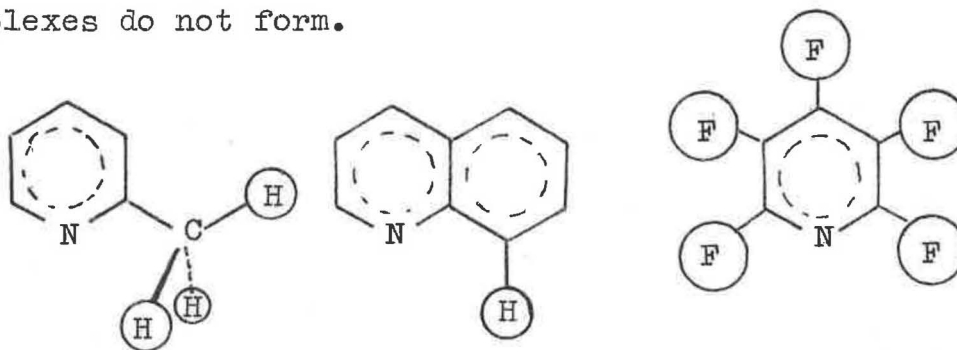


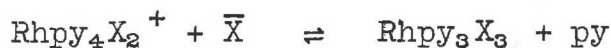
Figure 1.1. \dagger Rhpy_2X_2 unit (Not to scale)

Returning to the problem of the instability of certain of the complexes, one sees that replacement of an α -proton by a bulkier moiety such as $-F$, $-CH_3$, $-NH_2$, $-Cl$ will aggravate the nonbonding interaction with the axial ligand. Hence, the stabilities of even mono-complexes of ligands such as those below will be greatly reduced, and it is not wholly unexpected that tetrakis-complexes do not form.



Some difficulty was also experienced in preparing the complex trans-dichlorotetrakis(3-chloropyridine)-rhodium(III) cation. The steric effect cannot be invoked here; indeed one notes that the major product of the reaction ^{was}/(EtOH catalysed) 1,2,6-trichlorotris(3-chloropyridine)rhodium(III) molecule, so catalysis is effective, as the use of insufficient pyridine gives the analogous compound. It is very likely that this is merely a solubility effect; $Rh(Clpy)_4Cl_3$ itself is rather insoluble in water, as is the ligand, so that $Rh(Clpy)_3Cl_3$ will be very insoluble in the reaction medium and

precipitate rapidly (which it is observed to do) as it forms. Indeed the insolubility of the Rhpy_3X_3 compounds as opposed to their Rhpy_4X_3 salts may well be an important influence in the equilibrium

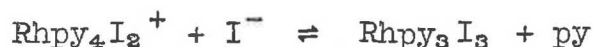


That the 3-chloropyridine case is not affected by electronic factors is discussed shortly.

1.4 Trans-Diiodotetrapyridinerhodium(III) Iodide

The catalytic effect of mild reductants⁽²²⁾ on the halide exchange reactions of the $\text{Rhpy}_4\text{X}_2^+$ ions as well as on their synthesis is well established now, and is re-considered later in this work. Although the replacement of chloride by bromide in $\text{Rhpy}_4\text{Cl}_2^+$ is preparatively well known, the reaction with iodide is less readily accomplished; it is discussed in Chapter 3. Moreover, it has been reported⁽¹²⁾ that the species $\text{Rhpy}_4\text{I}_2^+$ is only difficulty synthesised by the usual procedure, and that "attempting to dry it or wash it with water, alcohol or ether causes ready loss of pyridine and a material Rhpy_3I_3 remains as a water insoluble material". (Rhpy_3I_3 is characterised in Chapter 3). These observations may

have resulted from the presence of hypophosphorous acid causing catalysis of the reaction



which would proceed to the right as pyridine was removed by washing.

Initial attempts to effect the reversal of the above equilibrium by heating rhodium iodide or Rhpy_3I_3 in water/ethanol/pyridine mixtures were unsuccessful. However, when a stream of hydrogen⁽²³⁾ was used as catalyst on a cold reaction mixture, prolonged bubbling resulted in the dissolution of the solids and then crystallisation of golden-brown platelets of $\text{Rhpy}_4\text{I}_3 \cdot 3\text{H}_2\text{O}$. Synthesis of the perchlorate salt evidenced the presence of the $\text{Rhpy}_4\text{I}_2^+$ ion (Table 1.1a).

The complex is indeed relatively unstable in the absence of free pyridine, but also appears to hydrolyse in the sense



Although the hydrolysate has not been characterised, the reaction is a logical extension of the observations

(Chapter 3, Section 3), on the hydrolysis of its chloro- and bromo-analogues. The figures in Table 1.1a are reflective of the compound's relative instability.

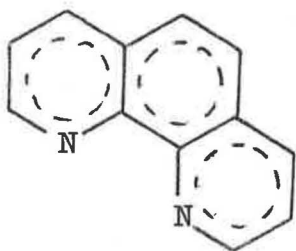
In continuation, it was later discovered that the reaction of Rhpy_3I_3 with pyridine under vigorous conditions (2:1:1 v/v py:H₂O:EtOH, added NaI, prolonged boiling) gave low yields of well-crystallised trans-diodotetrapyridinerhodium(III)iodide. The fate of the bulk of the rhodium remaining in the orange solution is unknown, but it is undoubtedly present as a pyridine complex; the basicity of the solution may well have forced the above hydrolysis reaction.

One now recalls the steric arguments advanced regarding the stability of the Rh-N bond, and realises that by implication, the Rh-I bond may also be destabilised. Poë and Vaidya⁽²⁴⁾ have proposed that ionic size may predominate among factors affecting the stability of much less "crowded" halide complexes.

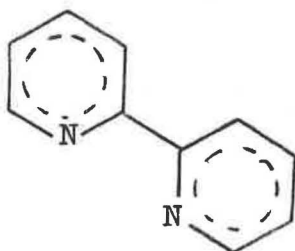
1.5 Other Heterocyclic Ligands

In order to investigate further the relationship between characteristics of the ligands and the structure

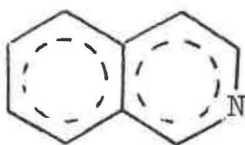
and reactivity of their complexes, the following heterocycles were used to complex with rhodium(III).



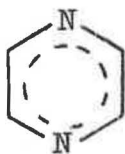
1:10-phenanthroline



2,2'-bipyridyl



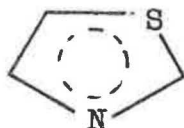
isoquinoline



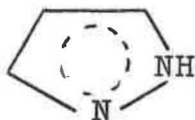
pyrazine



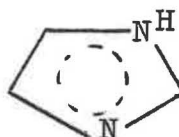
pyrimidine



thiazole



pyrazole



imidazole

cis[Rhphen₂Cl₂]⁺ and cis[Rhbipty₂Cl₂]⁺ are well known species⁽²⁵⁾, and this work confirms their preparation by the catalytic method.

As might be expected, iso quinoline, the steric restraint of quinoline removed, acts as a substituted pyridine, and yields cream crystals of trans-[Rhiquin₄Cl₂]Cl.3H₂O.

The presence of two heteroatoms in the monocyclics above introduced the possibility of polymerisation of the rhodium complexes via bridging ligands. Indeed, rhodium chloride even with a large excess (50:1) of pyrazine, yields a bright yellow crystalline substance, $\text{Rhpyz}_3\text{Cl}_3$. That this is not merely 1,2,6-trichlorotripyrazine-rhodium(III) is proved by its reflectance spectrum, which contains a band at 407 nm., indicative of the trans RhN_4Cl_2 chromophore. Also, it is insoluble in water, ethanol, acetone, chloroform, MeCN, MeNO₂, and strong HCl but soluble in boiling pyridine (or pyrazine) which suggest that it is polymeric and dissolves only in those reagents which can displace one function of a bidentate pyrazine.

Pyrimidine, on the other hand, on catalysed reaction with rhodium chloride, leads to an orange-yellow solution which required the addition of a large counter-ion (perchlorate) before a crystalline product was obtained. This is trans-dichlorotetrapyrimidinerhodium(III)perchlorate [$\text{Rhprm}_4\text{Cl}_2$] ClO_4 , as shown by its spectroscopic and analytical properties.

One deduces that the 1,3-dinitrogen arrangement in a six-membered planar ring is stereochemically unsuited for bidentacy, whereas the 1,4-configuration is suitable. Moreover, it seems likely that a heteroaromatic with a

heteroatom which is (a) capable of hydrogen bonding with water and (b) in the 3-position of the six-membered ring with respect to the Rh-N bond, will greatly solubilise the complex, and this is akin to the hydrophilic and lipophilic effects endowed by acetyl or alkyl respectively.

It is this same effect which prevented isolation of an imidazolrhodium complex. Even the perchlorate salt formed as an oily gum and was not investigated further.

Thiazole proved to be very similar to pyridine in its behaviour with rhodium(III)chloride. Reaction in the usual way produced a good yield of beautiful yellow glistening platelets, similar in appearance to $\text{Rhpy}_4\text{Cl}_3 \cdot 5\text{H}_2\text{O}$, but marginally less soluble in water. The reaction with RhBr_3 was less satisfactory, and gave a low yield of orange-yellow crystals which tend to crumble on drying. The remaining solution appeared from its electronic spectrum to contain mostly the trans- $\text{RhN}_4\text{Br}_2^+$ chromophore, but the addition of excess NaBr produced only a small amount of the bromide salt. The two compounds obtained are shown to be trans $[\text{Rhthz}_4\text{Cl}_2]\text{Cl} \cdot 5\text{H}_2\text{O}$ and trans $[\text{Rhthz}_4\text{Br}_2]\text{Br} \cdot 2\text{H}_2\text{O}$ by virtue of their analytic and spectroscopic properties.

Pyrazole, with RhBr_3 , similarly yielded only an orange-yellow solution, from which no crystalline material

was obtained; the preparation was not repeated. In contrast, after reaction with rhodium chloride, in the usual way, there was obtained a crop of bright orange-yellow prisms, again following the desired pattern of reaction in being trans[Rh₂Cl₂Cl₂]Cl.5H₂O; the formulation is supported by the analytical and spectroscopic results obtained.

Hence, in a five-membered ring, it is probable that the other ligands guard the 2-position against solvation to some extent, while the 3-position H-bonds with the solvent when possible. The >NH group in the 2-position does not interfere with the coordination behaviour.

In order to avoid the hydrophilic influence of the >NH group in imidazole, N-methylated ligand was reacted with rhodium bromide and chloride. The products are possibly the [Rh(Meim)₅X]²⁺ ions. Both have the electronic spectroscopic properties associated with the RhN₅X chromophores, and are 1:2 electrolytes as their perchlorate salts, but satisfactory analyses have not yet been obtained for [RhMeim₅X](ClO₄)₂. Their reactions are not EtOH catalysed.

1.6 Structure and Electronic Spectra

The d-d spectra of halogenoamminerhodium(III) species have been well documented^(10,26). Thus the trans-dihalo-tetraminerhodium(III) species such as $\text{trans}[\text{Rhen}_2\text{X}_2]^+$ give rise^(14,26) to absorption bands at 406 nm. (X = Cl), 425 nm. (X = Br) and 462 nm. (X = I) which are due to one (or both) of the components ${}^1\text{A}_{1g} \longrightarrow ({}^1\text{E}_g, {}^1\text{A}_{2g})$ of the d^6 Rh^{3+} ion in the tetragonal ligand field. The precise understanding of this phenomenon in rhodium(III) complexes does not yet seem to have been attained. On passing to the cis-diacidotetramine complexes, the ${}^1\text{T}_{1g}$ state recovers its degeneracy⁽²⁷⁾ and the band moves to higher energy, to a position similar in wavelength to the acidopentamine complex. The results in Table 1.2 for the heterocyclic base complexes are the best guide to their structures. The trans- Rhp_4X_2^+ (X = Cl, Br) ions have been studied before^(10,11,14,28) and the results are in good agreement with these. The chloro-complexes in the tables which have not been previously published all have λ 406-411 nm. and therefore have trans-stereochemistry. One notes that the trans- Rhp_4X_2^+ ions with X = Br, I, have their first d-d band at lower energy than their $\text{Rhen}_2\text{X}_2^+$ analogues (800 and ca. 1200 cm^{-1} respectively). This implies a lower ligand field in the heterocyclic base complexes, but one cannot distinguish between

Table 1.2

Electronic Spectra of Rhodium Pyridine Complexes

Compound	Characteristic d-d Band		Other Bands		Medium
	λ	ϵ	λ	ϵ	
[Rhp ₄ Cl ₂]Cl·5H ₂ O	410	78	a		MeOH
	410	77			H ₂ O
[Rhp ₄ Cl ₂]ClO ₄	410	77			MeCN
[Rhp ₄ BrCl]BF ₄	425	64	(480)	30	
[Rhp ₄ Br ₂]Br·5H ₂ O	441	118	323	185	
			(270)	16000	
			(261)	29000	
			257	31100	
			(220)	34000	
[Rhp ₄ Br ₂]ClO ₄	441	117			MeCN
[Rhp ₄ I ₂]I·3H ₂ O	(490)	460	400	12500	MeOH
			308	25000	
[Rhp ₄ I ₂]ClO ₄	(490)	440	402	11000	MeOH
			308	22000	
			267	14500	
			261	14500	
[Rhp ₄ Cl ₂]Cl·3H ₂ O	410	87			EtOH
[Rhp ₄ Cl ₂]ClO ₄	411	87			MeCN
[Rhp ₄ Cl ₂]BF ₄	411	90			CHCl ₃
[Rh(4Etpy) ₄ Cl ₂]ClO ₄	409	103			CHCl ₃
[Rh(3Clpy) ₄ Cl ₂]Cl·5H ₂ O	410	106	(282)	10000	CHCl ₃ /MeOH
			275	13100	
			269	12900	
[Rh(3Acpy) ₄ Cl ₂]ClO ₄	408	80	(300)	650	MeCN/MeOH
			(279)	7500	
			272	10400	
			266	10300	
			225	54000	

continued

Compound	Characteristic d-d Band		Other Bands		Medium
	λ	ϵ	λ	ϵ	
[Rh iquin ₄ Cl ₂]Cl·3H ₂ O	410	102	331 317 (304) (285) (278) (267) 234	3300 3000 2300 3200 5800 7100 ca 40000	MeOH
[Rhthz ₄ Cl ₂]Cl·5H ₂ O	409	89	232	41000	MeOH
[Rhthz ₄ Br ₂]Br·2H ₂ O	440	144	312 (262) 237 222	2200 22000 30000 30000	EtOH/H ₂ O
[Rhpzl ₄ Cl ₂]Cl·5H ₂ O	406	88	(265) ^b 216	3000 41000	MeOH
[Rhprm ₄ Cl ₂]ClO ₄	409	105			MeCN
[Rhpzn ₃ Cl ₂] _x Cl _x	407		(310) 257		Solid reflectance
[Rhphen ₂ I ₂]I·2H ₂ O	417	1400	354 (335) (325) (300) 273 223	4000 5200 6800 19500 55500 89000	MeOH/H ₂ O

a: see table 3.5 a.

b: broad absorption 300-350 nm.

reduction of the axial and reduction of the in-plane components of the ions' tetragonal fields. It does introduce the possibility that the steric effects discussed in 1.3 lead to increases in the metal-ligand bond distances in comparison with the $\text{Rhen}_2\text{X}_2^+$ ions, and this could lead to progressive lowering of the ligand field splitting, $10Dq$, since it depends inversely on the sixth power of the cation-dipole separation. On the other hand, the absorption spectra can be rationalised empirically without invoking this effect (Chapter 4).

Progressive lowering of the $\text{Rh} \leftarrow \text{X}^-$ charge transfer band energy is obvious in the di-iodide, where what is presumably the ligand field band at $485\text{-}495\text{ cm}^{-1}$ is partially obscured by the 400 nm. charge transfer band. Comparison of λ , ϵ values for a given complex ion with different solvents and anions show that these do not vary outside experimental limits.

The spectrum of the rhodium phenanthroline iodide complex is in accord with the formulation $\text{cis}[\text{Rhphen}_2\text{I}_2]\text{I}\cdot 2\text{H}_2\text{O}$; $\text{cis}[\text{Rhen}_2\text{I}_2]^+$ absorbs at 375 nm. while in the quartet $\text{cis}[\text{Rhen}_2\text{Cl}_2]^+$, $\text{cis}[\text{Rhen}_2\text{Br}_2]^+$, $\text{cis}[\text{Rhphen}_2\text{Cl}_2]^+$ and $\text{cis}[\text{Rhphen}_2\text{Br}_2]^+$ the phenanthroline complexes⁽²⁹⁾ absorb ca. 2500 cm^{-1} below their ethylenediamine⁽²⁶⁾ analogues, so $\text{cis}[\text{Rhphen}_2\text{I}_2]^+$ is expected to have a d-d band at ca. 415 nm.

One now finds parallel behaviour to that observed⁽²²⁾ for the replacement of chloride by bromide in the trans $[\text{RhL}_4\text{Cl}_2]^+$ complexes. Qualitative examination (visual and spectrophotometric) proves that the reaction



is catalysed by ethanol when L = alkylpyridine, acetylpyridine, pyrimidine, pyrazole, isoquinoline, or thiazole.

1.7(i) The Reaction of $\text{trans}[\text{Rh}(\text{thiazole})_4\text{Cl}_2]^+$ with Bromide

In the last case, the experiment was performed quantitatively. Firstly, by monitoring the absorbance at 310 nm., the reaction of a $5.65 \times 10^{-4}\text{M}$ solution of $\text{trans}[\text{Rhthz}_4\text{Cl}_2]\text{Cl} \cdot 5\text{H}_2\text{O}$ in 0.2M NaBr was followed at 82°C. The pseudo-first order plot of $\log(A_\infty - A_t)$ vs time which was obtained is depicted in Figure 1.2. A_∞ was then estimated of a $2.92 \times 10^{-4}\text{M}$ solution of $\text{trans}[\text{Rhthz}_4\text{Br}_2]\text{Br} \cdot 2\text{H}_2\text{O}$ at 310 nm. in 0.2M NaBr at 80°C. The fit of the points obtained to a straight line is not good, but quite adequate for the purposes of this discussion. The line has a slope of 4.7×10^{-6} , hence $k = 1.08 \times 10^{-5} \text{ s}^{-1}$, or the reaction has a half-life of $6.4 \times 10^4 \text{ s.} = 18 \text{ hours.}$ In contrast Fig. 1.3 depicts the plot of absorbance at

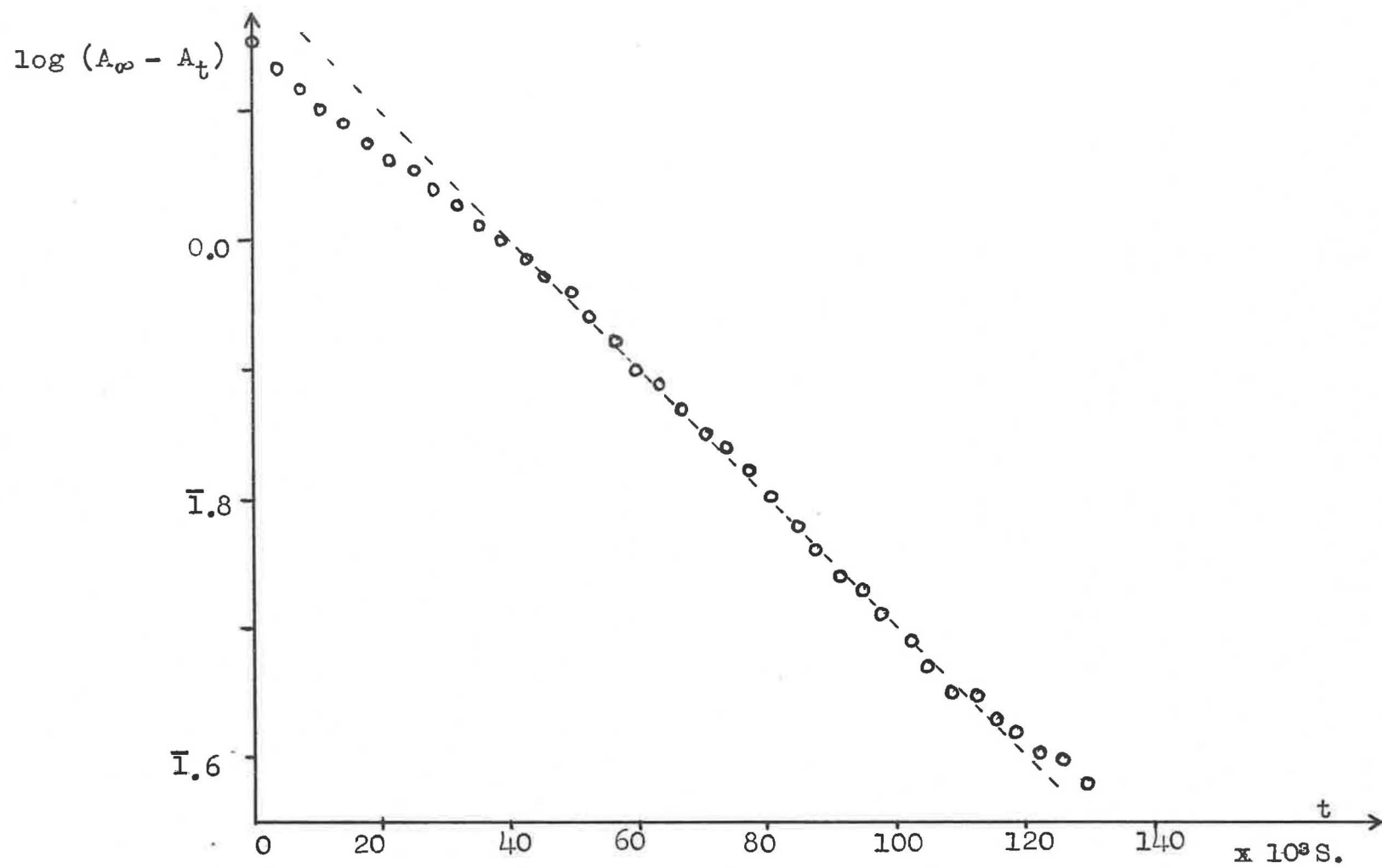


Fig. 1.2 Rate plot for halide exchange in thiazole complex

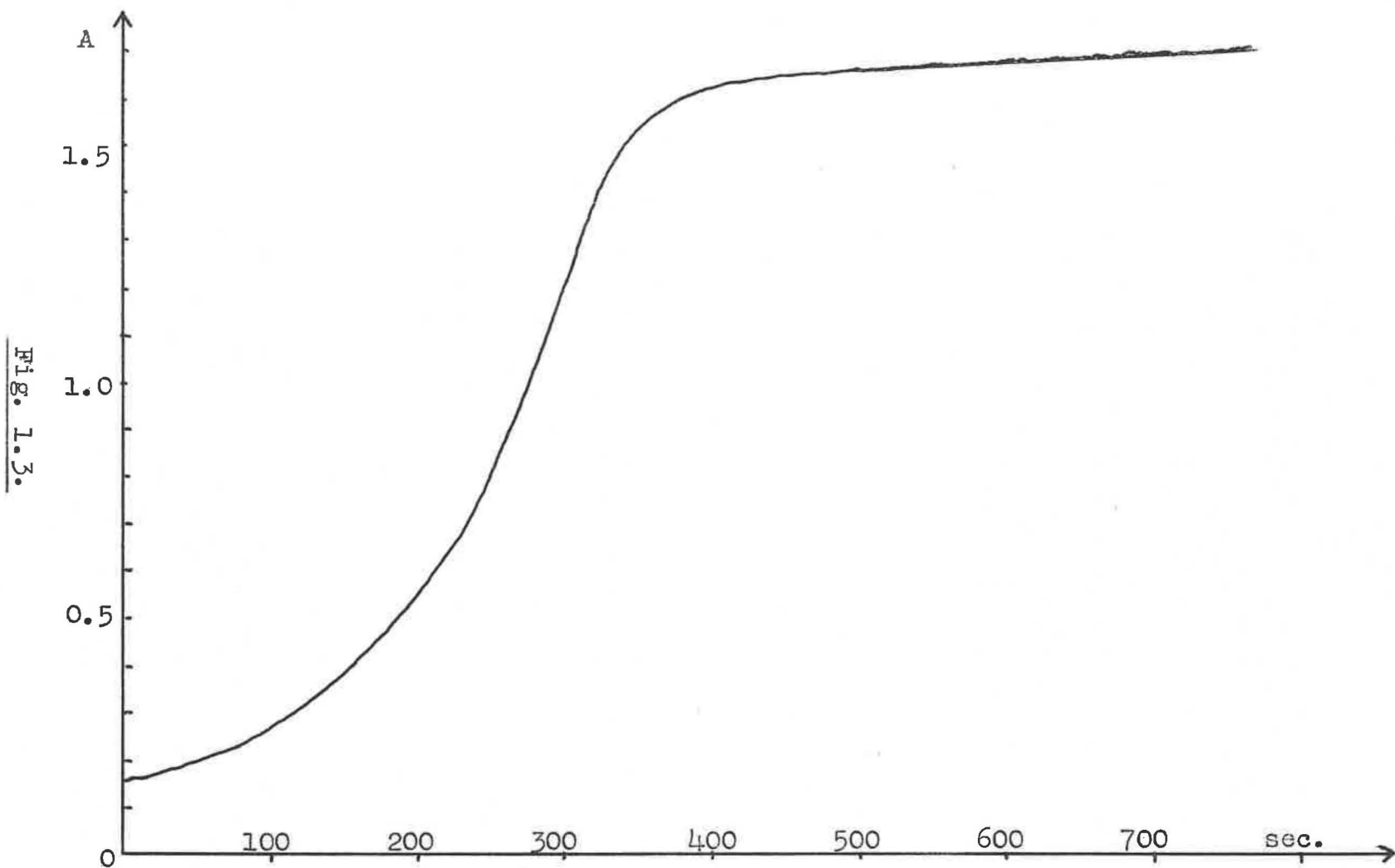


Fig. 1.3.

Absorbance vs time trace for EtOH catalysed reaction of $(\text{Rh thz}_4\text{Cl}_2)^+$ with Br^- .

320 nm. vs time when the same reaction is carried out in 30% v/v ethanol-water mixture. The reaction is complete within about seven minutes, but the absorbance continues to rise slightly, due to decomposition of the product, and after twelve minutes the solution is cloudy. The relatively slow initial rate reflects the induction period required for even the ethanol catalysed substitutions in the presence of oxygen, as in the case of the pyridine systems⁽²²⁾. Thus the rate is accelerated by a factor of ca. 500 through ethanol catalysis.

1.7(ii) Electronic effects arising within the heteroaromatic ligands are best discussed in terms of their pKa values⁽³⁰⁾ for the reaction



One sees from Table 1.3 that substituted pyridines have a fair span of pKa values; those listed are by no means the extremes. Quinoline and 2-methylpyridine bracket pyridine itself, so steric and not electronic factors are responsible for their complexes' instabilities. The extremely acid and basic pyridines have substituents in the 2-position and would not be very suitable for complex formation.

Table 1.3

Basicities of Nitrogenous Heterocycles

<u>Compound</u>	<u>pKa</u>
pyrazine	0.65
3-nitropyridine	0.81
pyrimidine	1.30
pyrazole	2.47
thiazole	2.53
3-chloropyridine	2.84
quinoline	4.80
pyridine	5.17
<u>isoquinoline</u>	5.40
3-methylpyridine	5.68
2-methylpyridine	5.97
4-methylpyridine	6.02
4-ethylpyridine	6.02
3,5-dimethylpyridine	6.15
4-methoxypyridine	6.62
imidazole	6.95
N-methylimidazole	7.33
ammonia	9.25

The failure of past (and present) workers⁽¹²⁾ to prepare the $[\text{Rhpy}_6]^{3+}$ ion has been attributed⁽¹⁰⁾ to the steric restraints involved in placing six ligands about the rhodium ion. Indeed, the problem is the same if one considers a cis $[\text{Rhpy}_4\text{X}_2]^+$ or $[\text{Rhpy}_5\text{X}]^{2+}$ species, in terms of "crowding" of the rings.

Recent claims for genuine hexapyridinmetal complexes are those based on the electronic spectra of some cobalt(II) species⁽³¹⁾ and, indisputably, the X-ray crystal structure of⁽³²⁾ the $[\text{FePy}_6][\text{Fe}_4(\text{CO})_{13}]$ complex salt. Dahl and Doedens found that the paramagnetic $[\text{FePy}_6]^{2+}$ has a regular octahedral array of pyridines (R-factor 0.12). The Fe-N bonds are longer (2.26\AA) than in $\text{Rhpy}_4\text{Cl}_2^+$ (2.09\AA). One might suggest that base strength and steric hindrance are the two competing factors which determine whether a rhodium(III) complex becomes $[\text{RhL}_5\text{X}]^{2+}$ or t- $[\text{RhL}_4\text{X}_2]^+$. Possibly, the use of a very basic 6-membered hetero-aromatic will lead to a pentakis complex. In the pyridine series, 4-methoxy-pyridine is one of the most basic without a 2-substituent, but may not be basic enough - 3,5-lutidine (pKa 6.15) only forms the tetrakis complex. That the Lewis acid behaviour of a metal ion toward a nitrogenous base is related to that same behaviour of a proton is demonstrated by recent studies⁽³³⁾ which showed the order of stability

toward first transition row ions as (cf. Table 1.3)

4-methylpyridine > 3-methylpyridine ~ pyridine

Among the bifunctional ligands, pyrazine is capable of donating to a second rhodium even though its first pKa is only 0.65 and hence its second pKa is probably negative as a result of the inductive effect of the rhodium. Nor does variation of pKa affect the ligand field contribution, but that is a reflection of the ionic part of the metal-ligand bond.

The non-catalysis of many complexes may therefore be due to the requirement of breaking a strong, covalent Rh-N bond, if the catalysis proceeds via the Rh^{I} route suggested⁽²²⁾. One notes that catalysis is effective up to a point in the synthesis of $[\text{RhA}_5\text{Cl}]^{2+}$, that the catalysed substrate in the synthesis is mainly a readily reduced (Chapter 3) chlororhodium complex. Addition of ammonia (pKa 9.25) to rhodium trichloride in warm aqueous ethanol gives a good yield of the above.

1.8 Solvates and Adducts

The ability of trans[Rhpy₄X₂]⁺ to crystallise with unusual anions has been well studied^(19,34) in the case of the hydrogen dinitrate salts [Rhpy₄X₂](HN₂O₆) (X = Cl, Br) one type of the so-called "acid adducts" of this complex. The salts may also include apparently cationic addends, such as the [H₅O₂]⁺ ion⁽³⁵⁾ in [Rhpy₄Br₂][H₅O₂]Br₂, while one may look upon the water of crystallisation as a neutral addend (or as an [X(H₂O)_n]⁻ ion).

The stabilisation of charged species by appropriate counter-ions has been discussed by Basolo⁽³⁶⁾, and the tribromide and triiodide salts of [Rhpy₄Br₂]⁺ have been characterised⁽¹¹⁾.

When an aqueous solution of Rhpy₄Cl₃ is shaken or allowed to stand under an atmosphere of chlorine, there are deposited cream, silky crystals. The infrared and Raman spectra (300-4000 cm⁻¹) show only bands associated with the trans[Rhpy₄Cl₂]⁺; there is no C-Cl bond stretching absorption, and the compound is anhydrous. It has the composition Rhpy₄Cl₅ (Table 1.4). A very similar compound is formed in the same way with trans Irpy₄Cl₃, analogous in composition. However, both have very strong i.r. absorption centred at ca. 220 cm⁻¹ and a remarkably strong Raman band at ca. 270 cm⁻¹. Evans and Lo⁽³⁷⁾

Table 1.4

Analytical Data for the Adducts

Compound	%C		%H		%N	
	f.	c.	f.	c.	f.	c.
[Rhpy ₄ Cl ₂]I ₃	27.6	27.6	2.0	2.3	6.1	6.4
[Rhpy ₄ Cl ₂]Cl ₃ a	40.4	40.3	3.4	3.4	9.7	9.4
[Rhpy ₄ Cl ₂][Br ₂ Cl]	34.0	35.0	3.0	3.0	8.0	8.2
[Rhpy ₄ Cl ₂]Br ₃	33.1	32.9	3.0	2.8	8.0	7.7
[Irpy ₄ Cl ₂]Cl ₃	35.0	35.0	3.6	3.0	8.5	8.2
[Rhpy ₄ Cl ₂]ClO ₄ .MeNO ₂	39.4	38.8	3.9	3.6	11.4	10.8
[Rhpy ₄ Cl ₂]ClO ₄ . <u>n</u> -PrNO ₂	38.9	40.7	4.0	4.0	11.4	10.3
[Rhpy ₄ Cl ₂]ClO ₄ .NC(CH ₂) ₄ CN	44.7	44.8	4.4	4.0	11.7	12.0

a: Cl, found 28.9, calculated 29.7%

b: calculated

f: found

characterised spectroscopically tetrakis (n-propyl) ammonium trichloride and showed it contained the $[\text{Cl}_3]^-$ ion, which had the spectroscopic properties of the above compounds, which are therefore formulated trans $[\text{Mpy}_4\text{Cl}_2]$ (Cl_3). Similarly, $[\text{Rhpy}_4\text{Cl}_2]\text{I}_3$ and $[\text{Rhpy}_4\text{Cl}_2]\text{Br}_3$ have been prepared, the latter by addition of bromine to the bromide salt in chloroform. The addition of Br_2 to a chloroform solution of Rhpy_4Cl_3 gave a bright orange compound with very strong vibrational bands at 183 cm^{-1} (i.r.) and 170 cm^{-1} (Raman). It is formulated as $[\text{Rhpy}_4\text{Cl}_2][\text{Br}_2\text{Cl}]$, but the analysis was 1% low in carbon.

The trans $[\text{Mpy}_4\text{X}_2]^+$ therefore seem to be the cations par excellence for the stabilisation of large uninegative anions. Thus the perchlorate, tetrafluoroborate, hexafluorophosphate, thiocyanate, tribromide, triiodide, trichloride [tetrachlorodipyridinerhodate] and dibromochlorate salts are all insoluble in water. The stabilisation aspect is recognised in that Chattaway and Hoyle⁽³⁸⁾ stated that Cl_3^- was stable only below 25° even in the presence of a large cation, while $[\text{Rhpy}_4\text{Cl}_2]\text{Cl}_3$, $[\text{Rhpy}_4\text{Cl}_2](\text{Br}_2\text{Cl})$ and $[\text{Rhpy}_4\text{Cl}_2]\text{Br}_3$ do not show any change in ~~enthalpy~~^{heat capacity} on differential thermal analysis until 260°C . $[\text{Rhpy}_4\text{Cl}_2]\text{Cl}_3$, $[\text{Irpy}_4\text{Cl}_2]\text{Cl}_3$ may be oven-dried at 120°C without loss of weight, but while wet, they lose chlorine as the equilibrium $\text{Cl}_3^- \rightleftharpoons \text{Cl}^- + \text{Cl}_2$ becomes effective,

presumably through preferential solvation of chloride.

When recrystallised from certain organic solvents, the perchlorate salts of $RhL_4X_2^+$ may retain solvent of crystallisation, even though they form as anhydrates from water.

The methyl cyanide solvate of $[Rhpy_4Cl_2]ClO_4$ forms as yellow, translucent rhombs, but rapidly loses solvent to the atmosphere and becomes opaque. Higher boiling solvents lead to more stable solvates. These have been analysed spectrophotometrically by measuring their absorbances in MeCN solution. The results are in Table 1.5 while analytical data for some very stable ones are in Table 1.4. The spectrophotometric method relies on the insensitivity of ϵ of the 410 nm. band to the environment, although the anion and solvent used have been held constant. An outline of the method is appended, whereby one obtains "n" in the formula $[RhL_4X_2]ClO_4(\text{solvent})_n$.

Thus $[Rhpy_4Cl_2]ClO_4$ forms hemisolvates with propionitrile and nitroethane, monosolvates with nitromethane, nitropropane (n and iso) and adiponitrile (1,4-dicyanobutane) and a much less stable disolvate with methyl cyanide. Isobutyronitrile appears to be too bulky or too paraffinic for inclusion, while benzonitrile is almost certainly too bulky.

Table 1.5

Compositions of Solvates $[\text{RhL}_4\text{X}_2]\text{ClO}_4 \cdot (\text{Sol})_n$

Substrate	Solvent	n
$[\text{Rhpy}_4\text{Cl}_2]\text{ClO}_4$	acetonitrile	2.2
"	propionitrile	0.56 a
"	<u>isobutyronitrile</u>	0
"	adiponitrile	0.98 b,c
"	benzonitrile	0
"	nitromethane	1, b,d
"	nitroethane	0.65, 0.57
"	1-nitropropane	1.02, b
"	2-nitropropane	0.94
$[\text{Rhpy}_4\text{Br}_2]\text{ClO}_4$	nitromethane	0.87
$[\text{Rhpic}_4\text{Cl}_2]\text{ClO}_4$	nitromethane	1.0, b

a: $\nu(\text{C}\equiv\text{N})$ 2250 (w) cm^{-1}

b: see Table 1.4

c: $\nu(\text{C}\equiv\text{N})$ 2245 (s) cm^{-1}

d: $\nu(\text{N}-\text{O})$ 1560 (s), 1377 (m) cm^{-1}

1.9 Vibrational Spectroscopic Studies

1.9(i) The Coordinated Ligand

Vibrational spectroscopy has proved a valuable characterisation method in this work, and an empirical approach to the subject often reveals useful information. However, the burgeoning of qualitative investigation in the "organic" field is an established phenomenon in the literature⁽³⁹⁾. On the other hand, the detailed mathematical analysis of a polyatomic system such as the Rhp_4X_2^+ ion is beyond the intent of this work, and has indeed recently been undertaken elsewhere⁽⁴⁰⁾. For these reasons, attention will be directed principally toward the localised metal/ligand chromophore and comment on the heterocyclic ring systems minimised. In Table 1.6 are set down the i.r. bands of free pyridine and the corresponding bands in a typical complex, $[\text{Rhp}_4\text{Cl}_2]\text{ClO}_4$, when there is a significant frequency shift concomitant with coordination.

Two comprehensive qualitative studies of coordinated pyridines have been published^(41,42), while the vibrational analyses of free pyridine^(43,44) and its deuteriates^(44,45) seem well understood, in the first order at least.

Gill et. al⁽⁴¹⁾ observed that the two lowest frequency infrared bands of free pyridine (ν_3, ν_{27})* actually

* Notation used is that of reference 44(b).

Table 1.6

Free py. ^a	Rhodium Complex	Assignment
405 w	455 m 465 m	ν_{27}, B_2 : out of plane ring puckering
605 m	650 m	ν_3, A_1 : ring breathing laterally
703 vs	684 s 694 vs 708 m	ν_{26}, B_2 : out of plane δ (C-H)
752 s	748 s 757 sh 763 vs 778 s	ν_{25}, B_2 : out of plane δ (C-H)
992 vs (Raman)	1024 vvs	ν_1, A_1 : totally symmetric ring breathing
1148 m	1160 s	ν_{16}, A_2 : ring skeleton stretching + ν (C-H)
1439 vs	1452 s	ν_{18}, A_2 : ring skeleton stretching + ν (C-H)
1583 s	1608 s	ν_4, A_1 : ($C_2(6)-C_3(5)$) + ν (C-H)
3083 m	3110 w	ν_{19}, A_2 : ν (C-H) mostly

a: references 44, 45

b: references 44 (notation), 43 (description).
Symmetry referred to is C_{2v} of pyridine

appear to increase in frequency on coordination, while Clark and Williams⁽⁴²⁾ concluded that the shifts were dependent on the stereochemistry of the complex and increased down a group in the periodic table, although increasing the ionic radius across a transition row decreased the frequencies. Firstly, the absorption at 450-470 cm^{-1} attributed to ν_{27} of pyridine, as well as the ν_3 band, increase as the charge on the complex increases, as well as suffering the previously observed mass increase effect. This is revealed by Table 1.7 which incorporates results from this work and one from Clark and Williams' paper. Thus ν_{27} falls at 422 cm^{-1} in trans-Copy₄Cl₂, but in trans-[Copy₄Cl₂](BF₄) two bands appear, at 460, 470 cm^{-1} ; while the absorption assignable as ν_3 is now found 25 cm^{-1} higher, at 650 cm^{-1} .

It has been noted⁽⁴²⁾ that splitting of some of the bands e.g. ν_{27} , occurs in the complexes, and as all the vibrations of pyridine are necessarily nondegenerate (the molecule is of symmetry C_{2v}, whose irreducible representations are A₁, A₂, B₁, B₂) this implies that some coupling of the pyridine rings occurs. This may result, in the solid state from one or both of two effects. Firstly, intermolecularly from the imposition of the unit cell symmetry on the set of ligand rings, secondly and more likely, in an intramolecular fashion, from coupling of vibrations

Table 1.7

Pyridine Ring Modes in Selected Compounds

Compound	Raman ν_1 (vs)	i.r. ν_3	i.r. ν_4 (s)	Raman ν_6 (m)	i.r. ν_{27}
pyridine ^a	992	605	1583	1030	405
(pyI)(ICl ₂)	1006	660 s ^b	1597 s ^b	1029	c ^b
t-Copy ₄ Cl ₂	1011	626 vs	1599	1039	422 s
t-[Copy ₄ Cl ₂](BF ₄)	c	644 sh 651	1607	c	467 s 478 s
t-Copy ₄ Br ₂	1012	624 s 627 vs	1598	ca1040	426 s
t-[Copy ₄ Br ₂]Br ₃	c	646 m 652 w	1605	c	468 m
t-[Rhp ₄ Cl ₂]ClO ₄	1023	650 m	1608	1049	455w 460 m
K[cRhp ₂ Cl ₄]H ₂ O	1023	647 w 650 s	1608	1052	458 s 474 s
t[Rhp ₄ I ₂]I.3H ₂ O	1024	662 w	1607	c	c
[Ptp ₄](BF ₄) ₂	1022	662 w	1608	1081	470 w 477 w
t[Ptp ₄ Cl ₂](BF ₄) ₂	1028	663 s	1610	1046	460 m

a: reference 44

b: reference 47

c: not observed; the result of absorption of the exciting line by the coloured compound in the Raman spectra.

across a single ion (molecule), especially for the lower frequency vibrations, wherein the metal atom may transmit the effect.

It might be expected that the latter intramolecular effect would result in larger splittings, merely as a result of the greater proximity of additional rings. Various of the fundamental vibrations of free pyridine are split when the molecule's symmetry is changed from C_{2v} to D_4 , as in trans Mpy_4X_2 with its angled pyridine ligands. For example a B_1 mode goes to $E_g + E_u$ in a D_{4h} molecule (all py rings parallel) which in D_4 then coalesce as $2E$, and these, now both i.r. active, may lose their degeneracy by coupling in or out of phase with other pyridine rings. Thus A type vibrations are unsplit, B types are split. Table 1.6 may support this thesis, but it is not inviolable.

The ring breathing mode, ν_1 , which is the strongest Raman band in uncoordinated pyridine, is shifted to higher frequency on coordination, when it is often the strongest Raman band observed in pyridine complexes (this work); e.g. in $Rhpy_4Cl_2^+$ it occurs 32 cm^{-1} higher. Providing this assignment is correct, and it does seem likely to be so, since the shift increases as the M-N bond strength increases, it is difficult to explain why

the ring mode frequencies are, in general, raised by coordination. Nyholm et.al.⁽⁴¹⁾ invoked $d\pi - p\pi$ interaction to account for the phenomenon, while Mathieu's group⁽⁴⁶⁾ suggested that it is merely a mass effect at the nitrogen atom, although the increment in ν_{27} effected by the oxidation of Co(II) to Co(III) does solicit an explanation involving some electronic effect. Furthermore the ring breathing mode ν_1 , is seen (Table 1.7) to increase as the charge on the acceptor increases (Figure 1.4) whereas if it were a mass effect on ν_1 , iodine, being lighter than only platinum, would show a higher ν_1 value than it in fact does. The best rationalisation of the frequency increase effects has been offered by Russian workers⁽⁴⁷⁾ who proposed (i) that increasing the s-character in an sp^n hybrid bond increases the bond strength, and (ii), that coordination increases the amount of s-character in the nitrogen sp^2 σ -orbitals. This implies reasonably that the donor σ -orbital on pyridine is predominantly p in character. Their explanation appears to have been misinterpreted by Mathieu and coworkers⁽⁴⁶⁾.

1.9(ii) Metal-Ligand Vibrations

The i.r. spectrum of trans[Rhpy₄Cl₂]Cl.5H₂O has been examined by previous workers^(42,46), in the region

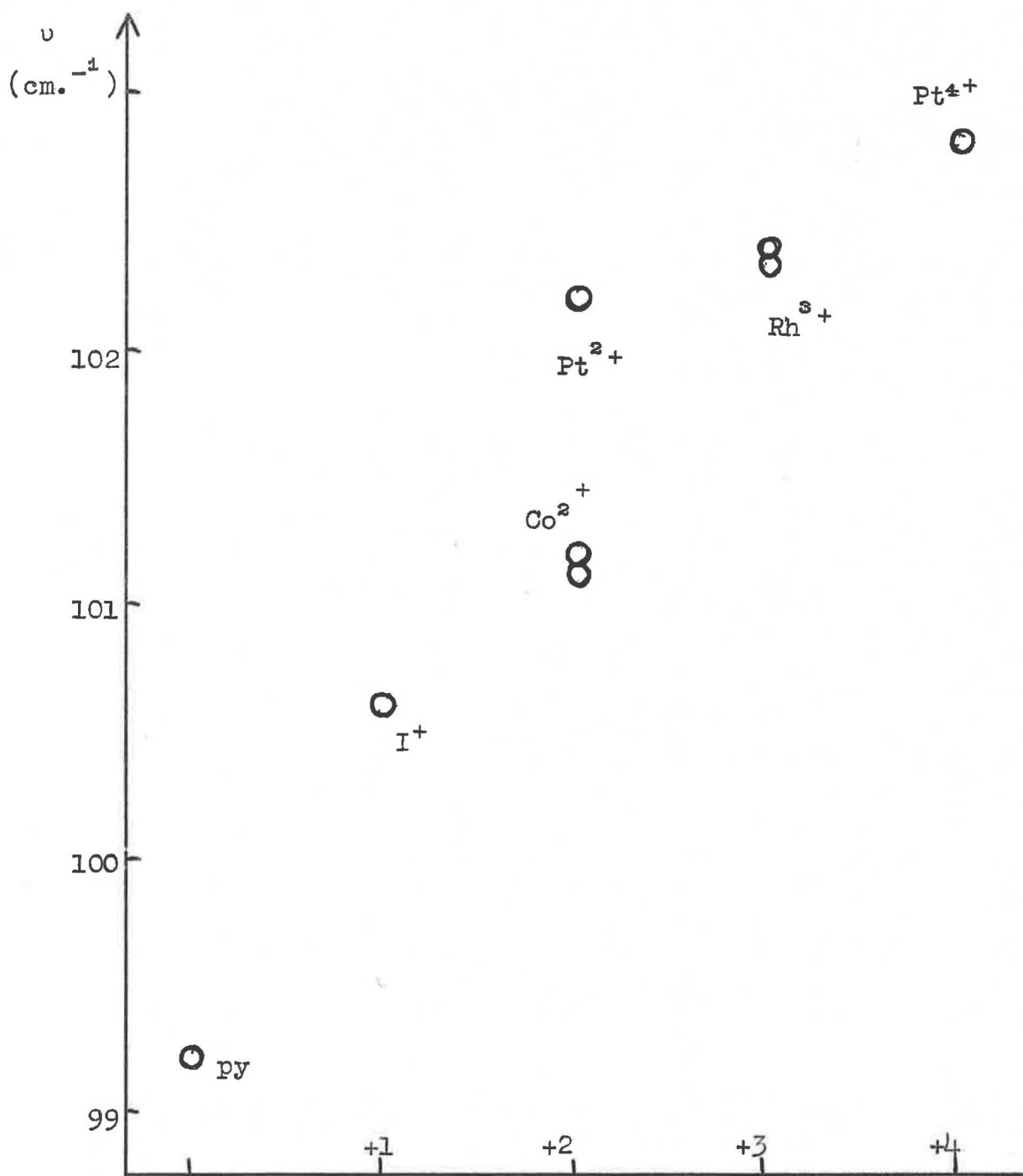


Fig. 1.4. The influence of acceptor charge on the pyridine ν_1 vibration frequency.

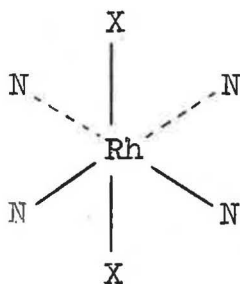
200-400 cm^{-1} , and assignments have been proposed for $\nu(\text{Rh-Cl})$ and $\nu(\text{Rh-N})$. Mathieu⁽⁴⁶⁾ found that the ratios of squares of the Raman band frequencies assignable as the symmetric Pt-N stretching modes in Ptpy_4^{2+} and PtA_4^{2+} were within 2% of the inverse ratios of the ligands' masses (79 and 17). Hence replacement of ammonia by pyridine could be expected to reduce the A_{1g} vibration of RhA_6^{3+} from 514⁽⁴⁸⁾ to ca. 240 cm^{-1} . This is the region (230-270 cm^{-1}) attributed to $\nu(\text{Rh-py})$ by Clark and Williams, whose assignments⁽⁴²⁾ of $\nu(\text{M-py})$ for a large range of metals have since formed the basis for the location of this vibration in the i.r.⁽⁴⁹⁾.

The location of $\nu(\text{M-Cl})$ is a lesser problem, as halogenometallate species such as $[\text{RhCl}_6]^{3-}$ are well known and have been investigated by i.r.⁽⁵⁰⁾, so that $\nu(\text{Rh-Cl})$ has been observed at 322 cm^{-1} in the above anion, for example.

Mathieu's above demonstration of the probability that increased ligand mass was the principal influence on the frequency of $\nu(\text{M-N})$ allows the proposition that the pyridine can be considered to act as a heavy "point" mass to the first approximation.

With this in mind, an assignment of metal-ligand vibrations in $\text{Rhpy}_4\text{X}_2^+$ might be rendered in terms of a

model of simple tetragonal (D_{4h}) symmetry, viz.



although the rigid interpretation requires that coupling with of internal ligand modes be included^(40,51). The choice of D_{4h} symmetry contains the simplification that the conformations of the heterocyclic rings are ignored; i.e. that the idealised symmetry is higher than the real symmetry of the cation (D_4) and this in turn is reduced by the properties of the unit cell in the solid state, so that $[\text{Rhpy}_4\text{Cl}_2]^+$ is at a site of C_2 symmetry in its hydrogen dinitrate salt⁽¹⁹⁾, for example.

The number, type and spectroscopic activity of the $\nu(\text{M-X})$ and $\nu(\text{M-L})$ modes expected for trans MN_4X_2 in D_{4h} are given in Table 1.8.

Table 1.8

<u>Type</u>	<u>$\nu(M-X)$</u>	<u>$\nu(M-L)$</u>	<u>Raman active</u>	<u>i.r. active</u>
A _{1g}	1	1	yes	no
B _{1g}	0	1	yes	no
A _{2u}	1	0	no	yes
E _u	0	1	no*	yes

* Active in D₄

The observed vibrational spectra are given in Table 1.9: $tRhpy_4Cl_2^+$ and $tPtpy_4Cl_2^+$ have been investigated previously^(42,46) by far i.r. spectrometry and the results given are in good agreement with those reported, 200-400 cm⁻¹. Raman spectra were unobtainable for the $trans[CoPy_4X_2]^+$ compounds as the result of absorption of the exciting line (6328 Å) by the compounds' d-d bands. The compounds $CoPy_4Cl_2$, $CoPy_4Br_2$ did not yield bands attributable to $\nu(Co-X)$; this may well be because increasing the ionicity of a bond decreases the Raman effect intensity, so that $\nu(Co(II)-X)$ is swamped out by the exciting line scattering at low wavenumber values. Unfortunately, without Raman data, the trivalent cobalt-nitrogen vibration cannot be assigned with absolute certainty.

Table 1.9

Low Frequency Vibrations in Ionic Heterocyclic Base -

Halide Complexes

(cm.⁻¹)

<u>Compound</u>	<u>Raman(ρ)</u>	<u>Infrared</u>	<u>Assignment</u>
[Copoly ₄ Cl ₂]Cl.5H ₂ O	a	385s 346s 242s 220w	A _{2u} , ν (Co-Cl) E _u , ν (Co-py)
Copoly ₄ Cl ₂	a,b	230s 217s	A _{2u} , ν (Co-Cl) E _u , ν (Co-py)
[Copoly ₄ Br ₂](Br ₃)	a	358w 342m 244m 183vs	E _u , ν (Co-py) A _{2u} , ν (Co-Br) and ν_3 (Br ₃)
[Rhpy ₄ Cl ₂]Cl.5H ₂ O	304vs(0.5) ^c 253m(0.9) 215s(0.65)	367s 314m 250s 178s	A _{2u} , ν (Rh-Cl) A _{1g} , ν (Rh-Cl) (Rh-py) A _{1g} , ν (Rh-py) δ (Rh-Cl)
[Rhpy ₄ Br ₂]Br.5H ₂ O	254m(0.9) 224m(0.3) 186vs(0.7) 93s	328m 311m 260w 194s 88	ν (Rh-py) A _{1g} , ν (Rh-py) A _{2u} , ν (Rh-Br) A _{1g} , ν (Rh-Br) δ (Rh-Br)
[Rhpy ₄ I ₂]I.3H ₂ O	131s ^d	311m 220w 155vs 78s	A _{2u} , ν (Rh-I) A _{1g} , ν (Rh-I) δ (Rh-I)
[Ptpy ₄]Cl ₂ .3H ₂ O	229m 210s	306m	A _{1g} , ν (Pt-py)

(a: too deeply coloured.)
(b: from reference 42.)

Table 1.9 continued

Table 1.9 (continued)

(c:Raman ρ from MeNO ₂ soln.)		d:in DMSO soln.)	
Compound	Raman(ρ)	Infrared	Assignment
[Ptpy ₄ Cl ₂](BF ₄) ₂	334vs	360vs	A _{2u} , ν (Pt-Cl)
	271m	270s	A _{1g} , ν (Pt-Cl)
	236s	242m	E _u ?, ν (Pt-py)
	214m	214w	B _{1g} , ν (Pt-py)
	136s	180m	A _{1g} , ν (Pt-py)
	102s		δ (Pt-Cl)
	85s		
[Ptpy ₄ Br ₂](BF ₄) ₂		304m	
		282m	
	269m	241s	ν (Pt-py)
	241s	214s	ν (Pt-py)
[Rh(thz) ₄ Cl ₂]Cl.5H ₂ O	198vs		A _{2u} , ν (Pt-Br)
			A _{1g} , ν (Pt-Br)
[Rh(thz) ₄ Cl ₂]Cl.5H ₂ O	307vs	375s	A _{2u} , ν (Rh-Cl)
	269m	325s	A _{1g} , ν (Rh-Cl)
		258s	B _{1g} , ν (Rh-thz)
		227m	E _u , ν (Rh-thz)
	207w		
[Rh(thz) ₄ Br ₂]Br.3H ₂ O		345s	
		324s	
		277m	
		246m	
		222w	
		185vs	A _{2u} , ν (Rh-Br)
[Rh(pz1) ₄ Cl ₂]Cl.3H ₂ O		400s	A _{2u} , ν (Rh-Cl)
		328s	
	307vs	262s	A _{1g} , ν (Rh-Cl)
	252m	253vs	ν (Rh-pz1)
		245s	
	222m	225m	
[Rhpy ₄ BrCl](BF ₄)	346w	346s	A ₁ , ν (Rh-Cl)
		312m	
	263vs	263s	
	212m	212m	
	191s		
	153m		A ₁ , ν (Rh-Br)

Raman spectroscopy enables two types of vibrational transition to be recognised readily, namely the two $\nu(M-X)$ and $\nu(M-L)$ of type A_1 or A_{1g} , as these totally symmetric modes give rise to Raman effect transitions which are, as a general rule, strongly polarised. That is, one expects that when the plane of polarisation of the incident (exciting) beam is perpendicular to that of the emitted beam, then the ratio of emitted intensity to that intensity observed with the two planes of polarisation parallel is less than $\frac{6}{7}$.

Thus the solution spectra of the trans[Rhpy₄X₂]⁺ ions (X = Cl, Br) exhibit this effect (Table 1.9) and the A_{1g} $\nu(Rh-py)$ band is deduced to be at $219 \pm 5 \text{ cm}^{-1}$. The highly symmetric metal-pyridine vibration frequency is ideally independent of the mass of the metal atom, and is a function only of the metal-nitrogen bonds' force constant. This is concluded from Wilson's treatment⁽⁵²⁾ of the normal frequencies of such an idealised square planar AB₄ system, giving $4\pi^2\nu^2 = K/M_b$, where K is the relevant stretching force constant and M_b is the mass of B. Indeed, this vibration alters but slightly in passing from platinum(II) to rhodium(III) to platinum(IV). The averages of the assignable values are 210, 219, and 239 cm^{-1} for these three central ions.

In general, the locating of $\nu(M\text{-py})$ is more difficult for the i.r. than for the Raman spectra. In the cobalt(III) compounds it will be the 242/244 cm^{-1} band, if the assignments suggested by previous workers are to be regarded as a guideline. This means that $\nu(\text{Co-N})$ has increased little from cobalt(II) to cobalt(III) (ca. 30 cm^{-1}). The 344 ± 2 cm^{-1} bands are in a region more akin with $\nu(\text{Co-Cl})$ which has been assigned at 353 cm^{-1} in the trans $[\text{CoA}_4\text{Cl}_2]^+$ ion⁽⁵³⁾. Inasmuch as there is already absorption at 385 cm^{-1} attributable thus, and the vibration only occurs in the dibromocobalt complex (342 cm^{-1}), it is more likely to be the analogue of the vibration leading to the absorption at 310-315 cm^{-1} in the rhodium pyridine complexes. Note that a similar absorption occurs at ca. 305 cm^{-1} in two of the platinum compounds, and it has been proposed⁽⁴⁰⁾ that these are combination bands. Hence the frequency decrease must be associated with the changes in the internal pyridine vibrations, incurred in passing from one metal to another.

In the rhodium and platinum compounds there occur some coincidences and near coincidences of Raman and i.r. bands: ca. 252 cm^{-1} in Rhpy_4Cl_3 ; 214 and 270 cm^{-1} in $[\text{Ptpy}_4\text{Cl}_2](\text{BF}_4)_2$; 241 cm^{-1} in $[\text{Ptpy}_4\text{Br}_2](\text{BF}_4)$; ca. 224 and 252 cm^{-1} in $\text{Rh}(\text{pzl})_4\text{Cl}_3$.

Now E_u , into the D_4 symmetry of the Mpy_4X_2 ion with its "propeller" of pyridines, as opposed to the D_{4h} symmetry of the local environment, MN_4X_2 , transforms as E, since the removal of the two mirror planes, and hence of the centre of symmetry, cause E_u and E_g to coalesce. Thus the mode now becomes Raman active as well although the i.r. activities are unaffected (Table 1.8), and the appearance of three Raman bands in $PtPy_4Cl_2^+$ in the region of $\nu(M-py)$ for example, may be rationalised as: $A_1 + B_1 + E$. Again though, the difficulty of differentiating between the B_{1g} and E_u modes arises for all the other species of type ML_4X_2 , as there are now only two Raman bands in this region, which implies that the coincidences observed cannot be explained as above. Therefore a distinction cannot be made between the B_{1g} and E_u vibrations. Assignment made on the basis of i.r. inactivity for B_{1g} seems unreliable, as the positions appear to vary from compound to compound. Although the $A_{1g} \nu(Rh-L)$ modes decrease in frequency as the ligands' masses increase (pyrazole, pyridine, thiazole), it is not possible to differentiate between mass effects and electronic effects on $\nu(Rh-L)$ within the small number of ligands used in the rhodium(III) complexes examined. Moreover, substituents on the pyridine ring tend to complicate the far i.r. spectra, while by no means all the compounds are suitable

for Raman spectroscopy.

Assignment of $\nu(\text{Rh-Cl})$, $\nu(\text{Rh-Br})$ is more readily accomplished. Thus, the A_{1g} vibration manifests itself as an intense, polarised Raman band at about 30-80 cm^{-1} below its A_{2u} i.r. counterpart in the chlorides. The lesser interval between the corresponding $\nu(\text{Rh-Br})$ (10-20 cm^{-1}) has been attributed⁽⁴⁰⁾ to interaction of the i.r. active mode with an internal ligand vibration, which is supported by a comparison with trans $[\text{Rhen}_2\text{Br}_2]^+$ which has $\nu(\text{Rh-Br})$ much higher (223 cm^{-1} , cf. 194 cm^{-1}) in the i.r.

If a gross approximation is made in that the XRHX portion of the ion is treated as a linear triatomic unit, then a SVFF calculation may be applied to obtain a crude estimate of the force constant involved in the Rh-X bond stretching. Herzberg^(55a) gives, for a linear MX_2 system

$$4 \pi^2 \nu_1^2 = \frac{a_{11} + a_{12}}{M_X}$$

and

$$4 \pi^2 \nu_2^2 = (a_{11} - a_{12}) \left(\frac{M_M + 2M_X}{M_M \cdot M_X} \right)$$

where a_{11} is the M-X bond's force constant, a_{12} is the interaction force constant for the two M-X bonds, M_M , M_X

are the masses of M and X, and ν_1, ν_3 are the frequencies of the vibrations of type Σ_g^+ and Σ_u^+ for a linear triatomic, and correspond to A_{1g} and A_{2u} in the MN_4X_2 model. The ν_2 is the bending mode which, here, would involve M-N stretching also.

Thus, observation of $\nu_1(304 \text{ cm}^{-1})$ and $\nu_3(367 \text{ cm}^{-1})$ for Rhp_4Cl_3 enables the above expressions to be solved as simultaneous equations in a_{11}, a_{12} , yielding $a_{11} = 1.81 \times 10^5 \text{ dyne cm}^{-1}$ and $a_{12} = 0.16 \times 10^5 \text{ dyne cm}^{-1}$ which are reasonable values for M-X force constants. The results for this naïve calculation performed on some other of the compounds of the Table 1.9 are shown in Table 1.10.

Table 1.10

Derived Force Constants (dyne $\text{cm}^{-1} \times 10^{-5}$)

<u>Compound</u>	<u>a_{11}</u>	<u>a_{12}</u>	<u>k</u>
Rhp_4Cl_3	1.81	0.16	2.16
Rhpz_4Cl_3	1.97	0.01	1.98
$\text{Rhthz}_4\text{Cl}_3$	1.85	0.12	2.15
Rhp_4Br_3	1.16	0.47	2.34
Rhp_4I_3	0.90	0.39	
$\text{Ptp}_4\text{Cl}_2(\text{BF}_4)_2$	2.16	0.18	2.60
$\text{Ptp}_4\text{Br}_2(\text{BF}_4)_2$	1.52	0.33	
$[\text{Ptp}_4]\text{Cl}_2$			2.06

The apparent increase in a_{12} in passing from chloride, through bromide to iodide is probably a reflection of the interaction between halide and heterocyclic ligands, classically an electronic effect, indicating that stretching one M-X bond makes it more difficult to simultaneously stretch the other, trans to it, so that the concomitant increase in the calculated k-values related to the metal-nitrogen bonds is not necessarily indicative of a genuine increase in the real k. The vibrational interaction between the halides and the nitrogenous ligands may even be a manifestation of the large size of the axial halides, as was pointed out in prior discussion. That is, that the stable configuration of ligands about the rhodium ion relies on cooperative nonbonding interactions between the ligands, and that gross motions, e.g. rotations, of the heterocyclics may effect the potential curve of a large axial substituent, such as I^- . Indeed, the lower the frequency of the $\nu(M-X)$ vibration, the more likely it is that it will be low enough for the aromatic ring torsion to follow it. This is invoked in addition to the interaction of the axial ligand vibrations with internal vibrations of the heterocyclic ligands, and can only be proposed on sufferance that the low energy vibrations have been essentially correctly assigned, i.e. that a band given as arising from $\nu(Rh-X)$ is indeed mostly (Rh-X).

Bounsall and Poë⁽⁵⁴⁾ have reported the i.r. spectra of trans[Rh₂Cl₂]⁺, and found ν (Rh-Cl) at 343 cm⁻¹, while for trans[Rh₂BrCl]⁺ that vibration's transition occurs at 343 or 333 cm⁻¹ and ν (Rh-Br) at 213 cm⁻¹. For trans[Rhpy₄BrCl]⁺, the RhN₄XY moiety's C_{4v} symmetry leads to the requirements of Table 1.11. One now expects each ν (Rh-X) to be both Raman and i.r. active, that is, ν (Rh-Cl) and ν (Rh-Br) should each appear in both types

Table 1.11

Vibrational Types and Activity in C_{4v}

<u>Type</u>	<u>ν(M-X)</u>	<u>ν(M-L)</u>	<u>Raman</u>	<u>Infrared</u>
A ₁	2	1	yes	yes
B ₁	0	1	yes	no
E	0	1	yes	yes

of spectra, while there should similarly be three bands arising from ν (Rh-py), one of which is Raman active only. The observed spectra show that ν (Rh-Cl) appears at 346cm⁻¹ while ν (Rh-Br) is at 191 cm⁻¹ in the Raman, but was not observed in the i.r. (here the limit of observation was 190 cm⁻¹). The reality or otherwise of the force constants a₁₁, set out in Table 1.10, may be tested by applying them to this cation. The relevant model is then a linear

triatomic of type XMY, in which the $\nu(M-X)$ and $\nu(M-Y)$ stretching vibrations of type Σ^+ correspond to the A_1 modes in the C_{4V} model. Herzberg^(18b) gives

$$4\pi^2(\nu_1^2 + \nu_3^2) = k_1 \left(\frac{1}{M_X} + \frac{1}{M_m} \right) + k_2 \left(\frac{1}{M_m} + \frac{1}{M_Y} \right)$$

$$\text{and } 16\pi^4 \nu_1^2 \nu_3^2 = \frac{M_X + M_Y + M_Z}{M_X \cdot M_Y \cdot M_Z} \cdot k_1 \cdot k_2$$

for the triatomic's Σ^+ modes.

Applying the prior determined values for the force constants (a_{11}) of the Rh-Cl and Rh-Br bonds means that $k_1 = 1.81 \times 10^5$ dyne cm^{-1} and $k_2 = 1.16 \times 10^5$ dyne cm^{-1} . The above equations may then be solved after combining, as a quadratic in ν_1^2 or ν_3^2 . The results are $\nu = 189 \text{ cm}^{-1}$ and 352 cm^{-1} . These values are remarkably close to those observed (191, 346 cm^{-1}), considering the simplicity of the model used. They imply that the shift down in frequency of the $\nu(\text{Rh-Cl})$ transition is the result of the increased mass of the trans bromide and of the lower force constant of the trans, Rh-Br, bond. These two factors both tend to decrease $\nu(\text{Rh-Cl})$, so there can be no conclusion made favouring the existence of a trans-influence of the bromide on the chloride in this

compound. The apparently independent nature of the trans halogen vibrations is a relevant point, to be brought to bear in Chapter 4. The result, if valid, means that the attribution of infrared frequency decreases in $\nu(\text{Rh-Cl})$ to the bond weakening influence of a trans-ligand should be performed cautiously, with the complementary use of Raman spectroscopy where possible. Thus the trans-influence sequence given by Shaw and Smithies⁽⁵⁶⁾ for some iridium(III) compounds,



is reasonable, but mass effects probably contribute to the sequence of $\nu(\text{Rh-Cl})$ frequencies found⁽⁵⁷⁾ found for the trans ligands $\text{Cl} > \text{Br} > \text{I}$, $\text{CO} < \text{CH}_3$, R_3P , $\text{R}_3\text{As} < \text{H}$ altering the trans influence sequence to:



while, on the basis of the final arbiter, X-ray diffraction studies, Mason and Towl⁽⁵⁸⁾ regard that the trans influence order for Rh^{III} is



References - Chapter 1

1. S.M. Jørgensen, J. prakt. Chem., 1883 27 478.
2. F.M. Jaeger, J.A. van Dijk, Z. anorg. Chem., 1936 227 319.
3. S.M. Jørgensen, J. prakt. Chem., 1891 44 50.
4. P.S. Cohen, Advan. Chem. Ser., 1967 62 8.
5. M. Delépine, Bull. Soc. Chim. France, 1929 45 235.
6. R.D. Gillard, G. Wilkinson, J. Chem. Soc., 1964 1224.
7. M. Delépine, Compt. rend., 1953 236 1713.
8. P. Poulenc, Ann. Chim. France, 1935 4 599.
9. H. Holtzclaw, J.P. Collman, J. Amer. Chem. Soc., 1958 80 2054.
10. C.K. Jørgensen, Acta Chem. Scand., 1957 11 151.
11. F.P. Dwyer, R.S. Nyholm, Proc. Roy. Soc. N.S.W., 1943, 76 275.
12. B.N. Figgis, R.D. Gillard, R.S. Nyholm, G. Wilkinson, J. Chem. Soc., 1964 5189.
13. R.D. Gillard, G. Wilkinson, J. Chem. Soc., 1963 3594.
14. R.D. Gillard, J.A. Osborn, G. Wilkinson, J. Chem. Soc., 1964 3168.
15. K. Thomas, J.A. Osborn, A.R. Powell, G. Wilkinson, J. Chem. Soc., 1968A 1801.
16. M. Delépine, Compt. rend., 1953 236 559.
17. C. Ouannès, Compt. rend., 1958 247 1202.
18. R.J. Bromfield, R.H. Dainty, R.D. Gillard, B.T. Heaton, Nature, 1969 223 735.
19. G.C. Dobinson, R. Mason, D.R. Russell, Chem. Comm., 1967 62.

20. H. Kwart, S. Alekman, J. Amer. Chem. Soc.,
1968 90 4482.
21. B.T. Heaton, unpublished work.
22. R.D. Gillard, B.T. Heaton, D.H. Vaughan, J. Chem. Soc.,
1969D 974.
23. R.D. Gillard, J.A. Osborn, P.B. Stockwell,
G. Wilkinson, Proc. Chem. Soc., 1964 284.
24. A.J. Poë, M.S. Vaidya, J. Chem. Soc., 1961 1203.
25. E.D. McKenzie, R.A. Plowman, J. Inorg. Nucl. Chem.,
1970 32 199.
26. F. Basolo, S.A. Johnson, Inorg. Chem., 1962 1 925.
27. C.R. Hare, "Spectroscopy and Structure of Metal
Chelate Compounds", Ed. K. Nakamoto, P.J. McCarthy,
Wiley-Interscience, New York 196 , pp. 100.
28. H.-H. Schmidtke, Z. phys. Chem. (Frankfurt),
1962 34 295.
29. R.D. Gillard, B.T. Heaton, J. Chem. Soc., 1969A 451.
30. A. Albert, in "Physical Methods in Heterocyclic
Chemistry", Ed. A.R. Katritzky, Vol. 1, Academic
Press, London, 1963, chapter 1.
31. W.C. Jones, W.E. Bull, J. Chem. Soc., 1968A 1849.
32. R.J. Doedens, L.F. Dahl, J. Amer. Chem. Soc.,
1966 88 4847.
33. D. Forster, K. Moedritzer, J.R. van Wazer,
Inorg. Chem., 1968 7 1138.
34. R.D. Gillard, R. Ugo, J. Chem. Soc., 1966A 549.
35. D. Dollimore, R.D. Gillard, E.D. McKenzie,
J. Chem. Soc., 1965 4479.
36. F. Basolo, Coord. Chem. Rev., 1968 3 213.
37. J.C. Evans, G. Y-S Lo, J. Chem. Phys., 1966 44 3638.

38. F.D. Chattaway, G. Hoyle, J. Chem. Soc., 1923 654.
39. Specialist Periodical Reports, Inorganic and Organometallic Spectra, Vol. I, Ed. N.N. Greenwood, The Chemical Society, 1968.
40. R.A. Davies, Ph.D. Thesis, 1970, University of Kent.
41. N.S. Gill, R.S. Nyholm, G.A. Barclay, I.I. Christie, P.J. Pauling, J. Inorg. Nucl. Chem., 1961 18 79.
42. R.J.H. Clark, C.S. Williams, Inorg. Chem., 1965 4 350.
43. C.H. Kline, J. Turkevich, J. Chem. Phys., 1944 12 300.
44. a. D.A. Long, E.L. Thomas, Trans. Faraday Soc., 1963 59 783.
b. F.S. Murfin, *ibid.*, pp.12.
45. E. Castellucci, G. Sbrana, F.D. Verderame, J. Chem. Phys., 1969 51 3762.
46. F. Herbelin, J.D. Herbelin, J.-P. Mathieu, H. Poulet, Spectrochim. Acta., 1966 22 1515.
47. V. Filimonov, D. Bystrov, Optics and Spectroscopy, 1962 12 31.
48. W.P. Griffith, J. Chem. Soc., 1966A 899.
49. J.R. Durig, D.W. Wertz, Appl. Spectrosc., 1968 22 627.
50. D.M. Adams, "Metal-Ligand and Related Vibrations", E. Arnold, London 1967, Ch. 2.
51. I.R. Beattie, M. Milne, M. Webster, H.E. Blayden, P.J. Jones, R.C.C. Killean, J.L. Lawrence, J. Chem. Soc., 1969A 482.
52. E.B. Wilson, J. Chem. Phys., 1935 3 59.
53. T. Shimanouchi, I. Nakagawa, Spectrochim. Acta, 1962 18 89.
54. E.J. Bounsall, A.J. Poë, J. Chem. Soc., 1966A 286.
55. G. Herzberg, "Molecular Spectra and Molecular Structure", Vol. II, D. Van Nostrand Co., Princeton, N.J., 1945. (a) pp.154, (b) pp.173.

56. B.L. Shaw, A.C. Smithies, J. Chem. Soc., 1968A 2784.
57. M.A. Bennett, R.J.H. Clark, D.L. Milner, Inorg. Chem.,
1967 6 1647.
58. R. Mason, A.D.C. Towl, J. Chem. Soc., 1970A 1601.

CHAPTER 2

Superoxide Complexes of Rhodium

2.1 Initial Observations

When mother liquors from the catalytic preparation⁽¹⁾ of the salts of the type $\text{trans}[\text{RhL}_4\text{X}_2]\text{X} \cdot n\text{H}_2\text{O}$, or slightly basic solutions of these salts containing a mild reductant are exposed to oxygen, the pale yellow solutions may become green over a period ranging from a few hours to several days. This colour change is associated with the growth of an absorption band in the region of 600 nm. in the electronic spectrum. Pure compounds with absorption in this region are generally blue in colour, so that it appeared likely that the green colour was the result of the presence of a blue compound in the otherwise yellow solutions. Indeed, attempts to separate the "green" substance from solutions containing $[\text{t-Rhpy}_4\text{Cl}_2]^+$ by addition of anions such as ClO_4^- , BF_4^- , SiF_6^{2-} , or large cations such as NEt_4^+ were unsuccessful, the anions causing the simultaneous precipitation of the $\text{trans}[\text{Rhpy}_4\text{Cl}_2]^+$ salt in a mixture, the properties of which were identical to those of the pure $[\text{Rhpy}_4\text{Cl}_2]^+$ salt, apart from the slight difference in the electronic spectrum.

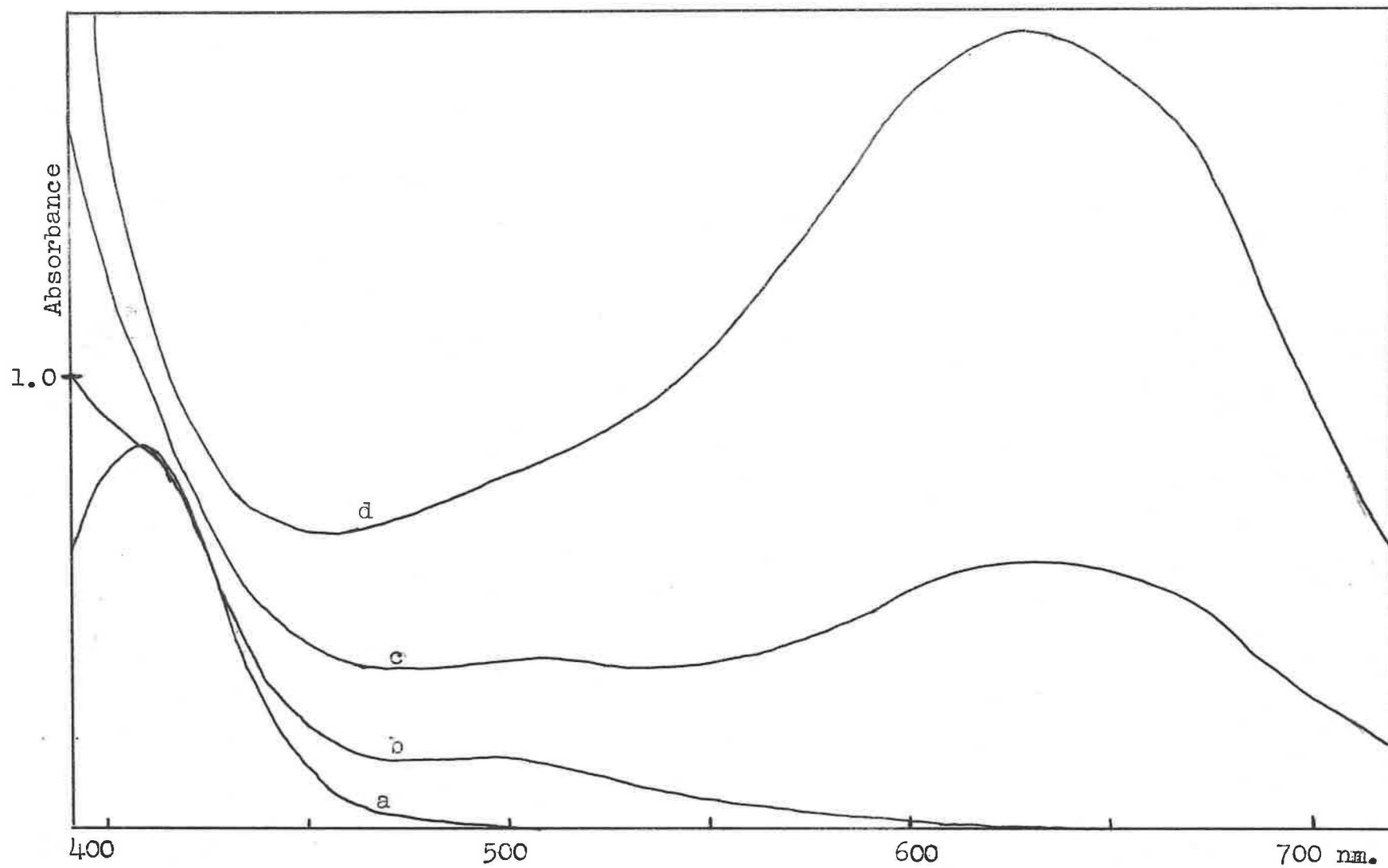


Fig. 2.1 Effect of ozonisation on the electronic spectrum of $\text{trans-Rhpy}_4\text{Cl}_3$ in alkaline aqueous ethanol.

2.2 Preparation of Compounds

On an attempt to increase the yield of the blue/green substance, O_2 was passed through a solution of $Rhpy_4Cl_3 \cdot 5H_2O$ in aqueous ethanol containing a small amount of base, but this procedure was ineffective. However, when the oxygen was replaced by a stream of 10% ozone in oxygen, there resulted a series of dramatic colour changes which are reflected by the series of visible spectra in Figure 2.1. The originally yellow solution (curve a) became orange in colour as strong UV absorption shifted toward the red, and a comparatively weak band appeared at 490-500 nm. (curve b). As ozonisation was continued the solution became brown as a band arose at ca. 620 nm. (curve c), and after 15 minutes, blue, as the 620 nm. band continued to grow (curve d) and dominate the visible spectrum, the intensity of colour increasing as passage of gas continued.

Difficulty was encountered in obtaining a pure product to investigate, because of the similarity of the properties of the products and starting materials. Before it was realised that hydrolysis of coordinated halide occurred to varying degrees, preparations of the blue chloro-complexes were contaminated by the corresponding diaquo (and presumably chloroaquo) species, or their hydroxo analogues if the precipitating medium was not acidic. Microscopic

examination suggested that cocrystallisation occurs within these very similar compounds as perchlorate salts as individual crystallites varied greatly in nature from blue plates to deep purple rhombs, while analytical data varied from sample to sample. Separation of the aquo- and chloro- complexes could be achieved by a solvent extraction procedure. The problem was better overcome by treating the crude products with HCl, to anate the aquo-complexes. Yields and purity were subsequently improved by using complexes of 4-methylpyridine instead of pyridine. In both cases, the blue compounds differed from the $[\text{RhL}_4\text{Cl}_2]^+$ salts by the latter's relative insolubility in 8-10M HCl.

2.3 Characterisation

That perchlorate, tetrafluoroborate and hexafluorophosphate were more effectively precipitating counter-ions than hexafluorosilicate (impure products) and much more so than sulphate and dithionate suggested that the blue cations carried an odd charge.

Analytical results (Table 2.1) for the blue picoline tetrafluoroborate salt (E), indicate that rhodium, heterocyclic ligands and chloride ligands are in the ratio 2:8:2

2.1

C		H		Cl		N		Other		a
f.	c.	f.	c.	f.	c.	f.	c.	f.	c.	Λ
34.7	34.7	3.6	4.1	12.3	12.8	7.9	8.1			218
39.7	40.0	3.0	3.3	6.3	5.9	9.2	9.3			192
41.6	41.5	4.4	4.4	12.9	12.8	7.8	8.1			193
44.4	44.7	4.6	4.7	10.6	11.0	8.5	8.7			154
43.4	43.8	4.6	4.3	5.4	5.4	8.6		Rh 15.3 15.7 F 16.7 17.3		210
31.7	31.8	3.7	3.3			7.4	7.5			-
32.5	32.4	3.3	3.2			6.6	6.3			184

a: in $\text{cm}^2\text{ohm}^{-1}\text{mole}^{-1}$ at 10^{-3}M in MeNO_2

c: calculated percentage

f: found percentage

and analyses of the perchlorates (A,C) show heterocyclic base to total chloride ratios of 8:5. Hence the complexes have ions of the type $[\text{Rh}_2\text{L}_8\text{Cl}_2\text{Y}]^{3+}$ where Y is a bridging ligand, or they have a metal-metal bond.

In aqueous solution they behave as oxidants toward iodide and iron(II) which cause fading of the blue colour. They do not reduce acidic hexanitratocerate(IV) ($E^\circ = +1.61\text{v}$) or permanganate ($E^\circ = +1.51\text{v}$). Indeed, titration with iron(II) sulphate in acid solution (Figure 2.2) shows that the blue colour is discharged after addition of one equivalent of iron(II) per two rhodium atoms. In addition, the blue colour may be restored quantitatively by cerium(IV) or chlorine. These facts rule out dirhodium(II,II) which would be a two electron reductant⁽³⁾ and also dirhodium(IV,IV) which would be a two electron oxidant. This leaves the mixed valence state dimer with Rh(III), Rh(IV), and Y dinegative (O_2^{2-} or O^{2-}); or the species which, taking the preparative method into consideration is most likely, i.e. two rhodium(III) centres with Y a superoxo bridge. Of the three, the μ -oxo formulation does not well satisfy the analytical data, while molecular models

Unless otherwise stated, all E° values are from Reference 2, and E values are calculated on the basis of these E° 's.

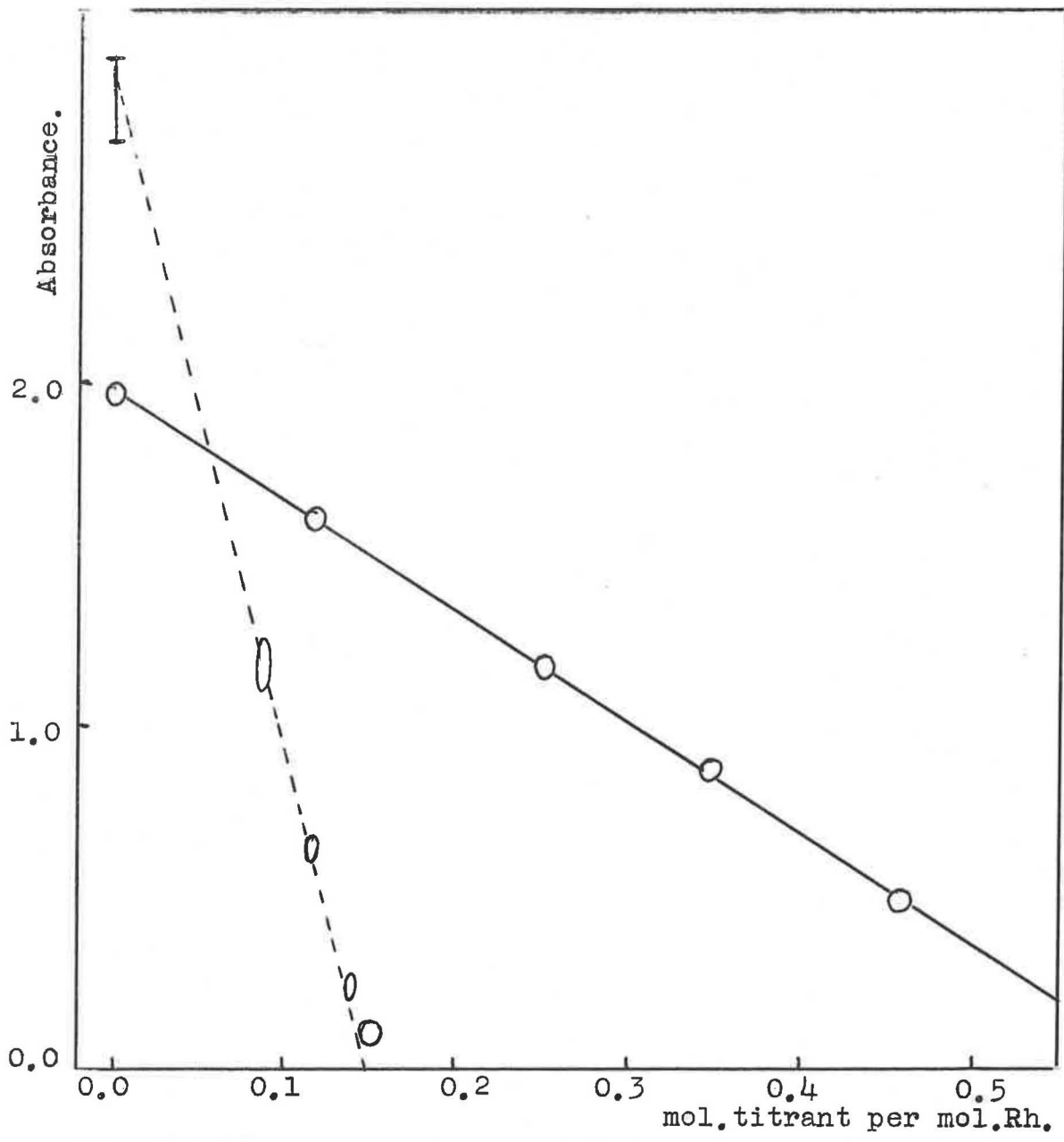


Figure 2.2 : Spectrophotometric titration of blue rhodium picoline/superoxide complexes; (—) with iron(II), (---) with thiosulphate.

indicate that the heterocyclic rings would lead to a sterically very crowded species even if the expected bent RhORh bridge were to become linear⁽⁴⁾. Moreover, known "mixed valence" μ -oxo species can be formulated as containing a symmetrical distribution of integral valence states. For example, the autoxidation product of V(II) can be written⁽⁵⁾ $[\text{V}^{\text{III}}\text{O}\cdot\text{V}^{\text{III}}]^{4+}$ while the same applies to more familiar species such as the "pyro"-oxy anions, $[\text{Cr}_2\text{O}_7]^{2-}$, $[\text{Mo}_2\text{O}_7]^{2-}$, $[\text{V}_2\text{O}_7]^{4-}$, and species such as^(6,7) $[\text{Re}_2\text{OBr}_{10}]^{4-}$, $[\text{Ru}_2\text{OBr}_{10}]^{4-}$, $[\text{Os}_2\text{OCl}_{10}]^{4-}$, $[\text{Zr}_2\text{OCl}_{10}]^{4-}$.

2.4 Magnetic Properties

Following this, the nature of the rhodium species is best described through comparison with the corresponding dioxygen bridged cobalt(III) dimers. Werner proposed⁽⁸⁾ that the green paramagnetic cobalt complexes contained the $[\text{Co}^{\text{III}}\text{O}_2^{\cdot-}\cdot\text{Co}^{\text{IV}}]$ moiety, and Malatesta⁽⁹⁾ pointed out that the two cobalt ions could be electronically equivalent through resonance. His electromers included the μ -superoxo-dicobalt(III,III) configuration first touched on but not adhered to, by Gleu and Rehm⁽¹⁰⁾; later being resurrected by Dunitz and Orgel⁽⁴⁾.

Table

Magnetic Properties of

Compound	ESR g(av.)	Medium	Reference
O_2^-	2.020	Pyridine	23
NaO_2	2.058	Solid	24
HO_2	2.016	H_2O	25
$K_5 [Co_2 (CN)_{10} O_2] \cdot H_2O$	2.019	Powder	15
$[Co_2 A_8 (NH_2)_2]^{4+}$	2.034	H_2O	15
$[Co_2 A_{10} O_2] (NO_3)_5$	2.025	H_2O	15
$[Co_2 A_{10} O_2] (NO_3)_5$	2.025	9M H_2SO_4	This work
$Co(acacen)py(O_2)$	2.026	Toluene, -74°	26
$[Rh_2 py_8 Cl_2 O_2] (ClO_4)_3 \cdot 8H_2O$	2.019	9M H_2SO_4	This work
$[Rh_2 pic_8 Cl_2 O_2] (BF_4)_3$	2.019	{ 9M H_2SO_4 Acetone Nitromethane	This work
$[Rh_2 pic_8 Cl_2 O_2] (ClO_4)_3 \cdot 2H_2O$	-	-	-
$[Rhpy_4 Cl_2] (ClO_4)$	-	-	-

Selected Superoxides

$10^6 \chi_g$	$10^6 \chi_m$	Magnetochemical		Reference
		$\mu(\text{B.M.})$	Medium	
-	-	-	-	-
33.0	1815	2.07	Solid	27
-	-	-	-	-
	1180	1.87	Solid	28 ^b
	1320	1.93	Sulphate, 18°	9 ^a
	1390	1.98	18°	9 ^a
-	-	-	-	-
3.40	1330	1.89	25°	29
0.320 ± 0.04	440 ± 60	1.67 ± 0.05	MeNO_2 , 33°	This work
0.357 ± 0.015	469 ± 20	1.64 ± 0.02	same	This work
0.263 ± 0.019	365 ± 25	1.63 ± 0.02	same	This work
-0.484	-285	0	22°	This work

a: The μ_{eff} results of Malatesta⁽⁹⁾ appear to be in error. The quoted χ_A values are less than the χ_m values implying that he had added rather than subtracted the (negative) diamagnetic corrections. The results (μ_{eff}) above are recalculated from his χ_m result.

b: Value of χ_m for monohydrate deduced from value for pentahydrate.

Electron spin resonance studies on the paramagnetic ammine^(11,12) amine^(13,14) and cyano⁽¹⁵⁾ complexes of cobalt led to the conclusion^(16,17) that the odd electron was shared equally between the cobalt atoms; the 15-line

fine structure resulting from the interaction of the electron with two ⁵⁹Co nuclei ($I = 7/2$), was observed, and agrees with the predicted number $2([I_1 + I_2] + \frac{1}{2}) = 15$.

The ESR spectrum of $[\text{Co}_2(\text{A})_{10}\text{O}_2](\text{NO}_3)_5$ is shown in Figure 2.3. The definitive crystallographic work of Marsh, Schaefer and co-workers^(18,19,20,21) proved the presence of the superoxide bridge in ammine and ethylenediamine complexes, where the O-O distances (Table 2.6) of ca. 1.32 Å are similar to those in ionic O_2^- , at ca. 1.29 Å⁽²²⁾.

The magnetic and ESR properties of the rhodium compounds are collected in Table 2.2. The ESR spectra (Figures 2.4, 2.5) are single line derivative curves, which show no fine structure under the conditions of the experiments, i.e. room temperature, in acetone or 50% H_2SO_4 . Although the ¹⁰³Rh (100% abundance) nucleus has a spin of $\frac{1}{2}$, the nuclear magnetic moment⁽³⁰⁾ is probably too small (-0.0879 nuclear magnetons) to cause observable splitting; cf. +4.6388 nuclear magnetons for ⁵⁹Co.

Quantitatively, the paramagnetism of the rhodium complexes corresponds to the doublet ground state expected

for the superoxo dimers. The susceptibilities were determined by Evans' NMR method⁽³¹⁾ using nitromethane as solvent (and references), at 33°C, the temperature of the probe. Errors quoted are estimated in relation to the accuracy with which the methyl resonance shifts (of MeNO₂) and the densities of the solutions were determined, these being the main sources of error in the calculation of χ_g from the data. The calculation is outlined in the appendix.

The ESR spectra unfortunately do not contain definitive information but are consistent with the superoxide formulation. The hyperfine coupling constants (A_{Co}), have been used previously⁽¹⁵⁾ to deduce relative spin densities at the metal centres in the cobalt complexes. The g values were found to parallel A_{Co} so that a small departure of g from the free electron value of 2.0023 could be indicative of a tendency for localisation of the odd electron on the O₂⁻ bridge. If this contention can be carried over into the rhodium amine complexes, then it implies that the amount of delocalisation over the metal ions is less than in the cobalt amines,

2.5 Redox Properties of the Compounds

The most obvious features of the superoxides are their colour and oxidising ability. The latter should be susceptible to polarographic examination, so the behaviour of the picoline superoxide and peroxide complexes (C,D) and the pyridine superoxide complex (A) of rhodium (all perchlorate salts) was investigated using the dropping mercury electrode.

Firstly, comparison of the currents observed at 0.0v* for the (picoline) μ -peroxide and μ -superoxide revealed that the latter was being reduced at $E < 0.0v.$, as there was a current generated significantly greater than the diffusion current of the KNO_3 used as supporting electrolyte. This is expected for a compound which is a strong oxidant; it means effectively that the μ -superoxide is capable of oxidising the (uncharged) metallic mercury. The same effect was observed⁽³²⁾ in the polarogram of the μ -superoxide $[Co_2en_4(NH_2)O_2]^{4+}$, but it should not be inferred⁽³³⁾ that the redox interconversion's potential is related to that value (Table 2.3).

*
All polarographic results quoted are relative to a saturated calomel electrode.

Table 2.3

Polarographic Properties of Superoxides

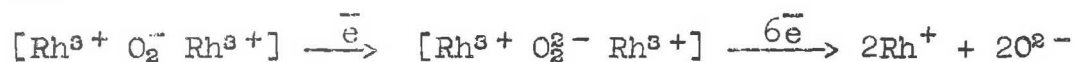
Species	$E_{\frac{1}{2}}$ (SCE)	Rel.n.	Medium	Reference
O_2^-	-2	1	Pyridine	35
$Co(salen)py(O_2)$	-0.6	1	Pyridine	36
$[Co_2(CN)_{10}O_2]^{5-}$	-0.12	1	Water	28
	-1.55	6	Water	28
$[Co_2 en_4 (NH_2)O_2]^{4+}$	0 a	1	Water	32
	-0.64	4	Water	32
$[Rh_2 py_8 Cl_2 O_2]^{3+}$	0 a	1	Water	b
	-0.58	6-7	Water	b
$[Rh_2 pic_8 Cl_2 O_2]^{3+}$	0 a	1	Water	b
	-0.79	6	Water	b
$[Rh_2 pic_8 Cl_2 O_2]^{2+}$	-0.79	6	Water	b, c

a: not a genuine wave, but non-zero current at 0.0v.

b: this work

c: pH 10.5; n relative to preceding compound

Secondly, in none of the three cases was a reduction wave observed in the region 0.0 to -0.5v., where most of the pyridine and substituted pyridine complexes of rhodium as yet studied exhibit a distinct two-electron reduction wave (Section 3.4). Such behaviour is strikingly similar to that of the dicobalt(III) μ -(su)peroxo compounds. After the one-electron reduction of superoxide to peroxide, the cobalt dimers are robust toward reduction in a region where monomeric complexes with similar (i.e. amine, oxygenous) ligands undergo the Co(III) \rightarrow Co(II) reduction⁽³⁴⁾, but at a more negative potential simultaneous reduction of both cobalt(III) and peroxide occurs, yielding a large wave. For example⁽³²⁾, $[\text{Co}_2\text{en}_4(\text{NH}_2)_2\text{O}_2]^{4+/3+}$ has a 4-electron reduction wave at $E_{1/2} = -0.64\text{v.}$ The polarographic results for the rhodium compounds (Table 2.3) confirm that qualitatively they are similar in behaviour to the cobalt complexes. The polarograms of the picoline compounds enable an estimate to be made of the relative numbers of electrons involved in the reduction. The picoline complexes incur a current increase at the -0.79v. wave which is six times the current involved in the continuous reduction from 0.0v., so the results are in excellent agreement with the sequence



The relative change in current observed for the pyridine compound is less satisfactory, but of the expected order, although it is not clear why the values for the second wave should differ as much as they do for the two types of ligand involved (ca. 0.2v.). It is noteworthy that the ratio of currents obtained for the pyridine and picoline superoxide compounds respectively is about 2.4:1, which all other factors being equal, implies that the pyridine compound diffuses much more rapidly than the picoline analog, which is not surprising in view of the number of hydrophobic methyl addends on the latter.

The superoxide compounds of rhodium and cobalt are, from the results in Table 2.3, reduced by mercury, and E° for the cobalt ammine superoxides has been estimated⁽²⁸⁾ at ca. +1v.

The rhodium picoline/superoxide in slightly acidic solution is correspondingly reduced to the μ -peroxo complex by tin(II) ($E^{\circ} = +0.15v.$), thiosulphate ($E^{\circ} = +0.08v.$) hexacyanoferrate(II) ($E^{\circ} = +0.36v.$), iodide ($E^{\circ} = 0.536v.$) and iron(II) ($E^{\circ} = +0.771v.$). It is readily reduced by sodium nitrite in neutral solution ($E \sim 0.43v.$) but reluctantly in NH_2SO_4 where the nitrite, as HNO_2 , can act as both reductant and oxidant, as can NO and N_2O_4 ; ($0.80v < E < 1.29v.$). The (kinetic) stability toward

peroxide ($E^{\circ} = 0.682\text{v.}$) and sulphurous acid ($E^{\circ} = 0.17\text{v.}$) may result from noncomplementarity with these two-electron reductants although it oxidises (sodium) sulphite ($E^{\circ} = -0.93\text{v.}$). Reduction by thiosulphate was poorly effective in very acid solution, but was found to be fast in methanolic solution. Spectrophotometric titration of a 10^{-3}M solution of $[\text{Rh}_2\text{pic}_3\text{Cl}_2\text{O}_2](\text{ClO}_4)_3 \cdot 2\text{H}_2\text{O}$ in methanol with aqueous 0.0050M sodium thiosulphate (Figure 2.2) resulted in the consumption of one mole of thiosulphate for every four moles of complex. It is unlikely that the equivalent weight of ca. 2300, calculated on the basis of thiosulphate being a two-electron reductant is the correct result for the complex. More probably, the half-reaction;

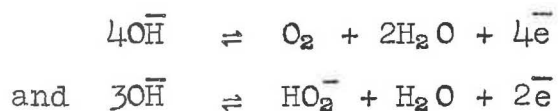


occurred, and indeed the solution after titration was acidic (pH ca. 3) and had the sulphurous odour characteristic of SO_2 .

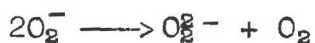
The μ -peroxide may be reoxidised quantitatively to the μ -superoxide by cerium(IV) ($E^{\circ} = +1.61\text{v.}$) or chlorine ($E^{\circ} = +1.36\text{v.}$). The superoxide does not oxidise bromide to bromine ($E^{\circ} = +1.07\text{v.}$) but bromine added to the peroxide produces a green precipitate, which is probably the Br_3^- salt of the superoxide. Finally, the μ -peroxo complex is reoxidised by μ -superoxodecamminedicobalt(III,III).

Therefore one may estimate that the one electron reduction of the superoxide corresponds to $+0.8v. < E^{\circ'} < +1.05v.$

The μ -peroxide was prepared both by iron(II) reduction and by base reduction of the superoxide. The latter follows the observation that hydroxyl ion causes fading of the blue colour, this being associated with the strong absorption band ca. 600 nm. The oxidation of hydroxyl may lead ultimately to peroxide or oxygen; the reduction half equations



have E° 's of +0.40v., +0.88v. respectively, so O_2 or H_2O_2 are possible products. However, no gas evolution was observed in any of the reactions with hydroxide, nor could peroxide be detected as a product, using the luminol-haemin reagent (see below). A control solution containing an amount of H_2O_2 equivalent to that expected as reaction product gave a very strongly positive result. The same difficulty has been encountered in the reduction of $[\text{Co}_2\text{en}_4(\text{NH}_2)\text{O}_2]^{4+}$ by OH^- . That the reaction is not a base catalysed disproportionation



is proved by the recovery (85%, 87% in two experiments) of the superoxide by acidification and reoxidation. This also shows that the $\text{O}\bar{\text{H}}$ reduction indeed gives the dimeric μ -peroxide, as it is unlikely that effective redimerisation would occur in the 10^{-4}M solution.

2-Aminophthalhydrazone ("luminol") in basic solution reacts⁽³⁷⁾ with peroxide. The organic oxidation product then luminesces strongly at ca. 440 nm. Haemin acts as a catalyst by producing hydroxyl radical from the peroxide, the radical being the reactive species. $[\text{Co}_2(\text{A})_{10}\text{O}_2]^{5+}$, $[\text{Rh}_2\text{py}_3\text{Cl}_2\text{O}_2]^{3+}$ and $[\text{Rh}_2\text{pic}_3\text{Cl}_2\text{O}_2]^{3+}$ (Figure 2.6) all react with the luminol-haemin reagent, giving strong emission at 438 nm. Moreover, $[\text{Rh}_2\text{L}_3\text{Cl}_2\text{O}_2]^{3+}$ rapidly oxidises luminol without⁽³⁸⁾ haemin present, suggesting that the compound initially gives hydroxyl radical:



This radical is known to attack a variety of substrates, with first order rate constants⁽³⁹⁾ of ca. $10^8 \text{ mole}^{-1}\text{sec}^{-1}$. Hence the ultimate product of the reaction is possibly an hydroxylated ligand. The μ -peroxide is less than 1% as reactive toward luminol/haemin as the superoxide, but is apparently still active, and this property is reminiscent of the cyanocobalt compounds' behaviour, where acid

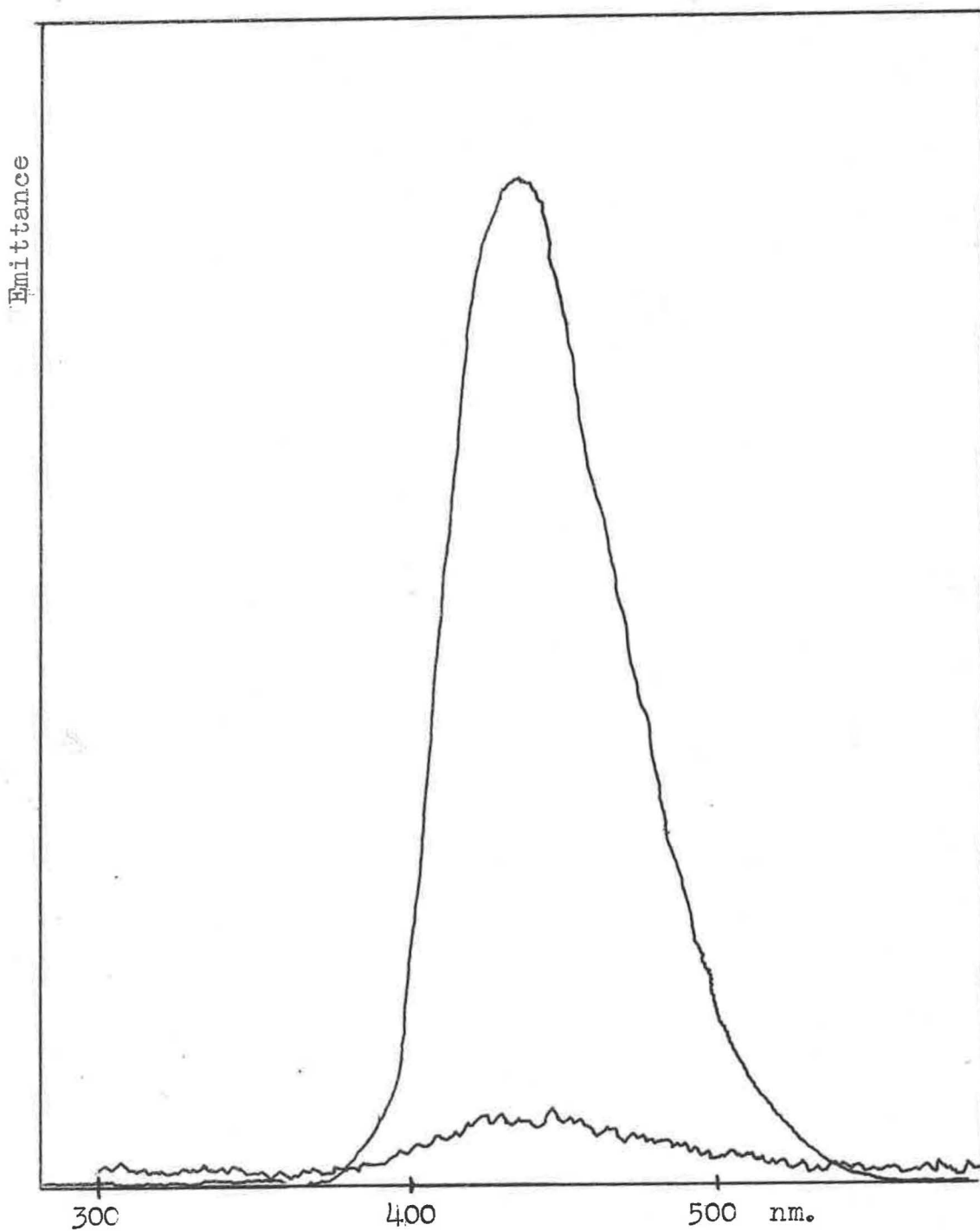
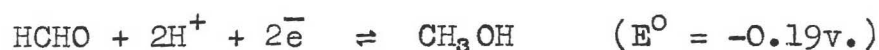


Fig. 2.6 Emission spectra from reaction of dimers with luminol-haemin: upper curve is picoline/superoxide C, lower is the peroxide D, at ca. 3 times the sensitivity of the instrument.

hydrolysis is required to free the bound peroxide⁽³⁸⁾.

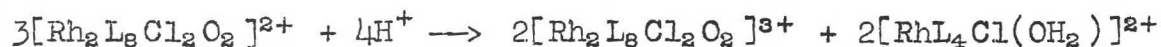
The reduction by base is more effective if aqueous methanol is used as solvent and it is noteworthy that the medium has increased reducing power⁽⁴⁰⁾



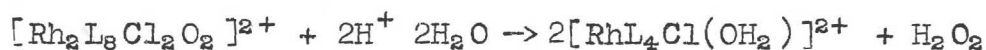
has $E = -0.19\text{v.}$ at pH 12.

The μ -peroxide is stable for several hours in aqueous alkali at room temperature, while in sulphuric acid solution, superoxide is regenerated slowly but only partially.

Iron(II) sulphate was added to an acidic solution (10^{-4}M) of the μ -superoxide to reduce it partially and then the sample was divided into two, oxygen was bubbled through one half, nitrogen through the other. 15% of the reduced superoxide was regenerated in both cases, suggesting that the process involves disproportionation;



rather than aerial oxidation, involving $\text{O}_2 + 2\text{H}^+ + 2\text{e}^- \rightleftharpoons \text{H}_2\text{O}_2$, say; and that hydrolysis;



is a competitive reaction, as the regain is much less than the possible 67%. In acidic solution, the μ -peroxide did

not reduce H_2O_2 ($E^\circ = +1.78\text{v.}$), and the iron salts present catalysed the decomposition of the added H_2O_2 . The redox disproportionation has been observed previously⁽⁴²⁾ for the $[\text{Co}_2(\text{NH}_2)_4\text{O}_2]^{3+}$ peroxide ion. An important difference between the rhodium and cobalt μ -peroxides is, that for fission reactions of the type⁽⁴³⁾;



the equilibrium lies well to the left for rhodium systems, as rhodium(II) is a strong reductant.

2.6.(i) Spectroscopy and Reactivity

Vlček⁽³⁴⁾ has demonstrated the correlation between (polarographically determined) redox potentials and spectroscopic properties of transition metals - a quantification of the rule-of-thumb that a coloured substance is a reactive one. The metal redox aspect is discussed further in Chapter 3, Section 4.

At present, the paucity of results available does not allow any real conclusion to be drawn regarding superoxides. However, it is clear that in the few cases where both the redox property and the electronic spectrum have been measured, a correlation exists. For the cases in

Table 2.4

Redox Property: Spectroscopic Correlations

System	Ox. power (v.)	ν_1 (kK)	References
O_2^- (Pyridine)	<u>ca</u> -2v.	22.6	23,35
$[Co_2(CN)_{10}O_2]^{5-}$	+0.25	20.6	15,28
$[Rh_2pic_3Cl_2O_2]^{3+}$	+0.9	16.4	This work
$[Co_2(A)_{10}O_2]^{5+}$	+1.0	15.0	28,44 This work

Table 2.4, oxidising power decreases as the energy of the first transition increases, although one should not neglect the fact that the ionic charge is increasing in the order
 $\text{Co/CN} < \text{Co/NH}_2\text{R} < \text{Rh}$.

2.6.(ii) Spectroscopy and Structure

Absorption in the red end of the visible spectrum is a characteristic feature of superoxide complexes⁽⁴⁴⁾. The source of this absorption has been the cause of some disagreement in the literature. Linhard and Weigel⁽⁴⁵⁾ first attributed the 670 nm. band in the $[\text{Co}_2\text{A}_{10}\text{O}_2]^{5+}$ ion to a typical cobalt(III) crystal field transition, and Barrett⁽⁴⁶⁾ has recently revised this assignment, interpreting the lowest energy bands in $[\text{Co}_2(\text{A})_{10}\text{O}_2]^{5+}$ and $[\text{Co}_2(\text{CN})_{10}\text{O}_2]^{5-}$ as crystal field bands arising from cobalt(III) in C_{4v} symmetry. This assignment is not tenable, and is discussed below and compared with other more likely assignments.

The first spin allowed transition of low spin cobalt(III) in an octahedral environment is the ${}^1\text{A}_{1g} \rightarrow {}^1\text{T}_{1g}$ band, as shown by Figure 2.7. Reduction of the local symmetry from O_h to C_{4v} by replacement of an ammonia in the hexammine, say, by an oxygenous ligand, causes the ${}^1\text{T}_{1g}$

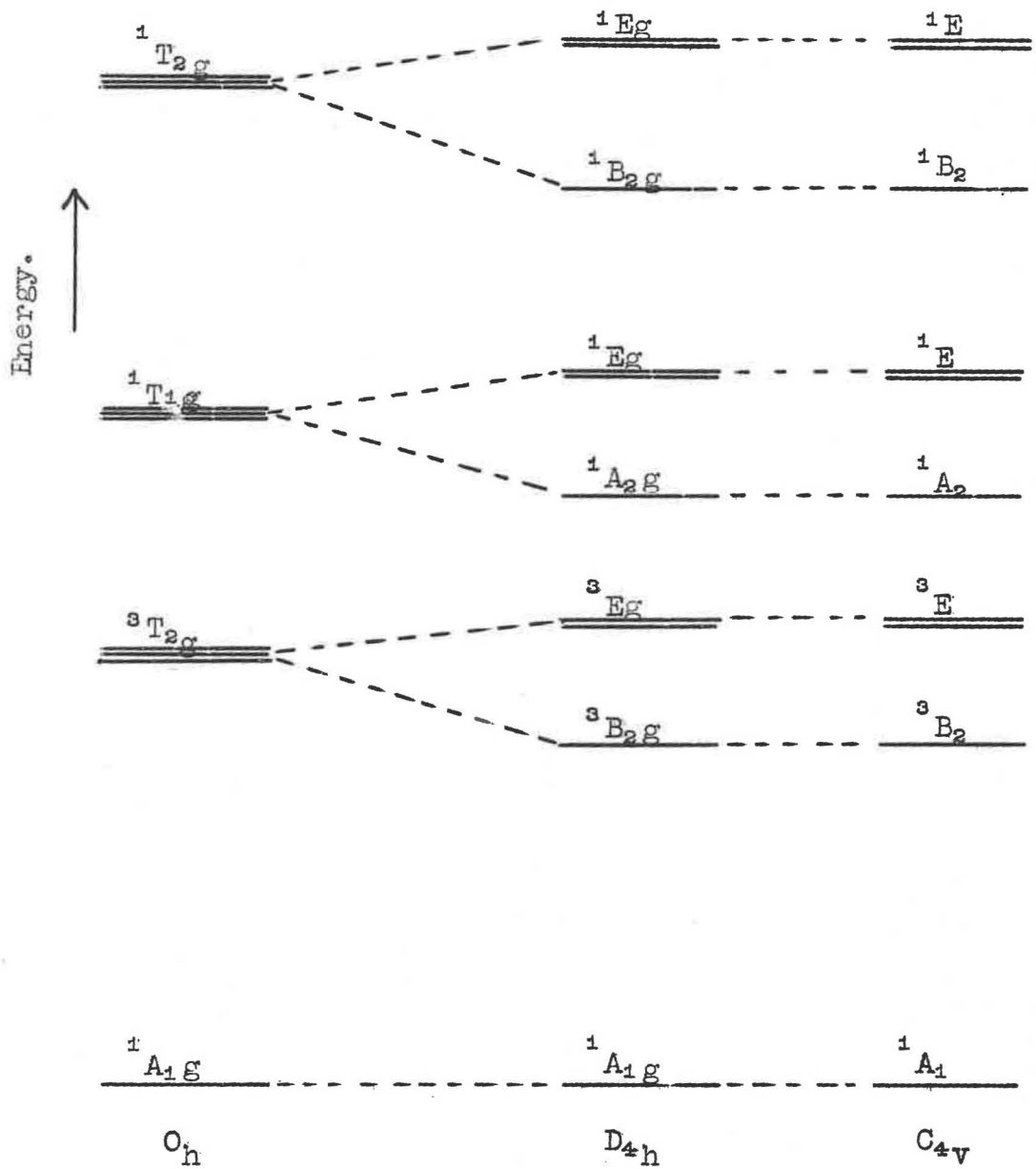


Fig. 2.7 The effect of decreasing the symmetry of a spin-paired d^6 ion (decreasing the axial crystal field) on some of its lower lying excited states.

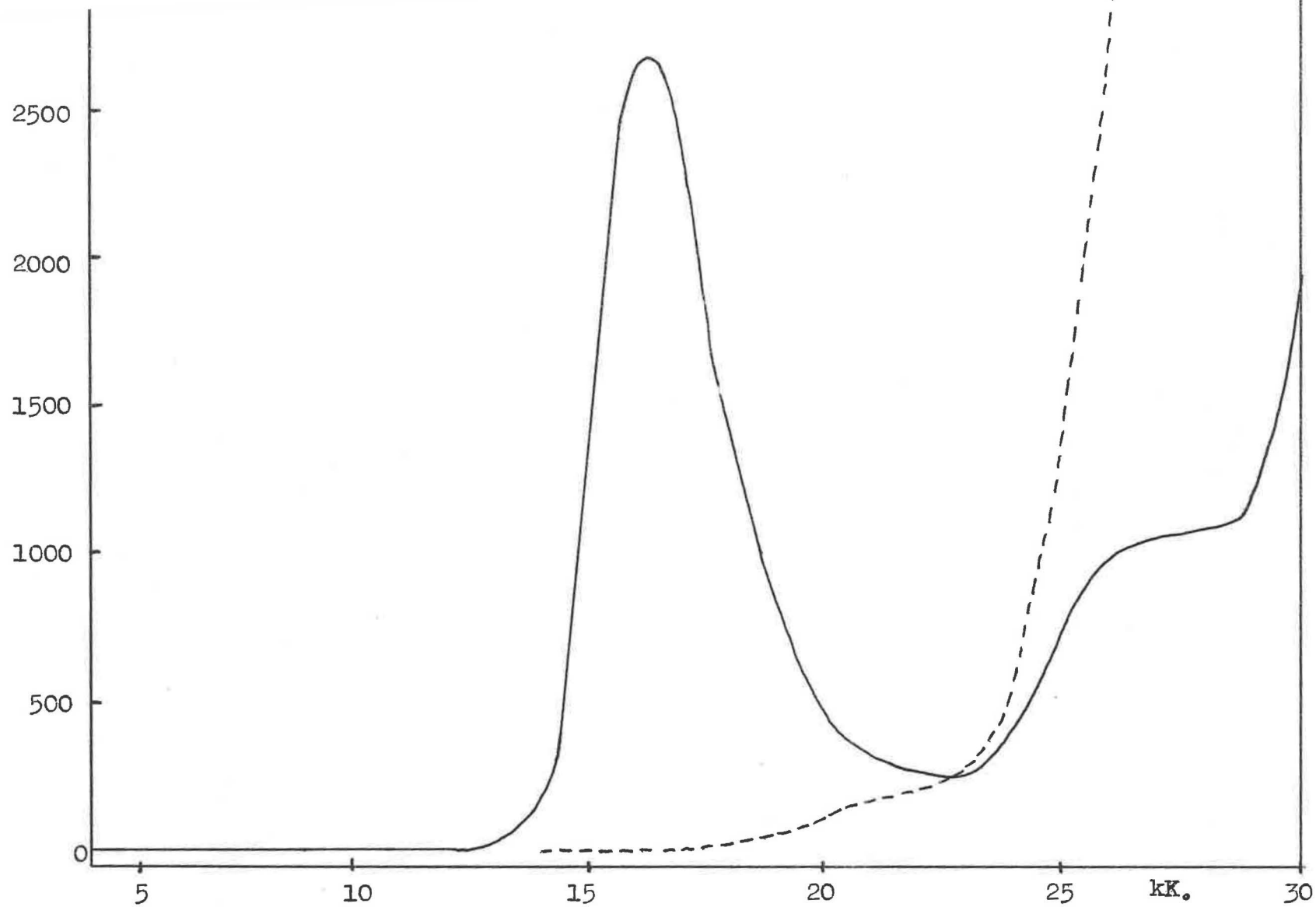


Fig. 2.8 Visible spectra of Rhodium Picoline Complexes (---) μ -peroxide,
(—) μ -superoxide.

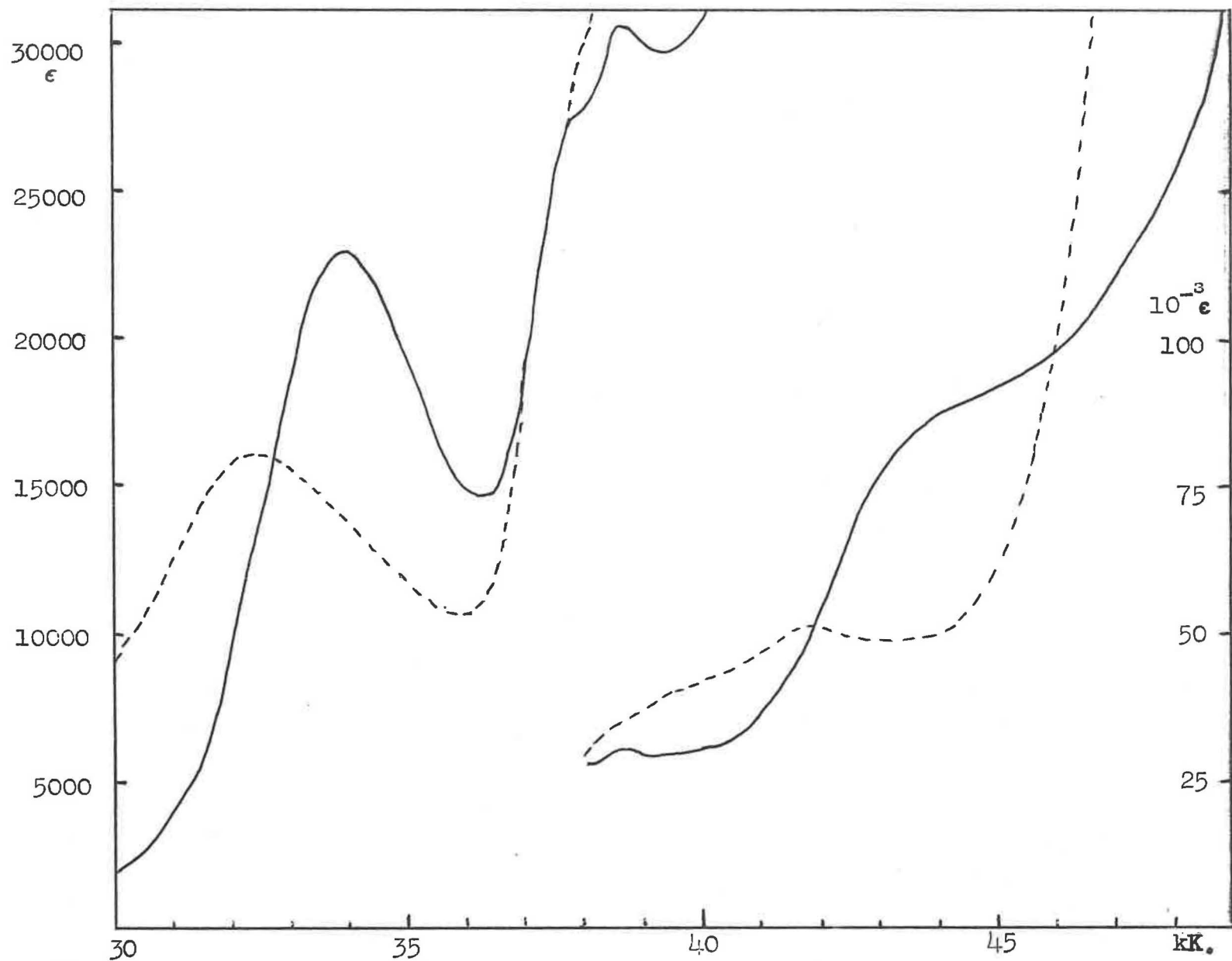


Fig. 2.9: UV spectra of Rhodium Picoline Compounds; (—) Superoxide, (-----) Peroxide.

Table 2.5

Electronic Spectra of (Su)peroxides

Ion	λ (nm)	ν (kK)	ϵ	Medium	Ref.
O_2^-	248	40.3		NaCl+KCN	47
O_2^-	370	27.0		NaO ₂ +Na ₂ O ₂	48
O_2^-	442	22.6		Pyridine	23,35
[Co ₂ (CN) ₁₀ O ₂] ⁵⁻	486	20.6	1130	H ₂ O	49
	360	27.8	2400		
	311	32.2	24800		
	276	36.2	5890		
	225	44.5	10000		
[Co ₂ (CN) ₁₀ O ₂] ⁶⁻	489	20.4	345	1M KOH	49
	370	27.0	6150		
	327	30.6	10120		
[Co(CN) ₅ (OH ₂)] ³⁻	380	26.3	360	H ₂ O	50
	235	42.5	7000		
[Co ₂ (DMG) ₄ Py ₂ O ₂]	1200	8.34	110	Benzene	51
	700	14.3	1200		
	550	18.2	3600		
[Co ₂ en ₄ (NH ₂)O ₂] ⁴⁺	685	14.6	400	H ₂ O	52
	463	21.6	465		
	305	32.8	6000		
[Co ₂ pn ₄ (NH ₂)O ₂] ⁴⁺	695	14.4	~ 500	H ₂ O	53
[Co ₂ phen ₄ (NH ₂)O ₂]	~ 700	14	500	HClO ₄	54
[Co ₂ (L-hist) ₄ O ₂] ⁺	672	14.9	-	HNO ₃	13
	478	20.9	-		
	314	31.8	-		
[Co ₂ tetren ₂ O ₂] ⁵⁺	704	14.2	1330	HClO ₄	14
	468	21.4	560		
[Co ₂ en ₂ dien ₂ O ₂] ⁵⁺	706	14.2	1210	HClO ₄	14
	472	21.2	385		

Table 2.5 Continued

Ion	λ (nm)	ν (kK)	ϵ	Medium	Ref.
[Co ₂ trien ₂ A ₂ O ₂] ⁵⁺	706	14.2	1190	HClO ₄	14
	469	21.3	447		
[Co ₂ dien ₂ A ₄ O ₂] ⁵⁺	707	14.1	1170	HClO ₄	14
	469	21.3	365		
[Co ₂ en ₄ A ₂ O ₂] ⁵⁺	693	14.4	1240	HClO ₄	14
	471	21.2	350		
[Co ₂ A ₁₀ O ₂] ⁵⁺	663	15.1	790	12M H ₂ SO ₄	a
	479	20.9	280		
	b,c(330)	30	~ 3000		
	297	33.7	23000		
[CoA ₅ (OH ₂) ²⁺	485	20.6	~ 60		55
	340	29.4	~ 60		
[Rh ₂ py ₈ Cl ₂ O ₂](ClO ₄) ₃ · 8H ₂ O	602	16.6	2850	1N H ₂ SO ₄	a
	288	34.8	19000		
	(268)	37.3	33100		
	262	38.2	35800		
	(255)	39.2	31400		
	(225)	44.4	42400		
[Rh ₂ py ₈ Cl ₂ O ₂](BF ₄) ₃	602	16.6	2850	1N H ₂ SO ₄	a
[Rh ₂ pic ₈ Cl ₂ O ₂](ClO ₄) ₃ · 2H ₂ O	611	16.4	2780	1N H ₂ SO ₄	a
[Rh ₂ pic ₈ Cl ₂ O ₂](BF ₄) ₃	611	16.4	2780	1N H ₂ SO ₄	a,d,e
	(370)	27	2100		
	295	33.9	22800		
	266	37.6	28700		
	259	38.6	31400		
	(225)(44.4)		31300		
[Rh ₂ pic ₈ Cl ₂ O ₂] (ClO ₄) ₂ ·2H ₂ O	(472)	(21.2)	170	MeCN+EtOH H ₂ O	d a,e
	(370)	(27.0)	3980		
	308	32.5	16000		
	(266)	(37.6)	27100		
	(259)	38.6	35800		
	237	42.2	52200		

Table 2.5 Continued

Ion	$\lambda(\text{nm})$ $\nu(\text{kK})$	ϵ	Medium	Ref.
$[\text{Rh}_2\text{py}_8\text{O}_2(\text{OH}_2)_2]^{5+}$	572 17.5	3300	1N H_2SO_4	a
$[\text{Rh}_2\text{py}_8\text{Cl}_2\text{O}_2]^{2+}$	(360)(28.0)	4300	NaOH 0.1M	a
	311 32.2	15000		
	(267)(37.5)	27500		
	261 38.3	33800		
	255 39.2	33600		
	242 41.3	33100		

a: This work

b: Unresolved shoulder

c: From Gaussian resolution in λ

d: See Figure 2.8

e: See Figure 2.9

L-hist:L-histidine.

DMG :dimethylglyoximate.

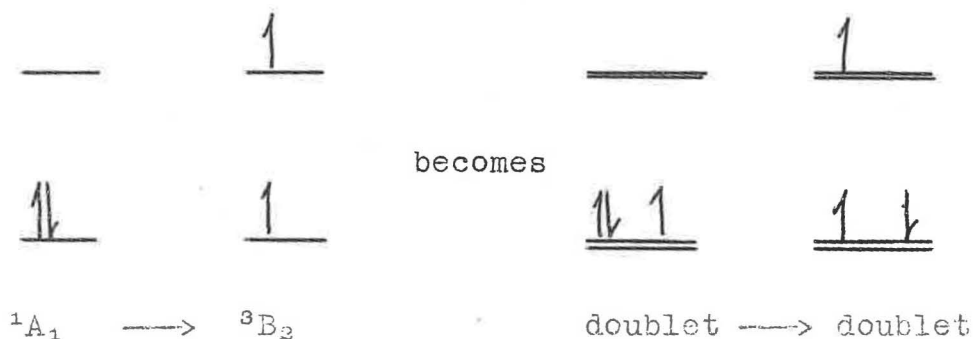
dien :diethylenetriamine.

tetren: tetraethylenepentamine.

term to split into 1E and 1A_2 , the latter at higher energy, while ${}^1A_{1g}$ now transforms as 1A_1 . The first transition in the superoxides cannot be ${}^1A_1 \rightarrow {}^1E_g$. The spectra of two cobalt(III) complexes with a local N_5O environment are given in Table 2.5, the second being a superoxide. It is obvious that the bands of pink $[Co(A)_5OH_2]^{2+}$ occur unshifted, within the spectrum of the $[Co_2(A)_{10}O_2]^{5+}$ ion, while the superoxide band occurs at an energy below that predicted for any cobalt pentammine ion from Jørgensen's⁽⁵⁵⁾ rule of average environment. Theory⁽⁵⁶⁾ regarding tetragonal splitting would require that the second and third bands be slightly shifted as well as the first.

The long wavelength transition has been studied in optically active complexes^(53,54,57) by circular dichroism, and found to have $\epsilon_L - \epsilon_R < 0.2$ at the wavelength of maximum absorption, and only slight optical activity at longer wavelength. This fact, combined with the high intensity of the bands, is interpretable as evidence against the transition occurring within the cobalt ions. The possibility exists, though, that a transition may occur to the term which is 3B_2 in C_{4v} (Figure 2.7) if mixing in (Figure 2.10) of the superoxide ligands' low lying doublet states were to remove the spin ~~re~~^{stt}action:

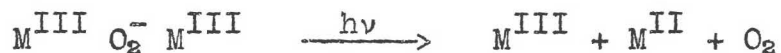
Figure 2.10



The $^1A_1 \rightarrow ^3B_2$ transition is not expected to appear in CD⁽⁵⁸⁾. The objection to this, and indeed to all the ligand field assignments, is that the low energy band is more intense than one would expect^(56a) for a Laporte forbidden band where intensity borrowing from a nearby strong absorption is not possible. There is no evidence for electronic coupling of the cobalt d-sets, and it has been shown^(59,60,61) that even for dimers with more than one bridge, the cobalt ions are electronically independent, in the d-d region at least. Coupling appears likely to occur only in special cases, such as in a linear^(4,62) metal-bridge-metal moiety.

One suggestion made by Sasaki and coworkers⁽⁵³⁾ and recently by Schrauzer and Lee⁽⁵¹⁾ was that low energy charge-transfer may occur between metal and ligand. Both the cobalt amines⁽⁴³⁾ and the rhodium complexes are stable toward visible light. The dirhodium picoline complex was unaffected by two hours' irradiation in solution by a 180mW

helium-neon laser (633 nm.). If the band involved ligand metal charge transfer, one might expect some dissociation to occur



At least in the rhodium case, the stabilities of rhodium(III)-superoxide and rhodium(IV)-peroxide are similar, this being shown by the recent isolation⁽⁶³⁾ of a complex probably containing a μ -peroxodirhodium(IV,IV) moiety⁽⁶⁴⁾. This supports the thesis that metal-to-ligand charge transfer could occur at low energy. It also reflects the parallel drawn in section 6.(i) between redox potential and transition wavelength, which are then indicative of the electron affinity of the superoxide ion for its given environment. Circular dichroism bands with $0.1 < \left| \epsilon_L - \epsilon_R \right| < 2$ have been assigned⁽⁶⁵⁾ as metal-to-ligand ($Co^{III} \rightarrow NO_2^-$) charge transfer bands, their wavelengths not necessarily corresponding to the absorption ($\epsilon_L + \epsilon_R$) maximum.

The simplest explanation of the low optical activity of the (cobalt) bands is that the transition occurs within the superoxide ligand, the ground and excited states thus being isolated from the centres of activity, and is the phenomenon of which the $^1A_1 \rightarrow ^3B_2$ transition idea is

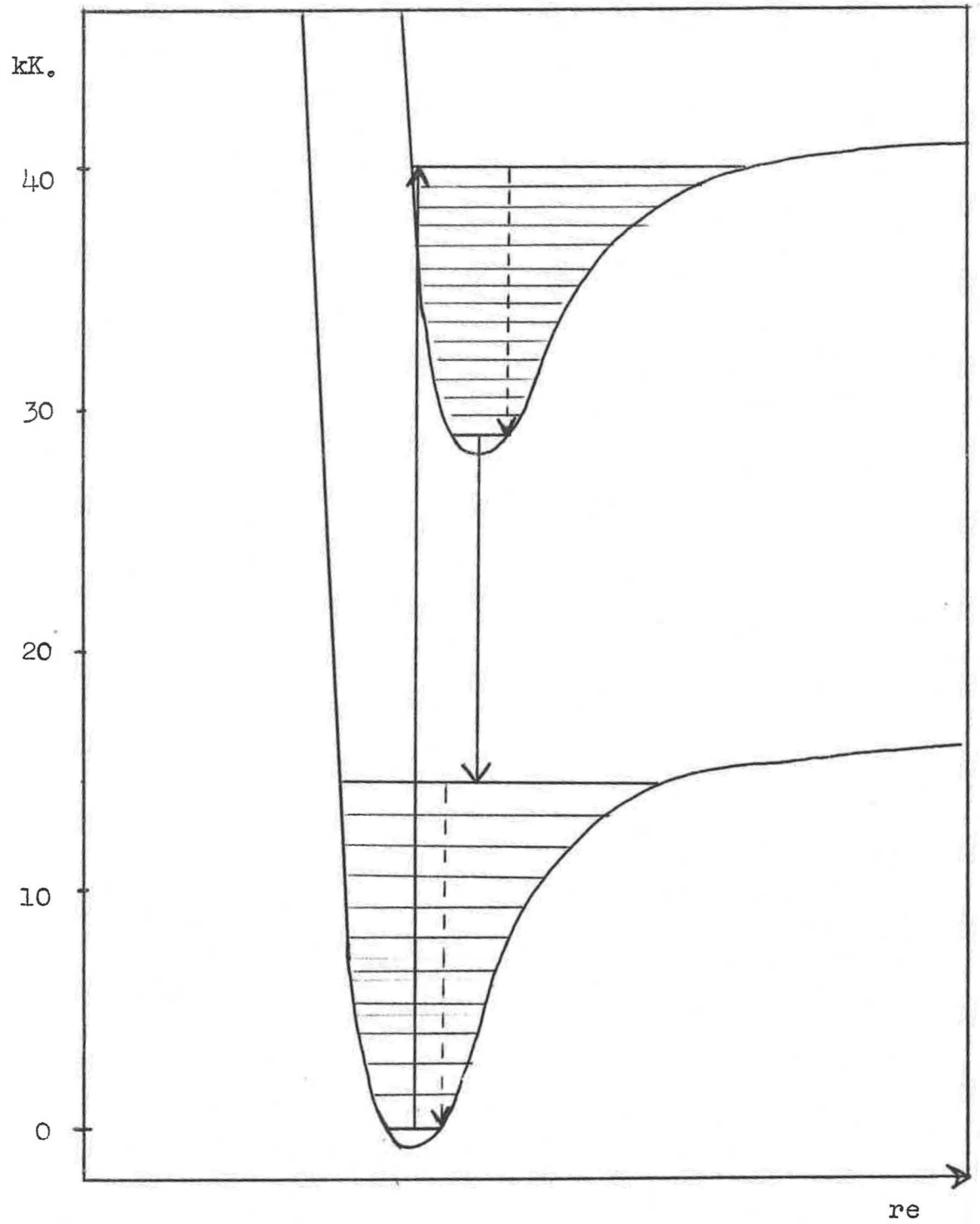


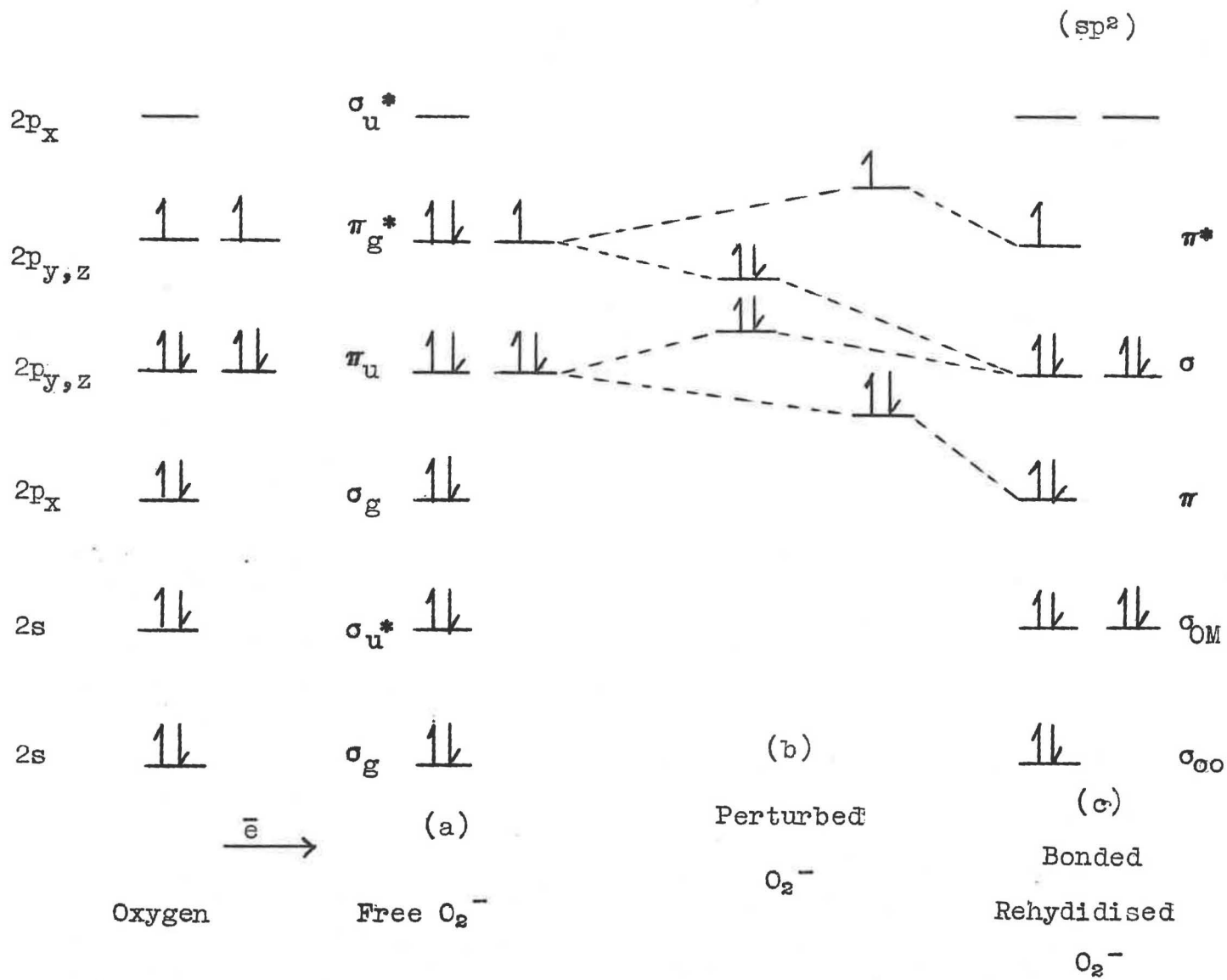
Fig. 2.11 Schematic idealisation of the fluorescence process in superoxide in an alkali halide lattice.

another extreme. The possibility of such a transition is an integral part of the structural properties of superoxide compounds.

The emission spectrum of the superoxide ion in alkali halide matrices has been examined⁽⁴⁷⁾ and bands in the 650 nm. region have been assigned⁽⁶⁶⁾ to transitions from $v' = 0$ in the excited state to large v'' in the ground state, thus giving the energy diagram of Figure 2.11. It is apparent that the vertical $O \rightarrow O$ excitation should require ca 29kK (350 nm.), but the lattices absorb⁽⁴⁷⁾ firstly at 40.3kK (248 nm.) although NaO_2 absorbs at 27kK (370 nm.)⁽⁴⁸⁾

The electronic structure of O_2^- (Figure 2.12a) is formed by adding an electron to the O_2 molecule, of which the structure is well described by LCAO-MO theory. The O_2^- ion is unique in that it is the only known ligand which formally contains an odd electron in a π^* orbital. This electron occupies an orbital whose corresponding charge cloud density is equally distributed on both O atoms and cylindrically symmetric about the O-O axis. It might therefore be expected that cationic addends would occupy axial sites on the O_2^- ion. However, Walsh's rules demand that $H_2O_2^+$ for example, should not be linear, and crystallographic studies show that the metal-superoxide-metal group is planar, but bent. The bending has the effect of removing

Fig. 2.12 Electronic structures of O_2 and O_2^-



the degeneracy of the π -orbitals; as shown in Figure 2.12a, with the XY plane as the M_2O_2 plane, the p_z orbitals are unaffected by bending, while the energy of the p_y set change (Figure 2.12b) as the metal cations orbitals approach, as in the familiar crystal field situation for d-orbitals.⁽⁶⁶⁾ There is then a net energy gain as a result of the relative change in the π -orbitals, because four electrons decrease in energy while only three increase. Fbsworth and Weil⁽¹²⁾ look upon this effect as being a Jahn-Teller distortion, but this is incorrect for the tetratomic M_2O_2 model as the theorem⁽⁶⁷⁾ states that a nonlinear nuclear configuration is unstable with an orbitally degenerate ground state. The bridge's nonlinearity may be described in terms of a lesser order effect. Halverson⁽⁶⁸⁾ found that there is coupling between nuclear and electronic motion of O_2^- in crystalline KO_2 . The bending of the O_2^- away from the MOOM axis is a coordinate which gives rise to quadratic terms in the electronic Hamiltonian relating to the electronic-nuclear coupling. In a linear system such as this, first order (Jahn-Teller) terms do not contribute; the distortion arising from the quadratic terms is analogous to the Renner effect observed in free molecules. That the O_2^- bridge is not free to precess about the M-M axis, is the constraint imposed by the preference for M-O bond formation in a given orientation, which is a consequence of the effects of the

other ligands on the d-orbitals of the metal. This reveals the interesting result that the MOOM geometry is a function of the electronic structure of the polyatomic ion as a whole, and it is therefore correct to invoke the Jahn-Teller theorem.

The distortion is paralleled by the change in orbital energies depicted in 2.12b, the end result being equivalent to (re)hybridisation to the situation of 2.12c. The depicted energy order of the p-orbitals is suspect, but the fact remains that the electronic structure of O_2^- becomes highly perturbed, and an energy gap appears between the doubly and singly occupied p-orbitals. A $\pi_u \rightarrow \pi_g^*$ transition can now occur at lower energy than in the isolated O_2^- ion, although one would expect the transition energy to increase as the distortion increases.

The rationalisation of the electronic structure of the superoxides will obviously require a sophisticated theoretical investigation. However it seems likely that a molecular orbital description will reveal that the low energy transition involves orbitals whose charge distributions over metals and ligand (O_2^-) are dissimilar, thereby entailing some charge transfer character in a transition which is predominantly (bridge) localised $\pi \rightarrow \pi^*$.

On reduction of superoxide to peroxide the electronic spectra are, of course, radically altered, as ligand orbitals' occupancy prevents charge transfer from the metal while the $\pi - \pi^*$ transition is prevented also. However, in the μ -peroxorhodium compound, 2D, an absorption band at 472 nm. may be resolved from an indistinct shoulder. In addition, the μ -peroxodicobalt compounds apparently also have low energy absorption, e.g. at ca. 600 nm. in $[\text{Co}_2\text{en}_4(\text{NH}_2)\text{O}_2]^{3+}$, also as an unresolved shoulder⁽⁵²⁾, this time reflecting the activity of the (resolved) complex in the ORD and CD spectra, suggesting that the transition occurs within the metal chromophore. The problem of assigning the transition is no less difficult than the superoxide case. However, it should be noted that compounds of the type trans - $\text{Rhpy}_4\text{X}(\text{OH}_2)^{++}$ have absorption bands well below the energy expected for an RhN_4XO chromophore (Section 3.3.2), so the 472 nm. band in the μ -peroxorhodium species is possibly akin to this. On the other hand, as the transition $A_1 \rightarrow E$ (in C_{4v}) involves rotation of charge distribution (as shown by the presence of a Cotton effect), one may suggest that the already helically bound peroxide linkage may serve to transmit the effect of the dipole charge to the other metal atom; i.e. that some coupling occurs. It was also observed that a band arose at ca. 490 nm. in the preparation (Figure 2.1); this

could possibly have the same origin, although interpolation between ionic and bidentate O_2 (Table 2.5) predicts that a monomeric superoxide might absorb in this region ($22,000\text{ cm}^{-1}$).

In the ultraviolet region, the electronic absorptions of the rhodium and cobalt species are very similar; there being a strong band (ca. 290 nm., $\epsilon \sim 10^4$) in the superoxides, which shifts to lower energy (ca. 310 nm., $\epsilon \sim 10^4$) in the corresponding μ -peroxide, the intensity decreasing slightly.

It is noteworthy that on increasing the ligand field at the rhodium centre, one achieves an increase in the energy of the strong visible region transition in the superoxides; i.e. on passing from chloride to hydroxyl to water as ligands, λ decreases from 602 to 590 (aquo complex at pH 7) to 572 nm. Similarly, replacing pyridine by γ -picoline raises the wavelength maximum from 602 to 611 nm.; this has been observed previously by Taube's group⁽⁶⁹⁾ in complexes of ruthenium(II) with substituted pyridines, and in that case the bands observed were attributed to charge transfer transitions, $Ru \rightarrow \pi^*(L)$.

60. A.W. Chester, C.H. Brubaker, J. Inorg. Nucl. Chem.,
1968 30 213.
61. Y. Inamura, Y. Kondo, J. Chem. Soc. Japan, 1953 74 627.
Chem. Abs. 1954 48 2476f.
62. T.M. Dunn, "Modern Coordination Chemistry", Ed. J. Lewis
R. Wilkins. Interscience, New York, 1960. pp.272.
- 63a. K. Thomas, Ph.D. Thesis, London University, 1968
- 63b. Private communication.
64. R. Mason, Private communication.
65. J. Bolard, A. Garnier, J. Phys. Chim. Physicochim. Biol.
1969 66 1919.
66. J.S. Griffith, "Oxygen in the Animal Organism", Intern.
Union Biochem.; Proc. Symp. 1963, Pergamon 1964
pp. 141.
67. H.A. Jahn, E. Teller, Proc. Roy. Soc., 1937 161A 220.
68. F. Halverson, Phys. Chem. Solids, 1962 23 207.
69. P. Ford, De F.P. Rudd, R. Gaunder, H. Taube, J. Amer.
Chem. Soc., 1968 90 1187.
70. N.-G. Vannerberg, Acta Cryst., 1965 18 449.
71. W.P. Schaefer, Inorg. Chem., 1968 7 725.
72. M. Calligaris, G. Nardin, L. Randaccio, A. Ripamonti,
J. Chem. Soc., 1970A 1069.
73. J.A. Creighton, E.R. Lippincott, J. Chem. Phys., 1964
40 1779.
74. J.C. Evans, J. Chem. Soc., 1969D 682.
75. B. Jeżowska-Trzebiatowska, J. Mrozinski, W. Wojciechowska,
Bull. Acad. Pol. Sci., Ser. Sci. Chim., 1968 16 521.
76. W.P. Griffith, T.D. Wickins, J. Chem. Soc., 1968A 397.
77. G.C. Dobinson, R. Mason, D.R. Russell, Chem. Comm.,
1967 62.
78. M. Mori, J.A. Weil, M. Ishiguro, J. Amer. Chem. Soc.,
1968 90 615.
79. B. Bosnich, C.K. Poon, M.L. Tobe, Inorg. Chem., 1966
5 1514.

80. R.D. Gillard, B.T. Heaton, D.H. Vaughan, J. Chem. Soc., 1969D 974.
81. J.V. Rund, Inorg. Chem., 1968 7 24.
82. M.C. Baird, D.N. Lawson, J.T. Mague, J.A. Osborn, G. Wilkinson, Chem. Comm. 1966 129.
83. K. Thomas, G. Wilkinson, J. Chem. Soc., 1970A 356.
84. J.A. Osborn, A.R. Powell, G. Wilkinson, Chem. Comm. 1966 461.
85. D.N. Lawson, M.J. Mays, G. Wilkinson, J. Chem. Soc., 1966A 52.
86. R.D. Gillard, J.A. Osborn, G. Wilkinson, J. Chem. Soc., 1965 4107.
87. K. Thomas, J.A. Osborn, A.R. Powell, G. Wilkinson, J. Chem. Soc., 1969A 1801.
88. C. Floriani, F. Calderazzo, J. Chem. Soc., 1969A 946.
89. S.A. Cockle, H.A.O. Hill, R.J.P. Williams, Inorg. Nucl. Chem. Letts., 1970 6 131.
90. J.H. Bayston, F.D. Looney, N.E. Winfield, Austral. J. Chem., 1963 16 557.
91. J.H. Bayston, M.E. Winfield, J. Catal. 1964 3 123.
92. R.D. Gillard, B.T. Heaton, D.H. Vaughan, J. Chem. Soc., To be published.
93. L.E. Johnston, J.A. Page, Canadian J. Chem., 1969 47 4241.
94. J.O. Edwards, P.D. Fleischauer, Inorg. Chim. Acta Revs., 1968 2 56.
95. B. Martin, W.R. McWhinnie, G.M. Waind, J. Inorg. Nucl. Chem., 1961, 23 207.

96. E. Fremy, Liebigs Ann., 1852 83 240.
97. H. Taube, J. Gen. Physiol., 1965 49 (1) II 29.
98. S. Fallab, Angew. Chem. (Intern. Edit.) 1967 6 496.
99. R. Mason, Disc. Farad. Soc., 1967 47, 20.
100. L. Vaska, Science, 1963 140 809.
101. S.J. La Placa, J.A. Ibers, J. Amer. Chem. Soc., 1965 87 2581.
102. J.A. McGinnety, R.J. Doedens, J.A. Ibers, Inorg. Chem., 1967 6 2243.
103. J.A. McGinnety, N.C. Payne, J.A. Ibers, J. Amer. Chem. Soc., 1969 91 6301.
104. C.D. Cook, P.-T. Cheng, S.C. Nyburg, ibid., 2123.
105. J.S. Griffith, Proc. Roy. Soc., 1956 235A 23.
106. A. Haim, W.K. Wilmarth, J. Amer. Chem. Soc., 1961 83 509.
107. R. Mason, Nature, 1968 217 543.
108. R.S. Mulliken, T.S. Tsubomura, J. Amer. Chem. Soc., 1960 82 5966.
109. P. Powell, H. Nøth, Chem. Comm., 1966 637.
110. D. van der Helm, J.D. Childs, S.D. Christian, J. Chem. Soc., 1969D 887.
- 111a. S.J. La Placa, J.A. Ibers, J. Amer. Chem. Soc., 1965 87 2581.
- 111b. idem., Inorg. Chem., 1966 5 405.
112. G. Herzberg, Molecular Spectra and Molecular Structure, D. van Nostrand Co., New Jersey, 1945
(a) Volume I pp. 459
(b) Volume III, Appendix.
113. L.A. d'Orazio, R.H. Wood, J. Phys. Chem., 1965 69 2550.

114. R. Ugo, G. Conti, S. Cenini, R. Mason, G. Robertson,
Chem. Comm., 1968 1948.
115. S. Fallab, Chimia, 1970 24 76.
116. J. Hanzlik, A.A. Vlček, J. Chem. Soc., 1969D 47.
117. F. Basolo, M.L. Morris, R.G. Pearson, Disc. Farad.
Soc., 1960 29 80.
118. R.D. Gillard, E.D. McKenzie, M.D. Ross, J. Inorg.
Nucl. Chem., 1966 28 1429.

Chapter 3

Reactions of $[\text{Rhpy}_4\text{X}_2]^+$

3.1 Catalysis and Inhibition of Substitution Reactions

Substitutions are one of the most significant types of reaction which occur at transition metal centres, and ligand replacements in tetramine rhodium complexes of the type* $[\text{RhL}_4\text{XY}]^{n+}$ have recently been the object of a considerable amount of investigation^(1,2,3,4).

Reactions such as



where A, X, Y are halides or pseudo halides have been found to proceed with rate constants, which are first order or pseudo-first order in rhodium, of the magnitude of $10^{-3} - 10^{-5} \text{ sec}^{-1}$. Similarly, the dihalo cation $\text{trans}[\text{Rhpy}_4\text{X}_2]^+$ in aqueous solution reacts with halide ions ($\text{Y}^- \neq \text{X}^-$) to yield $\text{t-Rhpy}_4\text{XY}^+$ and $\text{t-Rhpy}_4\text{Y}_2^+$. Moreover, these relatively slow reactions are susceptible to

* L is a nitrogenous donor, e.g. py, NH_3 , $\frac{1}{2}\text{en}$; X, Y, are other ligands.

two influences on their rate⁽⁵⁾, namely that primary and secondary alcohols catalyse the halide exchange, while oxygen has a pronounced inhibitory effect. The latter phenomenon is discussed further in another part of this work. Reaction rate may thus be increased by addition of ethanol, say, and/or by deoxygenation of the solution, and halide exchange equilibrium attained within a few seconds. The suggested⁽⁵⁾ mechanistic rationalisation of these observations is that there is formed in solution a small amount of a very reactive reduced rhodium species, i.e. rhodium(I), rhodium(II) or hydridorhodium(III), which acts as the real catalyst in a fashion similar to that of platinum(II) toward platinum(IV)⁽⁶⁾.

By adding small amounts of possibly catalytic reductants to aqueous solution of $t\text{-Rhpy}_4\text{Cl}_3$, 3A containing excess bromide and warming the mixture, one may observe (visually and spectrophotometrically) that effective catalysts are: sucrose, hydroquinone, ethanol, propanol, << hydrazine hydrate, sodium borohydride, and metallic zinc. Thiosulphate ($E^0 = +0.08\text{v.}$), hexacyanoferrate(II) ($+0.36\text{v.}$), dimethyl sulphoxide ($+0.23\text{v.}$), iron(II) sulphate, nitrite and sulphite do not assist the reaction. The passage of hydrogen assists the reaction, and this is probably a catalytic effect, but by this

qualitative method the distinction cannot be made between catalysis on one hand, and on the other, inhibition removal, which is accomplished by the passage of nitrogen or even the addition of diethyl ether which has the effect of deoxygenating the warm solution. Oxidants such as chlorite inhibit the exchange as indeed, does acid. When an ethanolic solution of t-Rhpy₄Cl₃ (3A) is treated with hydrobromic acid and sodium bromide and heated at ca. 70° for an hour, no exchange occurs, despite the presence of the large amount of catalyst. The product is an acid adduct of the Rhpy₄Cl₂⁺ ion. This is evidenced by: the strong acidity (pH 2) of an aqueous solution (ca. 10⁻²M); the presence of the above cation's absorption at 410 nm. in the electronic spectrum; 365 cm⁻¹ in the infrared, ν (Rh-Cl); and by the analytical data. These suggest the formulation [Rhpy₄Cl₂]Br.HBr.3H₂O for the pale yellow laths, 3B.

This has an important synthetic application, as it implies that in the rhodium pyridine complexes certain ligands may be replaced by halide, say, without displacement of already coordinated halide.

3.2 Some Substitution Reactions at the Rhpy₄X₂⁺ Centre

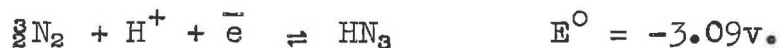
3.2.(i) Iodide

When a dilute aqueous solution of t-Rhpy₄Cl₃ is heated carefully with an excess of sodium iodide, the pale yellow colour deepens within a minute or so to orange and then rapidly changes to orange-brown, simultaneously orange-brown crystals are deposited. The product is [Rhpy₄I₂]I.3H₂O, (3C), its analytical* and spectroscopic properties being identical with those of a sample prepared as in Chapter 1. Use of borohydride or ethanol to catalyse a warm reaction mixture resulted in the precipitation of the plum-coloured crystalline compound, Rhpy₃I₃, discussed in Chapter 4.

*Analyses are tabulated in 3.9.

3.2.(ii) Azide

Azide itself is capable of acting as a reducing agent:



Cold aqueous solutions of t-Rhpy₄Cl₃ are relatively stable to azide in comparison with their reactivity toward

borohydride, for example. However, if nitrogen is bubbled through a cold aqueous ethanolic solution of 3A containing excess NaN_3 , the solution quickly becomes deep orange-yellow and within a couple of minutes deposits a yellow-orange precipitate of the nonelectrolyte $\text{Rhpys}(\text{N}_3)_3$, (3D). It is also formed by boiling an aqueous solution of 3A with a large excess of azide or (quantitatively) by adding a trace of NaBH_4 to a cold solution of 3A with excess azide (with or without ethanol). It is formed less efficiently by borohydride catalysis in warm aqueous ethanolic solution, when the other products, which have been isolated, are cationic diazidotetrapyridinerhodium(III) (as its azide, 3E, and tetrafluoroborate, 3F, salts) and the tetra-azidodipyridinerhodate(III) anion, as its Et_4N^+ salt, 3G. In this case, the triazido compound 3D forms as orange needles, but X-ray powder diffraction photographs show these needles and the orange-yellow powders to be identical. The diazido complex 3E may be prepared by boiling a solution of the dichloro complex 3A with a 15% excess of azide (2.3:1) to ensure complete removal of chloride.

The electronic spectra (Table 3.1) of the complexes are rather uninformative, consisting as they do of rather poorly resolved peaks. The first absorption band in the

Table 3.1

Electronic Spectra of Azides

Compound	λ (nm.)	ϵ	Solvent
[Rhpy ₄ (N ₃) ₂]N ₃ ·5H ₂ O (3E)	(445) ^a 386 311 (288) (267) 261 (256)	230 1470 8300 7200 12800 16000 14900	MeOH
[Rhpy ₄ (N ₃) ₂]BF ₄ (3F)	386 306 (285) (267) 261 (256)	1340 7600 7500 13400 16500 15600	MeCN
t-Rhen ₂ (N ₃) ₂ ⁺ b	375 282	780 12000	H ₂ O
Rhpy ₃ (N ₃) ₃ (3D)	(430) ^a (370) ^a (305) (269) 262 (257)	480 2000 14800 20000 21600 20500	MeCN
(NEt ₄)[Rhpy ₂ (N ₃) ₄] (3G)	(470) ^a 409 300 270 264 (257)	330 965 21300 13600 13300 12400	MeOH

a: from Gaussian resolution in wavelength.
Bands in brackets are shoulders in the spectrum.

b: reference 22.

necessarily trans-diazido cation is at 445 nm., and may be a spin forbidden band. Schmidtke⁽⁷⁾ observed a band at 395 nm. in $[\text{Rh}(\text{NH}_3)_5(\text{N}_3)]^{2+}$ which he attributed thus. The ${}^1\text{A}_{1g} \rightarrow {}^1\text{T}_{1g}$ transition has been assigned⁽⁸⁾ at 488 nm. (20500 cm^{-1}) in $\text{Rh}(\text{N}_3)_6^{3-}$, so that the cubic contribution to the diazidotetramine should be 26800 cm^{-1} (373 nm.) for the first band. Hence the 386 nm. band possibly contains ${}^1\text{A}_{1g} \rightarrow {}^1\text{E}_g$ in the tetragonal complex. The difficulties involved with this assignment are brought to light in Chapter 4. Basolo and coworkers⁽⁹⁾ found that Ru(III) and Ir(III) azidoammines gave nitrogen and coordinated nitrene on treatment with dilute H_2SO_4 , but with the trans-diazide 3E, no N_2 evolution occurs. Cold HCl does not affect the compound, but boiling a solution in 10M HCl causes the 311 nm. band to disappear. The reason for this is not known; the rest of the spectrum is unaffected, and replacement of N_3^- by Cl^- does not occur at an observable rate, as the 386 nm. band remains constantly and no band grows at 410 nm.

The infrared spectrum (Table 3.2) 3F shows one very strong band at 2010 cm^{-1} due to $\nu_{\text{as}}(\text{N}_3)$ and a medium intensity band at 398 cm^{-1} assignable as $\nu(\text{RhN}_3)$. Unfortunately, these absorptions do not allow a distinction to be made between a linear or bent RhNN unit. The former

Table 3.2

Selected Vibrational Bands of Azides

Compound	Raman (cm^{-1})	Infrared (cm^{-1})	Origin
KN_3 (a)	1344	645	δ
		2041	ν_s ν_a
$3D$ $\text{Rhpy}_3(\text{N}_3)_3$	389vvs 404vs 681m 1273m 1293m 2013w 2042m	302s	$\nu(\text{Rh-N}_3)$
		(386)	
		402s	δ
		(c)	ν_s
		1273s	ν_s
		1292s	ν_s
		(1295)	ν_a
		2008vs (b)	ν_a
2030vs			
$3E$ $[\text{Rhpy}_4(\text{N}_3)_2]\text{N}_3 \cdot 5\text{H}_2\text{O}$	380vvs 1287w 2035m	397s	$\nu(\text{RhN})$
		674s	$\nu(\text{RhN})$
		1277s	δ
			ν_s
			ν_s
		2010vs, br	ν_a
	ν_a		
$3F$ $[\text{Rhpy}_4(\text{N}_3)_2]\text{BF}_4$	380vvs 1280m 2040m	397s	$\nu(\text{RhN})$
		1280s	$\nu(\text{RhN})$
		2012s, br	ν_s
			ν_a
	ν_a		
$3G$ $(\text{NET}_4)[\text{Rhpy}_2(\text{N}_3)_4]$	(378vs) 387vvs 681s 1303m 2042s	388s	$\nu(\text{RhN})$
		402s	$\nu(\text{RhN})$
			$\nu(\text{RhN})$
			δ
		1288vs	ν_s
			ν_s
		2015vs	ν_a
	ν_a		
	$\nu_a + \nu_s$		

continued ...

Compound	Raman (cm^{-1})	Infrared (cm^{-1})	Origin
3H Rhpic ₃ (N ₃) ₃		355m (390) 400s 410s 1283s (1290)s 2012vs 2045vs	} } ν (ring) } ν (Rh-N ₃) } ν_s ν_s ν_a ν_a

- a: Reference 10a.
- c: difficult to distinguish, as pyridine has bands here.
- b: a in these compounds has a strong Christiansen effect in the nujol mull; reference 12.

would endow on $\text{RhL}_4(\text{N}_3)_2^+$ an approximately D_{4h} symmetry, the latter decreased symmetry, C_{2h} , but in each case, each of metal-ligand and (both) internal azide stretching vibrations are expected to give rise to one Raman active and one infrared active band (non-coincident) as observed. Structural studies⁽¹¹⁾ have shown coordinated azide to bond non-linearly, in accord with sp^2 hybridisation at the donor nitrogen.

The triazidotripyridine compound 3D has bands at 370 and 430 nm. The first spin allowed transition is expected to be at ca. 395 nm. on the basis of the cubic contributions estimated from previous work^(8,13). The band may drop below this in energy as in other RhN_3X_3 chromophores⁽¹³⁾. With a trans-precursor, the triazide 3D is necessarily the 1,2,6-isomer; this should have three metal-ligand vibrations, coincident in Raman and infrared, of species $2A_1 + B_1$ in the metals C_{2v} immediate environment*. The possibility arises that the band at 465 cm^{-1} in the i.r. spectrum is such a vibration, superimposed on the pyridine ring deformation modes near this frequency, and there is a weak Raman absorption at 468 cm^{-1} . However, examination of the analogous γ -picoline complex $\text{Rhpic}_3(\text{N}_3)$, (3H) shows that this has no absorption $440\text{-}490 \text{ cm}^{-1}$. The 302 cm^{-1} band in

*See Table 4.6.

$\text{Rhpy}_3(\text{N}_3)_3$ cannot be assigned reliably. The apparent non-occurrence of the predicted number of Raman bands is a demonstration of the shortcomings of applying vibrational spectroscopy in a simple qualitative fashion; cf. the relative success achieved in the analysis of the trans- RhL_4X_2^+ systems in Chapter 1. The i.r. absorption appears to be multiple in the region $370\text{-}410\text{ cm}^{-1}$ but is also to some extent in the diazido-cation. Thus, firm a priori distinction between cis and trans stereochemistry for the $[\text{Rhpy}_2(\text{N}_3)_4]^-$ ion by examination of $\nu(\text{Rh-N}_3)$ or of the electronic spectrum, is precluded. However, the trans-diazido complexes (3E, 3F) and the mer-triazides of rhodium with pyridine and γ -picoline (3D, 3H) show the expected number of bands resulting from the antisymmetric stretching vibrations of the azide ligands, denoted ν_a in Table 3.2. These two types of compound have respectively one and two $\nu_a(\text{N}_3)$ bands in the i.r. (and Raman), so the presence of only one band in $[\text{Rhpy}_2(\text{N}_3)_4]^-$ betokens the trans-isomer. This is more compatible with the mechanism proposed for these substitution reactions, while it is noted that attempts to prepare the cis isomer via the action of sodium azide on the cis- $[\text{Rhpy}_2\text{Cl}_4]^-$ ion were unsuccessful although a colour change was evident.

The stability of the rhodium azide complexes, shown above by their resistance to hydrochloric acid, is also demonstrated by the recrystallisation of $\text{Rhpy}_3(\text{N}_3)_3$ from the solution formed by boiling it in a mixture of pyridine, water and ethanol, under which conditions the chloro- and bromo- complexes yield $\text{Rhpy}_4\text{X}_2^+$.

Derivation of a rough force constant for the Rh-N_3 bond by the method used in Chapter 1 gives $k_{11} = 2.86 \times 10^5$ dyne cm^{-1} , which falls within the range $2.3-3.0 \times 10^5$ dyne cm^{-1} observed previously for metal azides⁽¹⁵⁾. However, it requires also a large bond interaction $k_{12} = 0.7 \times 10^5$ dyne cm^{-1} ; 25% of the k_{11} value.

Use of the asymmetric NN vibration frequency as a guide to the degree of covalency and hence the stability of the metal-azide bond^(10a) breaks down in the rhodium series here, as ν_{as} is relatively low, while the complexes are obviously quite stable. Nakamoto had correlated a high ν_{a} with a stable, covalent metal-nitrogen bond when comparing kinetic and spectroscopic results for chromium(III) and cobalt(III) azides^(10a).

Similarly to the result here, Chatt and coworkers have found no relationship between the relatively low $\nu(\text{N}\equiv\text{N})$ of a series of rhenium(I) nitrogen complexes and their

reactivity toward reductants⁽¹⁴⁾.

An attempt to form a BF_3 adduct of the triazido complex 3D gave an orange gum, the purification of which was not pursued successfully, as it appeared to be unstable.

3.2.(iii) Thiocyanate

By warming an aqueous solution of 3A with excess KNCS in vacuo there was obtained a yellow crystalline material, insoluble in most common solvents, which on recrystallisation from nitromethane gave yellow crystals (3K) which are merely the thiocyanate salt of $t\text{-Rhpy}_4\text{Cl}_2^+$. The electronic spectrum has λ 409 nm., $\epsilon = 98$ in DMSO; i.r. absorption at 2056s, $\nu(\text{CN})$; 736m, $\nu(\text{C-S})$; 365s, $\nu(\text{Rh-Cl})$, is consistent^(10b) with the formulation $[\text{Rhpy}_4\text{Cl}_2]\text{NCS}$ for 3K. Ethanol induced reaction of thiocyanate with 3A, but like borohydride led to a yellow colloidal suspension, (in the BH_4^- case orange in colour), accompanied by a sulphurous odour, hence a simple substitution reaction seems unlikely to occur.

3.2.(iv) Cyanate

Whether by merely heating an aqueous solution of 3A with sodium cyanate or by reaction in the cold catalysed by ethanol or borohydride, the same product, 3L, was obtained as yellow plates. The possibility of hydrolysis of cyanate:



had led to the expectation that the product might be an ammine complex. However, the infrared spectrum of the product showed ammonia to be absent, while there were strong absorptions at 2235, 2190 cm^{-1} $\nu(\text{C}\equiv\text{N})$ and a weaker band at 590 cm^{-1} , $\delta(\text{NCO})$. Analytical data showed the nonelectrolyte 3L to have the composition $\text{Rh}(\text{C}_5\text{H}_5\text{N})_3\text{Cl}(\text{NCO})_2$. That it is pure cis-dicyanate is implied by the failure of attempts to prepare $\text{Rhpy}_3\text{Cl}_2(\text{NCO})$ and $\text{Rhpy}_3(\text{NCO})_3$, of which a 1:1 mixed compound would have the same composition. Borohydride or ethanol catalysis of the reaction of the trans-dichloro complex 3A, with excess cyanate gave solutions which did not yield crystalline rhodium compounds. The question of linkage isomerism of the cyanate arises, as it may conceivably be either an N-donor or O-donor to the rhodium. Virtually all known cyanate complexes are

N-donors, i.e. isocyanate complexes⁽¹⁶⁾. Extrapolating from the $[\text{Pt}(\text{NCO})_4]^{2-}$ ion⁽¹⁷⁾, the isocyanate is expected to have a crystal field contribution about 0.86 of that of ammonia, so that one would predict the first spin allowed band to occur at 26700 cm^{-1} (375 nm.) by comparison with 1,2,6-Rhpy₃Cl₃. Indeed, the electronic spectrum (Table 3.3) has λ 376 (ϵ 327) which is a higher energy than the corresponding 'RhN₃O₂Cl' chromophore in Rhpy₃Cl.C₂O₄ (Chapter 4). Confirmation of this is provided by the infrared spectrum in nitromethane solution. The two C-N stretching peaks merge into one band centred at 2210 cm^{-1} , with a half-height width ($\Delta\nu_{\frac{1}{2}}$) of 110 cm^{-1} . Measurement of the transmittance enabled the absolute integrated intensity to be determined using Ramsay's equation⁽¹⁸⁾

$$A = \frac{\pi}{2Cl} \cdot \ln \left(\frac{I_0}{I} \right) \cdot \Delta\nu_{\frac{1}{2}}$$

which is essentially an integrated form of the more familiar Beer-Lambert law. The value obtained for the chloro-complex, 3L, was $A = 23.0 \times 10^4 \text{ l.mole}^{-1}\text{cm}^{-2}$ (per cyanate ligand) which is the upper limit of the range found for N-donor, isocyanate, by Norbury and Sinha⁽¹⁷⁾. The calculation is appended. The orange-yellow bromo-complex, 3M, $[\text{Rhpy}_3\text{Br}(\text{NCO})_2]$, has a

Table 3.3

Electronic Spectra of Isocyanate Compounds

<u>Compound</u>	<u>λ(nm.)</u>	<u>ϵ</u>	<u>Solvent</u>
3L	376	330	MeCN
	(320) ^a	395	
	(267)	11,500	
	(260)	16,200	
	255	17,800	
	249	17,600	
3M	397	280	MeCN
	(313) ^a	1,100	
	257	18,000	

a: Gaussian analysis in λ

consistent value for the first UV band (Table 3.3), of 25200 cm^{-1} . The shoulders at 320 nm., 313 nm., in the chloro- and bromo- compounds respectively are not necessarily ligand field bands, but may well be the $n \rightarrow \pi^*$ transition of NCO^- , shifted by coordination to the rhodium (See Chapter 4, Section 2(i).)

For the bromo- compound, the infrared intensity measurement (2200 cm^{-1} , $\Delta\nu_{\frac{1}{2}} = 95 \text{ cm}^{-1}$) gave $A = 17.3 \times 10^4 \text{ l.mol}^{-1}\text{cm}^{-2}$ which is within the range ($13\text{-}23 \text{ l.mole}^{-1}\text{cm}^{-2}$) for N-bonded cyanate ligands.

3.2.(v) Nitrite

Reaction of 3A with excess sodium nitrite in hot aqueous solution, or by warming such solution in vacuo produced a cream precipitate which did not have a sensible composition and which was a weak electrolyte ($\lambda \approx 0.05 \text{ cm}^2\text{ohm}^{-1}\text{g}^{-1}$ in MeNO_2). Recrystallisation from methyl cyanide gave pale yellow, solvated prisms of 3N, again a weak eletrolyte ($\lambda = 0.062 \text{ cm}^2\text{ohm}^{-1}\text{g}^{-1}$ in MeNO_2) the analysis of which demonstrated the presence of carbon, nitrogen and chlorine in the ratios 10.0:3.1:0.85 which implies pyridine:nitrite:chloride as 2:1:1. The properties of various preparations were found

not to be very reproducible, so the characterisation was not pursued.

Reaction of 3A under more vigorous conditions with excess NaNO_2 (warm aqueous ethanol, borohydride catalysed) gave cream crystallites of the nonelectrolyte 3P, which is formulated as $1,2,6\text{-Rhpy}_3(\text{NO}_2)_3$. Ultraviolet spectra of these compounds are similar and uninformative. One complication is that nitrite ion has $n \rightarrow \pi^*$ transitions^(19,20) at 354 nm. and 287 nm., and the intensities and positions of these may be affected by coordination. The general appearance of the absorption envelopes is of a slight shoulder at ca. 335 nm. ($\epsilon \approx 10^3$) rising to a more pronounced shoulder at ca. 280 nm. ($\epsilon \approx 10^4$) and then the pyridine $\pi \rightarrow \pi^*$ bands at 268, 262, 256 nm., ($\epsilon \approx 10^4$).

If a stoichiometric 2:1 ratio of nitrite to rhodium is used (under the above conditions), the resulting fluorescent apple-green solution slowly deposits pale yellow crystals of 3Q. Like the trinitro- complex, these are soluble in few solvents, such as methyl cyanide, nitromethane. 3Q analyses as $\text{Rhpy}_3\text{Cl}(\text{NO}_2)_2$. Infrared spectroscopy shows that the strong 1075 cm^{-1} band found by Basolo and Hamaker⁽²¹⁾ in (isomeric) nitrito complexes of platinoid metals is absent. Vibrational (infrared)

Table 3.4

Vibrational Spectra of Nitrites

Compound	Raman	Infrared	Origin
NaNO ₂	813a 1225 1325	828b 1261 1328	δ (ONO) ν _s (N-O) ν _a (N-O)
Na ₃ [Rh(NO ₂) ₆]	832a 847 1322 1380 1406	850s ^c 1350s 1425s	} δ } ν _s } ν _a
[Rh(NH ₃) ₅ (NO ₂)] ²⁺		848s ^d 1370w 1410m	δ ν _s ν _a
[Rh(NH ₃) ₅ (ONO)] ²⁺		848s ^d 1075vs 1370w 1450m	δ } ν _s } ν _a
3P [Rhpy ₃ (NO ₂) ₃]		823s 835s 1320vs 1343s 1410vs, br	} δ } ν _s } ν _a
3Q [Rhpy ₃ Cl(NO ₂) ₂]	335m 823s 835s 1314s 1342m ca.1430w	328s, br 348s 823s 836s 1315s 1325s 1342s 1410vs	(Rh-NO ₂) (Rh-Cl) } δ } ν _s } ν _a

a: reference 22
 b: reference 16
 c: reference 23
 d: reference 21

studies suggest that there is no definite basis for differentiating among N-bonded, O-bonded, O,O-chelated and N,O-bridging nitrite ligands. However, the apparent absence of absorption (other than pyridine ring bands) between 1250-1000 cm^{-1} seems to rule out the latter three isomers in 3Q (Table 3.4) while the strongest $\nu(\text{N-O})$ band occurs at 1410 cm^{-1} in 3P and 3Q, and this is associated with nitrorhodium complexes. Hence 3Q is formulated as 1-chloro-2,6-dinitro-3,4,5-tripyridine-rhodium(III).

3.2.(vi) Ethylenediamine

Treatment of 3A with basic materials tends to give hydrolysed products, so partly neutralised ethylenediamine was used, the mole ratios of 3A:en:HCl being 1:2:1. Meyer and Kienitz⁽²⁴⁾ claimed the preparation of $\text{Rhpy}_2\text{enCl}_3$ by the reaction of 3A with ethylenediamine, but this path has been disputed⁽²⁵⁾. However, after refluxing the above system in water, and evaporating down the solution, one obtains larger tabular yellow crystals of 3R. These have the properties expected of trans-dichloroethylenediaminedipyridinerhodium(III) chloride. The electronic spectrum is compared with that of the analogous bis-(ethylenediamine) and tetrapyridine compounds in Table 3.5.a

Table 3.5a

Electronic Spectra of Trans Dichlorotetramines

Compound	λ	ϵ	Medium
3R Rhpy ₂ enCl ₃	405	124	MeOH
	(295) ^a	300(200) ^a	
	(266)	5,200	
	260	6,800	
	254	6,800	
3A Rhpy ₄ Cl ₃	410	78	MeOH
	(305) ^a	230(170) ^a	
	(268)	8,300	
	262	11,600	
	256	11,800	
t-Rhen ₂ Cl ₃	406	75	H ₂ O ^b
	286	130	

a: Gaussian resolution in λ

b: Reference 26

They are, of course, very similar and although the positions (and intensities approximately) of the pyridine $\pi \rightarrow \pi^*$ bands and of the second ligand field band may be interpolated between $t\text{-Rhpy}_4\text{Cl}_2^+$ and $t\text{-Rhen}_2\text{Cl}_2^+$ to give those of 3R, the molar absorbance of the first ligand field band of 3R is well outside the experimental errors ($\leq 5\%$) in its greatly increased (59%) value. The infra-red spectrum ($400\text{-}4000\text{ cm}^{-1}$) contains the features of that of 3A and of $t\text{-Rhen}_2\text{Cl}_3$ ⁽²²⁾, thus offering no differentiation between the alternatives of 3R being a 1:1 mixed compound of Rhpy_4Cl_3 and Rhen_2Cl_3 . The powder photographs* of 3A, 3R and trans $[\text{Rhen}_2\text{Cl}_2]\text{Cl}\cdot 3\text{H}_2\text{O}$ are quite dissimilar: neither the lines of the last compound nor 3A are reproduced in those of 3R. The absence of the $\text{Rhpy}_4\text{X}_2^+$ unit in the lattice is suggested, as a piece of negative evidence, by the absence (or weakness) of the strong Raman bands which occur at ca. 215 cm^{-1} and 270 cm^{-1} in the Raman spectrum of 3A. $\nu_s(\text{Rh-Cl})$ occurs as a very strong band at 305 cm^{-1} , while there is also a medium intensity band at 356 cm^{-1} .

The best criteria remain the visible spectra and the powder photographs, which are positive evidence for the formulation of 3R as trans $[\text{Rhen py}_2\text{Cl}_2]\text{Cl}\cdot 3\text{H}_2\text{O}$.

* See Table 3.5(b)

trans[Rh_{en}Cl₂]Cl.3H₂O

trans[Rh_{enpy}₂Cl₂]Cl.3H₂O

trans[Rh_{py}₄Cl₂]Cl.5H₂O

		12.8 vs
7.4 vs	9.65 s	
	7.4 w	7.4 vs
	7.0 s	
6.6 vs	6.8 s	6.8 vs
		6.5 vs
6.4 vs	6.4 s	6.08 s
5.89 vs	5.93 s	
	5.40 s	5.25 s
	5.20 s	5.13 s
4.88 s	5.04 m	
4.74 s	4.86 m	
	4.63 m	
	4.52 m	
4.39 m	4.34 m	
		4.26 s
4.12 m	4.12 m	4.12 m
4.02 vs	4.03 m	
3.88 s	3.86 m	
3.80 w		
	3.72 m	
3.67 m	3.68 m	3.68 vs
3.63 w	3.59 m	
3.53 w	3.53 m	
3.48 w		
3.44 w	3.45 m	3.43 m
	3.35 m	3.37 m
a	a	3.23 s
2.80 vs		a
	2.70 s	2.62 s
	2.59 s	2.42 s
		2.42 s

a: medium and weak lines omitted from here down

Rh en₂Cl₂

Rh en₂py₂Cl₂

Rh py₄Cl₂

Table 3.5b.
X-Ray Powder Diffraction d-Spacings

3.2.(vii) 1,3-Dicarbonyls

Unlike the reactions with oxalate (Chapter 4), 3A did not react readily with sodium malonate in hot aqueous solution; the product isolated had λ 410 nm., suggesting that it was a salt of $\text{Rhpy}_4\text{Cl}_2^+$. Addition of borohydride as a catalyst yielded quite soluble, golden yellow crystals with the λ 388 nm. expected for an $\text{RhN}_3\text{O}_2\text{Cl}$ chromophore and strong broad infrared absorption at 1625 cm^{-1} , which is low for a carbonyl. However, analytical results indicated the incorrect C:N ratio (calculated 6:1, found 5.3:1) for the above formulation while the compound had a measurable conductivity ($\lambda = 0.038\text{ cm}^2\text{ohm}^{-1}\text{g}^{-1}$ in MeNO_2). The reaction with sodium acetylacetonate also required catalysis, but the product obtained was a yellow-brown gum which did not have the expected d-d band. Salicylaldehyde could not be induced readily to form a complex by reaction with 3A, the only products obtained being salts of $\text{t-Rhpy}_4\text{Cl}_2^+$ and its hydrolysate.

3.2.(viii) Phenanthroline and Bipyridyl

Surprisingly, perhaps, the addition to a 2:1 mole ratio of 1:10-phenanthroline to the chloro-complex of

3A, of degassed water in vacuo, did not lead to the formation of a 1:10-phenanthroline-rhodium complex, whereas $\text{Rhphen}_2\text{Cl}_3$ is the product formed when 3A is fused⁽²⁷⁾ in phenanthroline. In this connection, Rund⁽²⁸⁾ found that 1:10-phenanthroline has an inhibitory effect on reactions within the rhodium(III)-pyridine system, and attributed this to "scavenging" of the catalytic intermediate by the chelating agent.

When ethanol was added as catalyst for the reaction with phenanthroline, a pink colour developed in the solution, and an absorption band appeared at ca. 550 nm. The yellow product recovered was unchanged trans-Rhpy₄Cl₃ identified by its elemental analysis (C,H,N), UV spectrum (λ 410 nm.) and characteristic appearance.

The use of borohydride, intended to act as catalyst, led to similar results for the reactions with both 2,2'-bipyridyl and 1:10-phenanthroline. There appeared in each case a pink colour in the solution as above, and this is reminiscent of the observations of Martin and Waind⁽²⁹⁾ and of Kulasingam et al.⁽³⁰⁾ whose preparations of the bis- and tris- chelated species contained small amounts of coloured materials. Indeed, further addition of sodium borohydride, now in equivalent rather than catalytic proportion, caused deepening of the

colour to reddish-purple, and eventually resulted in the precipitation of purple solids from each solution. These are undoubtedly analogous to the "red-violet" compounds of rhodium with 2,2'-bipyridyl which were isolated by Martin et al.⁽³¹⁾, and characterised as bis-complexes of rhodium(I) and rhodium(II) (paramagnetic species). They were unable to define the exact nature of the compounds, i.e. whether they were four or six-coordinate about the metal ion, and consequently whether they were monomeric, dimeric, or even polymeric, the last being suggested by the compounds' low solubilities in common solvents. Similarly, the use of bis- or tris-chelates of rhodium(III) with 1:10-phenanthroline or 2,2'-bipyridyl as starting materials leads to the formation of coloured compounds. With chloride, hydroxyl and borohydride as possible ligands or counter ions, the deep purple compounds of rhodium obtained are stable in an inert atmosphere but not in the presence of oxygen. The 2,2'-bipyridyl species is aeri ally oxidised in a few hours to a brown substance, while its 1:10-phenanthroline counterpart is stable toward air for several days before any oxidation is apparent. Again, the product is a brown material. The oxidation is more rapid if the purple compounds are damp. The relative stabilities of the compounds toward oxygen parallels

their relative preparability; thus borohydride or sodium amalgam was shown to be necessary in the 2,2'-bipyridyl case^(31c), while ethanol is an adequately strong reductant to at least cause colouration of solutions of rhodium(III) phenanthroline compounds. Neither the purple bipyridyl nor the phenanthroline rhodium chelates gave satisfactory X-ray powder photographs, and although the time required for making exposures is 2-4 hours, the phenanthroline compound should have remained stable for that time, and this means that the substances obtained were too disordered to have reproducible interplanar spacings, which supports a polymeric formulation.

The 1:10-phenanthroline chelate, after drying, is fairly insoluble in water and ethanol, but moderately soluble in methyl cyanide, in which it gave a purple solution. The analytical figures indicated it was either impure or nonstoichiometric, as it contained boron (0.51%) from the borohydride and too little chloride (1.02%) to be a pure monomeric chloro-complex. Hence it may contain BH_4^- as counter-ion (partly) and would probably be purer if prepared by an electrochemical method. The magnetic properties were not investigated. The solution in MeCN had a peak at 547 nm. ($\epsilon \approx 3000$), a shoulder at ca. 440 nm. (~ 2500), and other strong

absorptions in the UV; the ϵ estimates are based on a formula weight derived from the analytical data (C, 56.0; H, 4.0; N, 11.1%) for a bis-chelated cation, by analogy with the known bipyridyl compounds. The colour of the solutions depended on the solvent used, thus in MeNO_2 the solution was redder than in MeCN, while in 12M nitric acid gave initially a red-purple solution, which rapidly turned deep blue, presumably as the result of oxidation of the complex. In contrast, ozone oxidises the compound (suspension in aqueous ethanol) only slowly, to give a pale yellow solution.

The 2,2'-bipyridyl chelate, when suspended in chloroform and subjected to passage of chlorine, faded from purple to tan in colour. The tan compound was recrystallised from methanol and gave a good yield of cis-dichlorobis(2,2'-bipyridyl)rhodium(III) chloride, as yellow prisms, their character confirmed by elemental analysis and their UV spectrum⁽²⁷⁾.

These observations support the contention that rhodium chelates are formed in which apparently low oxidation states are stabilised by the π -delocalising ligands. The oxidative decolouration of these substances corresponds to the formation of "normal" rhodium(III)

complexes. The intense absorptions in the visible spectra are attributable to metal-to-ligand, $d\pi^* \rightarrow p\pi^*$ transitions, signifying that the formally equivalent $Rh^{III}-L^0$ and $Rh^{II}-L^{-1}$ formulations cannot be reliably distinguished, though, of course, any real description of the compounds will be a hybrid of these extremes. The reaction with HNO_3 is less straightforward and may involve either oxidation to rhodium(IV), say, or not improbably, nitrosation of the heterocyclic ligand in a manner analogous to the reaction of salicylato-bis(ethylenediamine)cobalt(III) with nitric acid, which yields a highly coloured compound⁽³²⁾.

3.3 The Hydrolysis of $t-Rhpy_4X_2^+$

3.3.(i) Some Experimental Observations

When trans-dibromotetrapyridinerhodium(III)bromide is recrystallised from two molar aqueous sodium bromide solution there is obtained firstly a small amount of insoluble 1,2,6- $Rhpy_3Br_3$, then the trans $[Rhpy_4Br_2]Br \cdot 5H_2O$ while the remaining solution is still yellow and has an electronic absorption band at ca. 370 nm., there being no appreciable absorption at longer wavelength. Similarly, when an aqueous solution ($5 \times 10^{-3}M$) of

Rhpy_4Br_3 is heated at 85° for an hour, the 441 nm. peak diminishes in intensity by 11%, while the successive spectra share an isosbestic point at 413 nm. (Figure 3.1). No further change occurs over a period of three hours.

In an attempt to substitute bromide by fluoride, Rhpy_4Br_3 was heated at ca. 85° in approximately 4M potassium fluoride solution (initial pH 6.5). The 441 nm. band disappeared with a half life of ca. 5 min. and was replaced by a band at 370 nm., isosbestic points developing at 365 and 413 nm. The solution produced was examined by ^{19}F n.m.r. but any coordinated fluoride was too small in concentration to be detected. The product was separated from KF by dialysis and recrystallised as orange-yellow prisms of the perchlorate, 3S, which was found to contain no fluorine, but to be the salt of the hydrolysate $[\text{Rhpy}_4\text{Br}(\text{OH})]^+$.

One would expect the degree of hydrolysis observed to be a function of the pH attained by the solution, which will determine the rate of attack by hydroxyl ion. As bromide is lost, the overall reaction should lead to increasing acidity of the solution, as the cationic aquo-complex will be a stronger acid than unbound water. Hence only 10% is hydrolysed in water alone, but ca. 25% in sulphate ($\text{pK}_a \sim 2$) solution, virtually 100% in fluoride

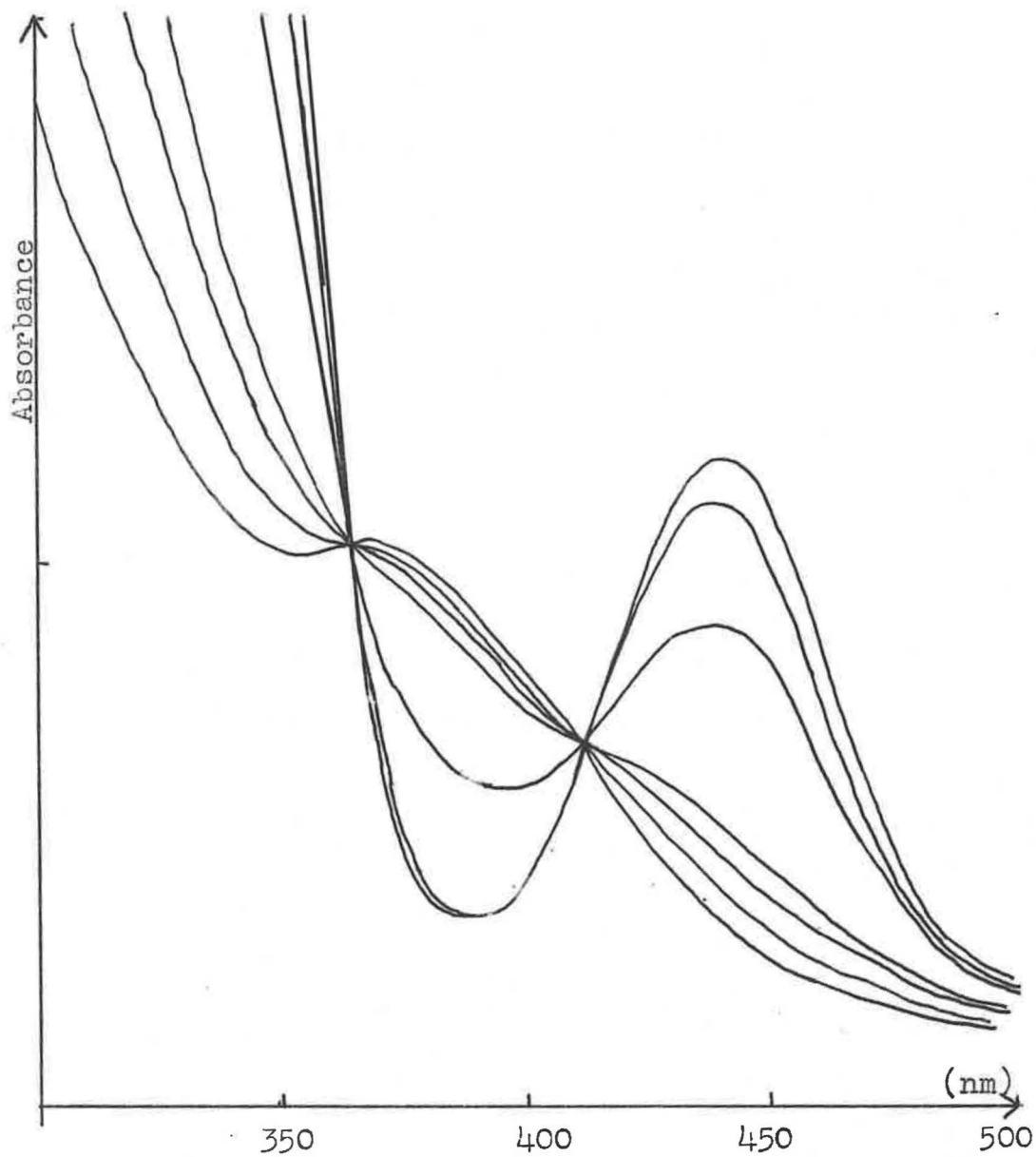


Fig. 3.1 Hydrolysis of trans- $\text{Rhpy}_4\text{Br}_2^+$ by F^-

($pK_a \sim 3.1$) and 100% in acetate ($pK_a \sim 4.5$) as buffer.

In view of the qualitative observations that $t\text{-Rhpy}_4\text{Br}_2^+$ is not hydrolysed rapidly even at 100° at pH 12-13, and quite slowly at pH 10-12 whereas KF can be effective as an hydrolysing agent, it is possible that ionic strength may be an important factor; Poë's group have recently found⁽³³⁾ that fluoride ions inhibit the anation of $\text{trans}[\text{Rhen}_2\text{Br}(\text{OH}_2)]^{2+}$ by chloride, so it is not surprising that it assists the reverse type of reaction. The anion (F^- , CH_3CO_2^-) may serve as the attacking species to form an intermediate which is highly vulnerable to hydrolysis, while the Br^- becomes effectively "lost" in the solution. Naturally, effective buffers against acidity increase are likely to be good donors toward a metal ion as well as toward a proton, and hence possible attacking species. Indeed, the use of sodium acetate leads to formation of varying amounts of the acetato complex ($1635s$, $1296s \text{ cm}^{-1}$ in i.r.).

The reaction with sodium hydroxide in equivalent or slightly excessive concentration is catalysed by ethanol. Any autocatalysis (hydroxyl assistance) could not be detected in the qualitative experiments performed. Irradiation (Hg arc) of $0.01M$ aqueous Rhpy_4Br_3 led to ca. 30% photolysis in an hour under the conditions used,

the products being Rhpy_3Br_3 and $\text{Rhpy}_4\text{Br}(\text{OH})^+$, the former in greater amount. The use of one equivalent of silver nitrate to aid removal of Br^- gave unsatisfactory results for both chloride and bromide.

Treatment of $t\text{-Rhpy}_4\text{Cl}_3$ with KF leads to hydrolysis also, but the rate is certainly lower under comparable conditions, and the same applies for acetate hydrolysis. The reaction with hydroxyl is catalysed by ethanol and the chlorohydroxo species may be prepared thus.

The bromohydroxo complex 3S takes up a proton in acid solution, to yield the trans-aquobromotetrapyridine-rhodium(III) dication, which may be crystallised as the orange perchlorate, 3T. This contains two molecules of water of crystallisation which are removed readily by desiccation to give the anhydrate 3U.

3.3.(ii) Spectroscopic Characterisation

Spectroscopic examination of the compounds reveals medium intensity absorption at 3565 cm^{-1} and a strong band at ca. 550 cm^{-1} in 3S, 3W. Recrystallisation of 3S from D_2O gives rise to a medium band at 2640 cm^{-1} . This is the position expected for $\nu(\text{O-D})$ shifted down from 3565 cm^{-1} (calc. 2595 cm^{-1}) while its relative

Table 3.6

Selected Vibrational Bands of Hydrolysates

Compound	Raman (cm^{-1})	Infrared (cm^{-1})	Origin
3S [Rhpy ₄ Br(OH)](ClO ₄)	226s	230s, br) ν (Rh-py)
	262s		
	321s	318s) ν_2 (ClO ₄ ⁻)
	463s		
	540m	547s	
	557s) ν (Rh-O)
		2640m	
	3565m	ν (O-H) (b)	
3T, 3U [Rhpy ₄ Br(OH ₂)] ²⁺	208m	208s (a)) ν (Rh-Br)
	225m	225m (a)	
	260m) ν (Rh-py)
	324m	316s (a)	
	436m		
		2520m, br	ν (O-D)
		3400m, br	ν (O-H)
	3440m, br (a)	ν (O-H) (c)	
3V [Rhpy ₄ Br(OH ₂)](PF ₆) ₂		557s	ν (PF ₆ ⁻)
		3560s	ν (O-H)
3W [Rhpy ₄ Cl(OH)]ClO ₄		315m) ν (Rh-Cl)
		328m	
		370m	
	552s	553s) ν (Rh-O)
		3565m	
3X [Rhpy ₄ Cl(OH ₂)](ClO ₄) ₂	366s		ν (Rh-Cl)
		3430s, br	ν (O-H)

a: 3U

b: coordinated OH⁻c: coordinated OH₂

sharpness also suggests the specificity of environment consistent with the bonded hydroxyl's.

The band at 550 cm^{-1} is a feature of the hydroxo complexes only, occurring in 3S and 3W but not in the aquo complexes 3T, 3U nor in salts of $t\text{-Rhpy}_4\text{X}_2^+$. Synthesis of the hexafluorophosphate salt, 3V, analogous to the perchlorate 3U enables it to be demonstrated (analysis, i.r.) that 3T, 3U are indeed aquo complexes and rules out the possibility of their being perchlorato-complexes. If the 550 cm^{-1} band is $\nu(\text{Rh-O})$ then it would be expected to appear in the aquo-complexes as well; a rationale for its absence is that the additional proton's effect is to greatly decrease the intensities in the Raman and i.r. and probably change the band's position also. Notably, a solution of commercial rhodium trichloride in 8M sodium hydroxide has a broad ($\Delta \nu_{\frac{1}{2}} \sim 80 \text{ cm}^{-1}$) Raman effect band centred at 535 cm^{-1} and such a solution must contain hydroxorhodium species as the first distinct electronic absorption (410 nm.) implies an environment with 3 or more oxygen ligands. Vibrational assignments are suggested in Table 3.6.

The electronic spectra of the hydroxo-complexes are as expected (Table 3.7). Trans $[\text{Rhpy}_4\text{Br}(\text{OH})]^+$ has $\lambda 371 \text{ nm.}$, cf. trans $[\text{Rhen}_2\text{Br}(\text{OH})]^+$ with $\lambda 370 \text{ nm.}$, ($\epsilon = 103$)(34).

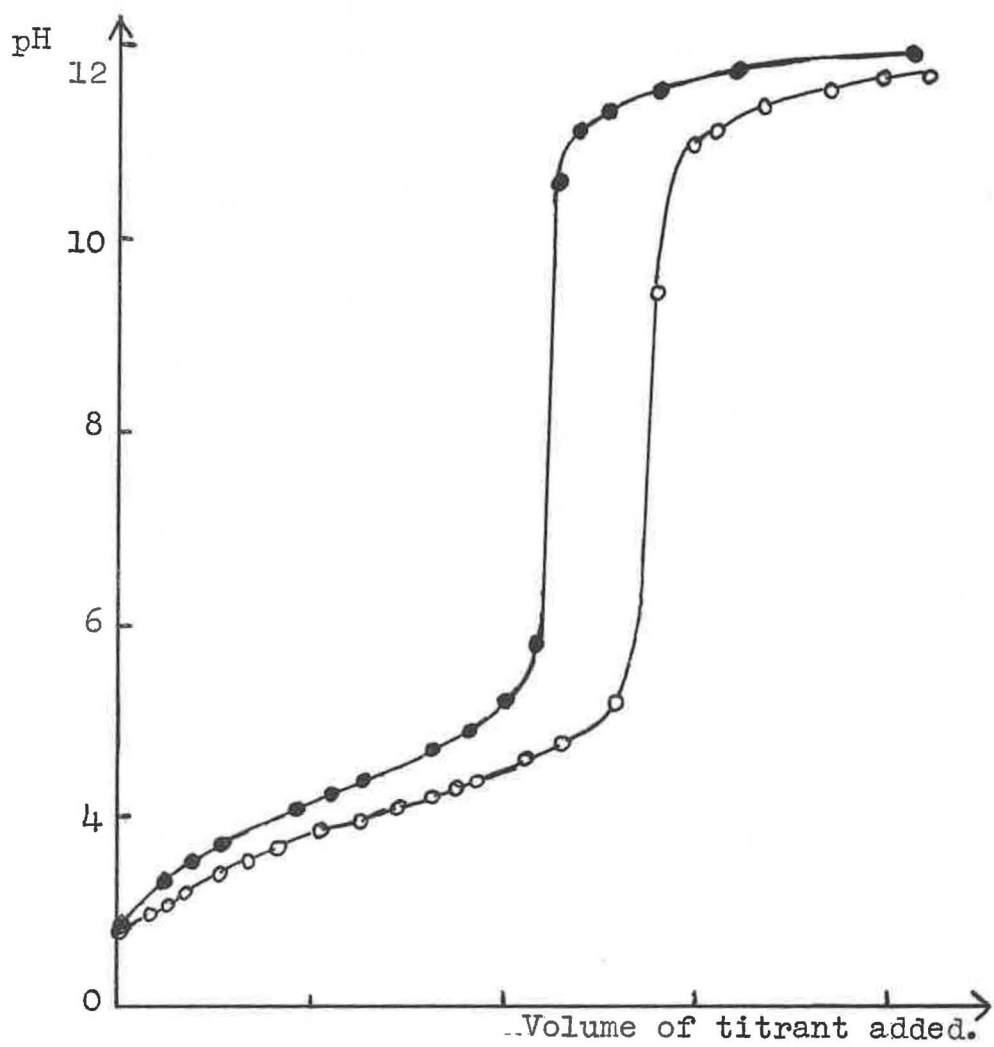


Fig.3.2 Titration curves for (○-○-○) trans- $[\text{Rhpy}_4\text{Cl}(\text{OH}_2)]^{2+}$ and (●-●-●) trans- $[\text{Rhpy}_4\text{Br}(\text{OH}_2)]^{2+}$ with sodium hydroxide in aqueous methanol.

In acidic solution, the aquo-bromo complex forms, and the spectrum changes accordingly. In order to find out which species predominates at any given pH, the pKa value of the coordinated water was determined by pH titration of the aquo-complexes 3T, 3X in 50% v/v aqueous methanol. The curves are shown in Figure 3.2. Duplicate titrations yielded equivalent weights, for 3T as an acid of 751 and 755 (calc. 752) and the pKa was estimated to be 4.21 ± 0.05 under these conditions. Any effect of the mixed solvent was not considered. The titration of 3X yielded an equivalent weight of 720 (calculated 688) and a pKa value of 4.00 ± 0.05 . The change in pKa observed is small (0.2 pKa units) but in the direction expected if one attributes to coordinated chloride a greater electron withdrawing power than bromide, in accord with the classical viewpoint. Similar compounds of ethylenediamine with rhodium(III) have higher pKa values⁽³⁴⁾ and as the trend may be attributed to increasing basicity of the nitrogenous donor, it would be interesting to see if the effect of variation of the pyridine pKa by substitution is transmitted via the metal ion.

Spectroscopic studies at pH 1-2 should therefore be concerned solely with the aquo-complex. The two bands

Table 3.7

Electronic Spectra of Hydrolysates

<u>Compound</u>	<u>λ(nm)</u>	<u>ϵ</u>	<u>Medium</u>
Br 3S	371	180	MeOH, pH 10 MeOH
	(283) ^a	2200	
	(267)	9200	
	261	12000	
	(255)	12500	
	234	28100	
Br 3T	(465) ^a	48	H ₂ O, pH 1.5 pH 1
	406	82	
	(268)	7600	
	261	9300	
	<u>ca.</u> 248	9800	
3T	<u>ca.</u> 470	1	Solid (b)
	<u>ca.</u> 408	1.2	
3T	500	53	11M. HClO ₄
	430	52	
Cl 3W	359	130	H ₂ O, pH 12
	(315)	200	
	(268)	8700	
	261	12000	
	255	11900	
	(235)	19000	
Cl 3X	390	63	H ₂ O, pH 1
	(315)	150	
Cl 3X	405	49	11M. HClO ₄
	(266)	7100	
	260	9400	
	254	8300	
	219	29000	

a: by Gaussian resolution in λ .

b: reflectance spectrum; relative peak heights in ϵ column will underestimate ϵ ratio of larger to smaller peak.

at 406, 465 nm. are comparable with those observed in trans[Rh_{en}Br(OH₂)]²⁺ at 395, 465 nm. ($\epsilon = 48, 26$ respectively), the shift to longer wavelength presumably being the result of tetragonal splitting of the first d-d band in the rhodium's C_{4v} environment. This follows from the generalisation that H₂O is considered to have a crystal field effect marginally stronger than that of OH⁻. The low energy bands are mentioned again in Chapter 4. The chloroaquo ion has only one distinct band in this region, which suggests that one of the bromoaquo ion's bands may arise from a spin-forbidden transition. The reflectance spectrum of crystalline 3T, the trans-bromo-aquotetrapyriderhodium(III) salt, confirms the nature of the chromophore at pH 1-2 in solution. It is noteworthy that in 11M perchloric acid solution the spectrum of the bromoaquo cation 3T is markedly changed; the 406 nm. band in particular shifts to longer wavelength and at the same time diminishes in intensity. Presumably further protonation occurs in these extremely acid conditions, probably at the coordinated water, forming a coordinated oxonium ion.

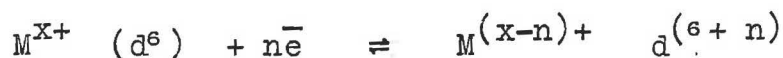
The anation of $t\text{-Rhpy}_4\text{X}(\text{OH}_2)^{+2}$ is readily accomplished by warming a solution in the appropriate acid. Hence, for $\text{X} = \text{Cl}$, $t\text{-Rhpy}_4\text{Cl}_2^+$ is formed with HCl ; for $\text{X} = \text{Br}$, HBr yields $t\text{-Rhpy}_4\text{Br}_2^+$; while the action of HCl on the bromoaquo compound 3T gives trans-bromochlorotetrapyridinerhodium(III). The orange-yellow fluoroborate salt 3Y has been characterised and some of its properties are discussed in Chapter 1.

3.4 Polarographic Studies of the Compounds

The interrelation between the polarographically measured redox potential and the spectroscopic properties of transition metal complexes has been elaborated by Vlček^v(35).

If a six-coordinated metal has $(6+n)$ electrons say, in the d-subshell, then it is apparent from the usual crystal field criteria that as the crystal field strength is increased, the tendency for spin-pairing into a $t_{2g}^6 e_g^n$ configuration increases. The point when the energy required for the transition ($10 Dq$) exceeds that expended in overcoming the interelectronic repulsions involved in pairing electrons in an orbital has been deduced for several metal ions from examination of their magnetic and spectroscopic properties. As the parameter $10 Dq$ increases, the t_{2g}^6 subset are stabilised and the e_g^n are raised in energy, the latter having an effect analogous to reducing the ionisation potential of an e_g electron. Hence it is easier to oxidise d^7 Co(II) by placing it in an environment of cyanide ions, where the large Dq tends to spin pair the $Co(CN)_5^{3-}$ ion, allowing removal of the destabilised e_g (approx) electron, than it is to remove the e_g electron from hexaquocobaltate(II),

say. Conversely, the process



will release more energy at the point of the n-electron transfer if $10 Dq$ is smaller, so that the e_g orbitals are lower in the potential energy well. Vlček's view is that a pre-excitation mechanism operates, such that following a $t_{2g} \rightarrow e_g$ promotion in the complex, the (reducing) electrons are accepted into the t_{2g} orbital vacated. This is an electron transfer mechanism in which electrons pass through the face of the coordination octahedron, while the first description (without prior electron promotion) applies to a process involving charge transfer through a coordinated ligand.

For complexes of trivalent rhodium and cobalt, distinct correlations have been found between $E_{\frac{1}{2}}$ and the energy of the first spin allowed transition. Notably, complexes of the type $[Rhen_3XY]^+$ have been studied^(36,37). Crow's data⁽³⁷⁾ yield a straight line with slope 4.4×10^{-5} v.cm. for the plot of the $E_{\frac{1}{2}}$ for the complexes versus Δv , (the difference between the energy of the first spin allowed transition in $[Rhen_3]^{3+}$ and the first singlet-singlet band in the complexes); those investigated had X, Y = NO_2^- , NCS^- , I^- , Br^- , Cl^- . For a similar group of trans- $Rhen_2XY^+$

Table 3.8

Polarographic Properties of Rhodium Complexes

Species	$-E_{1/2}$ (v. vs SCE)	ν (kK)	Source
\underline{t} -Rhpy ₄ Cl ₂ ⁺	0.21	24.4	a, 38
\underline{t} -Rhpy ₄ ClBr ⁺	0.22	23.5	"
\underline{t} -Rhpy ₄ Br ₂ ⁺	0.27	22.7	"
\underline{t} -Rhpy ₄ I ₂ ⁺	0.25 ^b	20.5	"
\underline{t} -Rhpy ₄ Cl(OH) ⁺	0.34	27.8	"
\underline{t} -Rhpy ₄ Br(OH) ⁺	0.26	27.0	"
\underline{t} -Rhpy ₄ (N ₃) ₂ ⁺	0.32	24.5	"
\underline{t} -Rh _{lut} ₄ Cl ₂ ⁺	0.11b	24.4	"
\underline{t} -Rh(4Etpy) ₄ Cl ₂ ⁺	0.36	24.4	"
\underline{t} -Rhp _{ic} ₄ Cl ₂ ⁺	0.39	24.4	"
\underline{t} -Rhp _{ic} ₄ Br ₂ ⁺	0.31d	22.8	f, 38
\underline{t} -Rh(3Mepy) ₄ Cl ₂ ⁺	0.24	24.4	"
\underline{t} -Rh(3Mepy) ₄ Br ₂ ⁺	0.26d	22.7	"
\underline{t} -Rh(3Etpy) ₄ Cl ₂ ⁺	0.27	24.4	"
\underline{t} -Rh(4NH ₂ py) ₄ Cl ₂ ⁺	0.47	24.4	"
\underline{t} -Rh(3NH ₂ py) ₄ Cl ₂ ⁺	0.20	24.4	"
\underline{t} -Rh(3Clpy) ₄ Cl ₂ ⁺	0.14	24.5	a, 38
\underline{t} -Rh(iquin ₄)Cl ₂ ⁺	0.22	24.4	"
\underline{t} -Rh(pz1) ₄ Cl ₂ ⁺	0.24	24.6	"
\underline{t} -Rh(thz) ₄ Cl ₂ ⁺	0.15	24.5	"
\underline{t} -Rh(thz) ₄ Br ₂ ⁺	0.18	22.8	"
\underline{t} -Rh(prm) ₄ Cl ₂ ⁺	0.12	24.5	"
\underline{mer} -Rhp _{ic} ₃ ClOx	0.41b	25.8	"
\underline{c} -Rhpy ₂ Cl ₄ ⁻	0.08	22.4	"
\underline{t} -RhA ₄ Cl ₂ ⁺	0.56	24.5	"
\underline{t} -Rhen ₂ Cl ₂ ⁺	0.70	24.6	26, 37, 38
\underline{t} -Rhen ₂ ClBr ⁺	0.77	24.0	26, 36
\underline{t} -Rhen ₂ I ₂ ⁺	0.60	21.6	26, 37
\underline{t} -Rhen ₂ Cl(NCS) ⁺	0.82	27.6	26, 37

continued

Table 3.8 - Continued

Species	$-E_2$ (v. vs SCE)	(kK)	Source
\underline{t} -Rhen ₂ (NO ₂) ⁺	1.14	33.3	26,37
\underline{c} -Rhen ₂ Cl ₂ ⁺	0.76	28.4	26,38
\underline{c} -RhtrienCl ₂ ⁺	0.70	28.4	26,38
Rhen ₃ ³⁺	0.72b	33.2	38,44
Rhpn ₃ ³⁺	0.54	33.2	38
RhA ₅ Cl ₂ ²⁺	0.94	28.7	43,44
RhA ₅ (OH) ²⁺	1.10e	31.2	7,45a
Rh(H ₂ EDTA)Cl ₂ ⁻	0.73	24.9	36
RhOx ₃ ³⁻	0.83	26.0	13,39
Rh(CN) ₆ ³⁻	1.54	44.5	41,42
Rh(SCN) ₆ ³⁻	0.39	19.6	42,43
RhCl ₆ ³⁻	ca. 0	16.1	a,38
\underline{t} -Rh(OH ₂) ₄ Cl ₂ ⁺	"	22.2	38,46
Rh(OH ₂) ₃ Cl ₃	"	21.2	38,46
Rh(OH ₂) ₆ ³⁺	0.35	25.2	38,44

a: this work

b: not a well-defined wave

c: 0.1M-KNO₃, pH 8.

d: in 0.1M KBr

e: variation by supporting electrolyte

f: reference 51

H₄EDTA : Ethylenediaminetetra-acetic acid.

ions, Gillard et. al.⁽³⁶⁾ quote a slope of -3.3×10^{-5} v.cm.⁻² ($\Delta\nu$ relative to $\text{Rh}(\text{NH}_3)_6^{3+}$) but related to Rhen_3^{3+} , their data fit well a line of slope 3.0×10^{-5} v.cm. The latter work revealed also that trans $[\text{Rhpy}_4\text{Cl}_2]^+$ and the dibromo-analogue did not fit the line. In Figure 3.3 is depicted the plot of $E_{\frac{1}{2}}$ vs. ν_1 the energy of the first observed (usually the singlet-singlet) transition, for a series of rhodium(III) complexes, from the data of Table 3.8. It was not appreciated by some electrochemical workers that the complexes of rhodium(III) are, as Jørgensen puts it⁽¹³⁾, quite robust, so that until recently polarographic studies have not always been performed on well-defined compounds. The complexity of behaviour of $t\text{-Rhpy}_4\text{Cl}_2^+$ complexes recently thwarted^(45b) the application of polarography as an analytical tool for rhodium.

Inspection of Figure 3.3 reveals that the bis(ethylenediamine)rhodium compounds do indeed lie in the region of a straight line, which is reinforced by other compounds with presumably innocent ligands, i.e. $[\text{RhA}_5(\text{OH})]^{2+}$, $[\text{RhOx}_3]^{3-}$, $[\text{Rh}(\text{CN})_6]^{3-}$. The relationship is approximately

$$E_{\frac{1}{2}} = -4.0 \times 10^{-5} \nu + 0.25 \quad (\text{sloped line, Figure 3.3})$$

where $E_{\frac{1}{2}}$ is in volts relative to a SCE, ν is in wave-numbers.

However, the correlation observed for these is violated by a large group of points with $E_{\frac{1}{2}}$ values more positive than would be predicted. These are the complexes of type trans[RhL₄XY]ⁿ⁺ where L is an heteroaromatic ligand, but the compounds are directly analogous to the trans[Rhen₂XY]⁺ type.

In the case of the ethylenediamine, cyanide and ammine compounds, hydridic species have been isolated and characterised, but only observed reliably in solution (by n.m.r.) for the pyridine and trien complexes. This suggests that the oxidising power of Rh(III) in the trien and heterocyclic compounds is sufficient to destabilise hydride by the equilibrium



This does not affect the observation that all the polarographic half waves observed correspond to a two-electron reduction, as the polarography is a probe for the primary process only.

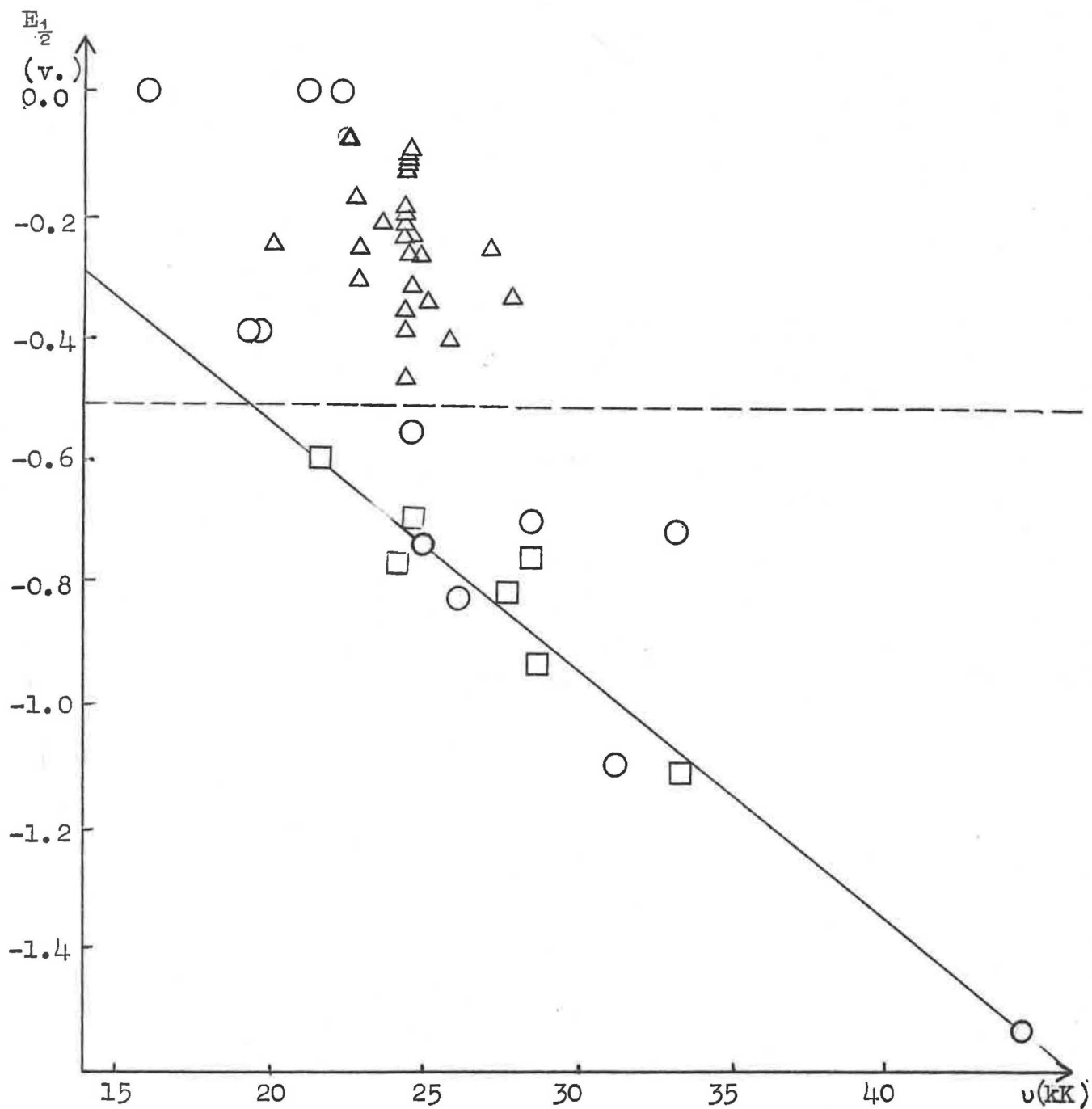


Fig. 3.3. Schema of the distribution of $E_{1/2}:\nu$ points for Rh^{III} compounds. See table 3.8 Δ : aromatic amine complexes; \square bis/en complexes; \circ others.

Coordinated water appears to have a discrepant effect, in that $t[\text{Rhpy}_4\text{X}(\text{OH}_2)]^{2+}$ have no waves, while there is probably a current increase near 0.0v., but this may be due to an anodic mercury wave. Even the $[\text{Rh}(\text{H}_2\text{O})_x\text{Cl}_{6-x}]^{3-x}$ species have $E_{\frac{1}{2}}$ values very close to 0v.

The points relating to the tetrapyridine complexes do not obey the thesis of inverse proportionality between $E_{\frac{1}{2}}$ and ν as the ethylenediamine compounds do; in $[\text{Rhpy}_4\text{XY}]^{n+}$, for example, the sequence $\text{XY} = \text{Cl}_2, \text{Br}(\text{OH}), \text{Br}_2$ is in fact the reverse of that expected. The pyridine chloro-complexes, inter alia, on a less sensitive scale, appear to have some correlation only in that $[\text{RhCl}_6]^{3-}$, cis $[\text{Rhpy}_2\text{Cl}_4]^-$ and trans $[\text{Rhpy}_4\text{Cl}_2]^+$ are in the expected order.

The points related to $[\text{Rh}(\text{SCN})_6]^{3-}$. " RhCl_3 " trans $[\text{RhA}_4\text{Cl}_2]^+$, $[\text{Rhpn}_3]^{3-}$ tend to lie in a "no man's land" as it were. Rationalisation of this observation for these propylenediamine and sulphur-donor ligand complexes of rhodium is evasive, as one would

reasonably expect them to behave similarly to their ethylenediamine analogues. Apart from these compounds, the first two may be accounted for within the category of the heteroaromatic base complexes in general. Thus there are two possible effects which can be proposed but which are not really distinguishable in any given case. Firstly, that the "oxidised" compounds are readily reduced by virtue of their electronic structure only, so that where there are ligands with a $d\pi$ -delocalising effect, the reducing electrons may enter via an orbital which is not localised on the metal ion, so that the d-d transition energies are not representative of the reducibility. This is applicable to the S-ligated hexathiocyanate and to the heteroaromatic ligands, which have both occupied and unoccupied π systems, so that electron transfer may occur through a pyridine π^* orbital, say, " RhCl_3 " which is probably polymeric⁽⁴⁷⁾ (or oligomeric) now appears, on the basis of the present results to be more "anomalous" than the other chloroaquo monomers, but the suggestion⁽⁴⁸⁾ that platinoid metal halide aggregates may have π -delocalising, "electron sink" properties may still be relevant.

The second explication follows from the stereochemical points raised in Chapters 1 and 4. The ease of reduction

of the heterocyclic ligand complexes may be related to the release of constraint applied to the heterocyclic rings by any rotation-restricting effect of the halogen ligands; i.e. one deduces that the process



for example, would involve a larger entropy increase than the cases where the (degree of) freedom of the nitrogenous ligands is unchanged. Hence ΔS would be greater than for similar complexes with ethylenediamine, or even 2,2'-bipyridyl or 1:10-phenanthroline. The latter ($\text{Rhphen}_2\text{X}_2^+$, $\text{Rhbipty}_2\text{X}_2^+$) unfortunately do not give distinct polarograms⁽³⁸⁾, but even that in itself may have little bearing on either approach. Restricted rotation of a monocyclic heteroaromatic ligand has been invoked⁽⁴⁹⁾ in the past to account for the entropy contributions to equilibrium constants involving metal complexes of such ligands.

It is noted that there seems to be little parallel between a species' charge and its $E_{1/2}$, which implies that this is probably not a factor which will enter into the discussion of the variation of $E_{1/2}$ with structure and composition. The effects of pyridine ring substituents

on $E_{\frac{1}{2}}$ may be summarised⁽³⁸⁾ thus: (i) β -substituted pyridines are similar to pyridine itself; (ii) γ -substitution has a greater effect on $E_{\frac{1}{2}}$; (iii) γ -substitution leads to $E_{\frac{1}{2}}$ values more negative than β -substituted pyridines; (iv) the dichloro complex is less readily oxidised than the dibromo complex for the γ -substituted pyridines, whereas the reverse is true for (β -substituted) pyridine(s). There is no palpable rationale for this behaviour, although even combined with the other heterocyclic ligands, the number of results available does not match the complexity of the problem.

Finally, the (dashed) horizontal line across Figure 3.3 at $E_{\frac{1}{2}} = -0.5v$. confines to the upper sector all those compounds whose substitution reactions are catalysed by ethanol, the exception being $[Rh(SCN)_6]^{3-}$, which has not been investigated in that connection.

In contrast, none of the species in the lower sector has been shown to be susceptible to ethanol catalysis in their substitution reactions. Moreover for the bis(ethylenediamine), and chloropentamine compounds, ethanol definitely has no catalytic effect.

The greater oxidising power of the heterocyclic base complexes is almost certainly the reason for the catalysis of their reactions by mild reductants, by which the

ethylenediamine compounds are unaffected. However, this interpretation may only be applied qualitatively, as the $E_{1/2}$ value is not necessarily a measure of E° for the given reduction process, but is related to it in that the difference between $E_{1/2}$ and E° is a measure of the rate of the reduction process⁽⁵⁰⁾. That is, $E_{1/2}$ is related to E° only for a "reversible" wave, for which $|E_{1/2} - E^{\circ}| < 0.05v$. and the reduction waves observed for the heterocyclic base complexes are irreversible⁽³⁸⁾.

Analytical Results for the Compounds

Compound	Code	%C		%H		%N		%Other	
		f.	c.	f.	c.	f.	c.	f.	c.
[Rhpy ₄ Cl ₂]Br.HBr.3H ₂ O	3B	33.6	34.1	3.2	3.8	8.2	8.0		
<u>trans</u> [Rhpy ₄ I ₂]I.3H ₂ O	3C	28.1	28.1	3.1	3.1	7.0	6.6	I,46.8	44.6
1,2,6-Rhpy ₃ (N ₃) ₃	3D	38.7	38.6	3.2	3.2	36.0	36.0		
<u>trans</u> [Rhpy ₄ (N ₃) ₂]N ₃ .5H ₂ O	3E	38.0	37.8	5.1	4.8	28.9	28.7		
<u>trans</u> [Rhpy ₄ (N ₃) ₂]BF ₄	3F	40.5	40.7	3.5	3.4	23.5	23.7	(Λ = 58)	
(NEt ₄)[Rhpy ₂ (N ₃) ₄]	3G	38.5	38.6	5.3	5.4	37.3	37.6		
1,2,6-Rhpic ₃ (N ₃) ₃	3H	42.7	42.5	4.2	4.2	33.3	33.1		
<u>trans</u> [Rhpy ₄ Cl ₂]NCS	3K	45.5	46.0	3.7	3.7	13.0	12.8	(Λ = 80)	
1,2-6-Rhpy ₃ (NCO) ₂ Cl	3L	44.5	44.4	3.4	3.3	15.1	15.2	O, 6.8 Cl, 7.6	7.0 7.7
1,2-6-Rhpy ₃ (NCO) ₂ Br	3M	40.0	40.5	3.0	3.0	13.9	13.9		
1,2,6-Rhpy ₃ (NO ₂) ₃	3P	37.9	37.7	3.1	3.2	17.2	17.6		
1,2-6-Rhpy ₃ (NO ₂) ₂ Cl	3Q	38.7	38.5	3.2	3.2	15.2	15.0	Cl, 5.9	7.6
<u>trans</u> [Rhpy ₂ enCl ₂]Cl.3H ₂ O	3R	29.8	29.9	6.3	5.0	11.3	11.6		
<u>trans</u> [Rhpy ₄ Br(OH)]ClO ₄	3S	38.7	39.0	3.6	3.4	9.6	9.1	Br,12.7 Cl, 5.5	13.0 5.8
<u>trans</u> [Rhpy ₄ Br(OH ₂)](ClO ₄) ₂ .2H ₂ O	3T	31.6	31.9	3.4	3.5	7.5	7.5	Br,11.4	11.2
<u>trans</u> [Rhpy ₄ Br(OH ₂)](ClO ₄) ₂	3U	33.3	33.5	3.5	3.1	7.7	7.8	Br,10.3 Cl, 9.3	11.1 9.9
<u>trans</u> [Rhpy ₄ Br(OH ₂)](PF ₆) ₂	3V	29.6	29.8	2.8	2.8	6.7	6.9		
<u>trans</u> [Rhpy ₄ Cl(OH)]ClO ₄ .H ₂ O	3W	40.7	40.8	3.9	3.9	9.4	9.5	Cl,14.0	12.1
<u>trans</u> [Rhpy ₄ Cl(OH ₂)](ClO ₄) ₂ .H ₂ O	3X	32.8	33.1	2.8	4.0	7.7	7.7	Cl,15.4	14.6
<u>trans</u> [Rhpy ₄ BrCl]BF ₄	3Y	38.6	38.7	2.9	3.2	9.3	9.0	Br,12.9 Cl, 5.8	12.9 5.7

Table 3.9

References - Chapter 3

1. A.J. Poë, K. Shaw, J. Chem. Soc., 1970A 393.
2. F. Basolo, R.A. Bauer, Inorg. Chem., 1969 8 2237.
3. C.S. Davies, G.C. Lalor, J. Chem. Soc., 1969A 445.
4. H.L. Bott, E.J. Bounsall, A.J. Poë, J. Chem. Soc., 1966A 1275.
5. R.D. Gillard, B.T. Heaton, D.H. Vaughan, Chem. Comm., 1969 974.
6. F. Basolo, M.L. Morris, R.G. Pearson, Disc. Farad. Soc., 1960 29 80.
7. H.-H. Schmidtke, Z. phys. Chem. (Frankfurt), 1965 45 305.
8. D. Garthoff, H.-H. Schmidtke, J. Amer. Chem. Soc., 1967 89 1317.
9. L.A.P. Kane-Maguire, F. Basolo, R.G. Pearson, J. Amer. Chem. Soc., 1969 91 4609.
10. K. Nakamoto, "Infrared Spectra of Inorganic and Coordination Compounds", J.A. Wiley and Son, New York, 1963. (a) pp.176, (b) pp.173.
11. J. Drummond, J.S. Wood, J. Chem. Soc., 1969D 1373.
12. W.J. Potts, "Chemical Infrared Spectroscopy", Vol. 1, J. Wiley and Son, New York, 1963.
13. C.K. Jørgensen, Acta Chem. Scand., 1957 11 151.
14. J. Chatt, J.R. Dilworth, G.J. Leigh, J. Chem. Soc., 1969D 687.
15. D.M. Adams, "Metal-Ligand and Related Vibrations", E. Arnold, London, 1967.
16. J.L. Burmeister, Coord. Chem. Revs., 1968 3 225.
17. A.H. Norbury, A.I.P. Sinha, J. Chem. Soc., 1968A 1598.
18. D.A. Ramsay, J. Amer. Chem. Soc., 1952 74 72.

19. M.J. Blandamer, M.F. Fox, Chem. Revs., 1970 70 58.
20. H.L. Friedman, J. Chem. Phys., 1953 21 319.
21. F. Basolo, G. Hammaker, Inorg. Chem., 1962 1 1.
22. J.-P. Mathieu, S. Cornevin, J. Chim. Phys., 1939 36 271.
23. M. Le Postollec, J.-P. Mathieu, H. Poulet, J. Chim. Phys., 1963 60 1319.
24. J. Meyer, H. Kienitz, Z. anorg. allgem. Chem., 1939 242 281.
25. R.D. Gillard, E.D. McKenzie, M.D. Ross, J. Inorg. Nucl. Chem., 1966 28 1429.
26. S.A. Johnson, F. Basolo, Inorg. Chem., 1962 1 925.
27. R.D. Gillard, B.T. Heaton, J. Chem. Soc., 1969A 451.
28. J.V. Rund, Inorg. Chem., 1968 7 24.
29. B. Martin, G.M. Waing, J. Chem. Soc., 1958 4284.
30. G.C. Kulasingam, W.R. McWhinnie, J.D. Miller, J. Chem. Soc., 1969A 521.
31. a. B. Martin, G.M. Waing, Proc. Chem. Soc., 1958 169.
b. idem, J. Inorg. Nucl. Chem., 1958 8 551.
c. B. Martin, G. Waing, W.R. McWhinnie, J. Inorg. Nucl. Chem., 1961 23 207.
32. A.G. Beaumont, R.D. Gillard, J. Chem. Soc., 1968A 2400.
33. H.L. Bott, A.J. Poë, K. Shaw, J. Chem. Soc., 1970A 1745.
34. H.L. Bott, A.J. Poë, J. Chem. Soc., 1967A 205.
35. A.A. Vlček, Disc. Farad. Soc., 1958 26 164.
36. R.D. Gillard, J.A. Osborn, G. Wilkinson, J. Chem. Soc., 1965 4107.
37. D.R. Crow, Inorg. Nucl. Chem. Letts., 1969 5 291.
38. D.H. Vaughan, unpublished results.

39. A. Wagnerova, Coll. Czech. Chem. Comm., 1961 26 2076.
40. R.D. Gillard, J.A. Osborn, P.B. Stockwell, G. Wilkinson, Proc. Chem. Soc., 1964 284.
41. W.P. Griffith, G. Wilkinson, J. Chem. Soc., 1959 2757.
42. H.-H. Schmidtke, Z. phys. Chem. (Frankfurt), 1964 40 96.
43. J.B. Willis, J. Amer. Chem. Soc., 1944 66 1067.
44. C.K. Jørgensen, Acta Chem. Scand., 1956 10 500.
45. a. L.E. Johnston, J.A. Page, Canadian J. Chem., 1969 47 4241.
b. ibid., 1969 47 2123.
46. W.C. Wolsey, C.A. Reynolds, J. Kleinberg, Inorg. Chem., 1963 2 463.
47. R.D. Gillard, P.B. Stockwell, G. Wilkinson, Proc. Chem. Soc., 1964 284.
48. M.F. Pilbrow, Ph.D. Thesis, University of Kent, 1970, pp. 86.
49. L. Sacconi, G. Lombardo, P. Paoletti, J. Inorg. Nucl. Chem., 1958 8 217.
50. A.A. Vlček, Prog. Inorg. Chem., 1963 5 211.
51. A.W. Addison, R.D. Gillard, B.T. Heaton, to be published.

Chapter 4

Tripyridinerhodium Compounds

4.1 Halooxalatotripyridinerhodium(III); Preparation and Properties

Chlorooxalatotripyridinerhodium(III) (4A) was first prepared by Tchugaev⁽¹⁾ by the action of potassium oxalate on a boiling aqueous solution of trans-dichlorotetra-pyridinerhodium(III) chloride. It may also be obtained through the reaction of rhodium trichloride with pyridine and potassium oxalate. The former method has also been applied⁽²⁾ to the synthesis of the bromo-analogue (4B) the formation of which is marginally more facile in aqueous solution than of the chloride.

The unusual 'synergic solubility' property of 4A has been investigated⁽³⁾ and the role of 4A in elucidating the stereochemistry of the rhodium pyridine complexes has been discussed⁽³⁾.

The reaction



is, predictably (Chapter 3) subject to catalysis, and quantitative yields of 4A, 4B may be obtained conveniently via the action of a trace of sodium borohydride on an aqueous solution of the reactants. The 4-methylpyridine and 3,5-lutidine analogues (4C, 4D) are obtained similarly; the former in lesser yield, as it crystallises from water as the tetrahydrate, which is soluble in water. The four H₂O are removable by vacuum desiccation at room temperature.

The compounds Rhpy₃XOx are kinetically quite inert, although a solution of Rhpy₃ClOx in aqueous pyridine may slowly hydrolyse, while a solution in 10M H₂SO₄ certainly does so, and Rhpy₃BrOx is slightly less stable in this medium, where loss of oxalate is more likely. The aqueous pyridine solution of Rhpy₃ClOx is unaffected by addition of sodium bromide or iodide, but again, a trace of sodium borohydride catalyses substitution of the halide, and this is the method utilised for the preparation of Rhpy₃IOx, 4E. An attempt to prepare Rhpy₃(N₃)Ox by this method gave a product which still contained a lot of 4A, while more forcing conditions produced only Rhpy₃(N₃)₃.

The electronic spectra of the oxalato-complexes (Table 4.1) are as expected; the chloro-compound 4A has

Table 4.1

Electronic Spectra of Oxalato Complexes. mer-

Rhpy₃XOx

Compound	λ	ϵ	Medium
4A (X = Cl)	391	150	py + H ₂ O
	396	160	py, H ₂ O (3)
	394	130	8M H ₂ SO ₄
	(310)	500	
	(266)	9800	
	260	13000	
	253	14000	
208	47000		
4B (X = Br)	408	125	8M H ₂ SO ₄
	(310)	630	
	(266)	6500	
	(258)	10000	
	(250)	13000	
	(230)	24000	
4E (X = I)	398	3700	MeOH/MeCN
	308	7700	
	(267)	10500	
	(256)	13600	
	(253)	15200	

has the first d-d band at ca. 25,400 cm^{-1} , and the average environment rule predicts a cubic contribution of 25,700-26,600 cm^{-1} . The band moves to lower energy as substitution by bromide is effected, though it is masked by charge transfer in the iodide.

The possibility of reliably assigning bands in the vibrational spectra (Table 4.2) is small, as the low frequency transitions involving metal-ligand stretching and bending coordinates will be heavily coupled with deformation modes of the chelating oxalate ion, and the low local symmetry (C_S) of the rhodium ion does not impose any selectivity between infrared and Raman activity of the expected modes. Even in Rhpy_3ClOx , the $\nu(\text{Rh-Cl})$ absorption is probably obscured in the i.r., as the bromide also has two strong bands in this vicinity (340, 355 cm^{-1}); and the iodide, one (356 cm^{-1}). However the strong Raman-i.r. coincidence at 356 cm^{-1} may be attributed thus. In the region 400-4000 cm^{-1} the infrared spectra of 4A, 4B, 4C are virtually superimposable, and they are very similar between 200-400 cm^{-1} also. The tentative assignments of Table 4.2 follow the work of Hester and Plane⁽⁴⁾ and Gillard et.al.⁽⁵⁾. The pentadeuteriopyridine analog of the chloro-complex is included as compound 4F. The transition at ca. 550 cm^{-1} is assigned as being mainly

Table 4.2

Selected vibrational bands of oxalate complexes.

Rhpy₃XOx.

<u>Compound</u>	<u>Raman</u>	<u>Infrared</u>	<u>Assignment</u>
4A (X=Cl)	220s	226s)	ν(Rh-py)
	277s	275s)	
	317s	316s	
	356s	356vs	ν(Rh-Cl), (OCO)
		408m	ν(Rh-O)
	557s	556s	ν(Rh-O) (a)
			1668vs)
		1700vs)	
		1722sh)	
	4B (X=Br)	199s	197vs
231s		231s)	ν(Rh-py)
		274m)	
		312s	
		345vs)	δ(OCO)
		359vs)	
		396m)	chelate ring deformations
		407m)	
		465m)	
		535w)	ν(Rh-O) (a)
		554s)	
	1672vs)	ν(C=O)	
	1705vs)		

Table 4.2 continued

Table 4.2 (continued)

<u>Compound</u>	<u>Raman</u>	<u>Infrared</u>	<u>Assignment</u>	
$4E^b$ (X=I)		222s)	ν (Rh-py)	
		271s)		
		311s		
		356vs)	chelate ring deformations	
		409m)		
		465m)		
		555s	ν (Rh-O) (a)	
		1668vs)	ν (C=O)	
		1702vs)		
	$4F^c$ (X=Cl)	212s)	ν (Rh-py)
270s				
313s				
354m				
		465m		
		529s)	δ (C-D)	
		540s)		
		554s))		
557s)	ν (Rh-O) (a)	
985vs			py ring breathing	
1673m	1667vs)	ν (C=O)		
1697m	1700vs)			

(a) not purely (Rh-O).

(b) too deeply coloured to obtain satisfactory Raman spectrum. Limit of observation in i.r., 200 cm^{-1} .

(c) tris(pentadeuteriopyridine) complex.

$\nu(\text{Rh-O})$ on the basis of Chapter 3, Section 3.2, but like the bands below it in energy, is probably not a simple fundamental. The infrared absorption at ca. 315 cm^{-1} occurs in nearly all the pyridine complexes of rhodium, but the Raman activity at this energy in the oxalates suggests that it may here be coupling with a vibration of the chelating ligand. A band, $440\text{-}500 \text{ cm}^{-1}$ has previously been attributed⁽⁴⁾ to an oxalate deformation. Deuteriation of the pyridine ring removes the pyridine ring mode near here to lower energy but a medium intensity band indeed remains at 465 cm^{-1} ; it is absent in the absence of oxalate, while crystalline $\text{K}_2\text{C}_2\text{O}_4 \cdot 2\text{H}_2\text{O}$ has a Raman band at 473 cm^{-1} .

Replacement of chloride by bromide (4A \rightarrow 4B) has the effect of producing a strong new band at 198 cm^{-1} in Raman and i.r. spectra which is likely to be $\nu(\text{Rh-Br})$. The symmetry of the complexes cannot be greater than that of point group C_3 , that of the RhN_3XO_2 unit, whence all vibrations should be coincidentally Raman and i.r. active.

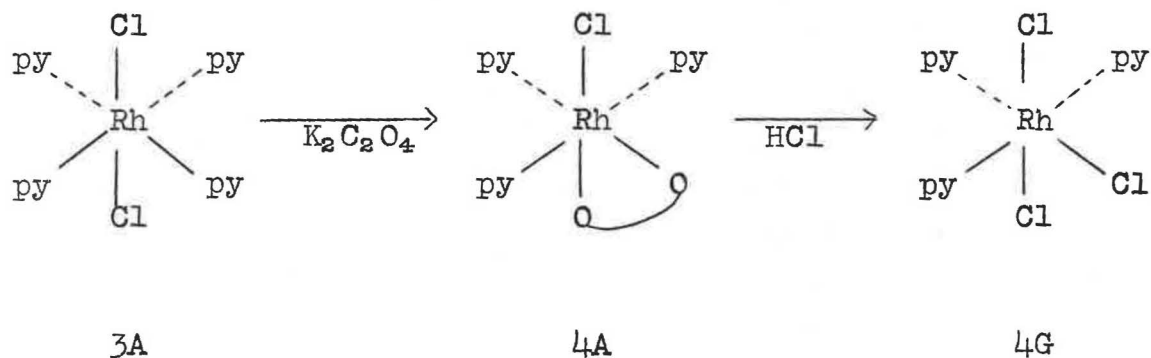
The oxalato-complexes are insoluble in most common solvents, but dissolve to some extent in aqueous pyridine or dimethyl sulphoxide. The complex Rhpy_3ClOx was shown⁽³⁾ to be insoluble in water or pyridine, but in a 50% v/v

mixture, these acted synergically to give a 0.0013 M solution of the complex. This was attributed to the ability of the mixed system to solvate both the hydrophilic (oxalate) and hydrophobic (aromatic hydrocarbon) halves of the molecule simultaneously. They are soluble in strong acids, and 4A hydrolyses slowly in this medium.

4.2(i) Reaction with Hydrohalogenic Acids

It has been found previously⁽³⁾ that the oxalate 4A when dissolved in concentrated hydrochloric acid, slowly deposits orange crystals of Rhpy_3Cl_3 (4G), which is the compound Delépine⁽⁶⁾ prepared by the action of pyridine on aqueous hexachlororhodate.

As the chloro-oxalate 4A is the uncharged complex formed from the known trans- $\text{Rhpy}_4\text{Cl}_2^+$ ion, the stereochemical rigidity of rhodium(III) complexes implies that the trichloride 4G can only be the 1,2,6-(mer-)isomer.



1,2,6-Rhpy₃Cl₃ is also formed often when insufficient pyridine is used in the ethanol-catalysed preparation of t-Rhpy₄Cl₃, especially if the pyridine is added to the rhodium(III) solution before the ethanol. However, none of the 1,2,3-(fac)isomer is isolatable under these conditions, whereas Collman and Holtzclaw⁽⁷⁾ obtained both isomers (without catalysis); the 1,2,6-isomer they referred to as their "orange-brown" isomer. 4G is the product obtained when t-Rhpy₄Cl₃ is heated for a considerable time in either ethanol or neat pyridine. It seems that the equilibrium



is influenced strongly by the ability of the given medium to solvate the chloride ion involved, hence it is displaced

to the right in pyridine, despite that reagent's excess.

The observation (Chapter 3, Section 1) that halide exchange at the Rh(III) centre is inhibited by acid leads to the possibility that the coordinated halogen in $[\text{Rhpy}_3\text{XOx}]$ is retained during the displacement of oxalate by HX. Obviously, this cannot be tested by the reaction of Rhpy_3ClOx with HCl or of Rhpy_3BrOx with HBr, the latter yielding 1,2,6- Rhpy_3Br_3 (4H) as expected. However the reactions



occur as written when the chloro- or bromo-oxalato compounds are dissolved in warm hydrobromic or hydrochloric acids, respectively.

The products, $\text{Rhpy}_3\text{ClBr}_2$ (4J), and $\text{Rhpy}_3\text{Cl}_2\text{Br}$ (4K), are obtained as deep red and deep orange crystals, respectively, and purified by recrystallisation from chloroform. Their virtually quantitative formation supports the implication of Section 1 of this Chapter that halide exchange at $[\text{Rhpy}_3\text{XOx}]$ occurs via a similar mechanism to that observed for the $\text{trans-Rhpy}_4\text{X}_2^+$ ions.

The tri-iodo complex, 4M, was obtained as plum-coloured crystals by boiling a solution of $t\text{-Rhpy}_4\text{Cl}_3$ in aqueous ethanol with excess iodide and a small amount of added pyridine. This reaction is mentioned in Chapter 1.

The reaction of iodide in acidic solution with the oxalate complexes did not give readily purifiable products and was not pursued.

The compounds with both chloride and bromide coordinated are the first well-characterised species with both halogens bonded to the same rhodium atom in an uncharged complex.

4.2(ii) Electronic Spectra

Table 4.3 contains the electronic spectra of the trihalotripyridine complexes. Substitution of chloride by bromide progressively lowers the energy of the first absorption band in a monotonic fashion. Agreement with previously reported^(8,10) values for the tribromo-complex (4K) is good. Solid reflectance spectra have been obtained for the trihalides and they correspond to the solution values and in addition show absorption due to pyridine at ca. 257 nm. It is not clear why Schmidtke⁽¹¹⁾ observed

the peak in the reflectance spectrum of mer-Rhpy₃Cl₃ at 440 nm. rather than at 425 nm. Moreover, there is no evidence for a band at 370 nm., either in the solid state or in chloroform solution, although Schmidtke claims to have observed it in both reflectance and DMSO solution. His method of preparation however, could lead to an impure product, while the method used here is unambiguously selective. The reflectance spectrum possibly has a shoulder at ca. 290 nm., but it is unlikely that $^1A_{1g} \rightarrow ^1T_{2g}$ would occur this high. Jørgensen⁽⁹⁾ has commented on the position of the d-d band in 1,2,6-Rhpy₃Cl₃, suggesting that in compounds of symmetry significantly lower than that of the octahedral chromophore model, splitting of, and configurational interaction amongst, excited states is likely to lower the energy of the transitions. The basis for this suggestion is presumably that the two lowest lying singlet excited states in Rh(III) are T_{1g} and T_{2g} , in an octahedrally symmetric field, but on reduction of the local symmetry to C_{2v} (mer-RhN₃X₃) these give rise to $A_2 + B_1 + B_2$ and $A_1 + B_1 + B_2$ respectively, and mixing of the B_1 and B_2 terms will occur, all transitions except $A_1 \rightarrow A_2$ being spin and orbitally allowed. Further reduction of the field symmetry to C_s (mer-RhN₃X₂Y) actually reduces the degree

term splitting, but both the 1T states now transform as $A^1 + 2A^{11}$, so that interaction is more likely.

Inspection of the absorption wavelengths in Table 4.3 shows that (except for the trichloride) there are three bands in the range 300 - 700 nm. These would be attributed generally to the ligand field singlet-singlet transitions ${}^1A_{1g} \rightarrow {}^1T_{1g}$, ${}^1A_{1g} \rightarrow {}^1T_{2g}$ and the third as a ligand-to-metal charge transfer process, where the representations are those of octahedral symmetry. However, the restrictions of the previous paragraph require that caution be exercised in interpreting the spectra. For the triiodotripyridine complex 4M, it is obvious from the high ϵ values of the lower energy bands that intermixing of charge transfer process is significant. For the sake of comparison, the parameters $10Dq$ and B have been derived by virtue of the above assignment. Jørgensen⁽¹¹⁾ gives the means of calculation of $10Dq$ and B by using the result that the separation of the ${}^1T_{2g}$ and ${}^1T_{1g}$ levels is $16B$, and the correction for configurational interaction is then

$$\frac{-84B^2}{10Dq} \text{ so that bands occur at } \nu_1 = 10Dq - 4B + \frac{84B^2}{10Dq}$$

and at $\nu_2 = 10Dq + 12B$. The results which emerge are rather inconsistent with expectation. Schmidtke's figure⁽¹⁰⁾ (238 cm^{-1}) for B in the trichloro compound

is surprisingly small, implying that

$\beta = \frac{B(\text{complex})}{B(\text{ion})} = 0.33$, which is comparable with the value quoted by Jørgensen⁽¹¹⁾ as being remarkably low (0.29) in

tris(diethyldithiophosphato)rhodium(III), so one must conclude that Schmidtke's result is invalid. The uncertainty of the procedure is exemplified when one compares the tribromo compound with the two chlorobromo complexes, and finds that mer-Rhpy₃Br₃ has a larger 10Dq than mer-Rhpy₃Br₂Cl while chloride is known to have invariably a stronger field effect than bromide. It is the field strength which is reflected by 10Dq, as 10Dq corresponds to the splitting of the t_{2g} and e_g levels in the 4d-orbital subshell of the rhodium ion. The implication is that the changing symmetry affects the splitting of the excited states significantly enough to destroy the validity of comparisons between complexes of different symmetry. Within the same symmetry the approach seems appropriate, as in the series Rhpy₃X₂Y for which X = NCO, Br, Cl, where 10Dq increases in the expected direction, Br < Cl < NCO. The interference of charge transfer is apparent in the triiodide and prevents derivation of 10Dq and B, while for the triazide compound it may be detracting from the relevance of the calculation.

The Racah parameter B is directly an indication of the interelectronic repulsion among the d-orbitals of a

metal ion. The d-d spectra of transition metal ions are rationalised in terms of B decreasing from the free ion value (720 cm^{-1} for Rh^{3+}) when the metal is ligated. Ligands may be arranged, for a given metal, in the order in which they decrease B; this nephelauxetic series is roughly paralleled, in the opposing sense, by the more familiar spectrochemical series. Qualitatively, it may be considered that B is somewhat a measure of the degree of charge transferred from ligand to metal in the ground state of the complex, i.e. the degree of covalency of the metal-ligand bond. A more polarisable ligand has the effect of increasing the total charge in the d-orbitals, causing them to expand to achieve electrostatic harmony with the kernel. Concomitant with the radial expansion, the intrasubshell repulsions decrease. However, the effect leads⁽¹¹⁾ to a defiance of the baricentre rule, as the radial parts of the functions relating to the t_{2g} and e_g orbitals are dissimilar. Hence the eventual result that the ${}^1T_{2g} \rightarrow {}^1T_{1g}$ separation is not simply $16B \text{ cm}^{-1}$. Precise information is difficult to obtain, as the t_{2g} and e_g sets will each have a related B-value, and the two cannot be separated without a knowledge of the spin-forbidden ${}^1A_{1g} \rightarrow {}^3T_{2g}$ band energy. Such bands are usually apparent in the compounds of iridium(III)⁽¹²⁾ but are usually very weak in those of rhodium(III) and

indistinguishable in cobalt(III) complexes. Within the halo-complexes, B is seen to decrease steadily as chloride is replaced by bromide, and again increase when halide is replaced by isocyanate, and these observations agree with the expected order of these donors in the nephelauxetic series.

The nature of azide as a ligand is partly revealed by the low value observed for B (250 cm^{-1}), which is remarkably similar to that (270 cm^{-1}) observed by Schmidtke⁽¹³⁾. It is possibly a reflection of the ability of N_3^- to delocalise the rhodium d π -orbitals over the π -system of the anion. The ligand-field strength of azide is markedly low for a nitrogen donor, however, and it may be that this is merely the result of π -electron density about the NNN axis reducing the ability of N_3^- to differentiate between the t_{2g} and e_g orbitals of the rhodium. In this regard, there do appear to be low-lying, occupied π -orbitals on N_3^- . The presence of nonbonding electron density at the donor atom has been invoked previously⁽¹⁴⁾ to account for ligand field strengths, and the above argument seems relevant to similar systems (isothiocyanate, isocyanate) which have occupied π -orbitals and lower ligand field strengths than would be expected for a nitrogen donor, in particular when the

M-NR angle is 180° or close to it, so that the π -system of the ligand interacts equivalently with all the t_{2g} orbitals.

With regard to the isocyanate compounds, mer-Rhpy₃X(NCO)₂, the B-values are the inverse of those expected. Notably, the second UV band is at shorter wavelength in the bromide than in the chloride, and it is a related, apparently anomalous property which causes the discrepancy in the trihalide compounds, where the first charge transfer band at ca. 320 nm. does not vary rationally in wavelength as chloride and bromide are interchanged. Assignment of the first band in the isocyanates does introduce the possibility that the 313 and 320 nm. bands correspond to the ligands' internal $n \rightarrow \pi^*$ transition, attributed to the 350 nm. absorption observed⁽¹⁵⁾ in square planar isocyanatoplatinoids.

4.2(iii) Empirical Rules for Rhodium(III) Spectra

Although the derivation of B and $10Dq$ for the compounds herein has led to some inconsistencies, it seems that the procedure is revealing whether or not expected ligand field bands are in fact being observed. It is useful to be able to deduce, from the appearance

of an absorption spectrum, the nature of the chromophore.

To this end the position of the first spin-allowed d-d band is usually the most readily accessible piece of information. This is generally obtained via the "average environment" procedure, using collected data on spectra of various compounds⁽¹⁶⁾. The nonisolation of the hexpyridinerhodium(III) ion has required that previous workers used an estimated value for the ${}^1A_{1g} \rightarrow {}^1T_{1g}$ transition energy of this as yet hypothetical species, whence Jørgensen⁽⁹⁾ suggested that a value of $30,000\text{cm}^{-1}$ would be appropriate for ν_1 , but no proposals have been made for a B-value. Because of this, and also to avoid the necessity of calculations involving both parameters it is desirable to have a better estimate of ν_1 for Rhpy_6^{3+} which will agree with the values observed in this work and enable more accurate predictions of band positions.

Toward acquiring a set of empirical values of ligand contributions to band energies, firstly the effects of term splitting by symmetry changes will not be considered; secondly, values derived from compounds already containing pyridine will be used where possible, as changing from one nitrogenous base to another certainly changes the first band position, and could possibly have an effect on the contribution from other ligands.

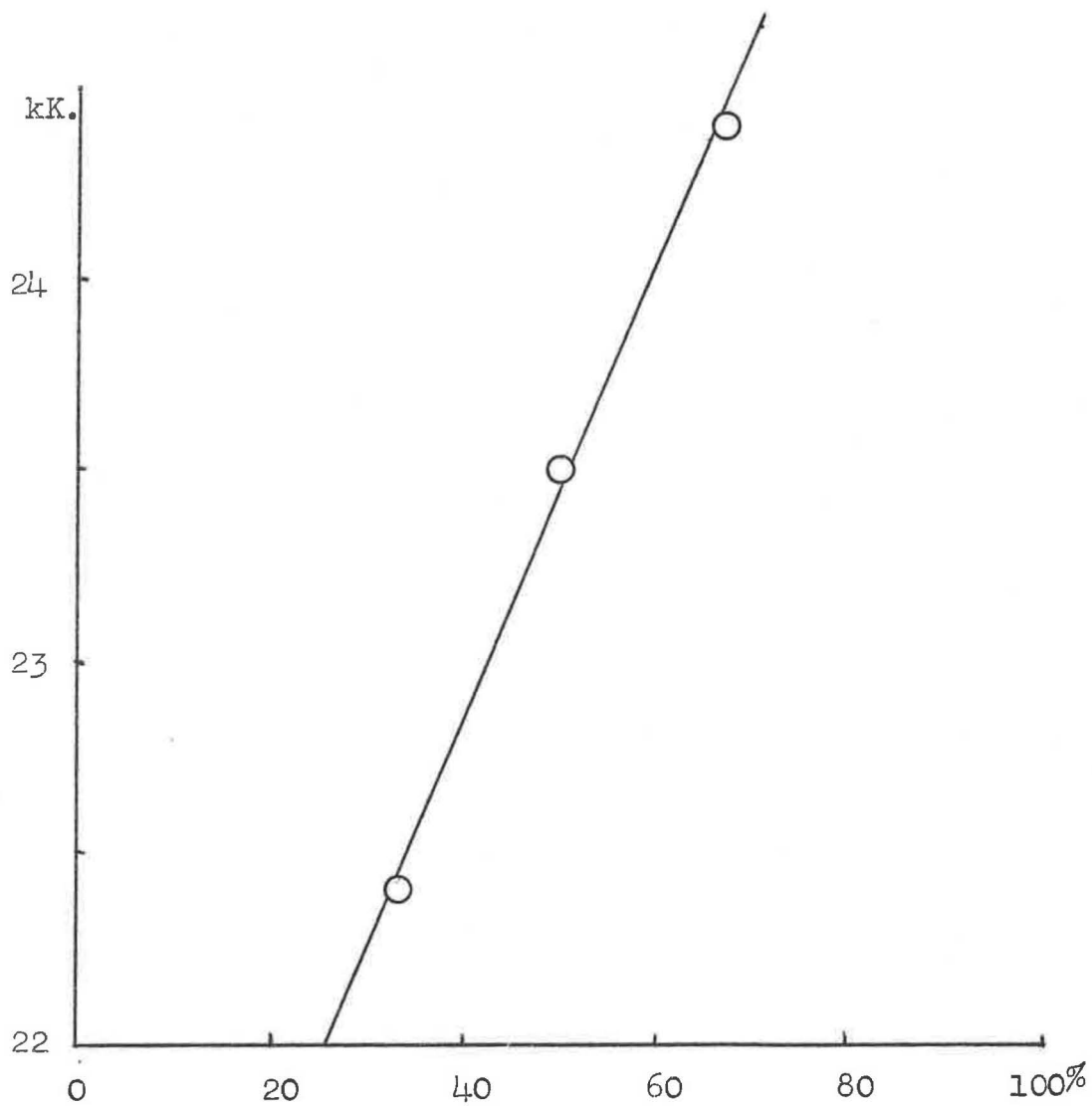


Fig. 4.1 Plot of ν_1 vs. proportion of chloride
in $\text{Rhp}_n\text{Cl}_{6-n}$ compounds.

Consider the simple diagram 4.1 on which are positioned the species $t\text{-Rhpy}_4\text{Cl}_2^+$, $\text{mer-Rhpy}_3\text{Cl}_3$ and $\text{cis-Rhpy}_2\text{Cl}_4$. The line drawn to fit these three points approximately, yields the value $\delta.\text{Cl} = 3,400 \text{ cm}^{-1}$, $\delta.\text{py} = 4,410 \text{ cm}^{-1}$ where $\delta.X$ represents the contribution of each ligand X to the energy of the first transition. These values have been fed back into Table 4.5 which compares observed λ values with those predicted from Table 4.4. Each $\delta.X$ is derived from the species preceding it in Table 4.4. Thus $\delta.\text{Br}$ is obtained by simply taking the mean of the values obtained when $\delta.\text{py}$, $\delta.\text{Cl}$ are used to compensate for those species in a bromo-compound. In this way a fairly consistent set of δ values have been assembled and in most cases excellent matching of observed and predicted energies are found, although this is not surprising as most of the predictions are not a priori estimates.

In Table 4.4, the values required for δX are compared with those found from previous work, usually with the corresponding $[\text{RhX}_6]^{n+}$ ion, and assembled by Jørgensen⁽¹⁶⁾. It brings to light some interesting features. Most of the values are close to those found for the $[\text{RhX}_6]^{n+}$ species, but the notable exceptions are the azide and hydroxyl ions. All the azides have a long λ shoulder and then an intense band at higher energy. The

Table 4.4

Ligand Contributions to Band Energy

<u>Ligand</u>	<u>$\delta(\text{cm}^{-1})$</u>	<u>$\delta(\text{lit.})\text{cm}^{-1}$</u>
Pyridine	4410	
Cl^-	3400	3220
Br^-	2630	3200
I^-	1220	
N_3^-	4200	3420
OH^-	6800	3980
H_2O	4450	4250
$-\text{NCO}^-$	4840	
$\frac{1}{2} \text{Ox}^{2-}$	4330	4180

Table 4.5

Comparison of Observed and Predicted Absorption
Wavelengths

Species	Predicted $\nu(\text{cm}^{-1} \times 10^{-3})$	Observed $\nu(\text{cm}^{-1} \times 10^{-3})$	$\lambda(\text{nm.})$
Rhpy ₂ Cl ₄ ⁻	22.4	22.4	447
Rhpy ₃ Cl ₃	23.4	23.5	425
Rhpy ₄ Cl ₂ ⁺	24.4	24.4	410
Rhpy ₄ Br ₂ ⁺	22.9	22.7	441
Rhpy ₃ Br ₃	21.1	22.0	455
Rhpy ₃ Br ₂ Cl	21.9	21.9	456
Rhpy ₃ BrCl ₂	22.7	22.6	442
Rhpy ₄ ClBr ⁺	23.7	23.5	425
Rhpy ₄ I ₂ ⁺	20.1	20.4	490
Rhpy ₃ I ₃	16.9	16.6	603
Rhpy ₃ Cl(NCO) ₂	26.3	26.6	376
Rhpy ₃ Br(NCO) ₂	25.5	25.2	397
Rhpy ₃ (N ₃) ₃	{ 23.5 a 25.8 b	23.2	430
Rhpy ₄ (N ₃) ₂ ⁺	{ 24.5 a 26.0 b	27.0	370
Rhpy ₂ (N ₃) ₄ ⁻	{ 20.7 a 25.6 b	22.5	445
		25.9	386
		21.3	470
		24.5	409
Rhpy ₃ ClOx	25.3	25.3	395
Rhpy ₃ BrOx	24.5	24.5	408
Rhpy ₃ IOx	23.1	not observed	
Rhpy ₄ Cl(OH) ⁺	27.8	27.9	359
Rhpy ₄ Br(OH) ⁺	27.1	27.0	371
Rhpy ₄ Cl(OH ₂) ²⁺	25.5	25.6	390
Rhpy ₄ Br(OH ₂) ²⁺	24.7	24.6	406

a: shoulder, $\epsilon \sim 10^2$ energy calculated using $\delta = 3.42$
 b: peak, $\epsilon \sim 10^3$ energy calculated using $\delta = 4.20$

$\delta.N_3^-$ obtained applies to the intense band, while the literature value has been used to match with the lower energy shoulder, which it fits better. The values are not at all consistent, so not even an empirical method can be used for deducing the structures of azidorhodium(III) chromophores. If the results in Table 4.4 have any real meaning, they suggest that the effects of delocalisation and bond covalency in such compounds overwhelm the simple ligand field calculations used. The high value ($6,800\text{cm}^{-1}$) obtained for hydroxyl implies either that OH^- is an extraordinarily strong ligand toward rhodium(III) (and the derivation of $10Dq, B$ yields $28,700\text{ cm}^{-1}, 261\text{ cm}^{-1}$ respectively for these quantities) or, more likely, that the 359 nm. transition simply does not correspond to $^1A_{1g} \rightarrow ^1T_{1g}$, but to $A_1 \rightarrow E$ in C_{4v} (see Figure 2.7) say, where by inference $E > A_2$ in energy. Indeed, there are possibly weak shoulders (ca. $390\text{-}410\text{ nm.}$) in the UV spectra of the hydroxy compounds, but the absorption envelopes are too complex for unambiguous analysis. The agreeable result for the aquo-complexes enables the final entry to be made in Table 4.4. Charge transfer absorption in the trans $[\text{Rhpy}_4\text{Br}(\text{OH}_2)]^{2+}$ is too strong for ν_2 to be assigned.

For iodide, it becomes apparent that in many compounds ν calc. will be obscured by the intense charge transfer ($I^- \rightarrow Rh(III)$) which occurs at about 400 nm., $\epsilon \sim 10^4$.

Using literature values for ligands other than chloride, an assemblage of δ py values were derived from the compounds in 4.5. The mean of twelve values was 4,420 cm^{-1} , which is insignificantly different from the value used here generally. The deviations from the mean were greater, of course, up to almost 10% in the worst individual case.

The wavenumber values listed in Table 4.4 should be a useful guide, but it must be remembered that the wavelength obtained must not necessarily be expected to correspond to $\nu_1(^1A_{1g} \rightarrow ^1T_{1g})$.

4.2(iv) Vibrational Modes of $Rhpy_3X_2Y$

The four compounds considered in this section are the 1,2,6-trihalotripyridine complexes, $Rhpy_3Cl_3$, $Rhpy_3Cl_2Br$, $Rhpy_3ClBr_2$, $Rhpy_3Br_3$. In Chapter 1 it was demonstrated that the low frequency vibrational spectra of the rhodium pyridine halide complexes were explicable

in terms of $\nu(\text{Rh-Cl})$ occurring at 300-400 cm^{-1} , $\nu(\text{Rh-Br})$ at 180-200 cm^{-1} , and less well, of pyridine, acting as an albeit heavy, one particle ligand, with $\nu(\text{Rh-py})$ 200-280 cm^{-1} .

Clark and Williams⁽¹⁷⁾ have examined the two isomers of Rhpy_3Cl_3 by i.r. spectroscopy (200-400 cm^{-1}) and assigned $\nu(\text{Rh-X})$ and $\nu(\text{Rh-py})$ in them on the basis of the symmetry of the RhN_3X_3 cluster. For the mer- Rhpy_3X_3 compounds, that unit has the symmetry of point group C_{2v} . The expected vibrational mode types and their spectroscopic activities are laid down in Table 4.6.

Table 4.6

Type	$\nu(\text{Rh-X})$	$\nu(\text{Rh-py})$	Activity Raman Infrared
A_1	2	2	All Raman and i.r. active
B_1	1	0	
B_2	0	1	

Hence all normal modes are predicted to be both i.r. and Raman active, and there are no opportunities for the removal of state degeneracies by the effects of environment

Table 4.7

Low Frequency Vibrational Transitions in mer-RhL₃X₂Y

L	X	Y	<u>Raman</u>	<u>Infrared</u>	<u>Assignment</u>	
py ^(a)	Cl	Cl	359w	358s(348s) ^(a)	$\nu(\text{Rh-Cl}), B_1$	
			336m(328m)	334s(328s)	$\nu(\text{Rh-Cl}), A_1$	
			299vs(298vs)	297m(290m)	$\nu(\text{Rh-Cl}), A_1$	
				(279sh)		
			268m(261m)	267s(256m)	$\nu(\text{Rh-py}), A_1$	
			251w(220w)	249s(225s)	$\nu(\text{Rh-py}), A_1$	
				236m(202m)	$\nu(\text{Rh-py}), B_2$	
lutidine	Cl	Cl		345s	$\nu(\text{Rh-Cl}), B_1$	
				331s(0.36) ^c	333s	$\nu(\text{Rh-Cl}), A_1$
				300vs(0.37) ^c	298m	$\nu(\text{Rh-Cl}), A_1$
				<u>ca.</u> 245w	245m	$\nu(\text{Rh-L}), A_1$
				<u>ca.</u> 237w		$\nu(\text{Rh-L}), A_1?$
					222s	$\nu(\text{Rh-L}), B_2?$
					356sh	}) }) })
	346m	342s	$\nu(\text{Rh-Cl}), A'$			
	334m	333s				
py	Cl	Br	297m	294s	$\nu(\text{Rh-Cl}), A'$	
			270s	265s, br	$\nu(\text{Rh-py})$	
			241m		$\nu(\text{Rh-py})$	
			230w	234w	$\nu(\text{Rh-py})$	
				195sh		
			192s	190s	$\nu(\text{Rh-Br}), A'$	

Table 4.7 continued

Table 4.7 (continued)

L	X	Y	<u>Raman</u>	<u>Infrared</u>	<u>Assignment</u>		
py	Br	Cl		337s	$\nu(\text{Rh-Cl}), A'$		
				317sh,w			
				310m			
				289m			
				260s)	$\nu(\text{Rh-py})$		
				232w)			
				220w)			
			193s	$\nu(\text{Rh-Br}), A'$			
py	Br	Br		337m			
				315m			
				305m			
				283m			
				<u>ca.</u> 275s	$A_1?, (\text{Rh-py})$		
				259m)	$\nu(\text{Rh-py})$		
				232w)			
				216w, sh			
				<u>ca.</u> 190s		192s	$\nu(\text{Rh-Br})$

a: figures bracketed refer to perdeuteriated complex.

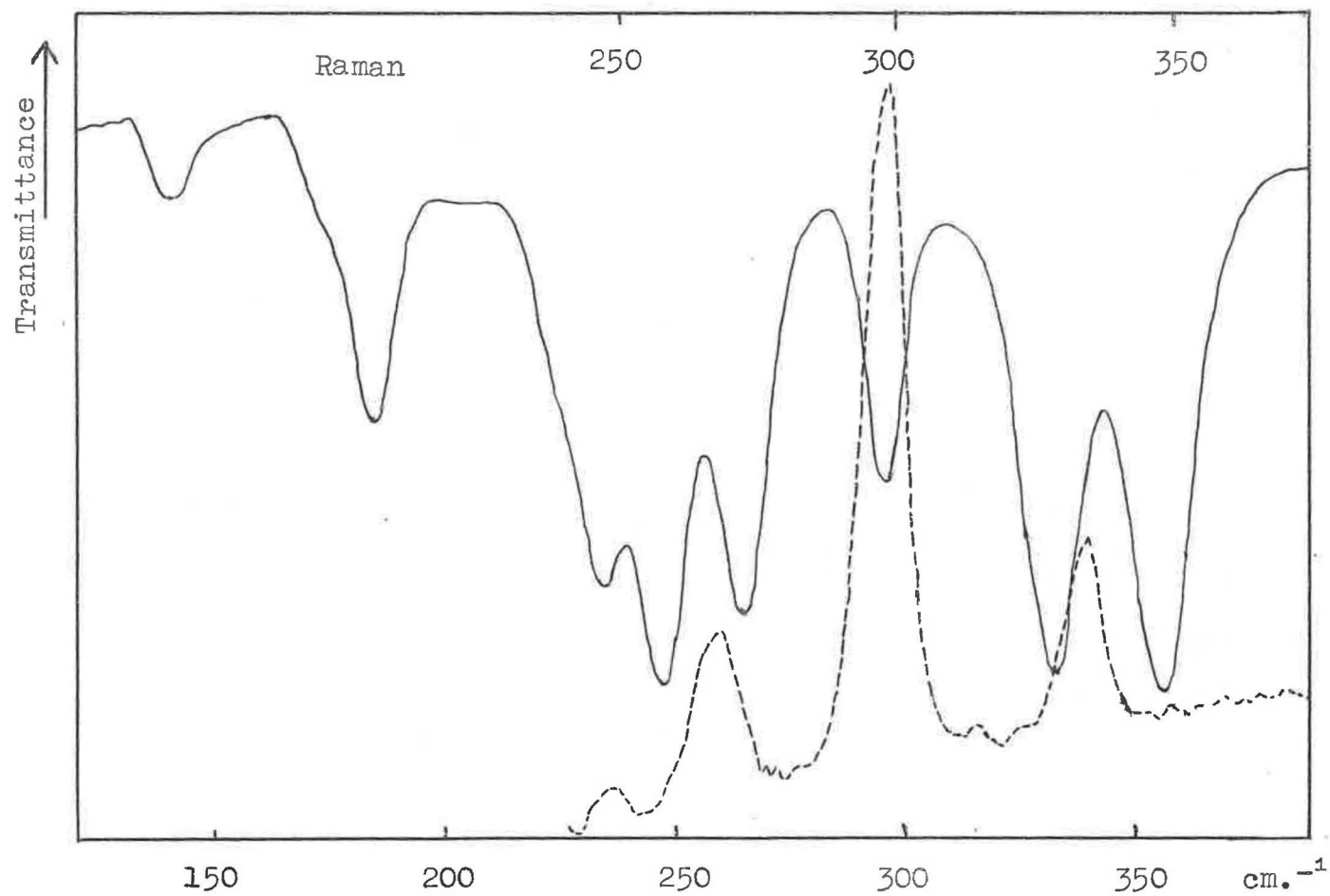
b: limit of observation 190 cm^{-1} .

c: figures bracketed are depolarisation ratios, in MeNO_2 solution. Lower limits, 200 cm^{-1} .

etc., as A and B type modes are nondegenerate.

Solubility limitations have required that Raman effect spectra be run on crystalline samples of mer-Rhpy₃X₃ and Rhpy₃X₂Y, so band depolarisation ratios are not available for these compounds. However, compound 4N, mer-Rhlut₃Cl₃, is sufficiently soluble for Raman spectroscopic investigation in nitromethane solution, and the results are added to Table 4.7.

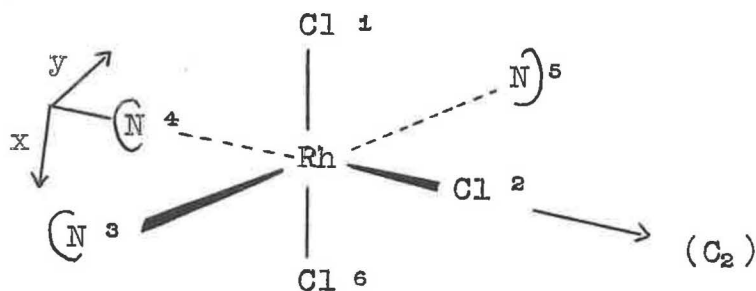
Clark and Williams assigned the bands they observed at 355, 332, 295 cm⁻¹ to $\nu(\text{Rh-Cl})$, and this is in agreement with this work. Differentiation between the A₁ modes on one hand, and the B₁ and B₂ modes on the other may be made possible by the Raman spectrum of the tris(3,5-dimethylpyridine)rhodium(III) compound 4N. Thus the two bands observed at 331 and 300 cm⁻¹ are both strongly polarised ($\rho = 0.36, 0.37$) so that they are undoubtedly the A₁ type transitions. Unfortunately, the 345 cm⁻¹ i.r. band was not observed in the Raman effect spectrum, so a depolarisation ratio cannot be obtained, although the fact that it is weak implies that the transition is less allowed in the Raman effect than the 331 and 300 cm⁻¹ bands, and hence that it is of type B₁ rather than A₁, thereby supporting the above A₁



Infrared (—) and Raman spectra of solid $\text{mer-Rhpy}_3\text{Cl}_3$

FIG. 4.2.

assignments. The B_1 vibration is that corresponding to the asymmetric Rh-Cl(1,6) bond stretching in the diagram below, which depicts the numbering scheme used for the octahedral coordination positions.



Now the only B modes are those associated with the trans Ch-Rh-Cl and N-Rh-N units. The modes pertaining to $\nu(\text{Rh-py}^4)$ and $\nu(\text{Rh-Cl}^2)$ are of type A_1 but may not mix in with the other A_1 stretching modes as these are orthogonal.

It seems probable that, being mutually trans, they might interact in a predictable fashion. Invoking the linear heteronuclear triatomic model of Chapter 1, and this time considering pyridine as one of the point masses, the A_1 then correspond to Σ^+ vibrations of the Cl-Rh-py unit. Calculation on this basis yields $\nu = 368$ and 247 cm^{-1} . There is indeed a $\nu(\text{Rh-py})$ band remarkably close to the calculated value, at 250 cm^{-1} , and like the

$\nu(\text{Rh-Cl})$ vibrations, only two appear in the Raman. On the other hand, the A_1 fundamental of the $\text{Rh-Cl}(2)$ bond is deduced to fall at 335 cm^{-1} , leaving the 298 cm^{-1} and 358 cm^{-1} bands agreeing with the A_1 and B_1 modes respectively, of the trans chlorides. The assignment of the 250 cm^{-1} band as A_1 , $\nu(\text{Rh-py}^4)$ implies, not disagreeably, that the 268 cm^{-1} transition belongs to the A_1 vibration of the $\text{py}(3)\text{-Rh-py}(5)$ moiety and the 236 cm^{-1} absorption is its B_2 vibration, thus being similar to the B_1 , $\nu(\text{Rh-Cl})$ mode in that it appears in the i.r. but not in the Raman.

The frequency for $\nu(\text{Rh-Cl}^2)$ is predicted above about the same as for chlorides mutually trans (on rhodium(III)) whereas in trans $[\text{Rhpy}_4\text{ClBr}]^+$, $\nu(\text{Rh-Cl})$ was calculated to decrease by 15 cm^{-1} (and actually fell by 21 cm^{-1}). The higher value expected for chloride trans to pyridine is the effect of the larger force constant used ($2.16 \times 10^5 \text{ dyne cm}^{-1}$) for the Rh-py bond, in contrast with the lesser value ($1.52 \times 10^5 \text{ dyne cm}^{-1}$) for the Rh-Br bond, even though the two ligands were considered to be isobaric ($\pm 1\%$). Repeating the calculation with the 3,5-lutidine compound, compensating for the mass change only, leads to $\nu = 365$ or 228 cm^{-1} . Hence a marginal drop (3 cm^{-1}) in the $\nu(\text{Rh-Cl})$, A_1 frequency is predicted but underestimated

(observed, 345 cm^{-1} , down 13 cm^{-1} from pyridine).

However, mer- $\text{Rh}(\text{lut})_3\text{Cl}_3$ does have a strong band at 222 cm^{-1} in the infrared, which may therefore be the A_1 , $\nu(\text{Rh}-\text{L}^4)$ vibration.

The drop in the A_1 frequencies from the values predicted for $\nu(\text{Rh}-\text{Cl})$ may either be the result of a trans-influence of heteroaromatic ligand or merely be unaccounted for by the crudity of the calculation. The latter is more probable, as a decrease of 7 cm^{-1} is engendered by deuteration of the pyridine, which leads to a mass increase, while the electronic effect should be unaltered. The matching of band assignments for the pyridine and deuteriopyridine compounds was accomplished mainly on the basis of the relative intensities of the various bands. The A_1 transition assigned to the mutually trans chloride is little altered ($\pm 2 \text{ cm}^{-1}$) by changing the heterocyclic base, and is close to the value (304 cm^{-1}) for $\text{trans}[\text{Rhpy}_4\text{Cl}_2]^+$. $\nu(\text{Rh}-\text{Cl})$ trans to pyridine falls at 341 and 325 cm^{-1} in the i.r. spectrum of fac- Rhpy_3Cl_3 ⁽¹⁷⁾ although the solution Raman spectrum has ⁽¹⁸⁾ bands at ca. 340 cm^{-1} and 310 cm^{-1} , despite the expectation that the $\nu(\text{Rh}-\text{Cl})$ vibrations in this molecule should coincide, being of type A_1 and E in C_{3v} symmetry.

Overall, there are good grounds for firm assignment of the ν (Rh-Cl) vibrations, but application to the bands belonging to ν (Rh-py) is less reliable in terms of definition of symmetry type of the vibrations, mainly because of lack of Raman polarisation data. The linear triatomic model which met with moderate success in Chapter 1 proves to be much less effective here, as the result, presumably of mixing in of ligands' internal modes due to the nonrigidity of the rings.

Replacement of a chloride ion by bromide, i.e. passing to 1,2,6-Rhpy₃Cl₂Br, lowers the local symmetry to C_S, in which condition all the stretching modes of the metal-ligand chromophore are both Raman and i.r. active.

Table 4.8

Rhpy₃X₂Y: C_S Vibrations

Type	(Rh-X)	ν (Rh-Y)	ν (Rh-py)	Activity
A'	2	1	2	All Raman and i.r. active
A''	0	0	1	

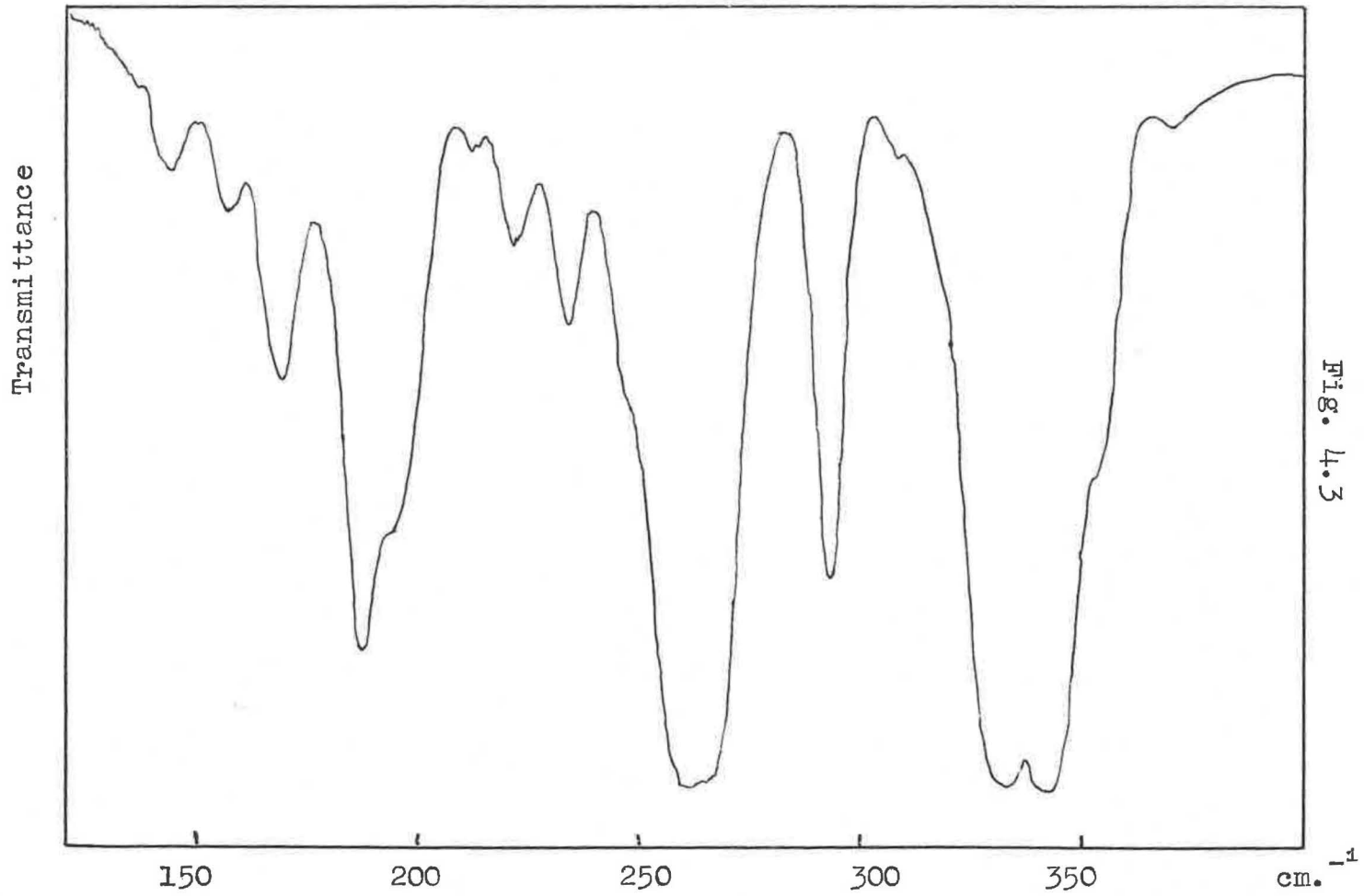
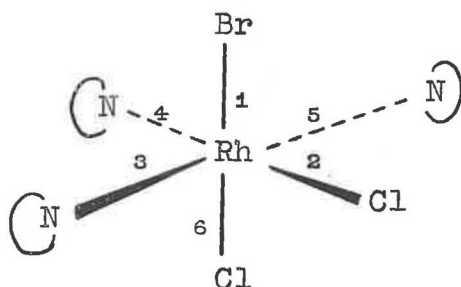


Fig. 4.3

Far infrared spectrum of 1-bromo-2,6-dichlorotripyridinerhodium(III)

The outcome of this is, that the advantage of being able to use Raman and i.r. spectroscopy as complementary probes is lost.

For $\text{Rhpy}_3\text{Cl}_2\text{Br}$, many features of the Rhpy_3Cl_3 spectrum are preserved, but the assignment is less reliably made. Strong, structured absorption arising from three overlapping bands, is centred at ca. 340 cm^{-1} and is due to $\nu(\text{Rh}-\text{Cl})$. As both the $\nu(\text{Rh}-\text{Cl})$ modes in the mer- $\text{Rhpy}_3\text{Cl}_2\text{Br}$ molecule (below) are of type A' , it



is possible that they may interact, so that the two centres of absorption, i.e. at $340, 295\text{ cm}^{-1}$ may be attributed to in-phase and out-of-phase vibrations of the two chlorides. The occurrence of more than one band at the higher energy could be the result of a crystal lattice effect, causing coupling within a unit cell, say, as one expects only two rhodium-chlorine stretching vibrations to appear. The compound is insufficiently

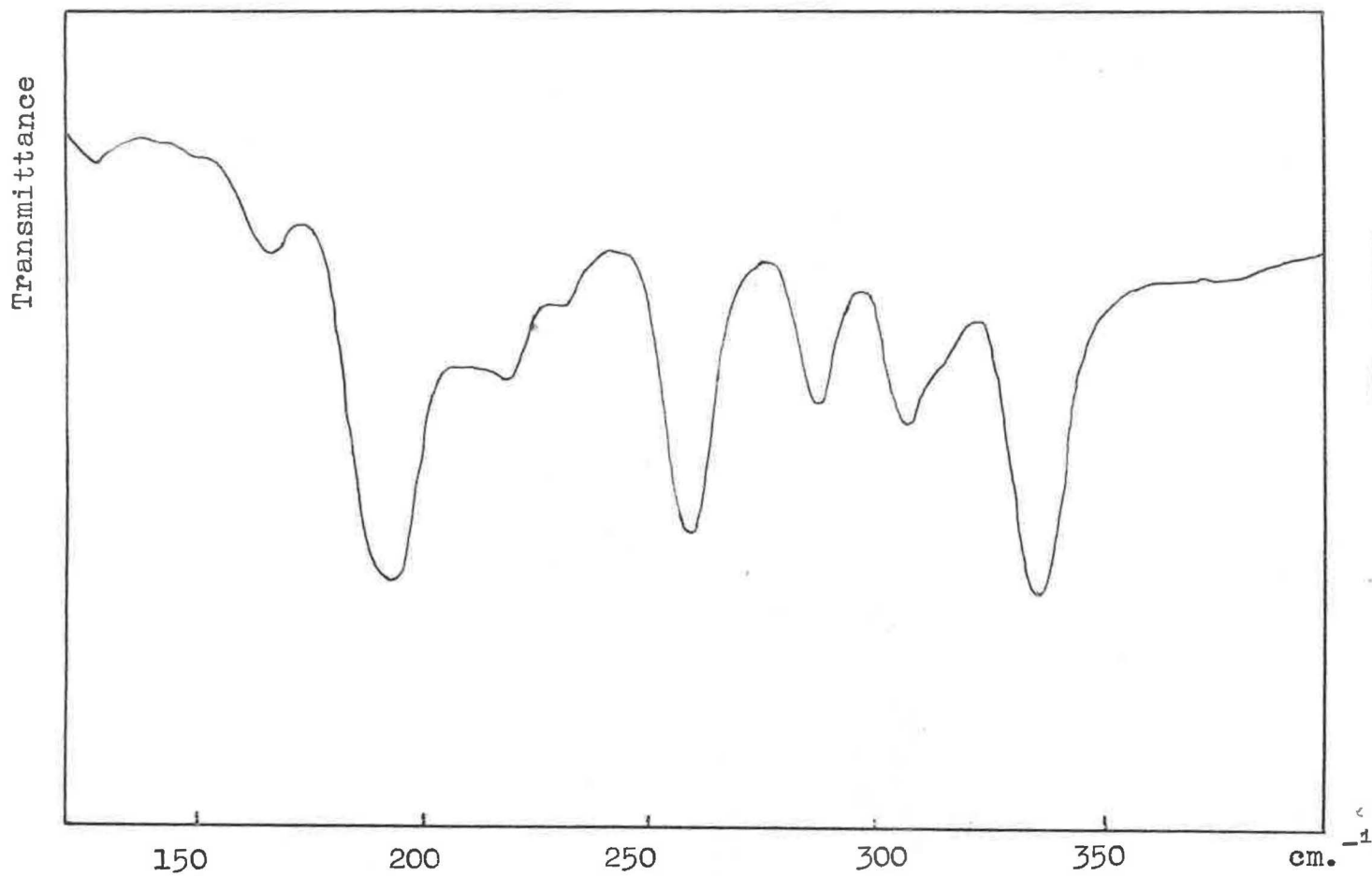


Fig. 44

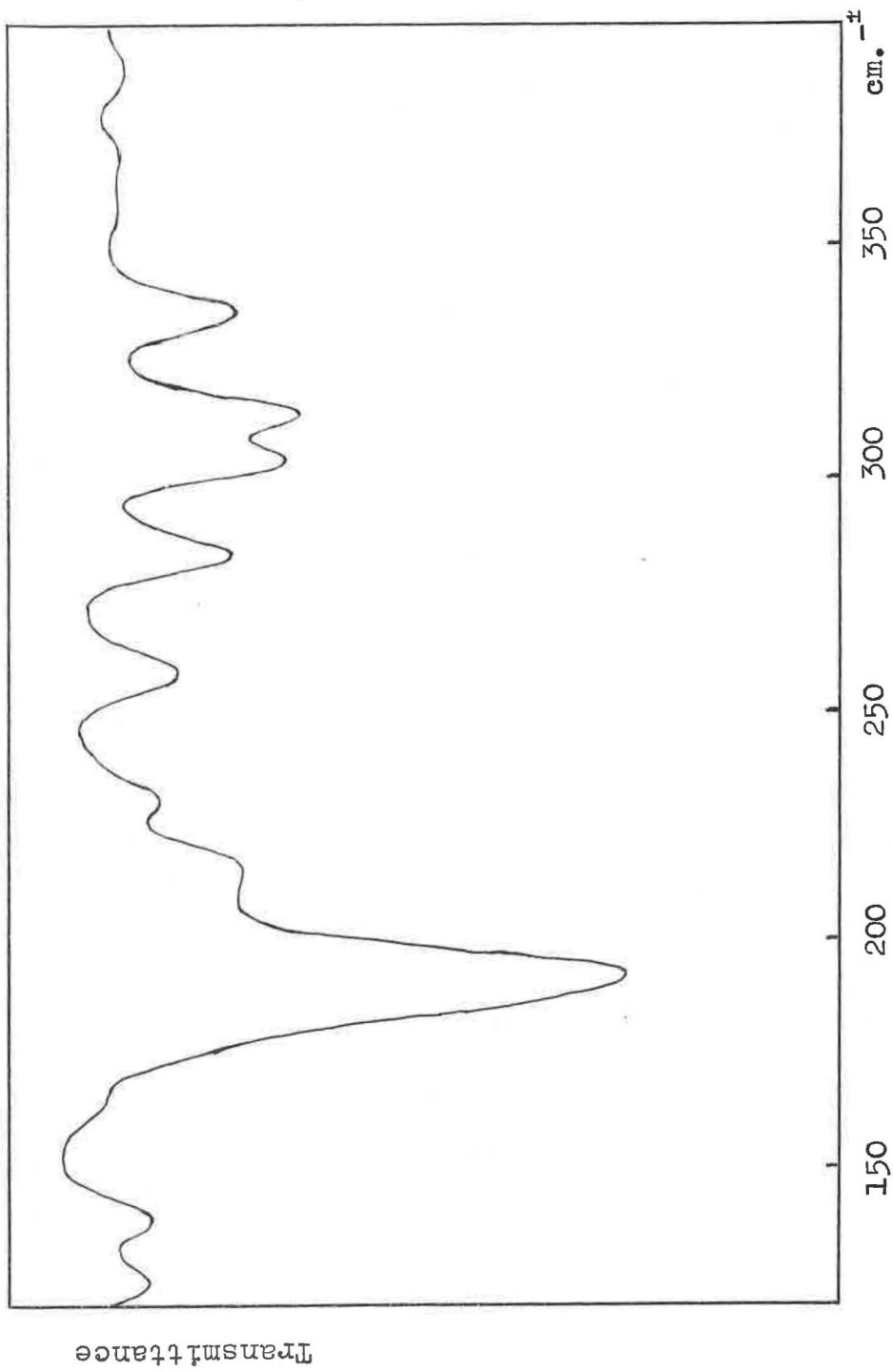
Far infrared spectrum of 1-chloro-2,6 dibromotripyridinerhodium(III)

soluble for solution Raman spectroscopy to determine whether the multiplet structure coalesces without a crystal lattice. In any case, it would not provide more information leading to better assignment, as five of the six modes expected are of the same type, A' .

The conclusions of Chapter 1 enable it to be deduced however, that the strong absorption at 191 cm^{-1} is due to $\nu(\text{Rh-Br})$, an A' mode, for which only one band is expected. Those bands at $230, 241\text{ cm}^{-1}$ may reasonably be attributed to $\nu(\text{Rh-py})$, but the band at $265\text{-}270\text{ cm}^{-1}$, strong in both its Raman effect and i.r. absorption is analogous to the very strong Raman band at 269 cm^{-1} in trans $[\text{Rhpy}_4\text{ClBr}]^+$.

Unexpectedly, the situation partly improves on passing to the compound $1,2,6\text{-Rhpy}_3\text{Br}_2\text{Cl}$, as the previous surfeit of strong absorption bands transforms itself into an apparent deficiency. There is a strong band at 337 cm^{-1} which may be assigned on the basis of its intensity and position, to the A' , $\nu(\text{Rh-Cl})$ stretching vibration. However, the expectation of two $\nu(\text{Rh-Br})$ absorptions is not fulfilled, there being only one strong band at 193 cm^{-1} . This is also the case in mer $\text{-Rhpy}_3\text{Br}_3$, which has one strong i.r. band at 192 cm^{-1} , while a sample of Rhpy_3I_3 gave absorption attributable to $\nu(\text{Rh-I})$

Fig. 4.5



Far Infrared spectrum of mer-Rhpy₃Br₃.

(cf. $[\text{Rhpy}_4\text{I}_2]^+$) only at 158 cm^{-1} (medium) (and, less likely, a weak band at 201 cm^{-1}).

In mer- $\text{Rhpy}_3\text{ClBr}_2$ and mer- Rhpy_3Br_3 appear a number of lower intensity bands, $280\text{--}350\text{ cm}^{-1}$, which are not accountable for. The decreasing solubility encountered as chloride is replaced by bromide, combined with the deepening colour (and possibly an increasing refractive index) prevents observation of all but the strongest Raman effect bands.

The occurrence of the intense transition at $265\text{--}270\text{ cm}^{-1}$ in trans- $[\text{Rhpy}_4\text{ClBr}]^+$, mer- $\text{Rhpy}_3\text{Cl}_2\text{Br}$ and mer- $\text{Rhpy}_3\text{ClBr}_2$ may be attributed to an enhanced rhodium-pyridine stretching vibration, as it occurs also in the Raman spectrum of fac- Rhpy_3Cl_3 ⁽¹⁸⁾. The coupling of the two cis chlorides in mer- $\text{Rhpy}_3\text{Cl}_2\text{Br}$ should be looked upon as an electronic effect. In contrast, mass coupling will be very significant in systems where the chemically different ligands have similar weights, i.e. with pyridine and bromine (79 and 80 a.m.u. respectively), and again when the central atom is of comparable mass also. The supposed non-appearance of the expected number of vibrations in the di- and tri-bromides may result from such coupling leading to "stealing" of intensity from the $\nu(\text{Rh-Br})$ transitions otherwise expected. Low symmetry in these compounds implies the

probability of fundamental modes mixing with one another in these ways. In conclusion, it is apparent that the metal-ligand vibrational spectra can only be understood very approximately from a qualitative viewpoint.

4.3 Halocarbon Solvates

4.3(i) Formation and Composition

Delépine⁽⁶⁾ observed that mer- Rhpy_3Cl_3 formed a chloroform solvate, and by drying the orange-red crystals at 120°C , he determined that they could be formulated as $\text{Rhpy}_3\text{Cl}_3 \cdot 2\text{CHCl}_3$. The same phenomenon was observed later by Holtzclaw and Collman⁽⁷⁾. The proclivity of rhodium pyridine complexes toward adduct formation has been demonstrated in Chapter 1. Those of definable structure involved a separate polyatomic anion which was not necessarily associated directly with the complex cation. Like the nitrile adducts of $[\text{Rhpy}_4\text{Cl}_2]\text{ClO}_4$, there is little reason to expect that a solvate of the above type should form between two molecules, neither of which is expected to be a donor or acceptor of any significance, for example. With a selection of compounds of the type mer- $\text{RhL}_3\text{X}_2\text{Y}$ available (L = substituted pyridine or

pyridine; X, Y = Cl, Br), an investigation of their behaviour toward a small number of halocarbon solvents was undertaken. The method followed naturally from the course of preparation of the compounds; they were simply allowed to crystallise from their solution in the given solvent. The results are given in Table 4.9. Two methods were used to determine the composition; either the crystals were weighed, dried and re-weighed, or else they were weighed out and the absorbance measured at a wavelength of known ϵ , at the maximum of a band if possible, to reduce error. The latter method, used in Chapter 1, has the advantage in that it incurs less error when determining the composition of a single crystal, a necessary measure taken when it was realised that more than one type of solvate can form. The first occasions on which attempts were made to grow crystals of $\text{Rhpy}_3\text{Cl}_3 \cdot 2\text{CHCl}_3$ met with failure, as the product proved to be unsolvated orange-red crystals. However, it was realised that the ambient temperature may have been a significant factor, affecting either solubility equilibria or simply rate of evaporation. Refrigeration of the solution, but still allowing slow evaporation of solvent, was found to induce crystallisation of the solvate.

Table 4.9

Compositions of Chlorocarbon Solvates

Compound	Appearance	% Solvent		Method
		Calc.	Found	
Rhpy ₃ Cl ₃ .2S ^a	orange rhombs	34.8	31.9	c
Rhpy ₃ Cl ₃ .D ^a	clusters of orange prisms	21.2	21.6	b
Rhpy ₃ Cl ₃ .2D	orange rhombs	35.0	34.9	b
Rhpy ₃ Cl ₃ .2CH ₂ Cl ₂	"	27.6	27.3	c
RhDpy ₃ Cl ₃ .2S ^d	"	34.0	34.6	b
Rhpic ₃ Cl ₃ .1.5S	"	26.8	26.9	b
Rhpy ₃ Cl ₂ Br.2S	orange-red rhombs	32.2	32.9	c
Rhpy ₃ ClBr ₂ .3S	deep red lozenges	40.0	38.8	b
Rhpy ₃ ClBr ₂ .S	deep red prisms	18.2	18.4 ^e	b,c

a: S = CHCl₃, D = CDCl₃

b: by oven drying

c: spectrophotometrically

d: pentadeuteriopyridine complex

e: mean of 17.8%, 18.9%

Although solvates could not be obtained with mer- Rhpy_3Br_3 with CHCl_3 , CH_2Cl_2 , or CH_2Br_2 this does not necessarily mean that they do not exist in the solid state, but probably that they are not stable. Solvate formation could not be induced for CH_2Br_2 or CHBr_3 with mer- Rhpy_3Cl_3 while CH_2Cl_2 formed a disolvate with Rhpy_3Cl_3 which was very unstable, and the rapid loss of CH_2Cl_2 made determination of the composition difficult. With CHCl_3 , Rhpy_3Cl_3 and $\text{Rhpy}_3\text{Cl}_2\text{Br}$ formed disolvates, which crystallised as brightly coloured, chunky rhombs up to more than 5 mm. in dimensions. The presumption that the monosolvate of chloroform on $\text{Rhpy}_3\text{ClBr}_2$ was the limiting degree of solvation for that compound, and that each rhodium compound formed one definite solvate, was dispelled when a crop of chloroform - solvated Rhpy_3Cl_3 crystals proved to be $\text{Rhpy}_3\text{Cl}_3 \cdot \text{S}$ (see footnote) the monosolvate. These were similar in appearance to the solvate $\text{Rhpy}_3\text{ClBr}_2 \cdot \text{S}$, both being in the form of roughly circular clusters (2-6 mm. across) of prisms, up to ca. 4 mm. long, but mostly smaller. In addition, an attempt to grow a crop of these crystals for X-ray powder photography resulted in the formation of a large (not single) crystal, about 10x4x2 mm.

S = CHCl_3 of solvation, D = CDCl_3 of solvation in 4.3

which was found to be the solvate $\text{Rhpy}_3\text{ClBr}_2 \cdot 3\text{S}$. Its stability towards loss of solvent to the atmosphere was comparable to that of $\text{Rhpy}_3\text{Cl}_3 \cdot 2\text{CH}_2\text{Cl}_2$, the product being orange-brown and remarkably micaceous in appearance.

A sample of $\text{Rhpy}_3\text{Cl}_2\text{Br} \cdot 2\text{S}$ was oven-dried for 10 minutes and then placed in a desiccator over chloroform and left for several days. After that, the unsolvated compound had not changed in appearance. That it had absorbed some chloroform was shown when redrying incurred a weight loss of ca. 18%, equivalent to previous uptake of ca. 0.9 CHCl_3 . Coupled with this observation, one notes in general that the relatively translucent, crystalline solvates, on desolvation, give products which are permeable, of a lighter colour, as they are quite opaque, and although the exterior morphology of the originally solvated crystal is retained, the products are very friable. The X-ray powder diffraction patterns are listed in Table 4.10, as d-spacing values, for three forms of mer- Rhpy_3Cl_3 ; these are (i) the unsolvated material, from the action of hydrochloric acid on the chloro-oxalate complex, (ii) the dichloroform solvate, with a small amount of chloroform added to the diffracting sample, and (iii) the desolvated material, from drying the disolvate at 110°C . It is immediately apparent that

Table 4.10

X-ray Powder Diffraction Data for Rhp_3Cl_3

(d-spacings)

(i)	(ii)	(iii)
7.75s	7.8vs	7.75s
7.3 s		7.35s
6.58s		6.65s
6.23w		
5.77vs	5.72m	5.78vs
		5.52m
5.33m	5.28s	5.30vs
5.06s		
4.84s		4.86s
	4.64m	
	4.57s	
4.48w	4.47m	4.50w
4.23w	4.26s	4.23w
4.17w	4.17s	4.18w
3.90s	3.90m	3.91s
	3.87m	
	3.80m	3.80w
3.64vs	3.65m	3.67m
3.55w	3.57m	3.56w
	3.49m	3.47w
3.37w	3.34w	
	3.28s	
3.04m	3.08m	3.03s
3.02m		
	2.93w	2.95m
2.88s		
	2.83w	
2.73w	2.76w	2.74m
2.66m	2.68w	2.66m
	2.60w	
2.55m	2.58w	
2.52m		
2.42m	2.41m	
2.39m		
2.38w		2.38m
2.36m		
2.34w		2.34m
2.28s	2.32m	2.28m
		2.17m
2.07m	2.08m	
2.00s		
1.72s		

(i) unsolvated; (ii) chloroform disolvate, $\text{Rhp}_3\text{Cl}_3 \cdot 2\text{S}$;
 (iii) desolvated at 110° .

inclusion of chloroform alters the crystal structure of the compound, as several strong lines associated with large interplanar spacings (4.8 to 7.3) in the parent compound are absent in the disolvate. When the chloroform is driven off, the crystal structure is changed again, this being suggested by two factors. Firstly, strong lines (7.35, 6.65, 4.86) appear in the desolvated compound, having been absent in $\text{Rhpy}_3\text{Cl}_3 \cdot 2\text{S}$. Secondly, the change in the lattice on desolvation is probably not merely a reversion to the original structure, since some lines which appear in the original crystals are changed in intensity in the desolvated material. For example, one observes that the $d = 5.33$ line is of medium intensity in the "unsolvate" (i), but very strong in the "desolvate" (iii). Other changes from (i) to (iii) are: 3.64, very strong, to medium; 2.88 strong, disappears; 5.06 strong, disappears. Hence on loss of included solvent, a new form of Rhpy_3Cl_3 is obtained, so the conclusion may be made that it, and presumably the other compounds, with the possible exception of mer- Rhpy_3Br_3 , are at least dimorphic. Although no diffraction pattern was obtained for a monosolvate, the facts that they form stoichiometrically and exhibit a crystal morphology different from that of the desolvated material, suggest that at least Rhpy_3Cl_3 (and $\text{Rhpy}_3\text{ClBr}_2$, by virtue of its trisolvate formation) will

be trimorphic, if not (literally) polymorphic.

The reaction



may therefore be expected to be irreversible, as desolvation does not merely remove the solvent molecules, but alters the lattice so that their re-entry is not favoured. It was noted that loss of therefore absorbed chloroform from desolvated $\text{Rhp}_3\text{Cl}_2\text{Br}$ was more rapid than from any of the solvates, implying that it corresponded merely to evaporation of the CHCl_3 from the large internal surface area.

These results are similar to those of Steinbach and Burns⁽¹⁹⁾ who found that the acetylacetonates of trivalent iron, chromium and aluminium which form chloroform disolvates on desolvation lead to formation of pseudomorphs of the original crystals. These, they claimed, could be held in equilibrium with the solvated material, their evidence being that linear plots of vapour pressure vs (reciprocal) temperature were obtained. This difference from the present work may be related to the possibility that there exists a polymorph of Rhp_3Cl_3 which is the immediate product of desolvation and which participates in a reversible equilibrium, but can also change to the form which will

not accept solvent again.

The apparently increasing stability sequence, trisolvate < disolvate < monosolvate is supported by a pair of differential thermal analyses, which gave endothermal maxima corresponding to loss of chloroform from $\text{Rhpy}_3\text{Cl}_2\text{Br} \cdot 2\text{S}$ and $\text{Rhpy}_3\text{ClBr}_2 \cdot \text{S}$ at a temperature higher for the latter (ca. 70-75°C) than the former (ca. 55-60°C). $\text{Rhpy}_3\text{Cl}_3 \cdot 2\text{S}$ had a well-defined endothermal peak but the maximum's position also varied somewhat (63-69°C over four runs) while the monosolvate peaked at ca. 105°. For comparison, the chloroform solvate⁽²⁰⁾ of $\text{Cu}(\text{salen})_2$ was prepared as red-purple prisms, and these lost chloroform to give an endothermal peak at 48°C.

The difference between the temperatures of maximum rate of chloroform loss (ca. 20°C) is well outside experimental error for those compounds, $\text{Rhpy}_3\text{Cl}_3 \cdot 2\text{S}$ and $\text{Cu}_2(\text{salen})_4 \cdot 2\text{S}$. Baker et. al.⁽²⁰⁾ proposed that in the copper complex, the $\text{Cu}_2(\text{salen})_4$ dimers are hydrogen bonded to the CHCl_3 via a ligand oxygen and the chloroform proton. Hence the qualitative thermochemical evidence suggests that ^ahydrogen bond from the CHCl_3 is probable for the rhodium pyridine complexes.

4.3(ii) Vibrational Spectra, and Structure

Firstly, the presence of the halocarbon is evident from the strong i.r. absorption at ca. 750 cm^{-1} in the CHCl_3 and CH_2Cl_2 solvates. This band, attributed to⁽²¹⁾ ν_5 in CHCl_3 and ν_9 in CH_2Cl_2 , unfortunately cannot be generally assigned an accurate position, as out-of-plane C-H bending bands of the ligands are also strong in this region. However, it can be distinguished in the following compounds: $\text{Rhpy}_3\text{Cl}_3 \cdot 2\text{CH}_2\text{Cl}_2$ (729 cm^{-1}), $\text{RhDpy}_3\text{Cl}_3 \cdot 2\text{S}$ (748 cm^{-1}) and $\text{Rhpic}_3\text{Cl}_3 \cdot 1.5\text{S}$ (751 cm^{-1}). These values are below those observed for liquid CH_2Cl_2 ⁽²¹⁾ (737 cm^{-1}) and more relevantly, for gaseous⁽²²⁾ or liquid⁽²¹⁾ CHCl_3 ($760\text{--}770\text{ cm}^{-1}$). The ν_3 (C-Cl) vibration of CHCl_3 occurs in all the solvates, only slightly shifted from the vapour value (672 cm^{-1}) to ca. $662\text{--}667\text{ cm}^{-1}$. It is appropriate to compare the values of the vibrational frequencies of the CHCl_3 molecule in the solvates with gaseous CHCl_3 as the latter should represent CHCl_3 in its state of least interaction with other molecules. Examination of the low frequency Raman effect bands of the solvates turns out to be not very informative, although the size and transparency of the solvate crystals allow one to obtain good Raman spectra, although the LASER beam tends to cause local heating which desolvates the crystal and makes it opaque.

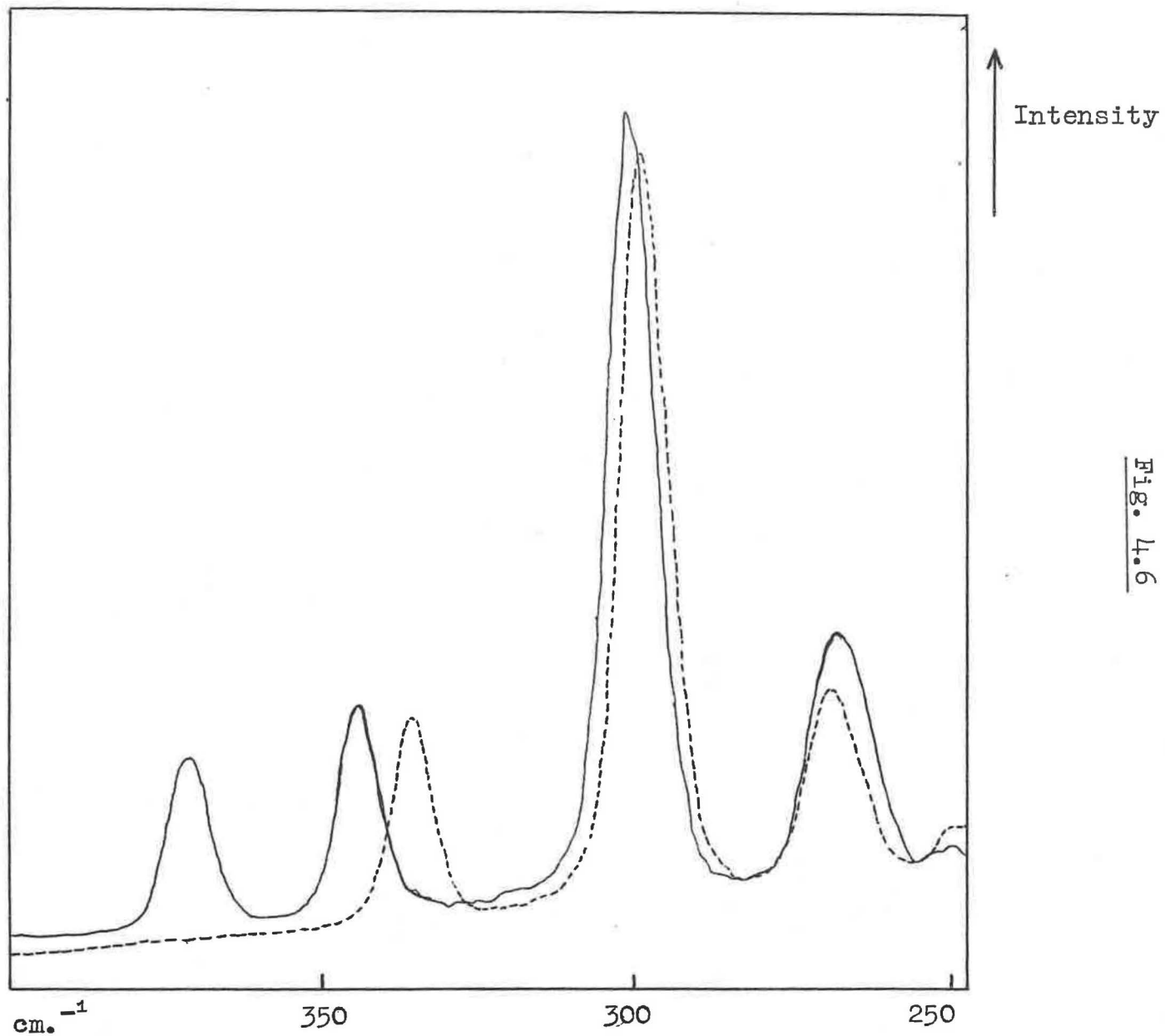


Fig. 4.6

Raman Spectra of Rhpy_3Cl_3 (----) and its CHCl_3 solvate (—)

Table 4.11

Raman Spectra of Chloroform Solvates

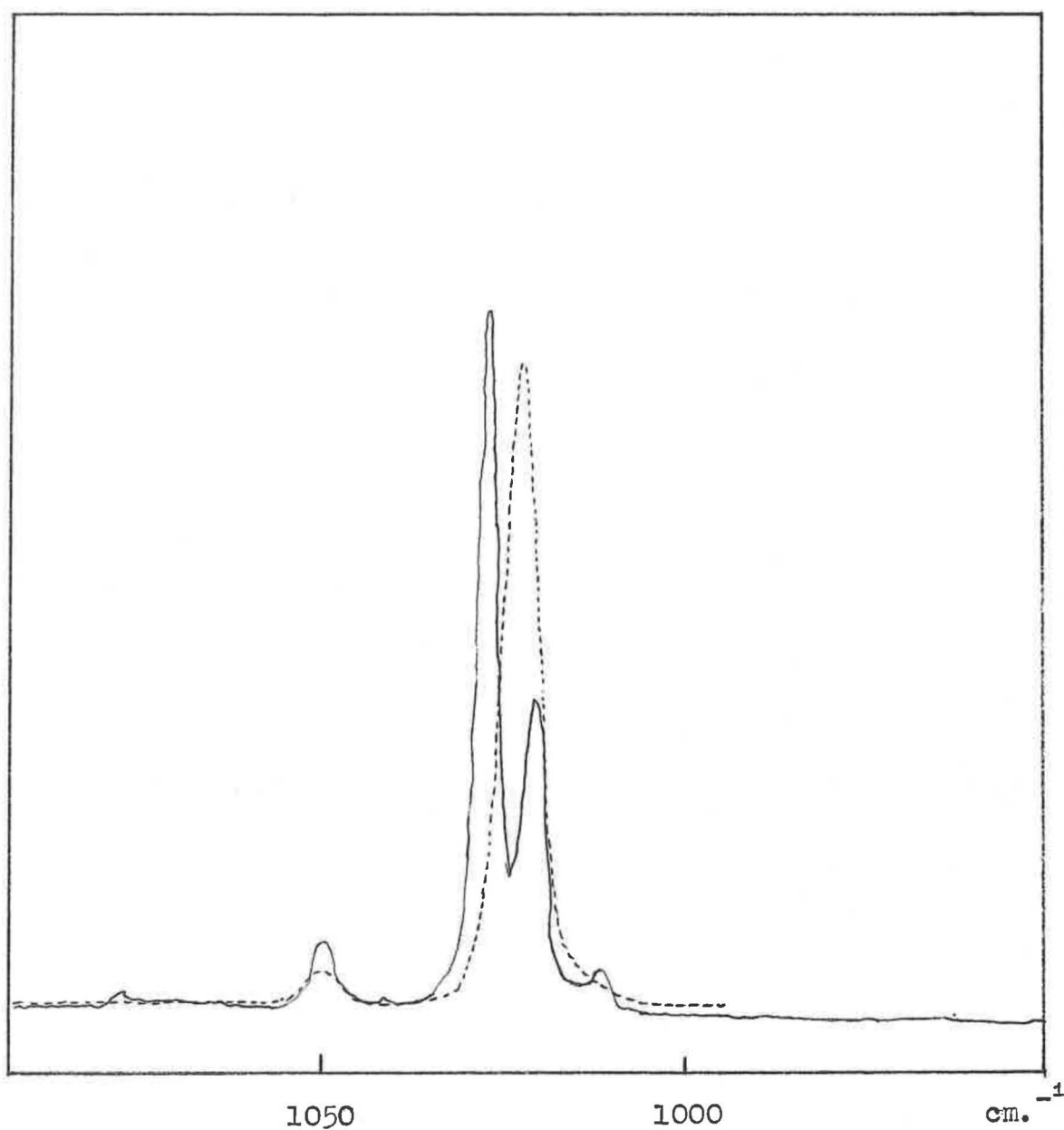
Compound	Wavenumber	Substrate	Solvent
Rhpy ₃ Cl ₃ ·2CHCl ₃	268 s	268 s	s 261 vs (a)
	301 vs	299 vs	
	342 s	336 s	s 363 s (a)
	369 s		
		1019 s	
	1021 s	1026 s	
Rhpy ₃ Cl ₃ ·CDCl ₃	218 s		s 262 s (b)
	268 s	268 s	
	300 vs	299 vs	s 366 s (t)
	342 s	336 s	
	363 s		
		1019 s	
1020 s	1026 s		
RhDpy ₃ ·2CHCl ₃	262 s	261 m	261 vs
	299 vs	298 vs	
	335 s	328 s	
	365 s		363 s
		987 s	
	985 s	979 s	

a: vapour phase energy, liquid phase intensity

b: liquid phase

There are three strong bands in the Raman spectrum of Rhpy_3Cl_3 between 200 and 400 cm^{-1} (Section 2.(iii)) at 268, 299, 336 cm^{-1} associated with the A_1 type rhodium-pyridine and rhodium-chlorine (latter two) stretches respectively, and the deuteriopyridine complex is similar. In $\text{Rhpy}_3\text{Cl}_3 \cdot 2\text{S}$, four strong bands are seen, and they are given in Table 4.11, as are those for the partially deuteriated compounds $\text{Rhpy}_3\text{Cl}_3 \cdot \text{D}$ and $\text{RhDpy}_3\text{Cl}_3 \cdot 2\text{S}$. Some changes are apparent, firstly the A_1 vibration associated with the chloride trans to the pyridine ligand moves up in energy by 6-7 cm^{-1} . Secondly, a strong band arises at ca. 365 cm^{-1} , due to ν_3 of the chloroform, only slightly shifted. In addition the ν_8 (C-Cl₃ bending) mode of the chloroform is not immediately apparent, although it is reported⁽²¹⁾ to give a very strong band at 262 cm^{-1} in CHCl_3 vapour. Possibly it is obscured by the band at 268 cm^{-1} in Rhpy_3Cl_3 and 261 cm^{-1} in $\text{RhDpy}_3\text{Cl}_3$. It may still be perturbed in the sense that it is therefore of reduced intensity in the Raman, even though it is known to be very strong in liquid CHCl_3 or CDCl_3 . Interaction of one (or two) of the chlorine atoms of the chloroform with another molecule would reduce the symmetry to C_s , but have no effect on the activity of the ν_8 mode.

Fig. 4.7



Raman spectra of Rhpy_3Cl_3 (—) and its disolvate (-----) showing change in pyridine ν_1 .

Another effect appears, at higher frequency. In the crystalline RhL_3Cl_3 compounds, there are two strong bands, not seen at low resolution, associated with the symmetric ring breathing mode of the pyridine. They are in a ratio of ca. 2.5:1 in intensity, occurring at 1026 and 1019 cm^{-1} in Rhpy_3Cl_3 , $\text{Rhpy}_3\text{Cl}_2\text{Br}$ and again separated by approximately 8 cm^{-1} in $\text{RhDpy}_3\text{Cl}_3$. They may correspond either to the ν_1 transitions of the pyridine rings which are trans to chloride (one) and mutually trans (two) respectively or result from in-phase and out-of-phase ν_1 modes. In the solvates, it appears that the more intense band at higher energy moves down and merges with the lesser band. The splitting in the solid state is reminiscent of the ^1H n.m.r. spectra of the compounds in solution, which show the heterocyclic ligands to be inequivalent in the ratio 2:1, but it is not determinable from the available data whether the Raman inequivalence in crystalline mer- Rhpy_3Cl_3 arises from the same cause or not. That is, it is possible that the single Raman peak observed in the solvates corresponds to the same degree of ring inequivalence as is indicated by solution n.m.r.

The i.r. spectra show a minor change in the environment of the pyridine rings in passing from unsolvated to solvated compound. In the Rhpy_3X_3 compounds there occurs

a group of three strong sharp bands due to pyridine's ν_{25} C-H bending mode e.g. at 757, 764, 783 cm^{-1} in Rhpy_3Cl_3 . The highest energy band is affected by solvation since it is absent from the spectra of $\text{Rhpy}_3\text{Cl}_3 \cdot \text{D}$ and $\text{RhDpy}_3\text{Cl}_3 \cdot 2\text{S}$ (otherwise 557 cm^{-1}) weak in $\text{Rhpy}_3\text{ClBr}_2 \cdot \text{S}$, but strong again in $\text{Rhpy}_3\text{Cl}_2\text{Br} \cdot 2\text{S}$, $\text{Rhpy}_3\text{Cl}_3 \cdot 2\text{D}$ and $\text{Rhpy}_3\text{Cl}_3 \cdot 2\text{S}$, so is no less enigmatic than the other spectroscopic properties.

Finally, however, there is one distinct piece of evidence regarding the solvent's environment. The $A_1 \nu_1$ (C-H) vibration of CHCl_3 occurs at 3019 cm^{-1} in the vapour phase Raman spectrum⁽²¹⁾ and is attributed to the quite weak 3034 cm^{-1} band in the vapour's i.r. spectrum;⁽²²⁾ CDCl_3 has ν_1 at 2265 cm^{-1} in the i.r. (weak band). In the solvates, medium to strong i.r. absorption⁽²²⁾ occurs between 2900 and 3000 cm^{-1} (Table 4.12). Unfortunately $\text{Cu}(\text{salen})_2$ has aromatic C-H stretching absorption in this region, which obscures the solvent ν_1 band, so the value for a ν_1 (C-H) shift in a known H-bonded solvate was not obtained. The ν_1 band was not strong enough for observation in $\text{Rhpic}_3\text{Cl}_3 \cdot 1.5\text{S}$ or $\text{Rhpy}_3\text{ClBr}_2 \cdot 3\text{S}$. The decrease in energy is compatible with the formation of a weak hydrogen bond with the substrate complex. The effect of H-bonding on the ν_1 frequency is well known; Allerhand

and Schleyer⁽²³⁾ examined this phenomenon, and concluded that the effect of merely changing the dielectric properties of the medium was much smaller than the shifts engendered by the presence of proton acceptors, such as pyridine ($\Delta\nu = 46 \text{ cm}^{-1}$). They disputed prior claims that $\Delta\nu$ paralleled the enthalpy of association of CHCl_3 with various proton acceptors, and Becker⁽²⁴⁾ proposed that ν_1 was insensitive to H-bond formation, but that ν_1 was indicative of it, and that ΔH for



could be less than zero even when $\Delta\nu$ was close to zero. The $\Delta\nu$ values found here are significantly large. They very probably correspond to H-bond formation states, rather than just being concomitant with the changes in the lower frequency vibrations, as these latter involve mainly the C-Cl bonds only; they certainly imply H-bonding on the Allerhand-Schleyer-Becker basis. Mason and Towl⁽²⁵⁾ have recently described the structure of the related but nonstoichiometric chloroform solvate $[\text{Rhp}_2\text{Cl}_2(\text{CP})] \cdot 0.61 \text{ CHCl}_3$ in terms of a weak hydrogen

CP = o-(di-o-tolylphosphino)benzyl anion

bond from the chloroform to a coordinated chloride cis to a pyridine, which thus prevents the solvent from becoming totally disordered throughout the lattice. One recalls the shift incurred in the A_1 , $\nu(\text{Rh-Cl})$ frequency, and the coalescence of the pyridine ν_1 bands in the Raman spectrum, and it seems likely that any H-bond will indeed be associated with the C_2 axis of the Rhpy_3X_3 molecule, although it is not possible to determine which of the trans ligands (py or Cl) is more affected. The $\Delta\nu$ values are greater for monosolvates than for disolvates, which means that proton acceptor sites are more available in the former. The changes in i.r. intensity of the CHCl_3 ν_1 band from the phase vapour reflect the perturbation expected along the C_3 axis on H-bond formation.

Table 4.12.

Position of ν_1 of CHCl_3 or CDCl_3 of solvation.

<u>Compound.</u>	<u>Position (cm^{-1})</u>	<u>Shift from vapour ($\Delta\nu$)</u>
$\text{Rhpy}_3\text{Cl}_2\text{Br}_2 \cdot \text{S}$	2978m	56
$\text{Rhpy}_3\text{Cl}_2\text{Br} \cdot 2\text{S}$	2992s	32
$\text{Rhpy}_3\text{Cl}_3 \cdot 2\text{S}$	2992m(a) 2993m	32
$\text{RhDpy}_3\text{Cl}_3 \cdot 2\text{S}$	2998m 2995m(a)	26
$\text{Rhpy}_3\text{Cl}_3 \cdot \text{D}$	2227m 2228s(a)	38
$\text{Rhpy}_3\text{Cl}_3 \cdot 2\text{D}$	2236s 2236s(a)	29

a: Raman spectrum.

Table 4.13

Analytical Data

Compound	Code	C		H		N		Other	
		f.	c.	f.	c.	f.	c.	f.	c.
Rhpy ₃ ClO _x	4A	44.0	44.1	3.1	3.2	9.2	9.1		
Rhpy ₃ BrO _x	4B	40.4	40.2	3.0	2.9	8.4	8.3		
Rhpic ₃ ClO _x ·4H ₂ O	4C	41.9	41.6	5.0	5.1	7.4	7.3	H ₂ O, 11.8	12.5
anhydrate		47.3	47.5	4.2	4.2				
Rhlut ₃ ClO _x	4D	50.2	50.4	5.0	4.9	7.6	7.7		
Rhpy ₃ I _{0x}	4E	36.1	36.8	2.2	2.7	7.8	7.6		
1,2,6-Rhpy ₃ Cl ₃	4G	40.2	40.3	3.4	3.4	9.2	9.4		
1-2,6-Rhpy ₃ Br ₃	4H	31.2	31.1	2.8	2.6	7.1	7.2		
1-2,6-Rhpy ₃ ClBr ₂	4J	33.7	33.7	2.9	2.8	8.1	7.9	Cl, 6.8 Br, 30.8	6.6 29.9
1-2,6-Rhpy ₃ Cl ₂ Br	4K	36.5	36.7	3.1	3.1	8.6	8.6	Cl, 14.7 Br, 16.5	14.4 16.3
1,2,6-RhDpy ₃ Cl ₃	4L	39.2	39.1			9.2	9.1		
1,2,6-Rhpy ₃ I ₃	4M	24.9	25.0	2.3	2.1	5.9	5.8		
1,2,6-Rhlut ₃ Cl ₃	4N	47.4	47.5	5.4	5.1	7.7	7.5		

References - Chapter 4

1. M.L. Tschugaev, Bull. Soc. Chim., 1919 25 234.
2. P. Poulenc, Ann. Chim., 1935 4 634.
3. R.D. Gillard, E.D. McKenzie, M.D. Ross, J. Inorg. Nucl. Chem., 1966 28 1428.
4. R.E. Hester, R.A. Plane, Inorg. Chem., 1964 3 513.
5. R.D. Gillard, S.H. Laurie, P.R. Mitchell, J. Chem. Soc., 1969A 3007.
6. M. Delépine, Bull. Soc. Chim., France, 1929 45 235.
7. J.P. Collman, H. Holtzclaw Jr., J. Amer. Chem. Soc., 1958, 80 2054.
8. J.A. Osborn, R.D. Gillard, G. Wilkinson, J. Chem. Soc., 1964 3168.
9. C.K. Jørgensen, Acta Chem. Scand., 1957 11 151.
10. H.-H. Schmidtke, Z. physik. Chem., 1962 34 295.
11. C.K. Jørgensen, Prog. Inorg. Chem., 1962 4 73.
12. C.K. Jørgensen, Acta Chem. Scand., 1956 10 500.
13. H.-H. Schmidtke, D. Garthoff, J. Amer. Chem. Soc., 1967 89 1317.
14. D.P. Graddon, E.C. Watton, Austral. J. Chem., 1965, 18, 625.
15. A.H. Norbury, A.I.P. Sinha, J. Chem. Soc., 1968A 1598.
16. C.K. Jørgensen, "Absorption Spectra and Chemical Bonding" Pergamon, Oxford, 1962 pp. 294.
17. R.J.H. Clark, C.S. Williams, Inorg. Chem., 1965 4 350.
18. H. Shaw, Unpublished work.
19. J.F. Steinbach, J.H. Burns, J. Amer. Chem. Soc., 1958 80 1839.

20. E.N. Baker, D. Hall, J.N. Waters, J. Chem. Soc., 1970A
406.
21. G. Herzberg, Molecular Spectra and Molecular Structure,
Volume II, D. Van Nostrand, New York, 1945 pp. 316-7.
22. A. Ruoff, H. Bürger, Spectrochim. Acta, 1970 26A 989.
23. A. Allerhand, P. von R. Schleyer, J. Amer. Chem. Soc.,
1963 85 1715.
24. E.D. Becker, Spectrochim. Acta, 1959 15 743.
25. R. Mason, A.D.C. Towl, J. Chem. Soc., 1970A 1601.

Chapter 5

5.1 On Certain Aspects of Transition Metal Autoxidation

The interaction of molecular oxygen with transition metal centres and its consequent fixation as a diatomic ligand has been known for some considerable time⁽⁹⁶⁾ and the chemistry of this interaction has been discussed recently by Taube⁽⁹⁷⁾ and by Fallab⁽⁹⁸⁾.

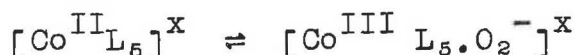
It is necessary for the formation of an O₂ adduct that the metal centre, in its low oxidation state, has a vacant coordination site otherwise oxidation may occur via an outer sphere mechanism, without the formation of an M-O₂ bond.

Structurally, monomeric oxygen complexes may be divided into two groups; those with the metal ion bonded to one of the oxygen's atoms ("end-on") and those with the metal ion equidistant from the two oxygen atoms ("side-on"). The first type of bonding is found to occur in the case of first transition row metals ligated by π -de-localising groups, e.g. [Coacacen]⁽²⁹⁾, [Cosalen]⁽³⁶⁾ and in the pentacyanocobaltate(II) anion⁽⁹⁰⁾. In these cases ESR spectroscopy^(26,90) demonstrates the presence of a doublet ground state for the Co-O₂ system, which is the result of the odd electron in these monomeric superoxo complexes;



The second type of geometry, with "side-on" bonded O_2 is known for the platinoid division metals with polarisable or π -delocalising ligands, the most notable example being Vaska's iridium complex⁽¹⁰⁰⁾ $[\text{Ir}(\text{CO})\text{Cl}(\text{PPh}_3)_2(\text{O}_2)]$, from which the O_2 molecule may be displaced by bubbling nitrogen through a solution of the compound. This and similar⁽¹⁰¹⁾ compounds have been characterised by X-ray crystallography.

Two factors appear to determine the structure of these transition metal oxygen complexes, namely oxidation state and stereochemistry of the precursor complex, although of course these two factors are not independent. The O_2 entity may be considered to be well-behaved as a ligand in terms of the stereochemistry of the O_2 adduct. In the case of the "end-bonded" cobalt species the metal is formally cobalt(III) and it appears necessary for well-defined oxygen uptake (whether or not it be reversible) that the resulting complex be six-coordinate. This is certainly true in the cases of the $\text{Co}(\text{CN})_5^{3-}$ adduct and the $[\text{Coacacen}]^{2+}$ adduct, where the fifth coordination position in the latter case must be occupied by a donor such as pyridine, DMF, etc.⁽²⁹⁾. Hence O_2 here acts as a one-electron oxidant and monodentate ligand;



Although it is required that the acacen = 4L residue be planar, thus preventing bidentacy of the O₂, neither is there any evidence that the cyano-anion loses CN⁻ to give [Co(CN)₄O₂]²⁻, with side-bonded O₂. When O₂ adds to IrCl(CO)(PPh₃)₂, IrI(CO)(PPh₃)₂, Ir(diphos)₂⁺ or Rh(diphos)₂⁺ in which the square planar four-coordinate metal is formally rhodium(I), or iridium(I), it may be considered to act as a bidentate ligand to give (albeit distorted) six coordinate structures^(101,102,103) and in these metals (unlike cobalt(II)) a two-electron oxidation step is possible, to M(III) whose complexes are almost invariably six-coordinate.

Moreover, the reaction of O₂ with ethylenebis(tri-phenylphosphine)platinum(0) results in the displacement of the C₂H₄ ligand to give a planar⁽¹⁰⁴⁾ pseudo-four-coordinate [Pt(PPh₃)₂O₂] where the O₂ may be thought of a (very approximately) a bidentate, two electron oxidant. It therefore appears that the mode of attachment of the O₂ moiety is predictable by consideration of the structure of the substrate. These criteria do, however, suggest a different bonding mode for the O₂ in the haemoglobin complex to that proposed by Griffith^(66,105).

The stability and reactivity of the O₂ adducts require a more detailed examination of the nature of the coordinated

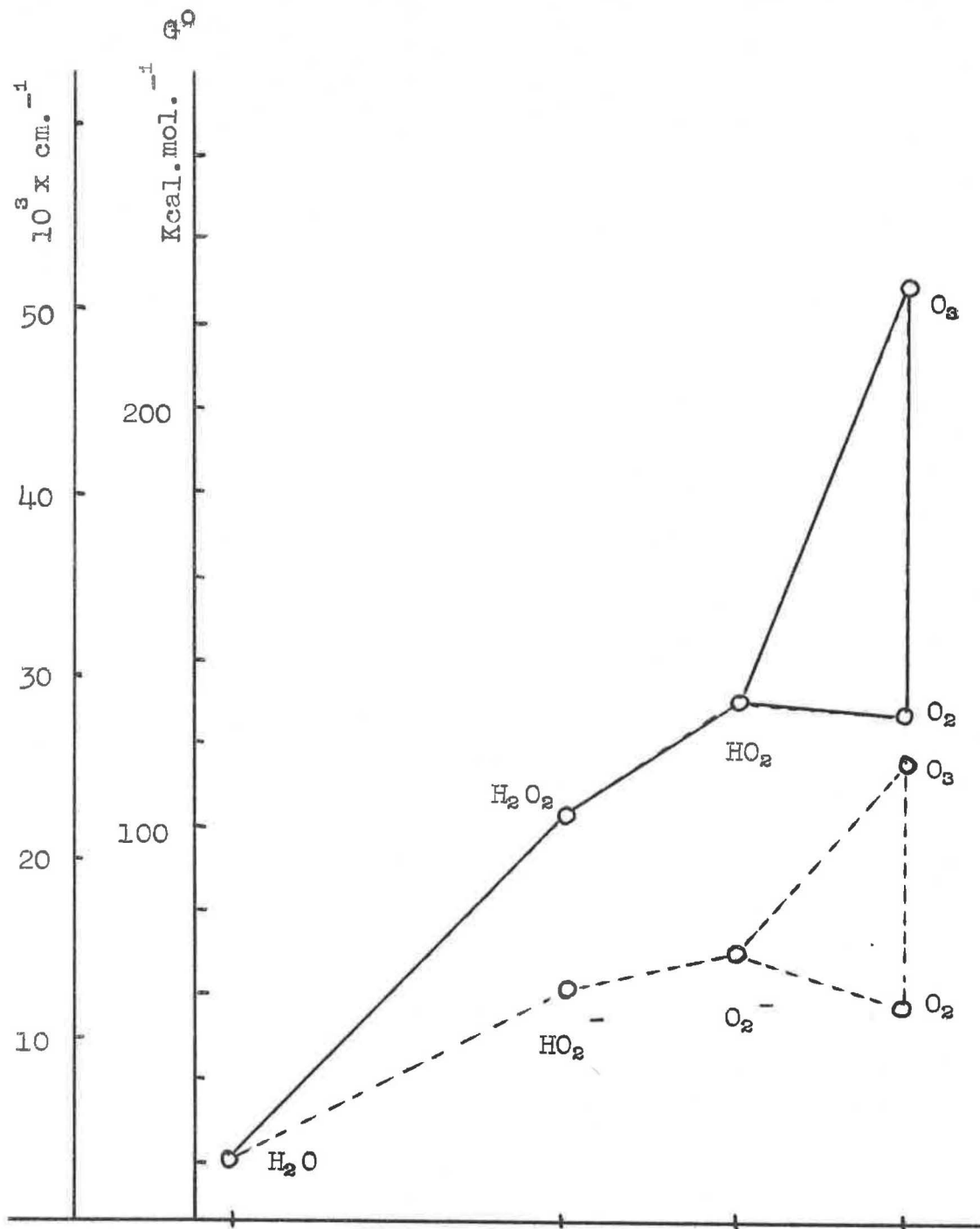


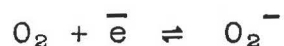
Fig. 5.1 Free energy diagram for oxygen vs water, (—) acidic, (---) basic.

O₂. As a thermodynamic criterion, for the reversible formation of an O₂ adduct, one requires that the redox potentials of the substrate and of the pertinent oxygen half-cell be similar, so that the idealised equilibrium



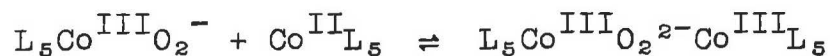
does not lie too heavily to one side.

Reference to Figure 5.1 shows that the free energies of the species constituting the oxygen-water redox system with respect to the standard hydrogen electrode are such that superoxide is destabilised with respect to O₂. In order to make the electron transfer step



reversible the O₂⁻ ion needs to be stabilised by 5-10 Kcal. mole⁻¹ relative to O₂ depending on pH and solvent, so a one-electron reducing metal ion needs an E⁰ in the region of -0.2v. to -0.5v.

In the case of the cobalt complexes, further reaction may occur, whence the monomeric superoxo-cobalt(III) complex may act as oxidant towards another cobalt(II) species, to give a peroxo bridged dimer;



and this sequence has been confirmed in the pentacyano and salen series (26,36,72,88,90,106). The O₂ adduct formed from [Co(salen)(DMF)]²⁺ in DMF is reversible (107) as is that formed when salen is replaced by acacen (29), where a value of logK = 2.11 was determined. In order to examine the factors which may determine the stability of the adducts, and also their reactivity, it is necessary to take into account the rather singular nature of the electronic structure of the O₂ ligand (Figure 2.12). Simple MO theory neatly explains the triplet ground state observed in free O₂ as a result of the degeneracy of the antibonding π -orbitals derived from the oxygen 2p atomic orbitals perpendicular to the O-O axis.

Mason (99,107) has pointed out the similarity between the geometry of a coordinated ligand (such as O₂) and the geometry of the excited state of the free ligand. Mulliken (108) has suggested that O₂ may act as a Lewis acid in organic bases, a property which may be enhanced (97) by electronic re-arrangement to the ¹Δ state (Diagram 5.2). Remarkably perhaps, halocarbonylbis(triphenylphosphine)rhodium(I) forms 1:1 adducts with boron trihalides (109) while S-bonded SO₂, also a strong Lewis acid (110), is found to occupy an apical coordination site in its square pyramidal adduct (111)

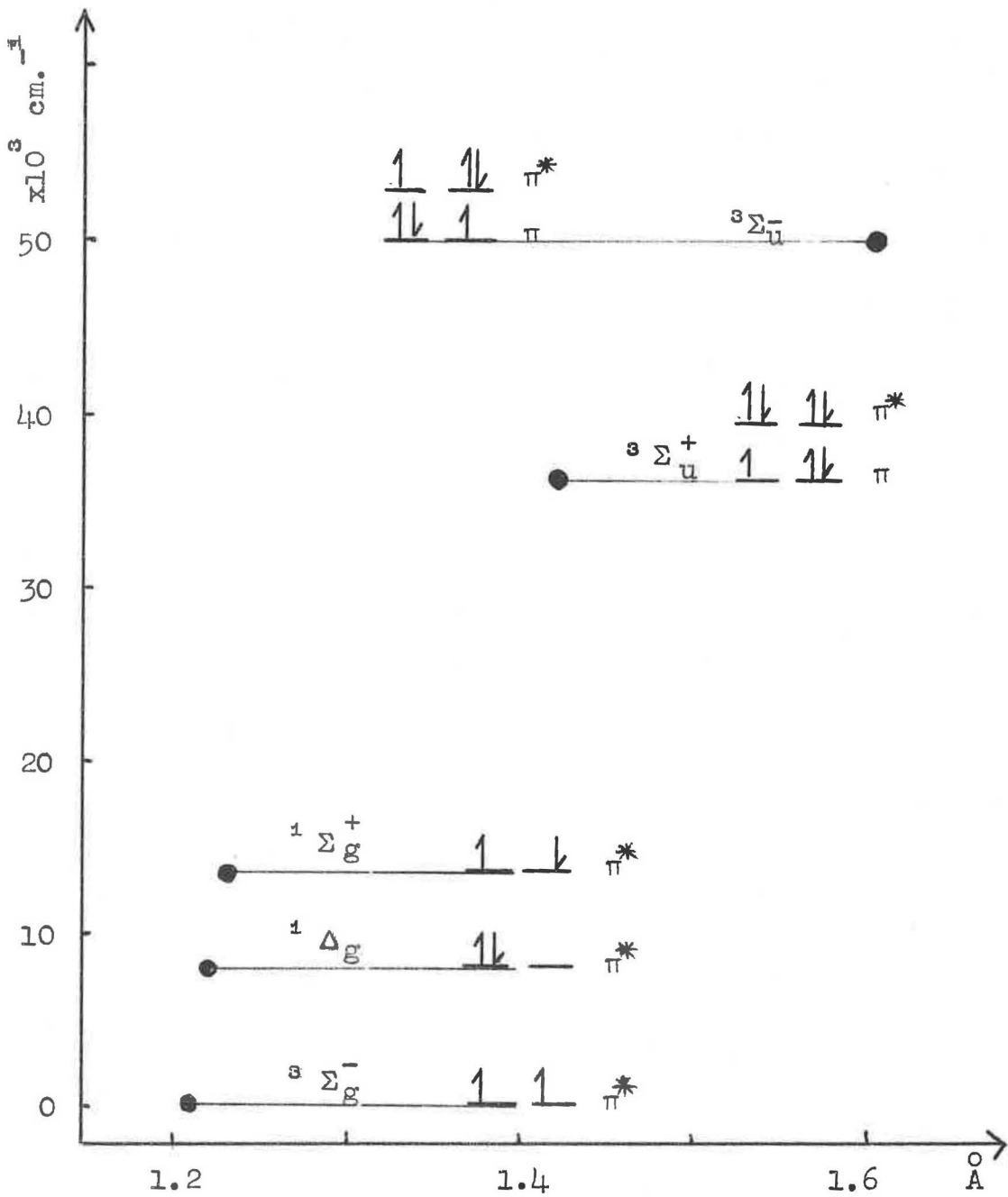


Fig. 5.2 Scheme of O_2 excited states as plot of spectroscopic energy vs. bond length.

of $\text{IrCl}(\text{CO})(\text{PPh}_3)_2$.

It appears then, that lower valence state metal complexes have a significant Lewis base capability, which would be important in their interaction with O_2 . Indeed, O_2 may be a poor donor as a result of its slightly higher ionisation potential⁽¹¹²⁾. (12.2 eV), compared to more familiar donors such as NH_3 (10.15 eV). N_2 is worse (15.6 eV) while ethylene (10.50 eV) is comparable to NH_3 , and CO (14.0 eV) is already polarised. On the other hand O_2 has a significant electron affinity⁽¹¹³⁾ (0.65 eV) and its oxidising properties are a familiar aspect of its chemistry. While the σ - and π -bonding components from platinum to ethylene in Zeise's salt are probably of roughly equal importance⁽¹¹⁴⁾, the latter will be preemptive in O_2 complexes of similar geometry. Consider now the Vaska adduct $\text{IrCl}(\text{CO})(\text{O}_2)(\text{PPh}_3)_2$. If the $\text{IrCl}(\text{CO})\text{O}_2$ moiety is in the XY plane, and the O-O axis therefore perpendicular to the XY bisectrix (Figure 5.3), forward donation (from base to acid) may occur from the $d_{x^2-y^2}$ orbital in the metal's antibonding e_g subset, to the antibonding $2p\pi_g$ orbitals on the O_2 , one of which will lie in the XY plane (Figure 5.3a). Overlap of the nonbonding d_{xy} orbital with the oxygens' bonding π_u subset allows "back donation" $t_{2g} \leftarrow \pi$ (Figure 5.3b). The O-O distance⁽¹⁰¹⁾ is 1.30Å

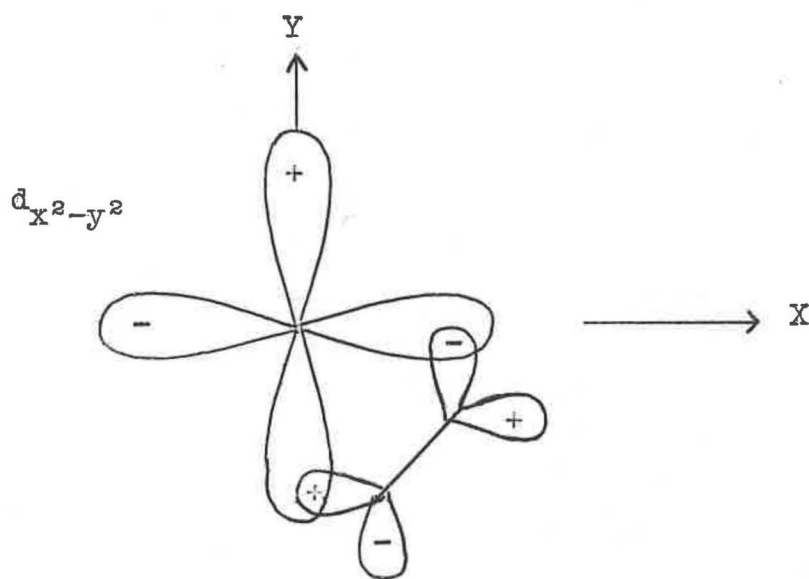


Fig. 5.3. (a) Base \rightarrow Acid donation involving e_g^* and π_g^* orbitals of the constituents.

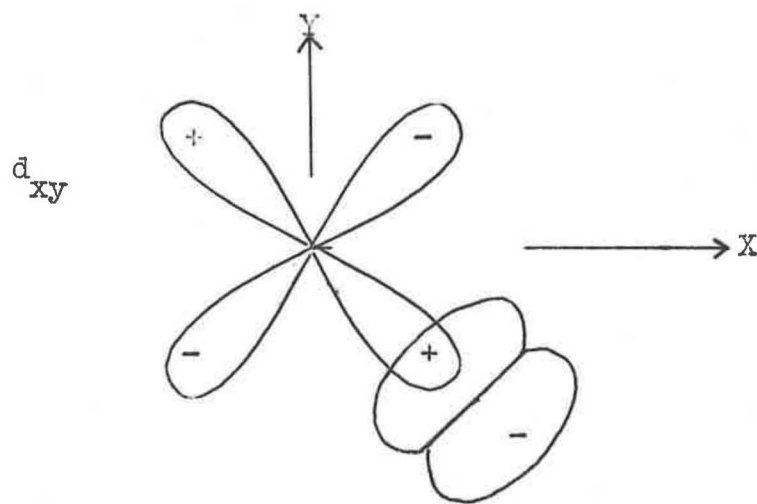


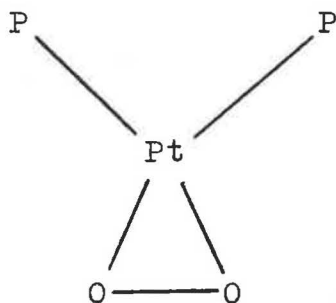
Fig. 5.3 (b) Acid \rightarrow Base back-donation involving t_{2g} - π_u overlap.

which corresponds approximately to a superoxide type O_2 ligand with the π -orbital occupancy roughly one electron more than the π^* (e.g. $\pi^4\pi^{*3}$).

As the other ligands in the XY plane are made more polarisable, the major effects should be to increase the $e_g \rightarrow \pi^*$ donation, accounting for the longer O-O bond (1.51Å) in the iodo-complex⁽¹⁰²⁾ as the π^* occupancy is increased.

When the trans-ligands are phosphines, the effect is greater still, and in $Ir(diphos)_2O_2$ the O-O distance⁽¹⁰³⁾ is 1.625Å which is similar to the ${}^3\Sigma_u^-$ state of O_2 (Figure 5.2). In the corresponding reversible rhodium complex, where the ionisation potential is greater (for the free ion) the expectedly worse donor metal gives a shorter (1.42Å) O-O bond⁽¹⁰³⁾ (cf. ${}^3\Sigma_u^+$ O_2) and a longer M-O bond.

For the pseudo-square planar platinum complex $[Pt(PPh_3)_2O_2]$, the d-orbital energy order is undoubtedly changed, but the structure⁽¹⁰⁴⁾ of the complex accommodates the overlap required by the preceding theory, as the trapezoidal planar geometry allows a metal orbital in the plane to extend past the ends of the O_2 moiety and overlap with the protruding π^*_g orbital. The reactivity of the coordinated oxygen⁽¹¹⁴⁾ is better explained by the excited



state concept for the ligand, in that the O-O distance (1.26Å) is similar to that of ${}^1\Sigma_g^+$ O₂ (1.23Å), although attack by a potential reductant at the unsaturated metal centre is probably the determinative factor in its reactivity.

Returning to the case of the pentacoordinate species, Co(CN)₅³⁻, [Cosalen(DMF)] etc., one foresees the opportunity here for the donor-acceptor (Co→O₂) interaction to occur. This will be more effective if the electronic density on the metal is increased, explaining the observation^(29,72) that the oxygen complexes form more readily for [Coacacen] and [Cosalen] when the donor orbital is also interacting with a base (py, DMF, etc.) in the position trans to O₂. The effect of the other axial ligand may be direct or indirect, i.e. it may "push" electronic charge directly through the (axial) d_{z²} orbital on to the O₂, or the O₂ may accept the charge from a d_{xz}/d_{yz} orbital. The latter case begs the postulate that the initial interaction

involves the O-O axis parallel to the metal-macrocylic plane. There is no direct evidence for this as yet, but Fallab⁽¹¹⁵⁾ has suggested the existence of a discrete, π -bonded state intermediate for an equilibrium of the type



The donor-acceptor model proposed here would not predict side-bonded O_2 in these systems when rigidly applied. Instead, the interaction would be expected to be $d_{z^2} - \pi_g^*$ and result in the O_2 being end-bonded to the cobalt, but with the CoOO angle $\neq 180^\circ$, by virtue of the spatial distribution of the π_g^a orbital, and this is the geometry proposed by Basolo and coworkers⁽²⁶⁾ for the (Coacacen) complexes.

If a rhodium(I) intermediate is responsible for the catalysis of the $\text{Rhpy}_4\text{X}_2^+$ systems' reactions, then only the steric factors discussed in Chapter 1 would prevent the formation of an octahedral adduct, $[\text{Rhpy}_4\text{O}_2]^+$, with the cis tetrapyridine geometry. If O_2 can overcome this constraint, the following would probably involve loss of pyridine, and further decomposition. Indeed, warm solutions of $\text{Rhpy}_4\text{X}_2^+$ are not stable to prolonged oxygenation, but become cloudy, suggesting the formation of insoluble tripyridinerhodium compounds.

The direct action of O_2 on a coordinatively unsaturated metal complex becomes mechanistically elegant and chemically, very rational. Recent results support the generality of this hypothesis. Vlček has shown that $[Co(CN)_5H]^{3-}$ may be deprotonated⁽¹¹⁶⁾ to yield $[Co(CN)_5]^{4-}$ a very reactive species, while $[Rhen_2(OH)H]^+$ may similarly lose water⁽⁹²⁾ to give $[Rhen_2]^+$.

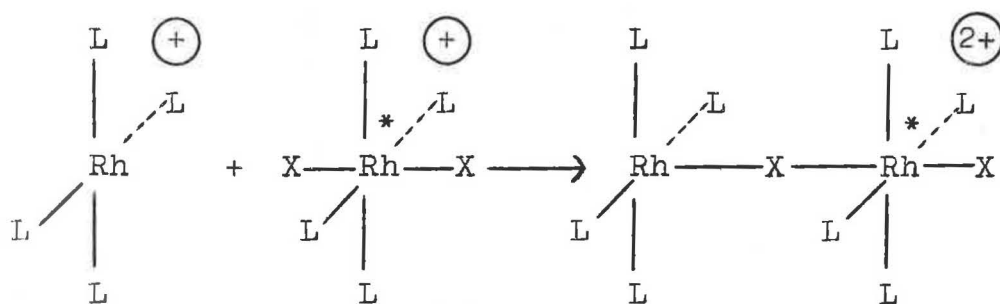
Thus the reaction of $Rhpic_4Cl_2^+$ with O_2 in basic reducing medium may be partly rationalised on these grounds. One notes that in the Rh^I case, there is an unfavourable spin restriction on the reaction with O_2 and it was observed that a basic ethanolic solution of $Rhpy_4Cl_3$ under O_2 could be turned blue-green by acid Ce^{IV} after standing in sunlight for a week, while an identical solution kept in the dark did not give any colouration. This agrees with the possibility of attack by $^1\Delta_g O_2$ produced by the action of sunlight (Figure 5.2) but by no means proves it.

5.2 Conclusion

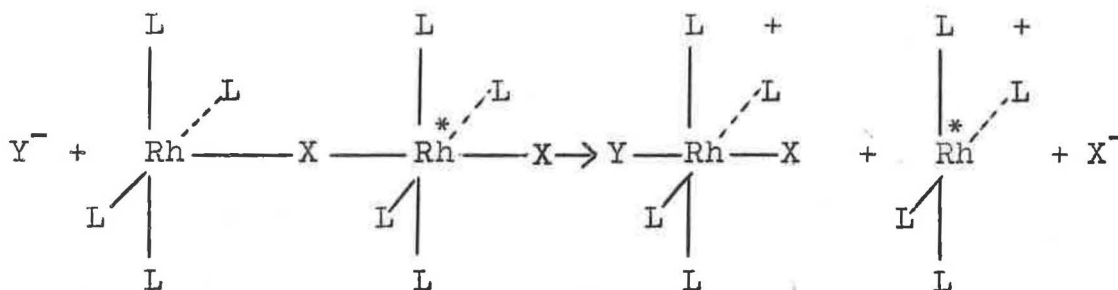
5.2(i)

The mechanism involving reduced intermediate catalysis is established for the rhodium(III) substitutions in this

system. The reactions studied may be interpreted in terms of the suggested⁽⁹²⁾ d^6-d^8 bridging mechanism, as in the chemistry of Pt(IV) substitutions⁽¹¹⁷⁾ catalysed by Pt(II) whence catalysis will involve one-step ligand transfers of the type:



(i)

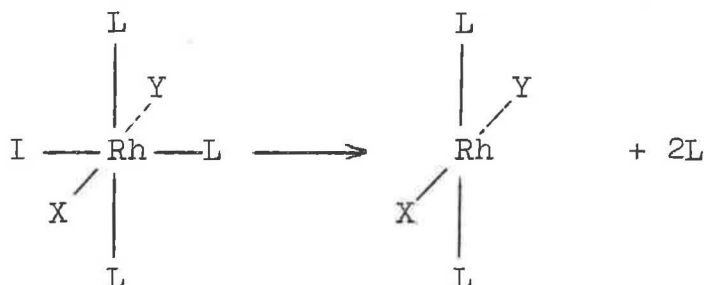


(ii)

Various factors may arise in substitutions involving specific types of ligands. First of all, a fundamental difference between the tetrapyridine and bis(ethylene-

diamine) systems is that loss of pyridine is possible, whereas loss of chelated ethylenediamine is very unlikely. One factor which might affect the pathway of a substitution in the tetrapyridine system is the ability of a given ligand to act as an electron transfer bridge between the d^6 and d^8 centre. In the reaction scheme presented above, if X and Y are halides, then substitution along the XRhX axis is thus allowed, as Cl^- , Br^- are known to form bridged species readily. The same applies for azide as axial ligand, and it may serve well as an electron transfer bridge, as it has an extensive π -system and is very polarisable (viz. the intense Raman band).

In addition, the halide complexes conform to a second possible source of constraint on the reaction pathway. This is, that axial substitution implies that the ligands perpendicular to the axis are associated with the Rh^I species, because they form strong bonds to rhodium, and by the same token, endow stability on the Rh^I intermediate. In that case, intermediates of the type below may form.



Thus, alternative pathways are opened, and in the case of the further reaction of the trans-diazido complex, the stabilised moiety may be $\text{Rhpy}_2(\text{N}_3)_2^+$, say, which would lead to the triazide product, itself very stable toward attack by pyridine or acids. The "strong" ligands nitrite, isocyanate probably give initially the Rhpy_4XY^+ complex but in the next stage of reaction, the factors above become important.

The catalytic mechanism involves a redox equilibrium step, and the polarographic survey of Chapter 3 showed that certain classes of ligands (monoheteroaromatics) lead to increased reducibility of the rhodium(III) complex, but in general, for other ligands, increased field strength leads to decreased reducibility.

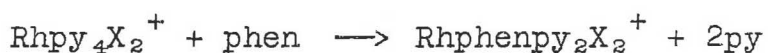
Hence catalysis occurs slightly less readily for the step in which chlorodinitrotripyridinerhodium(III) is converted to the trinitro-complex, the reaction requiring more vigorous conditions. In contrast, azides react more readily as they have lower ligand fields. The formation of the triazide complex, and of the cis disubstituted compounds with cyanide and ⁽¹¹⁸⁾iso cyanate bring to light a further simple influence on the outcome of a given reaction, which is that these are all quite insoluble products. Thus the tripyridine species by virtue of their

insolubility, and also of their uncharged nature, act as a barrier to further reaction. Note that reaction in the opposite direction (to cation rather than to anion) is also interfered with, e.g. in the case of tri-iodotri-pyridinerhodium(III). The solubility factor simply displaces equilibria in favour of the tripyridine species. The effect is further exemplified by the triazide's quantitative formation in cold solution, whereas in hot, ethanolic solution, it is precipitated much more slowly and the subsequent reaction to the tetra-azido-anion may occur. It was also observed, that in the tetramine cations' reactions, ethanol catalysed halide exchange leads more readily to insoluble species when the amine is pyrazole or thiazole, compared to the pyridine complex. Here, one expects the Rh-N bond to rupture more readily with the less basic five-membered ring amines. In accord with these views on solubility, soluble products do lead to further reaction, e.g. the displacement by ethylene diamine observed in Chapter 3, and the known reaction with ammonia⁽¹¹⁸⁾, leading to RhA_3Cl^{2+} .

It should be realised also that the possibility of generation of rhodium(II) species exists, and cis-disubstitution would be the result of attach of a ligand at a vacant coordination site. The argument becomes then a matter of degree rather than of assigning clear-cut

definitions of oxidation states and stereochemistry for intermediates; the bridged unit is formally equivalent to Rh_2^{II} .

It was noted (Chapter 3) that the reaction



does not occur under anaerobic conditions, let alone formation of bis- or tris- chelates, and this was explained in terms of the 1:10-phenanthroline 'scavenging' the reduced intermediate. The situation such as this where catalysis occurs in vacuo by virtue of a redox pre-equilibrium returns the question of the nature of the reductant in the autocatalytic systems. Either the ligands or the water are possibilities for the role or, again, rhodium itself undergoing disproportionation in an equilibrium where Rh^{III} is greatly favoured, unlike platinum, where the platinum(II) and platinum(IV) species are dominant.

Regardless of its precise formulation the reduced catalyst is also scavenged by oxygen. For a divalent species, one expects a monomeric rhodium(III) superoxide to result while for a rhodium(I) intermediate, either (i) formation of cis- Rhpy_4O_2 , the molecular oxygen side-

bonded complex, which then decomposes, or (ii) the formation of an end-bonded O_2 adduct, which will therefore become a rhodium(III) peroxide (or hydroperoxide) complex. There is little evidence for the cis oxygen complex in this system, but some for the other two, from the synthesis of the μ -peroxo and μ -superoxo dimers, although the exact conditions for their formation are still unknown in the tetrapyridine system.

5.2(ii)

The solubility properties of the tetrapyridine species are dramatically illustrated through the formation of unusual salts such as $[Rhpy_4Cl_2]Cl_3$, while $Rhpy_4Cl_3$ itself, though very soluble in hot solution has a K_S of only ca. $7 \times 10^{-4} \text{ mol}^2 \text{ l}^{-2}$ at 17°C . Crystallisation of the salts of $RhL_4X_2^+$ depends on the stabilisation of the lattice by the cooperation between a large counter-ion (NCS^- , ClO_4^- , $Cl^- + xH_2O$) and the complex cation.

The electronic spectra of the complexes are, on close examination, similar to but not identical with complexes of nonaromatic amine donors.

The vibrational transitions of the rhodium pyridine halide systems are fairly well rationalised by neglecting coupling of internal ligand modes in the simple complexes of high symmetry, and treating the ligands as point masses. In less symmetric systems, the coalescence of vibrational mode symmetry types allows for more interaction between ligands and with their internal motions, and motions of the metal ion also. $\nu(\text{Rh-Cl})$ modes are satisfactorily assignable in all cases, but $\nu(\text{Rh-Br})$ only with reliability in monobromo-complexes and in trans[Rhpy₄Br₂⁺]. Distinction can rarely be made between $\nu(\text{M-py})$ vibration types with the available data.

Note: the bibliography is addended to that of chapter 2.

Experimental

A. Instrumental Techniques

Electronic Spectrophotometry: A Perkin Elmer 450, Hitachi Perkin-Elmer 124, or Unicam SP 800 was used (the last for the kinetics).

Infrared Spectroscopy: Instruments were: Perkin-Elmer 337 or 457 ($400 - 4000 \text{ cm}^{-1}$). Samples were prepared as mujol or fluorocarbon mulls. Infrared absorbance measurements, and spectra ($190 - 400 \text{ cm}^{-1}$) were obtained with a Perkin-Elmer 225 grating instrument utilising a dry air purging unit. For infrared ($120 - 400 \text{ cm}^{-1}$) spectra were obtained as interferograms and processed in a RIIC FTC - 100/7. Fourier Transform Computer. Samples for this region were compressed ($50 \mu \text{ mol}$) in polythene (0.2g.) discs.

Raman Effect Spectroscopy: The instrument was a Coderg Raman spectrophotometer with an OIP 181B helium-neon continuous LASER as source, emitting 180 mW at 6328 \AA . Samples were examined as solutions (H_2O or MeNO_2), or in the crystalline state in glass sample tubes. Compounds with significant absorbance ca. 630 nm. , opaque or poorly crystalline samples were not suitable. Neon atomic transition lines were filtered out of the exciting beam, or used as calibrating lines. Spurious peaks arose

(800 - 900 cm^{-1}) at large slit width through excitation of the sample container and obscured weak bands in that region in solids.

Electron-Spin Resonance: Spectra were obtained on a Varian Associates A-3 spectrometer at Southampton University (Dr. G. Luckhurst).

Nuclear Magnetic Resonance: A Perkin-Elmer R10 60 MHz spectrometer was used. The 220 MHz spectrum was obtained from the S.R.C. unit, Runcorn, Cheshire.

Emission Spectroscopy: An Aminco-Bowman spectrofluorimeter fitted with a Bryans 2200 XY plotter was used. The testing of samples was done aerobically. Luminol reagent was prepared by the literature method. The reagent (1 ml.) in a 1 cm. silica cell was placed in the instrument and checked for background emission. The test sample (0.2 ml. or 20 mg.) was added and the emission spectrum scanned from 300 to 600 nm.

Differential Thermal Analysis: Qualitative calorimetry was performed on a Perkin-Elmer DSCI-B Differential Scanning Calorimeter. Samples (5 mg.) were run against air to obtain plots of enthalpy vs temperature (scan rate 8 $\text{C}^{\circ} \text{min}^{-1}$) the latter calibrated against the M.P.'s of organic standards in the range 60 $^{\circ}$ - 200 $^{\circ}$ C.

pH Titrations: Accurate pH measurements were obtained with a Radiometer model 4 pH meter, calibrated before runs against potassium hydrogen phthalate buffer (pH 4.00). The two aquo-complexes (Chapter 3) were titrated in aqueous methanol (50% v/v, 5 ml.) with standard sodium hydroxide. (i) 170 mg. $\text{Rhpy}_4\text{Br}(\text{OH}_2)(\text{ClO}_4)_2 \cdot 2\text{H}_2\text{O}$ required 2.25 ml. of 0.1 M-sodium hydroxide. (ii) 76.9 mg. required 5.12 ml. of 0.02M-sodium hydroxide. (iii) 98.8 mg. $\text{Rhpy}_4\text{Cl}(\text{OH}_2)(\text{ClO}_4)_2 \cdot \text{H}_2\text{O}$ required 2.75 ml. of 0.05 M-sodium hydroxide.

Polarography: Polarograms were obtained from a Beckman Electroscan 30 instrument. The DME had a flow rate of $1.41 \text{ mg. sec}^{-1}$ and a drop time of 4.56 sec. at -0.6v. in a 0.1 M - KCl solution. All $E_{\frac{1}{2}}$ values are reported in volts vs a (fibre junction) SCE (EMF = +2.42v. vs SHE at 25°C). The anode consisted of a platinum spiral in NaNO_3 solution and was separated from the working compartment by an agar gel/ NaNO_3 salt bridge.

Compounds were made up as 10^{-4}M solutions (100 ml.) on 0.1M - KCl, except for the superoxide complexes, which were in 0.1M - KNO_3 and the bromo-complexes, which were in 0.1M - KBr. The polarogram of the μ -peroxo-rhodium complex was measured in 0.1M - KNO_3 at pH 10.5. To remove oxygen, which gives a reduction wave ca. -0.4v.,

solutions were degassed for at least 15 minutes by the passage of a stream of "white spot" nitrogen. Polarograms were run down to ca. -1.2 to -1.4v., where K^+ reduction begins. A wave, near 0.0v. presumably due to mercury oxidation (e.g. in acidic solutions), sometimes prevented scanning of the region above -0.1v. Pronounced maxima occurred with many of the compounds, attributable to streaming of the (oxidising) ions in solution past the mercury drop. These maxima could be suppressed by the addition of 1% aqueous gelatin solution followed by further degassing (0.25 ml.). The addition of gelatin tended to alter the $E_{\frac{1}{2}}$ values slightly, and it was advantageous to use low rhodium concentrations, as less gelatin was needed to suppress the maxima, which increased greatly as the rhodium concentration was increased. Some of the compounds were not sufficiently soluble, due to the high counter-ion concentration of the supporting electrolyte. In such cases, either a saturated solution was filtered and used e.g. $Rh(Clpy)_4Cl_3$, or else aqueous methanol was used as solvent (up to 50% v/v MeOH) as in the case of $Rh(iquin)_4Cl_3$. Polarograms of $Rhpy_4Cl_3$ in 0%, 10% and 80% v/v MeOH/water were identical; nor was the $E_{\frac{1}{2}}$ affected by increasing the acidity of the solution (pH 2) but a maximum appeared at ca. -0.6v. which was not suppressed by gelatin.

Conductivities: were measured with a Philips PR 9500 A.C. bridge, and bright Pt electrodes. Values for molar conductivities (Λ , or "Cond" in the experimental) are in $\text{cm}^2\text{ohm}^{-1}\text{mol}^{-1}$ and refer to 10^{-3}M solutions in MeNO_2 , unless otherwise stated.

B. Analyses

C, H and N analyses were by the Alfred Bernhardt Laboratory (West Germany) or were obtained on a Hewlett-Packard F. & M. Scientific 185 C,H,N Microanalyser ; this machine has a sample preheat stage in its cycle, and some H-analyses are low, due to loss of water of crystallisation. Oxygen and halogen analyses were done by Bernhardt or by the Beller Laboratories (Göttingen).

Rhodium was determined gravimetrically as the metal by ignition of the sample (ca 1500°C , 10 minutes) cobalt by the pyridine/thiocyanate method.

C. Reagents

Reagents were of standard grade; analytical grade reagents were used for quantitative work. Gases other than chlorine (I.C.I. Ltd.) were supplied by B.O.C.

Heterocyclics were supplied by B.D.H. or Koch-Light Laboratories. Thiazole was from Fluka AG, N-methylimidazole a gift from Dr. M.V. Twigg.

Platinum metal halides were obtained from Johnson Matthey & Co. Ozone was generated with a B.O.C. Mk.II Ozoniser. Deuteriated reagents (pyridine, water, chloroform) were supplied by Prochem Ltd.

D. Preparation of Compounds

(i). Heterocyclic ligand complexes of rhodium(III)

The general method for the preparation of the complexes $[\text{RhL}_4\text{X}_2]\text{Y}\cdot n\text{H}_2\text{O}$ was as follows.

To rhodium trihalide (0.2 g.) dissolved in hot (80°) 50% v/v aqueous ethanol (25 ml.) was added a solution of the ligand (5-10 mol. per mol. Rh) in ethanol (10 ml.). Reaction was usually complete in a few seconds. If the rhodium trihalide solution was not heated before the addition of the ligand, precipitation of the insoluble RhL_3X_3 compound ensued. The solution was evaporated to dryness on a rotary evaporator, excess ligand being removed if possible. Sufficient water (ca. 40 ml.) was added to dissolve the compound when hot, and after

charcoaling, the complex was allowed to crystallise from the filtered solution as it cooled. When the ligand had an alkyl substituent (other than 4-methylpyridine), oils were often deposited from aqueous solution. This problem was best overcome by (re)-crystallising from aqueous methanol/ethanol, as described for the acetylpyridine complex perchlorate, below.

Yields were 80-90%, recovered as the chloride salts. The repetition of some preparations allowed recycling of the mother liquors for the first crystallisation. Recrystallisation yields very pure compounds as large yellow spangles (L = py, pic) or smaller pale yellow crystals for other substituted pyridines.

Prepared by this method were (i):

(a) trans-dichlorotetrapyridinerhodium(III)chloride pentahydrate. Yield 0.5 g. golden yellow laths⁽¹⁾.

(ii) Perchlorate and tetrafluoroborate salts were prepared by addition of the appropriate acid (5 ml.) to a solution of the compound (0.2 g.) in hot water. Yields are quantitative. Thus prepared were: (compound, followed by molar conductivity, in brackets, $\text{cm}^2\text{ohm}^{-1}\text{mol}^{-1}$ in MeNO_2 , 10^{-3}M): $\text{Rhp}_4\text{Cl}_2\cdot\text{ClO}_4$ (74), $\text{Rhp}_4\text{Br}_2\cdot\text{ClO}_4$ (72), $\text{Rhp}_{\text{ic}}_4\text{Cl}_2\cdot\text{ClO}_4$ (75), $\text{Rhp}_{\text{ic}}_4\text{Cl}_2\cdot\text{BF}_4$ (74).

By procedure (i).

(a) trans-dichlorotetrapyridinerhodium(III)perchlorate was prepared as in (i), but to the warm (charcoaled) aqueous solution was added NaClO_4 (lg.). Yield, 0.2 g. orange compound; Cond. 47.

(b) trans-dichlorotetakis(isoquinoline)rhodium(III)chloride trihydrate recrystallised from methanol-water giving 0.4 g. cream silky crystals; Cond. 61.

(c) trans-dichlorotetrathiazolerhodium(III)chloride pentahydrate. Yield 0.5 g. bright yellow platelets; Cond. 77.

(d) trans-dichlorotetrapyrazolerhodium(III)chloride pentahydrate. Yield 0.25 g. orange-yellow prisms, $\epsilon = 77$ $\text{cm}^2 \text{ohm}^{-1} \text{mol}^{-1}$ at 10^{-3}M in H_2O .

(e) trans-dibromotetrapyridinerhodium(III)bromide pentahydrate. Yield 0.4 g. orange crystals⁽¹⁾.

(f) trans-dibromotetrathiazolerhodium(III)bromide dihydrate. Yield 0.1 g. orange compound; Cond. 73.

(iii) (a) trans-dichlorotetrakis(3-acetylpyridine)rhodium(III)perchlorate was prepared by adding NaClO_4 (0.5 g.) to a solution of the crude product (oil)

obtained by the procedure (i) (after charcoaling). The precipitate was recrystallised from aqueous ethanol by adding sufficient water to cause slight turbidity of the warm ethanolic solution (15 ml.), then allowing it to cool. Yield 0.4 g. of pale yellow prisms; cond. 68.

(b) trans-dichlorotetrakis(4-ethyl — pyridine)rhodium-(III)perchlorate was prepared as in (a), yield 0.3 g. cream crystals; cond. 67.

(iv) mer-trichlorotris(3-chloropyridine)rhodium(III) was the major product when procedure (i) was used. The bright yellow precipitate was recrystallised from CHCl_3 , giving 0.4 g. orange needlelets which immediately effloresced, losing CHCl_3 of solvation. Found: C, 32.5; H, 2.1; N, 7.4%; $\text{RhC}_{15}\text{H}_{12}\text{N}_3\text{Cl}_6$ requires C, 32.8; H, 2.2; N, 7.6%. The chloroform solution had λ 422 nm. $\epsilon = 80$.

(v) trans-dichlorotetrakis(3-chloropyridine)rhodium(III)chloride pentahydrate was made by modifying (i) as follows. "RhCl₃" (0.1 g.) in 50% warm aqueous ethanol (10 ml.) was added slowly to the ligand (1 g.) in boiling 50% ethanol (10 ml.). The crude compound was recrystallised from ethanol. Yield 0.2 g. yellow powder; cond. 52.

(vi) poly(trans dichloro- μ -pyrazinedipyrazinerhodium(III)) chloride was prepared by method (i). Yield 0.4 g. bright yellow compound, insoluble in H₂O, EtOH, CH₃Cl, MeCN, MeNO₂, HNO₃, HCl, but soluble in hot pyridine.

(vii) 1:10-Phenanthroline and 2,2'-bipyridyl complexes (Rh chel₂Cl₂)Cl.nH₂O were prepared by adding the ligand (0.3 g.) to rhodium trichloride (0.25 g.) in hot aqueous ethanol (50% v/v, 15 ml.) as in (i).

(viii) cis-Di-iodobis(1:10-phenanthroline)rhodium(III) iodide dihydrate was prepared by refluxing the complex chloride (0.1 g.) in aqueous ethanol (50% v/v 40 ml.) with sodium iodide (1 g.) for 30 minutes. The brick-red crystals were filtered off and recrystallised from boiling (aqueous ethanol) sodium iodide solution. Conductivity 83.

(ix) trans-diiodotetrapyridinerhodium(III)iodide trihydrate was obtained by two routes.

(a) Rhodium iodide (0.1 g.) was suspended in a mixture of water (20 ml.), pyridine (40 ml.) and ethanol (20 ml.).

Hydrogen was bubbled through this mixture for 1 hour. The yellow-brown solution was filtered to remove unreacted material and concentrated to 20 ml. on the rotary evaporator, yielding golden brown crystals (0.07 g.) which were washed with cold water and air dried. Cond. 77.

(b) $\text{Rhpy}_4\text{Cl}_3 \cdot 5\text{H}_2\text{O}$ (0.2 g.) was dissolved in warm water (100 ml.). To the solution was added pyridine (1 ml.) and, slowly, sodium iodide (1.2 g.); care was taken not to heat unevenly, not to allow precipitation of the iodide salt. After ca. 30 s. at 80° the colour of the solution changed from pale yellow to light orange, and within 1-2 minutes, became deep orange-red, and golden-brown silky crystals appeared. These were filtered off from the cold solution, washed with cold water and air-dried. Yield 0.2 g.

(c) The perchlorate salt was obtained by precipitation from methanol as yellow-brown prisms, which were filtered off, washed with cold methanol and air-dried. Cond. 88.

(x) trans-dichlorotetrapyridinerhodium(III) trihalides
The trichloride salt was prepared by shaking an aqueous solution (100 ml.) of hydrated Rhpy_4Cl_3 (0.2 g.) under an atmosphere of chlorine, thus producing feathery cream

crystals which were filtered off, washed with cold water then ether (100 ml.) and dried in vacuo over sulphuric acid. Yield, 0.16 g. Conductivity 64. The iridium analog was prepared similarly. Conductivity 61. The triiodide salt⁽²⁾ resulted from an attempted Karl Fischer titration of the complex chloride salt, 0.44 g. of which gave 0.63 g. shiny brown platelets, conductivity 54. The tribromide salt⁽²⁾ was obtained by adding bromine to the chloro-complex's bromide salt in chloroform (λ 410 nm.) Orange crystals, conductivity 65.

(xi) trans-dichlorotetrapyridinecobalt(II) and trans-dibromotetrapyridinecobalt(II) were prepared by the literature method⁽³⁾, as pink and lilac crystals respectively, which readily lost pyridine to the atmosphere, turning deep blue, hence the analysis for the chloride (c, 51.9; H, 4.2; N, 11.9%) is low ($C_{20}H_{20}Cl_2CoN_4$ requires C, 53.0; H, 4.5; N, 12.5%). The bromide had Co 11.9% (calculated 11.0).

(xii) (a) trans-dichlorotetrapyridinecobalt(III)chloride pentahydrate was prepared by the method of Werner and Feenstra⁽⁴⁾. The green crystals had C, 41.7; H, 3.9;

N, 9.7%. $C_{20}H_{30}Cl_3CoN_4O_5$ requires C, 42.1; H, 5.3;
N, 9.8%. Desiccation (high vacuum, room temperature)
gave the anhydrate; found C, 49.7; H, 4.3; N, 11.6;
Cl, 21.9%. $C_{20}H_{20}Cl_3CoN_4$ requires C, 50.0; H, 4.7;
N, 11.7; Cl, 22.1%. The compound had 636 nm. ($\epsilon = 45$)
and 505 nm. (31) in water.

(b) The tetrafluoroborate salt was made as in(ii) from
cold water. Found C, 45.1; H, 3.6; N, 10.2%.
 $C_{20}H_{20}BCl_2CoF_4N_4$ requires C, 45.0; H, 3.8; N, 10.5%.
Conductivity 67.

(xiii) trans-dibromotetrapyridinecobalt(III)tribromide
was prepared by the procedure of Babaeva and Baranovskii
as⁽⁵⁾ insoluble brown needles; C, 31.1; H, 3.1; N, 7.1%.
 $C_{20}H_{20}Br_5CoN_4$ requires C, 31.0; H, 2.6; N, 7.2%. The
reflectance spectrum had peaks at 695, 455 nm.

(xiv)(a) Tetrapyridineplatinum(II)chloride trihydrate was
prepared by the standard method⁽⁶⁾. The colourless
crystals had C, 37.6; H, 3.5; N, 8.5%. $C_{20}H_{26}Cl_2N_4O_3Pt$
requires C, 37.8; H, 4.1; N, 8.8%.

(b) The tetrafluoroborate salt was prepared as in (ii) and obtained as white prisms. Found C, 34.4; H, 2.9; N, 7.9%. $C_{20}H_{20}B_2F_8N_4Pt$ requires C, 35.0; H, 2.9; N, 8.2%. Conductivity 149.

(xv) trans-dichlorotetrapyridineplatinum(IV).bis(tetrafluoroborate) was prepared by passing chlorine through a solution of the pyridineplatinum(II)chloride (0.2 g.) in water (40 ml.) and crystallised by addition of tetrafluoroboric acid (5 ml.). The white crystals (0.2 g.) had C, 32.0; H, 2.7; N, 7.3; Cl, 9.5%. $C_{20}H_{20}B_2Cl_2N_4Pt$ requires C, 31.8; H, 2.7; N, 7.4; Cl, 9.4%. Conductivity 186.

(xvi) trans-dibromotetrapyridineplatinum(IV).bis(tetrafluoroborate) was obtained by adding bromine (0.05 g.) to the platinum(II) tetrafluoroborate complex salt (0.2 g.) in water (50 ml.). Rotary evaporation reduced the volume to 15 ml. and the product was obtained as bright yellow crystals (0.22 g.) which had C, 27.9; H, 2.6; N, 6.3; Br, 19.5%. $C_{20}H_{20}B_2Br_2F_8N_4Pt$ requires C, 28.4; H, 2.4; N, 6.6; Br, 18.9%. Conductivity 164.

(xvii) μ -Superoxodecammine dicobalt(III)(III)pentanitrate was prepared by adding nitric acid to a filtered solution of the acid sulphate⁽⁷⁾ in 2M-sulphuric acid.

$H_3OCo_2N_{15}O_{17}.H_2O$ requires H, 5.0; N, 32.4%. Found H, 4.9; N, 32.6%. The electronic spectrum agrees with that previously reported⁽⁸⁾ (Chapter 2).

(xviii) N-iodopyridinium dichloriodate was obtained by the procedure of Jones et.al.⁽⁹⁾ and its i.r. spectrum (nujol mull, 400-4000 cm^{-1}) agrees with theirs.

(xix) μ -Superoxo-trans,trans-dichloro-octakis(4-methylpyridine)dirhodium(III)(III) triperchlorate dihydrate.

To a solution of $Rhpic_4Cl_3.3H_2O$ (0.6g.) in aqueous ethanol (20 ml., 20% v/v) was added 1M-NaOH (2 ml.). A stream of 10% ozone in oxygen ($0.5 l.min^{-1}$) was passed through this solution for ca. 2 hours when the now deep blue solution was chlorinated briefly to oxidise any of the μ -peroxo-compound present, and 10M- $HClO_4$ was added (5 ml.) or $NaClO_4$ (5g.) to recipitate the crude compound, often as a gum which was dissolved in concentrated hydrochloric acid (15 ml.) while carefully warmed. This is a critical point in the preparation. If the compound shows signs of fading while

impure at this stage, the warming should be carried out under chlorine. The deep blue solution was cooled, filtered to remove the precipitated $[\text{Rhpic}_4\text{Cl}_2]\text{ClO}_4$ and the compound crystallised by adding hot 0.5 M perchloric acid (20 ml.) to the warmed solution. The process was repeated, this time with stronger heating of the HCl solution (15 ml.) and addition of less perchloric acid (5 ml.). The hydrochloric acid treatment anates any aquorhodium species present. The deep blue crystals are washed with cold water and air-dried (0.1 g.).

(xx) μ -Superoxo-trans,trans dichlorooctakis(4-methylpyridine)dirhodium(III)(III)tris(tetrafluoroborate) was prepared as in (xix) but using 4M-tetrafluoroboric acid in place of perchloric acid. Yield 0.1 g. of deep blue compound.

(xxi) μ -Superoxo-trans,trans-dichloro-octapyridine dirhodium(III)(III) triperchlorate octahydrate was prepared as in (xix), but from trans $[\text{Rhpy}_4\text{Cl}_2]\text{Cl}\cdot 1.5\text{H}_2\text{O}$ as starting material, giving deep blue-purple crystals (0.08 g.). Excess base (5:1) gave the analogous aquo-complex,

(xxii) μ -superoxo-trans,trans-diaquo-octapyridinedirhodium(III)(III)pentaperchlorate, hexahydrate, which was separated before anation by extraction from nitromethane-chloroform mixture (15 ml., 8:1 v/v) into nitric acid (0.5 M, 50 ml.) and crystallised by addition of sodium perchlorate (10 g.). The dichloro-complex remains in the organic layer, but the procedure is not a good one. It is ineffective with the picoline compounds, which are too lipophilic.

(xxiii) μ -Superoxo-trans,trans-dichloro-octapyridine-dirhodium(III)(III)tris(tetrafluoroborate) was prepared as in (xx) using 4M-tetrafluoroboric acid instead of perchloric acid, and obtained on air-drying as deep purple-blue anhydrous crystals (0.07 g.). It may be prepared also by addition of tetrafluoroboric acid to a solution of the perchlorate in 0.1M hydrochloric acid.

(xxiv) μ -Peroxo-trans,trans-dichloro-octakis(4-methylpyridine)dirhodium(III)(III) diperchlorate dihydrate was obtained by two methods. (a) To the μ -superoxide, (xix), (0.2 g.) in ice-cold 0.2M sulphuric acid (200 ml.) was added iron(II) sulphate heptahydrate (0.05 g.). The

blue colour of the solution rapidly faded to pale greenish-yellow. Sodium perchlorate (1.0 g.) was added, the volume of the solution reduced to 25 ml. under reduced pressure and the product obtained as yellow-tan crystals (0.13 g.) which were washed with cold water and dried in vacuo over sulphuric acid. The ^1H n.m.r. spectrum has peaks at τ 1.73, 1.84, (α -protons) 2.79, 2.88 (β -protons) 7.41 (CH_3) and 8.20 (H_2O) from TMS as internal standard. (b) To the superoxide (0.2 g.) in aqueous methanol (60% v/v 20 ml.) was added slowly 1M sodium hydroxide solution (ca 0.1 ml.). The blue colour rapidly faded, and crystallisation commenced. Addition of sodium perchlorate (0.2 g.) in methanol (5 ml.) improves the yield to ca. 0.15g. yellow-tan crystals.

The products (a), (b) have identical analyses (C,H,N) and UV spectra.

(xxv) Borohydride catalysed reactions (Chapter 3) were usually performed as follows: $\text{Rhpy}_4\text{Cl}_3 \cdot 5\text{H}_2\text{O}$ (0.6g.) was dissolved in aqueous ethanol (30 ml., 25 % v/v). To the hot solution was added excess (0.5 - 3.0g.) of the reagent, followed by sodium borohydride (0.5 - 2.0mg.). The solution usually changed colour immediately, and was

filtered and allowed to stand overnight, after which filtrate and/or precipitate were recovered.

(xxvi) Reactions in vacuo were carried out by distilling 50 ml. of triply degassed water into a 100 ml. round flask containing the reagents, under high vacuum.

(xxvii) Trinitrotripyridinerhodium(III) was obtained as in (xxv) by adding sodium nitrite (2g.) to the solution and in addition, boiling the solution. Yield, after 2 days, 0.1g. white crystals, insoluble in H₂O, EtOH, CHCl₃ soluble in MeCN, MeNO₂.

(xxviii) Chlorodinitrotripyridinerhodium(III) was obtained as in (xxv) but by using a stoichiometric amount (0.13g.) of sodium nitrite. Yield 0.22g. insoluble greenish-yellow twinned crystals, soluble in MeNO₂, MeCN only.

(xxix) Tetraethylammonium tetra-azidodipyridinerhodate-(III)* was obtained as above by using 60% v/v aqueous ethanol, 2g. sodium azide and crystallised from the

filtrate by addition of tetraethylammonium chloride (0.5 g.). Yield 0.15 g. bright orange yellow salt, after washing with water and recrystallising. Conductivity 59.

(xxx) Trans-diazidotetrapyridinerhodium(III)azide pentahydrate* was obtained when $\text{Rhpy}_4\text{Cl}_3 \cdot 5\text{H}_2\text{O}$ (0.5g.) was refluxed with a slight excess of sodium azide (0.13g.) for 0.5 hour. The cooled orange solution was filtered, and sodium azide (4g.) was added to crystallise the compound. Recrystallisation was by addition of sodium azide solution to a lukewarm aqueous solution; care was needed lest the added azide react to produce the insoluble triazide. Yield 0.25 g. of orange needles; conductivity 73. The compound is also produced when excess azide is used, but more triazide is formed.

(xxxi) Triazidotripyridinerhodium(III)* was also obtained (orange needles) from the above solution (xxx), but this is best prepared by carrying out the same reaction with less sodium azide (0.4g.) at room temperature, giving an orange-yellow precipitate (0.38 g.) which was recrystallised

from acetonitrile to yield deep orange prisms (0.3g.).

The picoline analog was recrystallised from methanol.

* N.B.: All the azide complexes explode violently when heated.

(xxxii) Halo di-isocyanatotripyridinerhodium(III)

compounds were obtained by adding sodium cyanate (0.5g.) to warm aqueous solution (50 ml.) of the $Rhpy_4X_3 \cdot 5H_2O$ (X = Cl, Br) salt. Yellow platelets (chloride) or orange-yellow crystals (bromide) formed, which were filtered off, washed with water and ethanol and dried in vacuo over sulphuric acid. Yields were 85-95%.

(xxxiii) Trans-bromoaquotetrapyridinerhodium(III)diper-

chlorate dihydrate was obtained by heating a solution of $Rhpy_4Br_3 \cdot 5H_2O$ (1 g.) in 4M sodium acetate (60 ml.) at 90° until the 440 nm. band shifted to 370 nm. (ca, 15 minutes). To the solution was added $NaClO_4$ (5g.) and the voluminous yellow precipitate, mostly $Rhpy_4Br(OH)ClO_4$, was filtered off and crystallised from 10M $HClO_4$ (25 ml.) by adding an equal volume of warm water. The compound was recrystallised from hot water, to give 0.4g. orange-red prisms, conductivity 124. On vacuum desiccation these yield the anhydrate.

Hydrolysis may also be effected by 4M-KF, but dialysis is then required for removal of KF, since perchlorate would also precipitate KClO_4 . The reaction is also accomplished, ethanol catalysed, by heating with a 20% excess of NaOH (100°).

(xxxiv) Trans-bromohydroxytetrapyridinerhodium(III) perchlorate was prepared by neutralising an aqueous solution (25 ml.) of the aquo complex (0.2g.) with 0.1M - NaOH. Yield, 0.15g. orange-yellow prisms, conductivity 72.

(xxxv) Trans-chloroaquatetrapyridinerhodium(III)diperchlorate hydrate was synthesised by the acetate-effected hydrolysis of $\text{Rhpy}_4\text{Cl}_3 \cdot 5\text{H}_2\text{O}$ (1.0g.) (xxxiii) above, monitoring spectrophotometrically for shift of the 410 nm. peak to ca. 360 nm. and minimisation of absorption at ca. 390 nm.; yield 0.3g. cream platelets, conductivity 98.

(xxxvi) Trans-chlorohydroxytetrapyridinerhodium(III) perchlorate was obtained from the aquo complex by neutralisation, as yellow prisms, conductivity 59.

(xxxvii) Trans-dichlorodipyridineethylenediaminerhodium (III)chloride trihydrate was obtained by refluxing the tetrapyridine chloride (0.3g.) with ethylenediamine monohydrochloride (0.05g.) overnight in aqueous ethanol (40 ml., 25% v/v). The solution was concentrated (10 ml.) on the steam bath and allowed to cool, whence orange-yellow rhombs (0.08g.) were obtained, which were washed with cold water and air-dried.

(xxxviii) Halo-oxalatotripyridinerhodium(III) were obtained by the literature⁽¹⁰⁾ procedure, or by the borohydride catalysis of a warm aqueous solution containing the Rhp_4X_3 salt (0.5g.) and potassium oxalate (0.3g.) (which dissolves more readily than the sodium salt). Yields were 95-100% of feathery yellow (X = Cl) or orange (X = Br) needles.

(xxxix) Chloro-oxalatotris(3,5-dimethylpyridine)rhodium-(III) and others with paraffinic substituents were best prepared by adding potassium oxalate (0.8g.) to the complex chloride salt (0.4g.) in boiling aqueous ethanol (10% v/v, ca 60 ml.). Further boiling redissolved the cream flocculent precipitate (oxalate salt) (more ethanol

was added if needed) and after 2-3 minutes caused evolution of heteroaromatic (odour) and crystallisation of the compound, which was filtered off the cold solution and washed with warm water. Yield 0.3 g. yellow platelets, soluble in alcohols and chloroform.

(xl) 1,2,6-Trihalotripyridinerhodium(III) compounds were obtained from the $Rhpy_3XOx$ (0.5g.) by dissolving them in hot hydrochloric or hydrobromic acid (HY, 25ml.) and allowing the solution to stand overnight. The crystals (85-95% yields) were filtered off, washed with hot water and recrystallised from chloroform by evaporation. The halocarbon solutions are photosensitive, and also give solvates (Chapter 4). Oxalato-complexes with substituted pyridines (lutidine) required methanolic hydrohalogenic acid for the reaction. The γ -picoline compound in $CHCl_3$ solution had λ 425 nm., $\epsilon = 78$. The 1H n.m.r. resonances due to the 2 different methyl groups were coincident at 60 MHz but the 220 MHz spectrum showed 2 peaks at τ 7.59, 7.57 in the expected ratio, 2:1.

(xli) Trans-bromochlorotetrapyridinerhodium(III) salts were obtained by the above reaction (xl) also, using the

perchlorate salt of the bromo-aquo complex (0.15 g.) which yielded insoluble orange rhombs of the perchlorate (0.05g.) and orange plates, which later were converted to the tetrafluoroborate salt by metathesis in water with tetrafluoroboric acid. Yield, 0.07g. orange needlets. Conductivity 75.

(xlii) Reactions of a rhodium hydride. Chloropentammine-rhodium(III)chloride was made by a modification of (i), in that excess ammonia solution gave ca. 80% yield of the salt, [$\nu(\text{Rh-Cl})$ 322cm^{-1} , $\nu(\text{Rh-N})$ 489, 508cm^{-1} , Raman], whose UV spectrum agreed with the literature description (11). This was converted to $(\text{HRhA}_5)\text{SO}_4$ by the method of Thomas and Wilkinson (12); the white crystals had $\nu(\text{Rh-H})$ 2073 cm^{-1} . These (0.48g.) were dissolved in deoxygenated water (60 ml.) giving 300 nm. ($\epsilon = 285$), 259 nm. ($\epsilon = 300$). Oxygen was bubbled through the solution (ca. 1 l. min.^{-1}) and reaction required 25 minutes, the solution becoming apple-green (13) as the hydroperoxide formed (sh. 400 nm., $\epsilon = 40$; sh. 340 nm., $\epsilon = 90$; 237 nm., $\epsilon = 3700$, lit. (14) 237 nm., $\epsilon = 3800$) and isosbestic points appeared at 283, 331 nm. (lit. (14) 287 nm). Evaporation in low vacuum, or bubbling nitrogen through the solution overnight caused it to turn deep blue (590 nm., ϵ , ca. 10^8). Sodium perchlorate

precipitated the blue (impure) product, which was found to be stable to crystallisation from nitric acid, but which oxidised hydrochloric acid to chlorine. The blue compounds (from nitric acid) reacted only slowly with the luminol reagent (weak emission 445 nm.). ESR spectra⁽¹⁵⁾ (dilute nitric acid, -80° and 20°C) showed them to have doublet ground states (cf. 3-line signal for $\text{Rh}_2^{\text{N}}\text{O}_2^{2-}$ species⁽¹⁵⁾, $N = \text{II or IV}$).

In another experiment, the hydride in aqueous solution was turned blue immediately by the passage of ozone, (λ 590 nm.) or pink in 15M-ammonia solution.

E. Determination of the Redox Equivalent

(a) An attempted iodometric determination for the pyridine/superoxide as the perchlorate salt gave unsatisfactory results, owing to formation of a suspension which obscured the end-point. A minimum value of 1030 was indicated (calculated 1384) as 19.5 mg. of complex in 0.005M-sulphuric acid liberated iodine from added potassium iodide equivalent to not more than 1.90 ml. of 0.010N-sodium thiosulphate.

(b) To the same compound (22.0 mg.) dissolved in cold 1M-sulphuric acid (25 ml.) was added 0.0117M-iron(II)

sulphate (4.00 ml.). The solution was kept cold and oxygen-free under a carbon dioxide 'blanket' by addition of dry ice. Back titration of the excess iron(II) (ferroin indicator) required 3.05 ml. of 0.0100M-ceric ammonium nitrate, giving an equivalent weight of 1350 for the complex.

(c) For the tetrafluoroborate salt of the picoline/superoxide complex, the titration was performed under nitrogen at room temperature, and the end point was somewhat variable by the iron(II) - cerium(IV) method. This was probably the result of acid hydrolysis and/or further reduction of the peroxo bridged product. By titrating a solution of the compound (28.1 mg.) in 0.5M-sulphuric acid (30 ml.) under nitrogen, with 0.0154M-iron(II) sulphate, and plotting absorbance at 610 nm. vs volume of titrant added, a straight line was obtained, (Figure 2.2) which on extrapolation to absorbance 0.04 gave an equivalent weight of 1150 (calculated 1314).

(d) An attempt to titrate a solution of the perchlorate salt of the picoline/superoxide complex with thiosulphate in M-sulphuric acid was unsuccessful, as its reaction with that reductant was too slow. However, 38.9mg. of the compound in methanol (ca. 25 ml.) when titrated with 0.005M-sodium thiosulphate gave a linear plot of absorbance (610 nm.) vs titrant added (Figure 2, 2) which indicated

an equivalent weight of ca 2300. The solution had a sulphurous odour and when diluted by half with water had a pH of 2.5 - 3.0 (indicator paper), supporting the contention that H_2SO_3 is the oxidation product; the expected pH is ideally 3.2.

App. (i).

Determination of Magnetic Susceptibilities

Evans⁽¹⁶⁾ gives a simple n.m.r. method for the determination of magnetic susceptibility of a compound, relying on the relationship:

$$\chi_g = \frac{3 \cdot \Delta f}{2\pi f m} + \chi_o + \frac{\chi_o(d_o - d_s)}{m}$$

where Δf is the up-field shift (in Hz.) due to the paramagnetic at the concentration of $m \text{ g.ml.}^{-1}$, f is the instrument frequency (60M Hz), χ_o is the mass susceptibility of the solvent, d_o its density, and d_s the density of the solution at the probe temperature (33.5°C). For solutions with the required concentration (" $2-5 \times 10^{-2}\text{M}$ in free spin") the last term is usually negligible, but the formula weights of the superoxides (1000-1400) required that solutions contained 5-10% w/w of complex. The density change was estimated by comparing the weights of identical volumes (density bottle) of solvent and of a 5% w/w solution of $[\text{Rhpy}_4\text{Cl}_2]\text{ClO}_4$ which gave $d_s - d_o = 0.012$ for the nitromethane solution. For MeNO_2 , $d_t = 1.1639(1 - 0.001152t)$ ⁽¹⁹⁾ (density vs temperature) and $\chi_g = -0.346 \times 10^{-6} \text{ c.g.s.u.}$ ⁽²⁰⁾ Hence, one approach is to measure Δf for the paramagnetic, and estimate the density correction (applying it to m also). Thus for $[\text{Rh}_2\text{py}_8\text{Cl}_2\text{O}_2](\text{ClO}_4)_3 \cdot 8\text{H}_2\text{O}$, $\Delta f = 3.25 \text{ Hz}$,
 $m = \frac{7.94 \text{ mg}}{196 \text{ mg}} \times d_s = 0.0458$ so

$$10^6 \chi_g = 0.565 - 0.346 + 0.103$$

$$\therefore 10^6 \chi_g = 0.322$$

Note that the 3rd term contributes 31% of χ_g !

$$\therefore 10^6 \chi_m = 446 .$$

Alternatively, a solution of the diamagnetic may be used as the external reference; a 10% w/w solution of $[\text{Rhpic}_4\text{Cl}_2]\text{ClO}_4$ in MeNO_2 gave a downfield shift (from external MeNO_2) of 2.35 Hz (whence $10^6 \chi_g = -270$). This is satisfactory when the complexes are similar, and has the added advantage that close similarity compensates for most of the ligands' diamagnetism, the equation becoming

$$\chi_g^c = \frac{3 \cdot \Delta f}{2\pi f m .}$$

if $d(\text{ref}) = d(\text{sample})$ and χ_0 's equal also. The density correction may still be significant in the new equation and its estimation remains the greatest source of error in the results in table 2.2. Otherwise, obtaining χ_g gives χ_m directly, which is then corrected by the usual procedure⁽¹⁷⁾ (measured values or Pascal's constants) to χ_m^c (obtainable from χ_g^c directly) from which one computes

$$\mu = 2.84 (\chi_m^c \cdot T)^{\frac{1}{2}} \quad \text{B.M.}$$

App. (ii).

Prediction of Vibrational Activity

The i.r. and Raman (in) activity of a given vibration is calculated throughout by the method in ref. 18. It consists of finding the representation whose symmetry properties are as those of the vibration in the given point group. For example, consider the stretching vibration $\nu(M-X)$ in trans MA_4X_2 . Consider the incurred change in bond length, $\Delta r(M-X)$. Table 6.1 of ref. 18 gives values χ_R for the effect of the point group's operations on the Δr of a given type, depending on whether the operation R leaves Δr unshifted or not ($\chi_R=0$). For $\Delta r(M-X)$ in D_{4h} , one has:

R	E	$2C_4$	C_2	$2C_2'$	$2C_2''$	i	$2S_4$	σ_h	$2\sigma_v$	$2\sigma_d$
χ_R	2	2	2	0	0	0	0	0	2	2

whence the relationship

$$n^{(\gamma)} = \frac{1}{g} \sum_j g_j \chi_j^{(\gamma)*} \chi_j \quad (\text{ref. 18, p.107})$$

is used; $n^{(\gamma)}$ is the number of irreducible representations of type p related to $\Delta r(M-X)$; g , the total of operations of the group (16 for D_{4h}); g_j the number of operations in the class j (2 for C_4); χ_j the character associated with that class for the given representation.

Thus

$$n(A_{1g}) = \frac{1}{16} (1x_1x_2 + 2x_1x_2 + 1x_1x_2 + 0 \dots + 2x_1x_2 + 2x_1x_2) = 1$$

Hence $\nu(M-X)$ occurs as $1A_{1g}$ (Raman active only) in D_{4h} (character tables). The procedure is continued for the other representations in the group.

App. (iii).

Determination of Integrated Infrared Intensity

Ramsay (reference 18 of chapter 3) gives the equation for the calculation of absolute infrared absorbance A, as

$$A = \frac{\pi}{2cl} \cdot \ln\left(\frac{I_0}{I}\right) \cdot \Delta\nu_{\frac{1}{2}} \quad \text{l.mole}^{-1}\text{cm}^{-2}$$

where c is the molarity of the absorbing species, l is the cell path length in cm., I_0 is the transmitted infrared intensity without the sample present, I the intensity transmitted by the sample, $\Delta\nu_{\frac{1}{2}}$ the half-height width of the band, in cm^{-1} . For practical purposes, the definition $\frac{I_0}{I} = \frac{1}{T}$ where T is the transmittance, leads to a modification when the transmittance (T_R) of the solvent blank is determined and used in conjunction with the transmittance (T_S) of the compound's solution, so that

$$A = \frac{\pi}{2cl} \cdot \ln\left(\frac{T_R}{T_S}\right) \cdot \Delta\nu_{\frac{1}{2}} \quad \text{l.mole}^{-1}\text{cm}^{-2}$$

For the compound mer- $\text{Rhpy}_3\text{Cl}(\text{NCO})_2$, a 1.03×10^{-2} M solution in MeNO_2 had minimal $T_S = 0.24$ at 2210 cm^{-1} , with $\Delta\nu_{\frac{1}{2}} = 110 \text{ cm}^{-1}$. A 0.05 cm. cell was used, with cell + solvent transmittance, $T_R = 0.95$. These values give $A = 23.0 \times 10^4 \text{ l.mole}^{-1}\text{cm}^{-2}$.

For the corresponding bromo-complex, mer- $\text{Rhpy}_3\text{Br}(\text{NCO})_2$, a 0.010 M solution had $T_S = 0.295$ at 2200 cm^{-1} , $\Delta\nu_{\frac{1}{2}} =$

95 cm^{-1} giving $A = 17.3 \times 10^4 \text{ l.mole}^{-1}\text{cm}^{-2}$ per ligand.

The greatest error involved is in the determination of $\Delta\nu_{\frac{1}{2}}$, as there is some solvent absorption at 2247 and 2288 cm^{-1} . This reduces the accuracy of the $\Delta\nu_{\frac{1}{2}}$ to $\pm 10\%$.

App. (iv).

Spectrophotometric determination of solvates'

compositions simply uses the Beer-Lambert law,

$$A = \epsilon cl$$

if $l = 1$, and ϵ is known, then A is measured and

$$W = \frac{\epsilon m}{AV}$$

where W = apparent gram-formula weight, m = mass of solvate dissolved (mg.), V = volume of solution (ml.). Hence the difference between the apparent formula weight and the (unsolvated) formula weight gives the amount of solvation.

Sources: Chapter 6

1. Inorg. Synth., Ed. E.L. Muetterties, 1967 X 64.
2. Chapter 1, reference 12.
- 3a. F. Reitzenstein, Ann. Chem., 1894 282 276.
- b. H. Grossman, Ber. deut. chem. Ges., 1904 37 1256.
4. A. Werner, R. Feenstra, Ber. deut. chem. Ges., 1906 39 1538.
5. A.E. Babaeva, I.B. Baranovskii, Russ. J. Inorg. Chem., 1959 4 343.
6. Inorg. Synth., Ed. J. Kleinberg, 1964 VII 251.
7. Chapter 2, reference 10.
8. Chapter 2, reference 45.
9. B. Jones, G.T. Moody, J.D.R. Thomas, Inorg. Chem., 1970 9 114.
10. Chapter 3, reference 25.
11. Chapter 1, reference 14.
12. Chapter 1, reference 15.
13. Chapter 2, reference 63a.
14. Chapter 2, reference 93.
15. N. Atherton, R. Mason, private communication.
16. Chapter 2, reference 31.
17. P.W. Selwood, "Magnetochemistry", Interscience Publishers Inc., New York, 1956.
18. E.B. Wilson, J.C. Decius, P.C. Cross, "Molecular Vibrations", McGraw-Hill, New York, 1955.
19. Beilsteins Handbuch der organische Chemie, 1 75 (Or).
20. F.G. Badder, S. Sugden, J. Chem. Soc., 1950 308.



Table 4.3

Electronic Transitions in mer-Rhpy₃X₂Y

Compound	X	Y	Medium	λ (nm)	ϵ	Assignment	$10Dq$ (cm ⁻¹)	B (cm ⁻¹)	β
4G	Cl	Cl	CHCl ₃	425 (269) 262 256	84 8300 12000 13000	$^1A_{1g} \rightarrow ^1T_{1g}$) $\pi-\pi^*$)	24200 ^d	238 ^d	0.33 ^d
4K	Cl	Br	CHCl ₃	442 (345) ^a (320) ^a	105 630(190) ^a 1400(1000) ^a	$^1A_{1g} \rightarrow ^1T_{1g}$ $^1T_{2g}$ CT?	24600	450	0.63
4J	Br	Cl	CHCl ₃	(456) ^a (376) ^a (337) ^a	150(108) ^a 750(270) ^a 1020(730) ^a	$^1A_{1g} \rightarrow ^1T_{1g}$ $^1T_{2g}$ CT?	21100	330	0.46
			10% in MeOH	(270) (265) (255)	14000 19000 24000) $\pi \rightarrow \pi^*$)			
4H	Br	Br	CHCl ₃	(455) ^a 378 ^b (318) ^a	210 1220 4200	$^1A_{1g} \rightarrow ^1T_{1g}$ $^1T_{2g}$ CT?	22500 ^d	303 ^d	0.42
			10% in MeOH	258	26000	CT			
4M	I	I	CHCl ₃	(603) ^a 500 393 306	650 2200 8000 18600	$^1A_{1g} \rightarrow ^1T_{1g}$ CT? CT CT			
3K	NCO	Cl		376 (320) ^a		$^1A_{1g} \rightarrow ^1T_{1g}$ $n \rightarrow \pi^*$ or $^1T_{2g}$	27500	308	0.44
3L	NCO	Br		397 (313)		$^1A_{1g} \rightarrow ^1T_{1g}$ $n \rightarrow \pi^*$ or $^1T_{2g}$	26400	468	0.65
3D	N ₃	N ₃		(430) ^a (370) ^a		$^1A_{1g} \rightarrow ^1T_{1g}$ $^1T_{2g}$	24000	250	0.35
4L ^c	Cl	Cl		425	78	$^1A_{1g} \rightarrow ^1T_{1g}$			
4N	Cl	Cl		427	68	$^1T_{1g}$			
3X ^e	Cl	OH ₂		390 315		$^1T_{1g}$ $^1T_{2g}$	26700	423	0.59

- a: Gaussian resolution in λ .
b: λ_{\max} : resolves as 387 nm.
c: deuteriated analog of 4G.
d: from ref. 11.
e: trans-Rhpy₄XY.

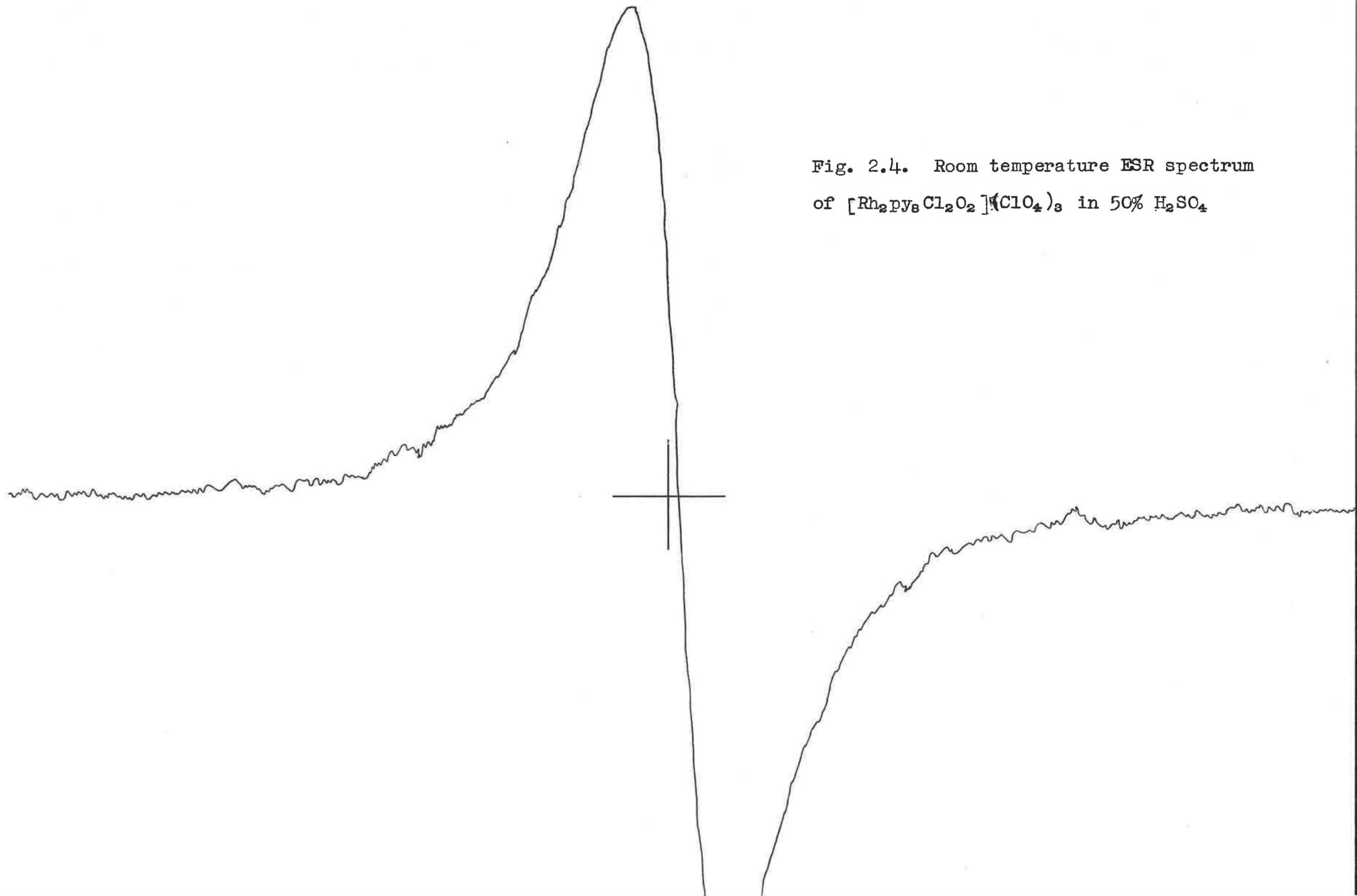


Fig. 2.4. Room temperature ESR spectrum of $[\text{Rh}_2\text{py}_8\text{Cl}_2\text{O}_2](\text{ClO}_4)_3$ in 50% H_2SO_4

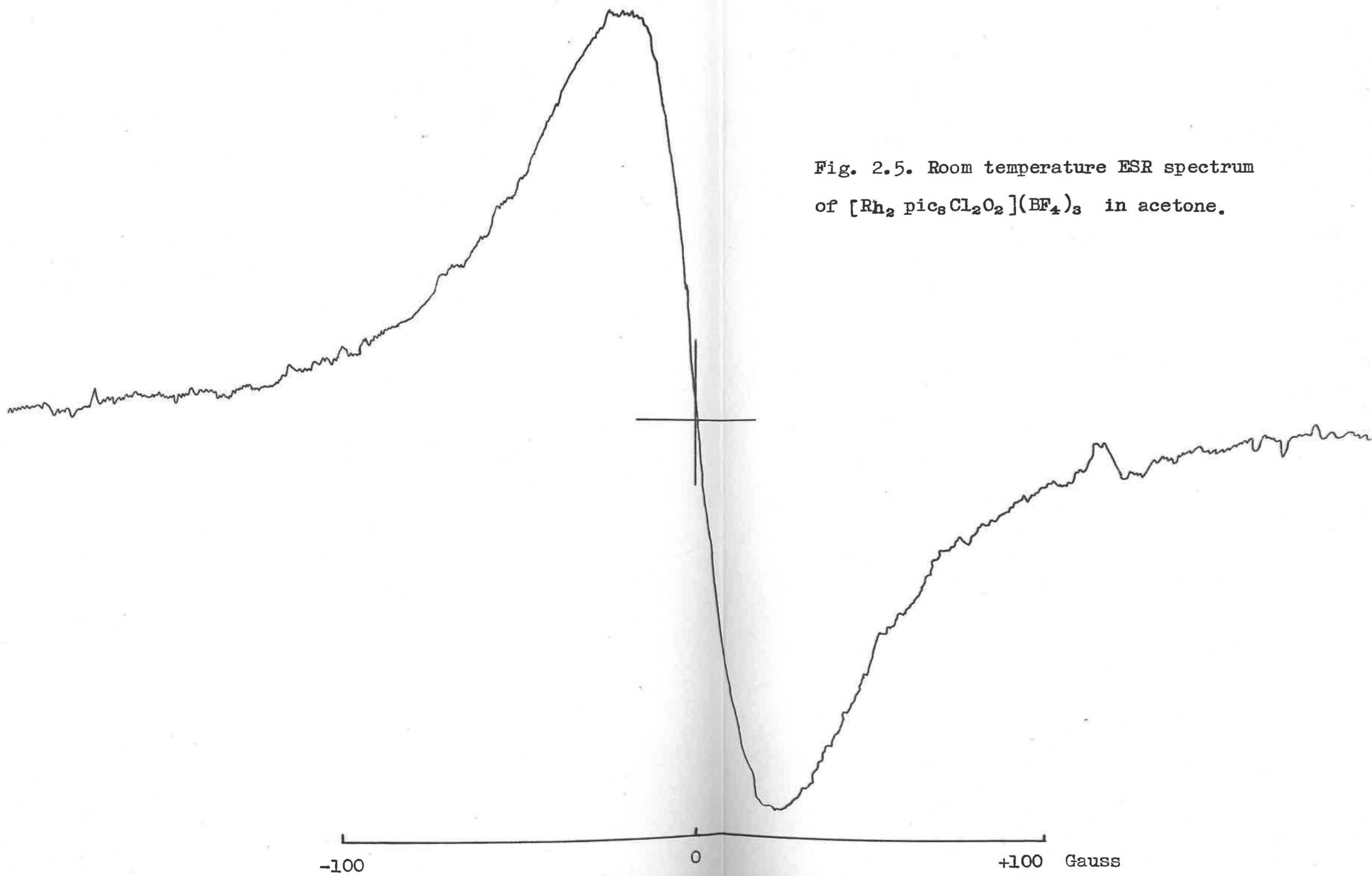


Fig. 2.5. Room temperature ESR spectrum
of $[\text{Rh}_2 \text{pic}_8 \text{Cl}_2 \text{O}_2](\text{BF}_4)_3$ in acetone.

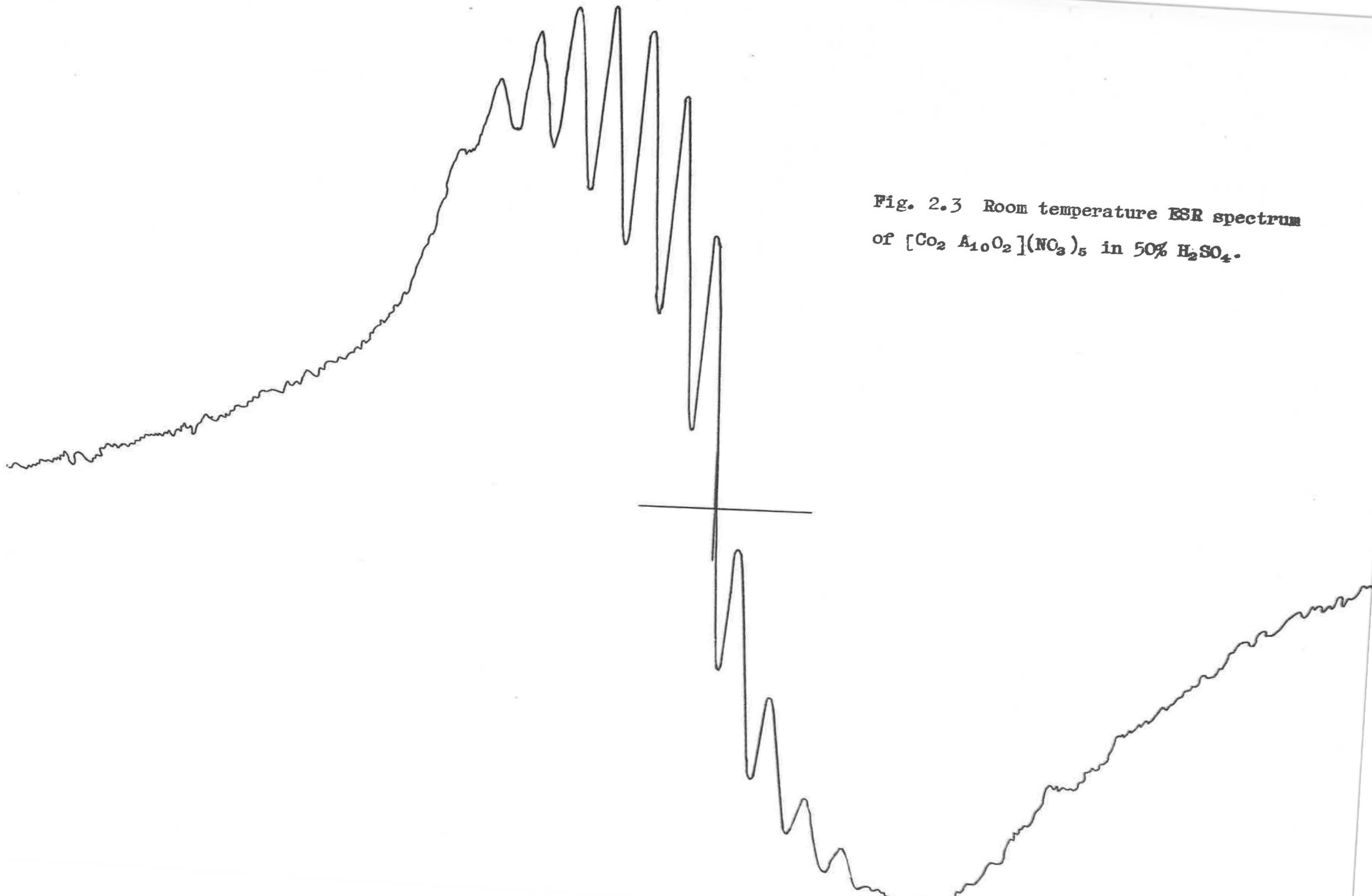


Fig. 2.3 Room temperature ESR spectrum of $[\text{Co}_2 \text{Al}_{10}\text{O}_2](\text{NO}_3)_5$ in 50% H_2SO_4 .